UNIVERSITY OF BIRMINGHAM

ASPECTS OF THE USE OF ELECTRIC ARC FURNACE DUST IN CONCRETE

by

FAHAD M. ALMUTLAQ

A Thesis submitted to
The University of Birmingham
For the degree of
DOCTOR OF PHILOSOPHY

School of Civil Engineering
College of Engineering and Physical Sciences
The University of Birmingham
August 2011

ABSTRACT

Electric arc furnace dust (EAFD) is a by-product of the electric steelmaking industry produced in large quantities around the world. In Saudi Arabia, a form of EAFD known as Bag House Dust (BHD) is being used in small amounts as concrete additive, because higher levels of addition caused excessive retardation of setting and hardening. The use of this material is recent, therefore little is known about its effects on durability. This research aims to examine effects of BHD additions on certain properties of cement pastes, mortars and concretes, particularly those believed to affect the susceptibility of embedded steel reinforcement to chloride-induced corrosion as this is a major cause of degradation of reinforced concrete structures in the Arabian Gulf region.

Studies of the effects of 2 % BHD addition on pore solution chemistry of hydrated-cement pastes with various levels of internal chloride contamination indicated that both free chloride concentration and hydroxyl ion concentration increased. Electrochemical monitoring of the corrosion behaviour of embedded steel in chloride-contaminated mortars showed that the rates of corrosion were reduced slightly in the presence of BHD.

Measurements of the coarse capillary porosities of hydrated-cement pastes revealed significantly lower results in 2-3 % BHD-specimens compared to plain cement pastes. Attempts to measure the consequent changes in apparent diffusion coefficients of chloride in related concrete specimens showed that the BHD additions caused no adverse effects on chloride penetration rates.

Electrochemical monitoring of the corrosion behaviour of steel bars embedded in mortars exposed to chloride ingress at 20 °C and 40 °C demonstrated that the threshold chloride level for the initiation of crevice corrosion was significantly increased by the presence of BHD. This was thought to be partly influenced by BHD in reducing bleeding which affects the integrity of the layer of hydration products formed around the steel surface.

Having found that 2-3.5 % BHD additions had no detrimental effects on the properties studied, the possibility of using chloride-free accelerators to increase levels of BHD addition without causing excessive retardation of cement hydration was investigated. Calcium nitrite and calcium formate were both found to be reasonably effective in increasing the rates of hardening of specimens with 8 % addition of BHD.

KEY WORDS: Electric arc furnace dust, corrosion of reinforcement, pore solution chemistry, coarse capillary porosities, apparent diffusion coefficients, chloride threshold value, bleeding, hardening of concrete, calcium nitrite, calcium formate.

ACKNOWLEDGEMENTS

The author would like to express his deep indebtedness and sincere thanks to Professor C. L. Page who supervised this research, for his valuable time and advice and for all his help and guidance in completing this thesis. I would like deeply thank Dr. Ian Jefferson, my co-supervisor, for his valuable help and comments.

I also wish to record my greatest thanks to Dr. M. M. Page for her assistance during my experimental work, Dr. J. Yang for his valuable comments and Dr L.Y. Li. for his mathematical explanations. Many thanks to Mr. J. Edgerton, Mr. D. Cope and other technical staff for their assistance. Special thanks to Mr. F. Biddlestone for his help and support with the thermal analysis studies and Dr. J. Deans for her help with XRF analysis.

My gratitude and appreciation to Dr. W. Al-Shalfan, general manager of SABIC Technology Centre in Jubail city, Mr. A. Al-Hazemi, the manager of the Materials and Corrosion section for their financial support and encouragement to improve my knowledge and skills in this field and to Dr. Z. Chaudhary for nominating me to continue my higher education in Civil Engineering department at the University of Birmingham and also for collecting and sending all necessary materials and information to complete this work. I would also like to acknowledge my debt to all my colleagues in SABIC Technology Centre.

Lastly, but not the least, I would like to express my special thanks to my family for providing me the much needed support and encouragement and my wife for her understanding; without their patience this work would not have been completed. Special thanks for my daughter, Miss Joman, for providing some of the fun after a long days work.

TABLE OF CONTENTS

ABBREVIATIONS

2 % BHD	specimens made with 2 per cent addition of BHD by weight of cement
3.5%CN/8%BHD	specimens made with 8 per cent addition of BHD and prepared with 3.5 per cent calcium nitrite by weight of cement
3.5%CF/8%BHD	specimens made with 8 per cent addition of BHD and prepared with 3.5 per cent calcium formate by weight of cement
0.4 % Cl	0.4 per cent addition of chloride, by weight of cement
20C01	specimens no. 1, contained steel bar without defects at the surface, made without BHD addition and exposed to 20 ºC temperature NaCl solution
40D23	specimens no. 3, contained steel bar with defects at the surface, made with 2 % BHD and exposed to 40 ºC temperature NaCl solution
A02	specimens no. 2, made without BHD addition and prepared at 0.5 w/c ratio
ASTM	American Society for Testing and Materials
B32	specimens no. 2, made with 3%BHD addition and prepared at 0.6 w/c ratio
BFS	blast furnace slag
BHD	bag house dust
BS	British standard
C_2S	dicalcium silicate
C_3S	tricalcium silicate
C_3A	tricalcium aluminate
C_4AF	tetracalcium aluminoferrite
C	cement
CA	coarse aggregate
$CaCO_3$	calcium carbonate
CaO	calcium oxide
$CaZn_2(OH)_6 \cdot 2H_2O$	calcium hydroxyl-zincate
CF	calcium formate

CH or $Ca(OH)_2$	calcium hydroxide
$[Cl^-]$	chloride ion concentration (mMol/l)
CN	calcium nitrite
Cs	the chloride concentration at surface (mass %)
C-S-H	calcium-silicate-hydrate
CO_2	carbon dioxide gas
D_{app}	apparent chloride diffusion coefficient (m^2/s)
DSC	differential scanning calorimetry
DTG	derivative thermogravimetry
DW	distilled water
ΔH	enthalpy change (J/g)
EAFD	electric arc furnace dust
E_{corr}	corrosion potential (mV)
EPA	environmental protection agency
E_{pit}	pitting potential
EWC	European waste catalogue
FA	fine aggregate
GGBS	ground granulated blast-furnace slag
I_{corr}	instantaneous corrosion rate ($\mu A/cm^2$)
K_2O	potassium oxide
KOH	potassium hydroxide
LPR	linear polarization resistance
LOI	loss of ignition
M	mole/litre solution
NaCl	sodium chloride
Na_2O	sodium oxide
NaOH	sodium hydroxide
$[OH^-]$	hydroxyl ion concentration
OPC	ordinary Portland cement
PFA	pulverized fuel ash
RH	relative humidity
S	sand

SBR	Styrene-Butadiene Rubber emulsion
SCE	saturated calomel electrode
SCM	supplementary cementitious material
SF	silica fume
TG	thermogravimetry
UPV	ultra pulse velocity
w/c	water to cement ratio
Wt.	weight
XRF	x-ray florescence
ZnO	zinc oxide

LIST OF FIGURES

LIST OF TABLES

Chapter 1

INTRODUCTION

1.1 BACKGROUND

Reinforced concrete is the most commonly used construction material. Concrete is moderately strong in compression but weak in tension. As a result, steel reinforcing bar is embedded in concrete to carry the tensile forces. The use of embedded steel in concrete was projected 150 years ago. Nowadays, most of the buildings, bridges and infrastructure in the world are reinforced concrete with consumption of billions of tonnes. In 2006, it was expected to reach 130 million or more metric tonnes in North America. Up to 2009, the annual rise of cement production is expected to reach 2.5 % (Broomfield, 2007).

It is important to everyone to live in a safe structure. Therefore, study of the major factors that may affect the durability, long-serviceability and stability of a concrete structure is important. Deterioration of concrete structures could be due to a variety of reasons, e.g. mechanical or chemical degradations. Since 1970s, corrosion of reinforcing steel was recognized to be a major cause of concrete structure deterioration in many parts of the world and it has becoming a significant financial problem (Page, 2007).

For instance, in a recent cost of corrosion study for US highway bridges, the estimated direct cost of corrosion was between $ 6.43 billion and $ 10.15 billion annually (Page, 2007). In a Transportation Research Board report, $50-200 billions were estimated as the cost of bridge deck repairs. In the United Kingdom, £616.5 million was the total estimate of salt-induced

corrosion damage on motorways and road bridges made as long ago as the 1980s in a study made for the former Department of Transport (Broomfield, 2007).

Thousands of millions of pounds (£) are therefore spent annually to repair damage caused by corrosion of the reinforcing bar in concrete structures. Many efforts have been made to conduct studies to assess several proposed methods to prevent the corrosion of reinforcing steel in concrete. These methods include the use of low permeability concrete with pozzolanic additions, corrosion inhibitors, epoxy coated rebars, galvanized steel bars, coatings and cathodic protection systems. One of the common prevention practices is to use concrete additives, by-products generated by different smelting industries, in potentially corrosive environments. The ingress of aggressive agents such as Cl^-, SO_4^{-2} and CO_2 etc. from the environment depends on the permeability of the concrete. So the use of concrete additions such as fly ash, ground granulated blast furnace slag and silica fume that show an improvement in the concrete durability parameters, and increase resistance to the ingress of the aggressive agents is sometimes favourable.

Another waste by-product material is electric arc furnace dust (EAFD). Recently, the production rate of EAFD has increased yearly as the steel industry grows internationally. The estimated quantity of EAFD produced annually, worldwide, is about 3.7 million tonnes, of which European sources account for some 500,000 - 900,000 tonnes. In the United States the approximate quantity of the EAFD produced every year is about 700,000 – 800,000 tonnes and this rate of EAFD production is increasing by 4-6 % each year (Machado et al., 2006). The disposal of EAFD is expensive. For example, the disposal cost in the United States only is approximately $200 million per year (Al-Zaid et al., 1997). According to many authorities

and to the European Waste Catalogue (EWC, 2002) EAFD is classified as a hazardous material (code 10 02 07) and thus disposal at landfill sites before treatment is not allowed due to the potential leachability of heavy metals such as Zn and Pb. Solidification and stabilization are the best techniques suggested by the Environmental Protection Agency (EPA) as a treatment option for some of the waste materials before final disposal (Pereira et al., 2007). When EAFD is solidified in a cement matrix, this will act as barrier between the waste and environment resulting in the reduction in both the permeability of the waste to water and the outward diffusion of heavy metals from it due to the reduction in the EAFD surface area (Hamilton and Sammes, 1999). The use of EAFD in concrete, which has not yet been widely investigated, could reduce some potential problems associated with the disposal of EAFD itself. Another advantage of using EAFD in concrete is that a partial replacement of cement raw materials in concrete reduces the high CO_2 emission generated during manufacture. Thus in situations where the recovery process of some heavy metals available in EAFD is not considered commercially feasible, the use of this waste material in concrete could be an effective means of disposal (Xia and Pickles, 1999).

1.2 SCOPE OF STUDY

Research into the use of EAFD is very limited and there is considerable scope for further work to investigate its possible application as a concrete additive. Most studies to date have tended to focus on stabilization/solidification rather than utilizing EAFD as an addition to concrete and studying its effect on the durability of reinforced concrete structures. Little attention has been paid to how to avoid the retardation effect when high levels of EAFD are used in concrete. The scope of the thesis, therefore, can be divided into two main objectives.

The thesis is divided into nine chapters. After this introductory Chapter, a review of the corrosion of steel reinforcing bar and its causes was carried out and followed by a literature review on the electric arc furnace dust (EAFD). The materials used and common experimental techniques were described in Chapter 3. In the remaining chapters, each experimental part stands with its own the main objective presented in an introductory section followed by a review of the relevant area and the detailed experimental work related to the corresponding experiment.

The abbreviation of "BHD" in this thesis was used to distinguish between the different electric arc furnace dusts (EAFD) generated in different countries and the one generated in Saudi Arabia referred to as "BHD". This distinction has to be made because EAFD composition may vary depending on the type of scrap used, type of additives used during the production stage and the type of steel manufactured (Salihoglu et al., 2007). For the first part, it was essential to investigate the effect of BHD addition on some of the main durability aspects that may cause deterioration of reinforced concrete structures, see part A in section 1.3. The second part was the study of the possibility of overcoming the retardation effect when using high levels of BHD in concrete, see part B.

1.3 OUTLINE OF THESIS

(A) Corrosion of steel reinforcing bar and its related studies

The major concrete durability problem is corrosion of steel reinforcing bar in concrete due to aggressive environmental conditions. In Chapter 4, the effect of BHD on the corrosion behaviour of embedded steel bar was investigated by monitoring the steel bar

electrochemically. To understand the implication of the behaviour of the steel bar, further studies were initiated to examine pore solution chemistry and chloride leaching tests. Investigations of the effect of BHD on porosity of cement pastes and the chloride ion ingress through concrete were carried out and reported in Chapter 5. The chloride ion ingress rate was assessed via two approaches; (i) determining the chloride ion apparent diffusion coefficients and (ii) estimating the depth at which the chloride level is critical. When chloride ions penetrate and reach a certain "threshold" level at the steel surface, the corrosion of steel reinforcing bar will be initiated. This threshold value was found to be affected by some parameters such as bleeding of concrete. Therefore, in Chapter 6, the effects of BHD on the chloride threshold value together with bleeding capacity of the concrete were considered. Another adverse effect of the bleeding process on durability of concrete is its effect on the concrete compressive strength development and thereby on bond strength at concrete-steel interface. Ambient temperature also has been found to have unfavoured effect on the concrete compressive strength. To examine this, the influence of temperature on compressive strength development of concrete containing various levels of BHD was investigated in Chapter 7. In the same chapter, concrete-steel bond strength was also examined.

(B) The possibility of overcoming the retardation effect of using substantial levels of EAFD in concrete

The main concern when using high levels of BHD in concrete is its effect of prolonging setting times and reducing early strength development. To overcome this adverse effect either low levels of BHD e.g. 2 and 3 % by weight of cement, as is the case now in Saudi Arabia (Maslehuddin et al., 2011), or non-chloride accelerator admixtures with higher level of BHD could possibly be utilized. In Chapter 8, the use of two non-chloride accelerators with high

level of BHD was studied and their effects on the setting time, consistence and the early hardening rate were investigated.

All the general conclusions derived from the experimental studies and the recommendations for further work are summarised in the last Chapter.

Chapter 2

LITERATURE REVIEW

2.1 CORROSION OF STEEL REINFORCING BAR IN CONCRETE

2.1.1 Introduction

Nowadays, the corrosion of steel reinforcing bar in concrete is the major cause of deterioration of the reinforced structures. Concrete normally provides a high degree of protection to the embedded steel reinforcing bar by: i) preventing the penetration of corrosive agents e.g. chloride ions, ii) providing a highly alkaline environment surrounding reinforcing bar that works to passivate the steel and hence, protect it against corrosion (Page and Treadaway, 1982). When water is available, soluble hydroxides e.g. NaOH and KOH will be formed. They provide a very highly alkaline condition in the concrete with a typical pH value between 13-14 (Page, 1998). A high degree of protection to the steel reinforcing bar can be achieved by producing a good quality, well placed and well cured concrete with an adequate amount of cover. The period of this protection will be affected by a number of factors. These include; maintaining a high level of pH hence, maintaining the integrity of the passive film, the physical integrity and thickness of concrete cover and the quality of the concrete and the barrier to the penetration of aggressive agents (BRE Digest 444, 2000).

Some factors, such as cement type, water to cement ratio, mineral admixtures, the condition of the concrete preparation and the site, ambient temperature, relative humidity, permeability of the concrete, etc., have been reported in many studies as significant influencing factors on

the corrosion rate of steel reinforcing bar embedded in concrete. In structures exposed to a marine environment it is important to take appropriate measures to keep the embedded steel reinforcing bar in a passive state and so prevent/control corrosion to ensure a durable concrete. For designing concrete resistant to corrosion of the reinforcement, the use of blended cements together with good compaction, a proper curing regime and a low water to cement ratio is required to achieve impermeable concrete of a high alkalinity i.e. minimizing the ingress of aggressive agents. Unfortunately, in practice, the aggressive agents will often find a way to reach the steel reinforcing bar when these factors are not achieved.

In the Arabian Gulf, many investigations along with professional experience of concrete durability have observed that the corrosion of steel reinforcing bar in the concrete is the first problem that leads to concrete deterioration (Al-Dulaijan et al., 2003, Chaudhary et al., 2008, Jarrah et al., 1995). Therefore, it is very important for site and industrial engineers to understand the corrosion process and to be familiar with the main causes of deterioration of reinforced concrete structures. The scope of Chapter 2 is to explain the mechanism of the corrosion process in a simple way supported with appropriate illustrations and to summarise the main causes of the corrosion of steel reinforcing bar in concrete. The fundamental factors that affect the corrosion rate of steel are discussed. In the same chapter, the BHD material as concrete additive is also reviewed.

2.1.2 Corrosion mechanism of steel reinforcing bar embedded in concrete

2.1.2.1 Principles of the corrosion process

The corrosion of steel reinforcing bar is considered to be an electrochemical process. Consequently, an electrolyte "aqueous solution" is required for anodic and cathodic reaction to occur. The electrolyte allows ions formed to move between the anodic and cathodic sites on the steel surface (Page, 2007). In high pH solutions and in the presence of moisture and oxygen, two different reactions can occur at two different areas of the metal surface. These are known as anodic and cathodic reactions. The process by which the ions formed move between the anodic and cathodic sites through the electrolyte, represents the corrosion current shown in Figure 2-1. In the anodic area, the anodic reaction occurs as follows;

$$Fe \longrightarrow Fe^{2+} + 2e^{-} \qquad [2.1]$$

In the anodic reaction, steel dissolves forming charged ions and provides electrons. These electrons are consumed on the steel bar surface in the other reaction [2.2] in the cathode area. This cathodic reaction will consume oxygen and water.

$$2e^{-} + H_2O + \tfrac{1}{2}O_2 \longrightarrow 2OH^{-} \qquad [2.2]$$

The cathodic reaction results in hydroxide ions being generated increasing alkanity in the concrete, thus enhancing the passive film (Broomfield, 2007).

These two reactions are considered to be the first steps in creating/generating rust. However, in humid and aggressive environments where oxygen and water are available, a series of further steps will take place as shown by [2.3], [2.4] and [2.5] reactions.

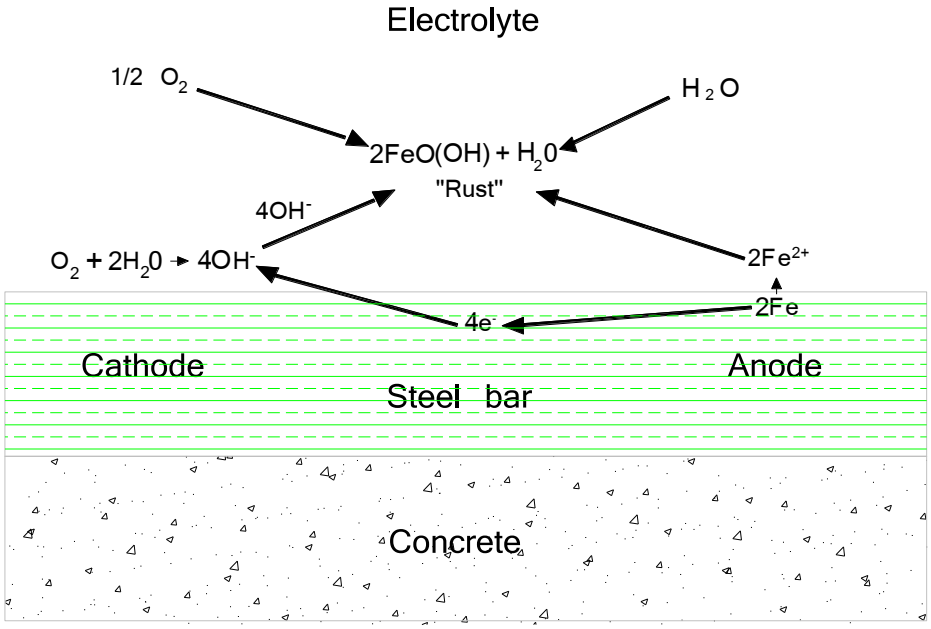

Figure 2-1 Anodic and cathodic reactions on the steel bar

$$Fe^{2+} + 2OH^{-} \longrightarrow Fe(OH)_2 \quad \text{Ferrous hydroxide} \qquad [2.3]$$

$$4Fe(OH)_2 + O_2 + 2H_2O \longrightarrow 4Fe(OH)_3 \quad \text{Ferric hydroxide} \qquad [2.4]$$

$$2Fe(OH)_3 \longrightarrow Fe_2O_3H_2O + 2H_2O \quad \text{Hydrated ferric oxide (rust)} \qquad [2.5]$$

Loosely adherent brown deposits of hydrated ferric oxide known as rust are thus formed. The corrosion product (rust) occupies a much larger volume that the original steel. This generates a tensile stress in the concrete and results in cracking and spalling of the concrete (Domone,

2010) and rust staining appears on the concrete surface, as shown in Figure 2-2. This visible evidence of corrosion is often considered to be a warning before there is any considerable risk of a structural collapse (Broomfield, 2007, Page, 2007).

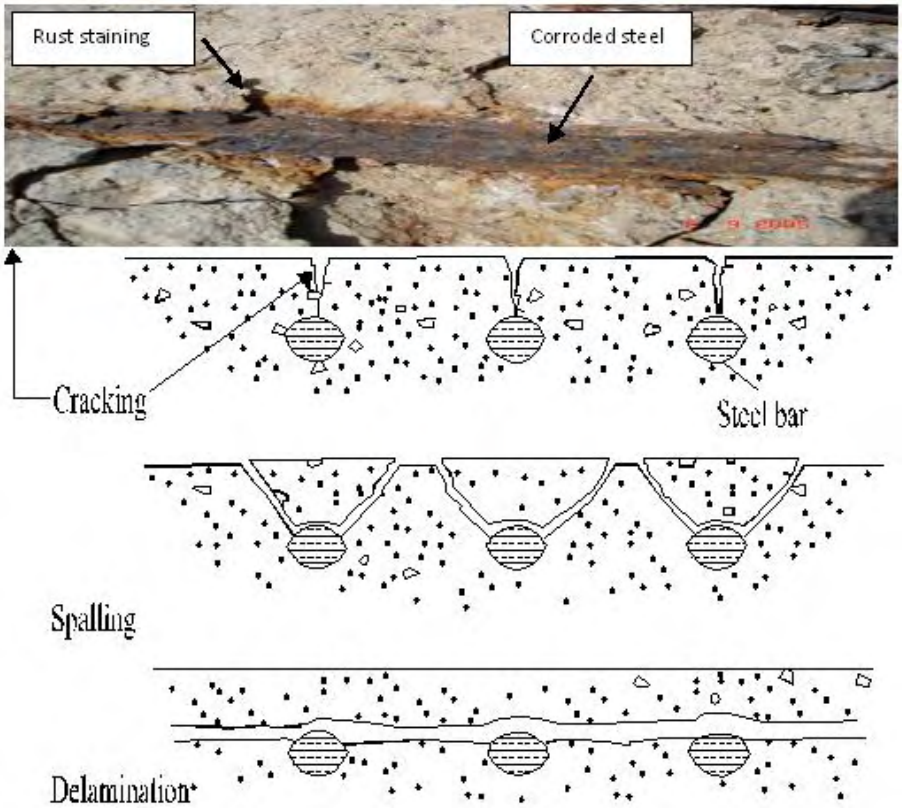

Figure 2-2 Shows how the expansion of corrosion products induce stress into the concrete and eventually leading to cracking

2.1.2.2 Passivity of steel reinforcing bar

In an alkaline environment where dissolved oxygen is available in abundance, the steel bar forms a surface oxide layer known as a passive film. This passive layer limits the loss of metal from steel surface due to corrosion (Domone, 2010). When steel is embedded in a highly alkaline environment, the corrosion of the steel will not proceed, although oxygen and water are available, due to formation of this passive layer. Furthermore, this passive film will

be maintained as long as the concrete surrounding the steel is very alkaline and not contaminated.

The anodic dissolution rate of steel bar is affected by the passive film. This can be illustrated experimentally by observing the applied potential and current density and their relationship for steel bars immersed in typically neutral and alkaline solutions. These relationships are defined as anodic polarization curves. In solution with a pH lower than 7, the anodic reaction rate increases as the steel potential in the anodic area increases. This phenomenon is known as "active dissolution" and is not observed in alkaline solution of pH > 11.5. The initiation of formation of the passive film is characterized, when the potential exceed a critical value of about - 700 mV (SCE), by a sharp decrease in corrosion current density. The formation of passive film can be expressed by the following equation;

$$2Fe + 3H_2O \longrightarrow Fe_2O_3 + 6H^+ + 6e^- \qquad [2.6]$$

This passive film will continue growing slowly together with rise in the steel potential until a critical potential is reached (Page, 2007). This passivity formation has been illustrated experimentally by showing the anodic polarization curve of the steel bar embedded in hydrated ordinary Portland cement pastes, as shown in Figure 2-3.

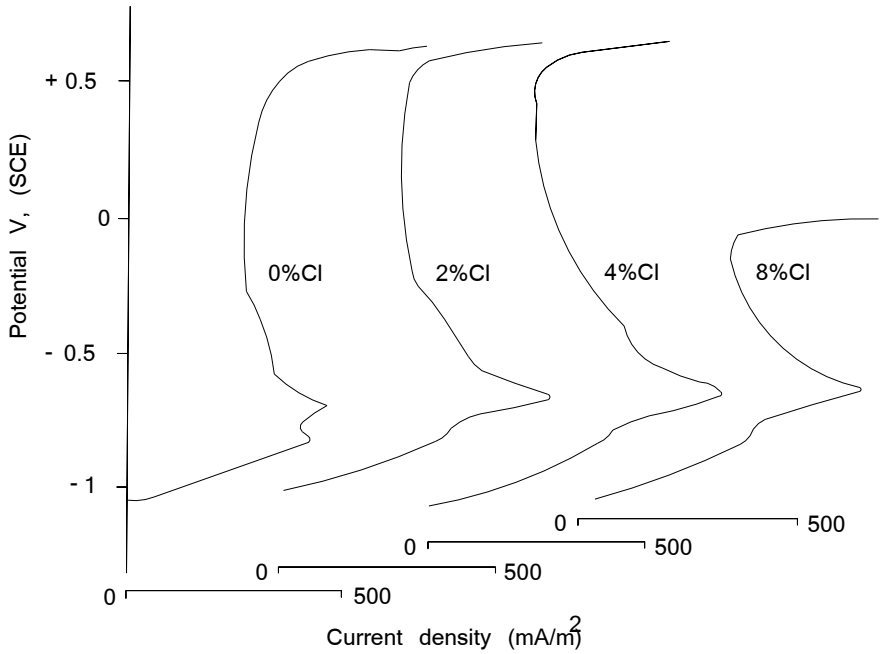

Figure 2-3 Typical anodic polarization curves of mild steel in hydrated ordinary Portland cement pastes of water/cement ratio of 0.4 containing various percentages of calcium chloride dihydrated by weight of cement. after (Page and Treadaway, 1982)

The thickness of the passive film is in the nanometer range (Page, 2007). This protective passive film is described as a tightly adherent, impermeable film and when it is maintained, will prevent any further corrosion of steel reinforcing bar embedded in concrete (Domone, 2010).

Diffusion of carbon dioxide, chloride ions and depletion of oxygen are the main processes that can break down the passive film. Further details related to these processes are discussed in the next sections. In some media that show low levels of pH (lower than 10) and some chloride ions, the passive film will not be stable. The passive film can break down when concrete is no longer highly alkaline (Page, 2007). Figure 2-4 shows the breakdown of the passive film on steel reinforcing bar in concrete. It follows, in the presence of moisture and

oxygen and breaks in the passive film, the active corrosion process will take place and rust may start appearing on the concrete surface.

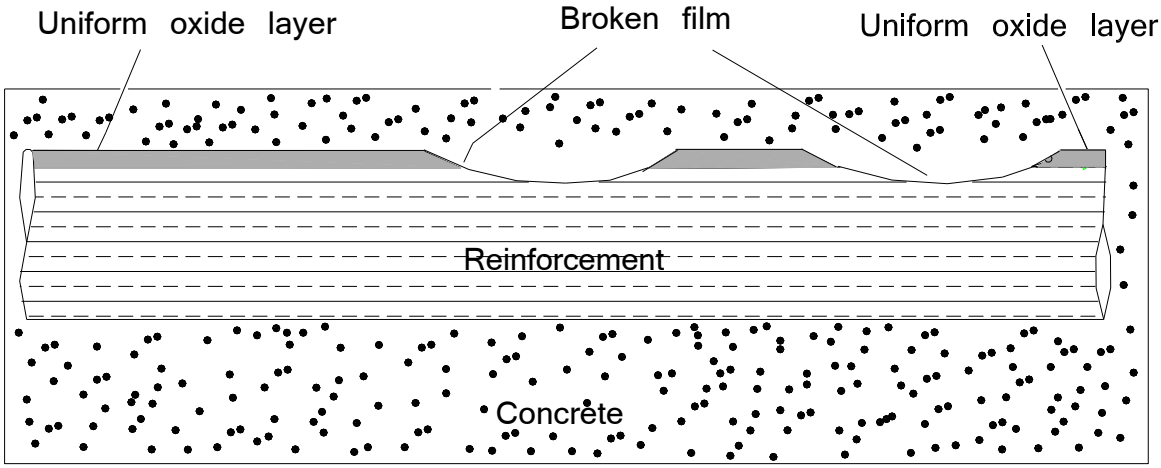

Figure 2-4 Break down of the passive layer on steel reinforcing bar in concrete

2.1.3 Pourbaix diagrams

To determine whether the corrosion of metals can occur under a given potential and pH, Pourbaix (1966) constructed maps that show the domains of thermodynamic stability of various phases of a metal and its oxidation products. Also, these diagrams show the tendency of metal to corrode in aqueous solutions at a given temperature and indicate how this tendency of metal corrosion is affected by changing potential (E, volt) and pH. From a Pourbaix diagram, three domains of thermodynamic stability can be identified;

a) "Immunity" domain: the dissolution of metal is impossible because the metal is thermodynamically stable.
b) "Corrosion" domain: the metal is unstable and corrosion can occur releasing metal ions in the solution.

c) "Passivation" domain: the metal dissolution is thermodynamically possible i.e. unstable metal depending on surrounding environment. However, the corrosion process produces an oxide surface layer i.e. Fe_2O_3. Figure 2-5 shows a simplified Pourbaix diagram indicating a protective layer is formed in the "Passivation" domain on the steel surface at 25 ºC temperature.

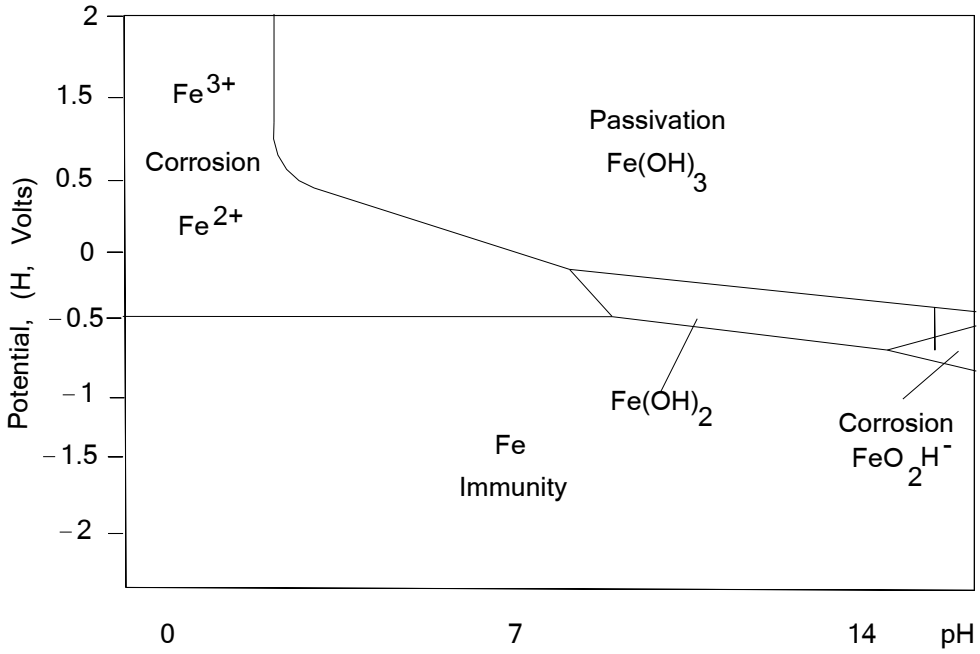

Figure 2-5 Protective passive layer is formed on the steel surface as per Pourbaix diagram after (Pourbaix, 1966)

2.1.4 Causes of corrosion of steel reinforcing bar in concrete

In some concrete structures, where concrete is not durable, with no protective measures used or when surrounded by an aggressive environment, there will be significant corrosion. Until the 1950s, the main cause of concrete deterioration was believed to be due to carbonation (Hunkeler, 2005). After that, chloride-induced corrosion became the most common cause of structural deterioration mainly because of either cast-in chlorides or exposure to external

sources of chloride such as deicing salt or a marine environment. The third mechanisms that causes breakdown of the passive film is depletion of oxygen as reviewed in the following section.

2.1.4.1 Depletion of oxygen

There are some environments where oxygen is depleted, including those where concrete is fully immersed in water or buried in saturated soil. The corrosion potential of passive steel bar in concrete may vary over a wide range between +200 to -700 mV (SCE) dependent on the availability of oxygen (Page, 1988). If this reduction of oxygen at the steel bar level is significant then it will have an effect on the cathodic reaction at the steel surface. In this case, the measurements of the corrosion potential (E_{corr}) of the steel bar will show more negative values as the oxygen level is reduced at the steel surface, as illustrated in an Evans diagram shown in Figure 2-6.

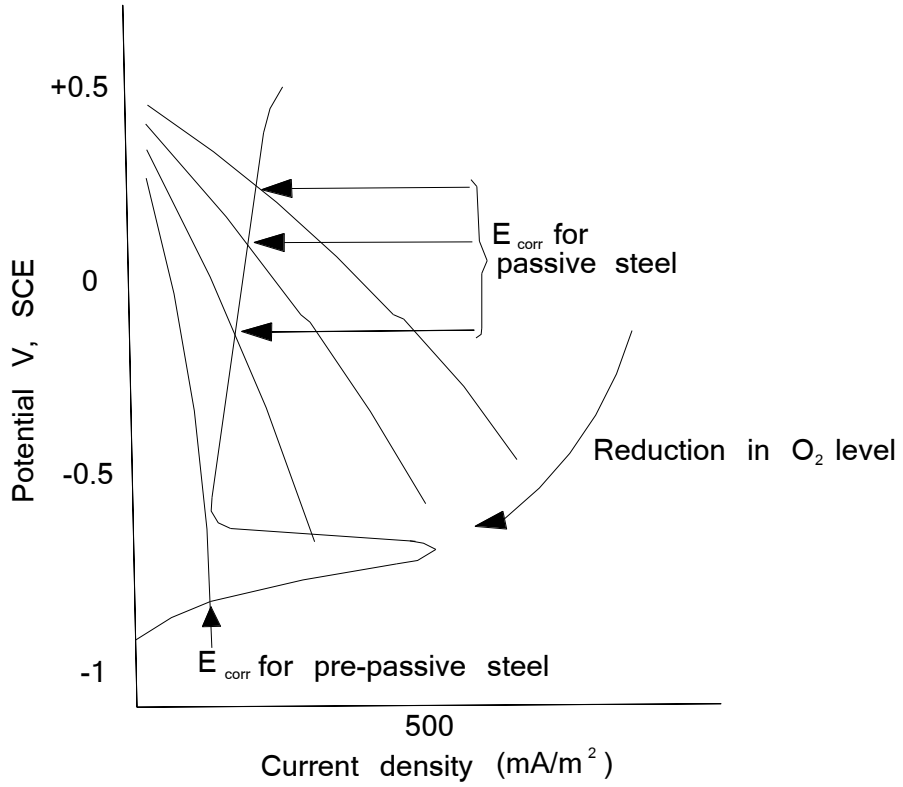

Figure 2-6 Evans diagram showing the effect of oxygen concentration on corrosion potentials on steel bar in concrete after (Page, 2007)

Figure 2-6 indicates steel in such an environment, where the steel potential reached a value of less than about – 700 mV (SCE), it will not be protected in the normal way i.e. by passivity of steel bar. The cathodic reaction will not proceed at a significant rate due to the reduction/absence of oxygen resulting in very small corrosion current density, see Figure 2-6. Hence steel embedded in concrete in this case will be protected due to the general depletion of oxygen leading to low corrosion density. This phenomenon is known as "cathodically restrained pre-passivity". In such situations, the well known passivity of the steel will be formed once oxygen is available again at the steel surface (Page, 2007).

On the other hand, there is more an important scenario which leads to a loss of cross section area of metal without showing signs of cracking or rusting of the concrete, which should not be confused with the one explained above i.e. effect of general depletion of oxygen. This process, occurs in corrosion macro cells as a result of depletion of local oxygen. It can result in the formation of a localized corrosion with black or green rust. The anodic and cathodic zones should be well separated on the reinforcing steel. The anodic zone is either located where there is voided or badly arranged and/or jointed concrete, saturated with oxygen depleted saline water. The saline water will reduce the alkalinity and thus increase the Fe^{2+} ions solubility. As a result of this, the metal will dissolve and produce ferrous compounds, hence a loss of steel cross section area without showing normal evidence of concrete deterioration e.g. cracking or rust staining. The corrosion products, e.g. ferrous compounds, are initially green in colour and when exposed to air the colour rapidly changes to black (Page, 2007). This localized corrosion could be considered the worst among the corrosion types.

2.1.4.2 Corrosion of reinforcing steel due to carbonation of concrete

To maintain the passivity of the steel reinforcing bar in concrete, a high pH environment is required. Neutralisation of the pore solution in concrete will change the alkaline condition in the pore solution to aggressive conditions (Page, 1998). Since concrete is a porous material, some aggressive gases may diffuse such as CO_2 or any other acidic gases, and then concrete loses its alkalinity and hence carbonation occurs. The carbonation process is usually a very slow process. The carbon dioxide is present in the air with a concentration of about 0.03 % (Gu et al., 2001). When concrete structures are exposed to the air for long time, the alkalinity of the concrete will be depleted, as illustrated by the following equations;

$$CO_2 + 2NaOH \rightarrow Na_2CO_3 + H_2O \quad [2.7]$$

$$Na_2CO_3 + H_2O + CO_2 \rightarrow 2NaHCO_3 \quad [2.8]$$

$$CO_2 + 2KOH \rightarrow K_2CO_3 + H_2O \quad [2.9]$$

$$Ca(OH)_2 + CO_2 \rightarrow CaCO_3 + H_2O \quad [2.10]$$

$$C\text{-}S\text{-}H + CO_2 \rightarrow CaCO_3 + SiO_2 \times H_2O \quad [2.11]$$

Practically, carbon dioxide from the air will penetrate through concrete cover, react with alkaline hydroxides in the concrete and form carbonate compounds. When more carbon dioxide diffuses into the concrete, more acid will be formed resulting in more depletion of the calcium hydroxide according to equation [2.10] and as illustrated in Figure 2-7. According to equation [2.11], calcium-silicate-hydrate (C-S-H) will react with carbon dioxide to form calcium carbonate and hydrated silica gel. Removal of the alkali hydroxides which are dissolved in the pore solution will lead to a significant reduction of alkalinity in the concrete, to a value of less than 10, and consequently, to an unstable passive film on the steel leading to steel corrosion (Page, 2007).

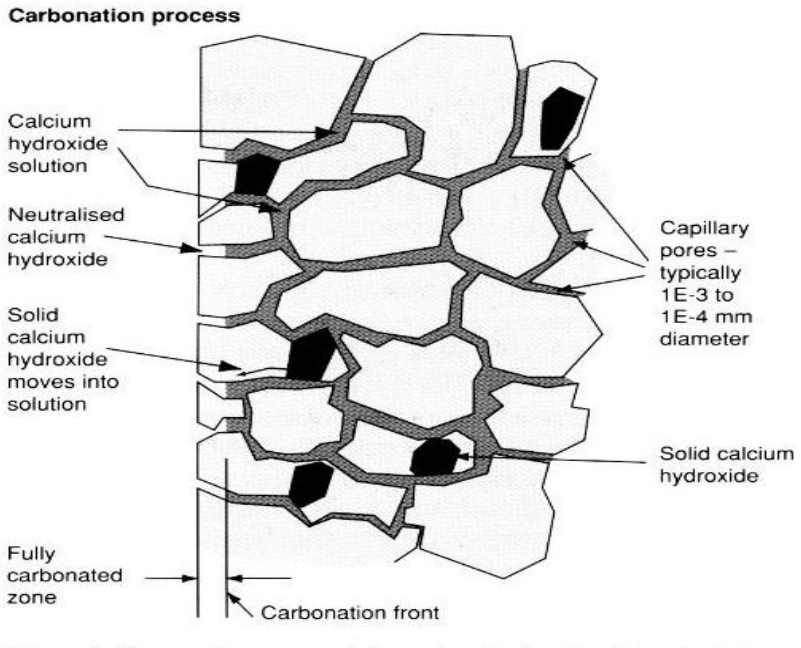

Figure 2-7 Schematic representation of alkalie neutralization in hydrated cement and the formation of a "carbonation front" after (Currie and Robery, 1994)

Once the concrete is carbonated, the condition of the electrolyte becomes more aggressive and as a result enhances corrosion of the reinforcement. The corrosion rates in the carbonated concrete were found to be governed mainly by the electrolytic material conductivity and they increase as the relative humidity (pore saturation) increases (Alonso et al., 1988). Chlorides (0.4 – 1.0 % by mass of cement) also influence the corrosion rates in carbonated mortar (Glass et al., 1991). High levels of industrial pollutants with the presence of chloride ions can accelerate corrosion of the reinforcement. For instance, in the Arabian Gulf region, many concrete structures deteriorated within a short period of time after the end of construction. The investigation carried out found that the main cause of the deterioration was corrosion of the reinforcing steel. The primary reason for corrosion of the reinforcement was due to a combination of the presence of chloride ions and the industrial pollutants (Kumar, 1998). Furthermore, it was found that, the corrosion rate of the reinforcing steel in concrete

contaminated with a combination of chloride ions and carbonation could be 5 to 20 times higher than the corrosion rate in concrete contaminated with chloride only (Yokota et al., 2005).

This enhancement in the corrosion rates of steel bar embedded in carbonated concrete could be due partly to a release of bound chloride ions in the concrete pore solution. Experimentally, the release of aggressive substances such as chloride and sulphate ions in the pore solution was confirmed by Anstice et al., (2005). In their study cement pastes were exposed for 30 min each day to various concentrations of CO_2; 100 %, 5 % (plus 21 % oxygen and 74 % nitrogen) and air. It was found that chloride and sulphate ions in the extracted pore solution were released and the concentration of these substances increased as the degree of carbonation increased as shown in Figure 2-8. The release of chloride ions was attributed to the decomposition of bound chloride from calcium chloro-aluminate hydrates according to the following equation;

$$3CaO.Al_2O_3.CaCl_2.10H_2O + 3CO_2 + 3H_2O = 3CaCO_3 + 2Al(OH)_3 + CaCl_2 + 10H_2O \quad [2.12]$$

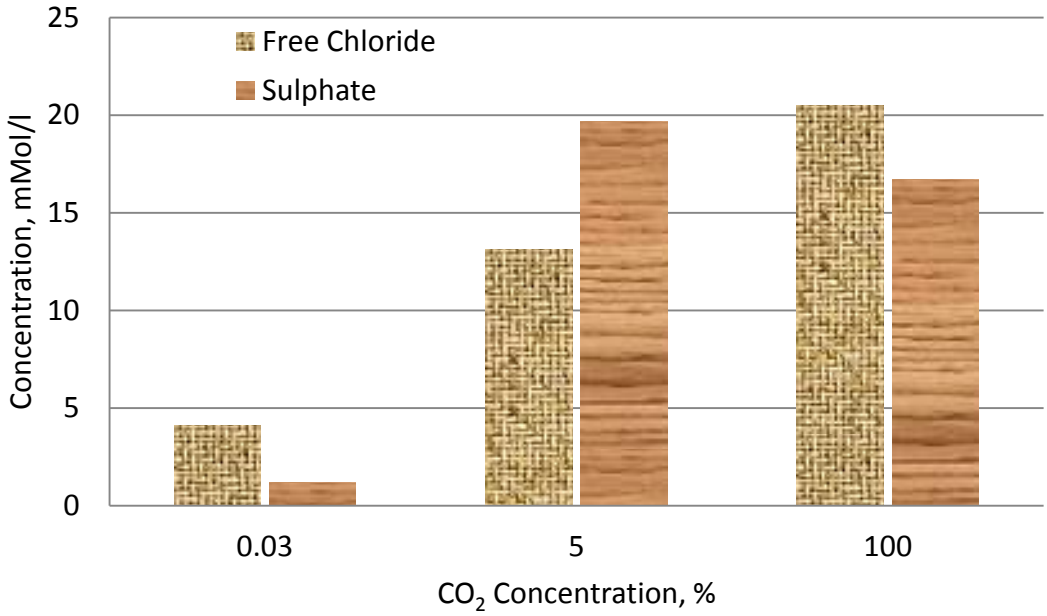

Figure 2-8 Concentration of chloride and sulphate ions found in the pore solution extracted from cement paste speciemns exposed to various levels of carbon dioxide after (Anstice et al., 2005)

Inadequate compaction, poor curing and failure to achieve the minimum specified concrete cover to the steel reinforcing bar are the most common problems that enhance carbonation-induced corrosion of reinforcement (Page, 1998). Three main parameters have been found to have an effect on the carbonation rate. These are the permeability of concrete, the total alkali content of the hydration products and the level of moisture in the concrete. Good quality concrete will result in low permeability and hence the rate of penetration of CO_2 is reduced. Carbonation rate is a function of relative humidity (RH). With low relative humidity, the penetration of the carbon dioxide is high. In practice, the pores are partly filled with water that allows the penetration of CO_2. At the same time, the reaction rate of $Ca(OH)_2$ with CO_2 is also high. Therefore, in the relative humidity range of 50 % - 75 %, the carbonation rate of concrete is most rapid, as shown in Figure 2-9, and thus, carbonation reaches the reinforcing steel faster (Richardson, 2002). This is verified in a study performed by Houst and Wittmann

(2002) where the depth of carbonation in mortar exposed to outdoors, one face was exposed directly to rain and the other face was sheltered, was found higher in the sheltered face than that in the exposed face because pores in the exposed face were blocked by rainwater. The carbonation depth in both faces of mortars made with different water to cement ratios and exposed to outdoors is illustrated in Figure 2-10.

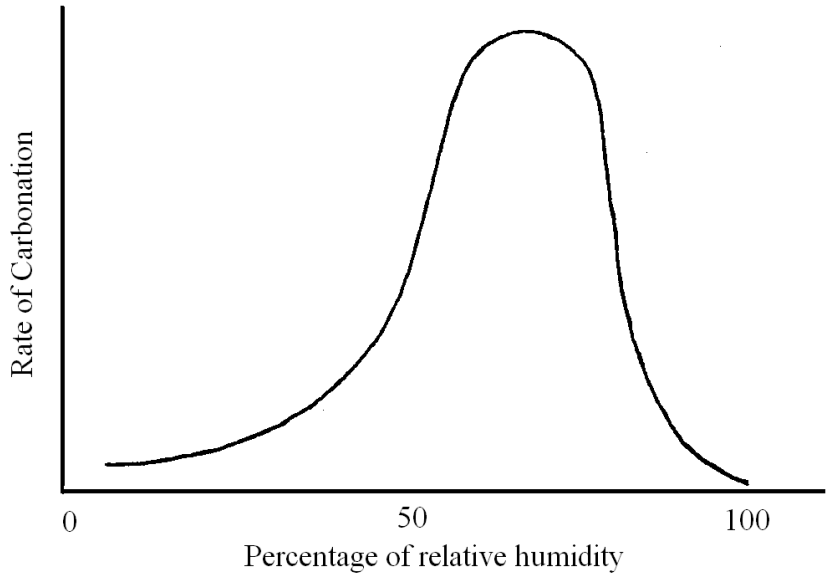

Figure 2-9 The effect of relative humidity on the carbonation rate of concrete

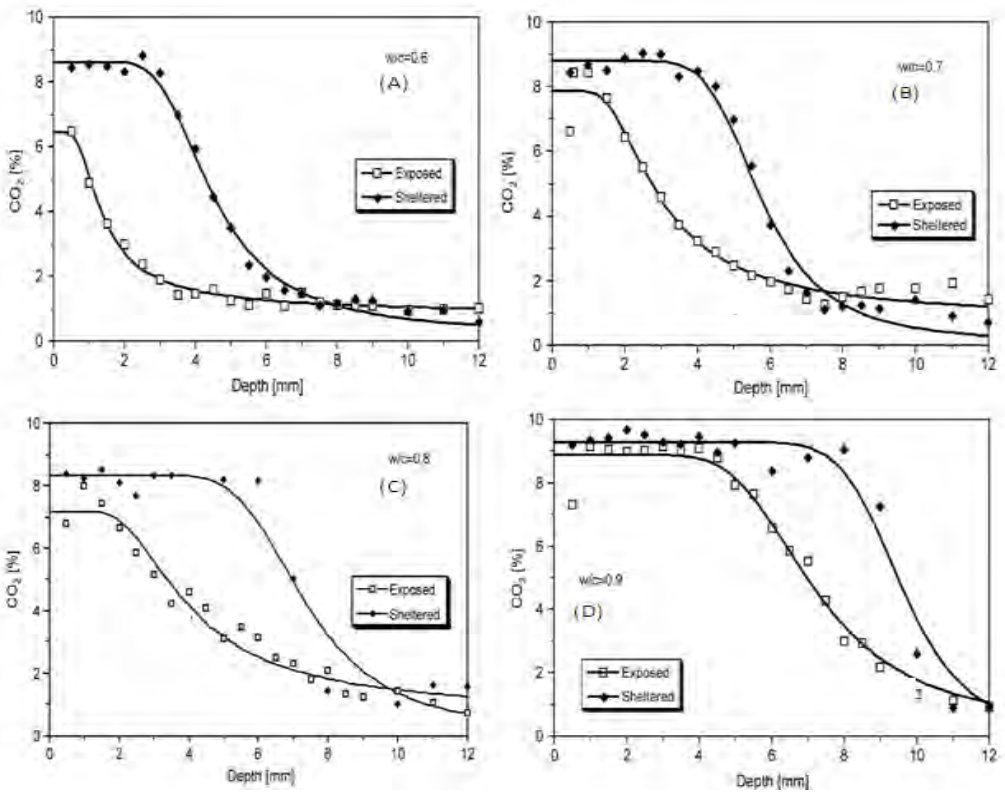

Figure 2-10 Carbonation profiles for mortars made of various w/c ratios: (A) 0.6, (B) 0.7, (C) 0.8 and (D) 0.9 and exposed to outdoors for 40.5 months after (Houst and Wittmann, 2002)

Furthermore, wet/dry cycling may enhance the carbonation process. When concrete is dry, carbon dioxide gas penetrates into concrete pores. Then, during wet cycles, the carbon dioxide dissolves in the water and leads to carbonation problems. Semi-dry and wet cycles are the most significant factor in carbonation induced corrosion (Hansson et al., 2007).

The rate of carbonation front penetration reduces with time. This could be attributed to three factors. First, carbon dioxide has to go further through the concrete. Secondly, continuous hydration of the concrete leads to more impermeable concrete. Finally, the carbonation may lead to precipitation of the carbonate in the existing pores and also, the carbonation reaction

releases water that may result in a wetter concrete internally than near surface and further hydration and hence more impermeable concrete (Hansson et al., 2007).

The carbonation of concrete is not like chloride–induced corrosion, general corrosion occurs rather than localized corrosion. The corrosion products will generate stresses in the concrete cover causing cracking before rust staining appears on surface of the concrete

2.1.4.2.1 Cover thickness and quality of concrete

The thickness and quality of concrete cover are very important factors in control of carbonation-induced corrosion. The carbonation rate increases when a poor quality of concrete is used. This concrete quality will lead to a structure with open pores. The diffusion of carbon dioxide will then be rapid since these open pores are well connected together. The most vulnerable area to carbonation attack is the corner of the structure. This is because a great surface area is exposed and hence, carbon dioxide can diffuse from both sides (Broomfield, 2007).

A good quality control is required and it is very important to ensure the required concrete cover depth is achieved. This is because a reduction in the expected time required for carbonation to reach the steel reinforcing bar of approximately 36 % when 20 % of the minimum specified cover is not achieved (Page, 2007). In practice, the latter is true and a survey carried out by Clark et al., (1997) showed that the 5 mm tolerance that should have been applied to nominal cover according to former standards i.e. BS 8110-Part 1 (1985) was commonly not achieved indicating poor quality control. The recommended allowance in

design for cover deviation has therefore been raised to 10 mm according to BS EN 1992-1-1 (2004) standard.

2.1.4.2.2 Depth of carbonation

For carbonation of concrete exposed to a constant atmosphere the rate of movement of the carbonation front can be modelled using Fick's first law of diffusion. From this, the carbonation depth (x) can be shown to have a parabolic relationship with the exposure time (t);

$$x = \left(\frac{2D(C_1 - C_2)}{a}\right)^{1/2} t^{1/2} = K\, t^{1/2} \qquad [2.13]$$

This equation was derived by Kropp (1995) where,

D is the constant diffusion coefficient and depends on porosity, pore size distribution, tortuosity and pore continuity, saturation degree, relative humidity and temperature;

C_1-C_2 is the concentration difference of CO_2 between the external surface (C_1) and the carbonation front (C_2) and depends on the concentration of CO_2 in the atmosphere;

a is the alkaline component and depends on the cement content and content of CaO in the binder;

t is exposure time;

K is carbonation coefficient.

The carbonation depth is simply estimated by spraying phenolphthalein (RILEM Committee, 1988). The colour will change from pink to colourless, around a pH value of 10, indicating

carbonated concrete in a freshly exposed concrete. It is important to know that, the carbonation coefficient (K) depends on the above parameters, D, (C_1-C_2) and a. In fact these parameters are related directly to the quality of concrete and to the condition of environment (Page and Treadaway, 1982). This form of relationship

$$x = K\,t^{1/2} \qquad [2.14]$$

is simple and provides a useful method to predict the depth of carbonation after an exposure period of time, (t). However, this equation cannot be expected to apply accurately in environments such as those of high relative humidity environments and wet/dry cycling for long time periods (Page, 2007).

2.1.4.3 Corrosion of steel reinforcing bar in concrete due to chloride penetration

2.1.4.3.1 Penetration process of chloride into concrete

Recently, the most serious cause of corrosion of reinforcing steel in concrete is the presence of chloride ions in the concrete. Chlorides can diffuse into concrete from the external environment when concrete structures are exposed to sea salt spray, direct sea water wetting and/or saline ground waters. The use of road-deicing salts is another significant source of chloride ions which caused a serious problem on bridge decks (Domone, 2010). In the United Kingdom, the main sources of chloride ions are from external sources and mainly from de-icing and seawater (BRE Digest 444, 2000). The ingress of chloride will be accelerated in the case of chloride-containing water, such as deicing salt water. This could result in a deep

chloride profile, as shown in Figure 2-11 , particularly in the area just above ground level i.e. 0.25 m, which is in direct contact with deicing salt water (Hunkeler, 2005). This chloride ingress can be accelerated by wetting and drying cycles of the concrete which in fact results in a greater depth chloride profile due to the building up of chlorides on the surface of the concrete.

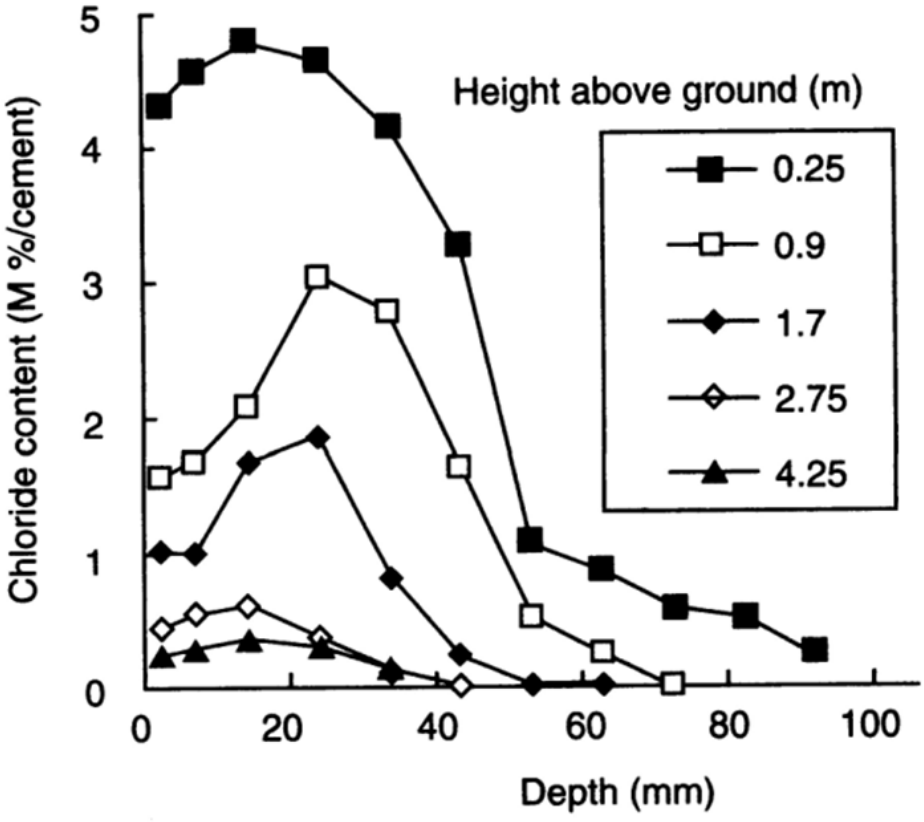

Figure 2-11 Chloride profiles of a backwall of a gallery for the traffic, exposed to deicing salt water after (Hunkeler, 2005)

Chloride induced corrosion is not like carbonation. The carbonation in concrete will proceed only when the pores are not completely filled with water. On the other hand, chloride ions are nearly unable to diffuse when the concrete is dry. Diffusion of ions takes place only in water. Initially, chloride ions can penetrate into concrete, when concrete is dry, by capillary suction

and then by a true diffusion process where chloride will diffuse further because of the differences in chloride concentration in the concrete. In a situation where the concrete structure is totally submerged the chloride ion movement is very slow and controlled purely by diffusion. Figure 2-12 shows the absorption and diffusion zone in the concrete structures. In fact, chloride penetration into concrete is a complex process. For instance, chloride ions are negatively charged and when the concrete is partly or fully saturated, the movement of chloride ions is affected by other ions' movement. Also, some of the penetrated chloride ions will react with, and turn into bound chloride either chemically or physically (Page, 2007).

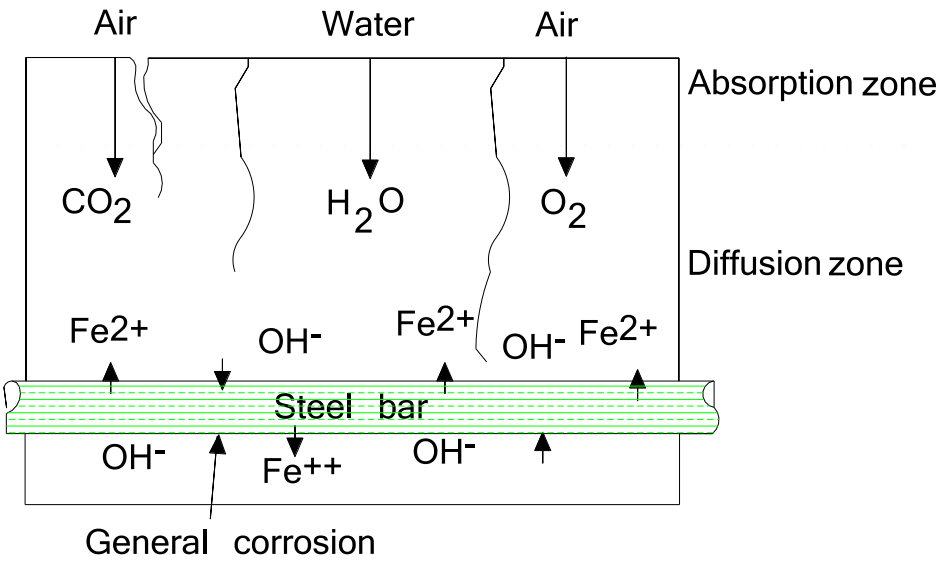

Figure 2-12 Shows the diffusion and absorption zone in the concrete structure

2.1.4.3.2 Presence of chloride ions in concrete

The chloride ions can be presented in concrete structures in two forms. There are many sources that lead to chloride contaminated concrete after the construction. The use of an accelerator such as calcium chloride is an example. The use of calcium chloride was

permitted until the mid-1970s. It was used in concrete as an accelerator with levels up to 1.5 % $CaCl_2$ by weight of cement. Other sources could be the use of seawater as mixing water and the use of contaminated aggregates. In the United Kingdom the risk of the corrosion due to chloride cast into the concrete, as a result of using admixtures and contaminated aggregates in the concrete mix, is now very low because of the limitation on chloride in mix materials (BRE Digest 444, 2000, Page, 2007). Also, some of the original mixed chloride will be bound. Some of the bound chlorides, however, will be released again when the pH value is further reduced due to the carbonation of the concrete (Anstice et al., 2005) and these chloride ions becoming free result in a more aggressive pore solution.

In the second form, where chlorides are allowed to penetrate from the external environment, it has been suggested that the free chloride ions found in concrete that is exposed to aggressive marine environments were high compared to those concretes where the chloride was introduced in the time of mixing (Page and Treadaway, 1982). These free chloride ions that are available in the pore solution are assumed to be the only chloride ions, and not the bound chloride, that take part in the corrosion reaction (Hussain et al., 1995). Furthermore, the concrete electrical conductivity, which is a characteristic of ion concentration, increases in the presence of chlorides (Hunkeler, 2005) consequently facilitating the flow of the corrosion current to anodic and cathodic sites giving higher corrosion rates (Goñi and Andrade, 1990, Gowers and Millard, 1999).

2.1.4.3.3 Pitting corrosion mechanism

When sufficient concentration of chloride ions reach reinforcing steel this will lead to a localized breakdown of passive film. A localized corrosion will result in intensive loss of cross sectional area of the metal before any evidence of significant damage to the concrete cover such as spalling or cracking. Some conditions must be achieved for localized corrosion to happen. These involve local breakdown of the passive layer, low concrete resistivity, and with contact of a conducting environment e.g. water or soil, ingress of chloride ions continues to the anodic site and therefore, reduction in pH, and availability of oxygen to support a high localized corrosion rate (Wilkins and Sharp, 1990).

A tentative explanation of the mechanism of the localized corrosion process is as follows. In case of local breakdown of the passive film, this area will act as anode whereas the intact film sites will act as a cathode. The oxidized iron reacts with chloride ions absorbed in the oxide layer and soluble iron complexes are formed at the anode site. In the presence of moisture, the iron complex reacts to form $Fe(OH)_2$. As a result of the reaction, more chlorides are generated and a reduction of pH occurs. When chloride is released on the metal surface, the process become self-generating. No further chloride is required. Further formation of $Fe(OH)_2$ and the release of H^+ and Cl^- due to the repetition of the reaction of Fe^{+2} with Cl^- ions occur. Consequently this produces a more acidic environment and destroys the oxide layer that then leads to pit formation (Ahmad, 2006). Figure 2-13 shows the pitting formation process and the composition of the electrolyte inside the pit (Page and Havdahl, 1985). Unlike carbonation, there is no overall drop in pH. The chloride ions act as a catalyst to corrosion but are not consumed in the process (Currie and Robery, 1994).

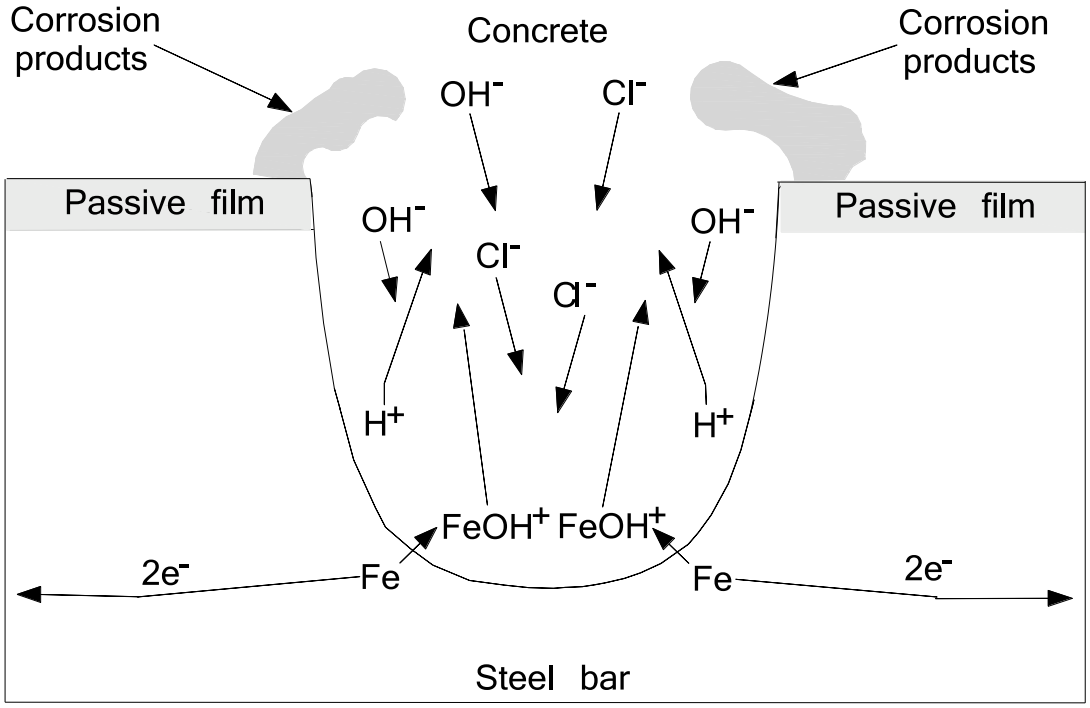

Figure 2-13 Illustration of the composition of electrolyte during the pit formation

When steel potential in the anodic area exceeds a critical value called the "pitting potential", the current density will increase sharply indicating pitting corrosion initiation. The value of "pitting potential" at a given temperature depends mainly on the concentration of chloride and on the electrolyte pH value (Page, 2007). The significance of the corrosion process increases as the $[Cl^-]/[OH^-]$ concentration increases near the steel bar surface (Lambert et al., 1991, Page et al., 1991). At a given level of chloride contamination, the risk of pitting corrosion of steel reinforcing bar embedded in concrete had been found to be affected by environmental conditions such as the availability of oxygen and ambient temperature and several material variables such as the condition of the steel bar surface and the presence of voids at the steel-concrete interface (Page and Treadaway, 1982). Moreover, the localized corrosion process can be extremely accelerated especially when the cathode area is bigger than anode area (Wilkins and Sharp, 1990). This is due to a large corrosion current developed by potential

differences between anodes and cathodes. As a result, an intensive corrosion rate occurs leading to faster deterioration rather than that occurring with general corrosion due to carbonation.

2.1.4.3.4 Effect of the combination of some aggressive substances on corrosion processes

Another ion that increases the aggressivity of the electrolyte and augments the risk of corrosion is the sulfate ion (Al-Tayyib and Shamim Khan, 1991). The situation will be made worse in the presence of chloride ions (Holden et al., 1983). Work carried out by (Al-Amoudi and Maslehuddin, 1993, Al-Amoudi et al., 1994, Dehwah et al., 2002) to study the effect of sulfate ions on the corrosion behaviour of steel bar showed that the corrosion rates of steel bar embedded in concrete specimens and subjected to a mixed solution of sodium chloride and sodium sulfate were higher compared with those steel bars embedded in concrete and exposed to sodium chloride solution only. This increase in the corrosion magnitude of the steel bar embedded in concrete and exposed to sodium chloride plus sodium sulfate was ascribed to the reduction in the cement binding capacity of chloride and in the concrete electrical resistivity (Dehwah et al., 2002). It was observed that the amount of free chloride ions, in the combined presence of both chloride and sulfate ions, was high compared to that of cement containing only chloride. This effect was attributed to the preferential reaction of tricalcium aluminate (C_3A) with sulfate ions and as a result hindering chloride binding reaction with C_3A and formation of calcium chloro-aluminate hydrate (Friedel's salt) (Holden et al., 1983).

It is believed that the exposure of concrete substructures to a medium containing a combination of aggressive species, such as sulfate-chloride-bearing soils and groundwater, is

the typical situation that leads to an increase in the density of the corrosion current in reinforced concrete in the Arabian Gulf (Al-Amoudi et al., 1994).

2.1.4.4 Cracking of concrete

Presence of cracks in the concrete will accelerate the corrosion process of the steel reinforcing bar. It will allow access (direct path) to the aggressive agents such as Cl^-, SO_4^{-2}, and other corrosion agents (fuel) oxygen and moisture. The corrosion rate of steel bar under cracks will be significantly influenced by the crack width and the quality of the concrete cover between the cracks (Bakker, 1988). In the case of carbonation only, the initiation of localized corrosion may occur under the cracked area as shown in Figure 2-14.

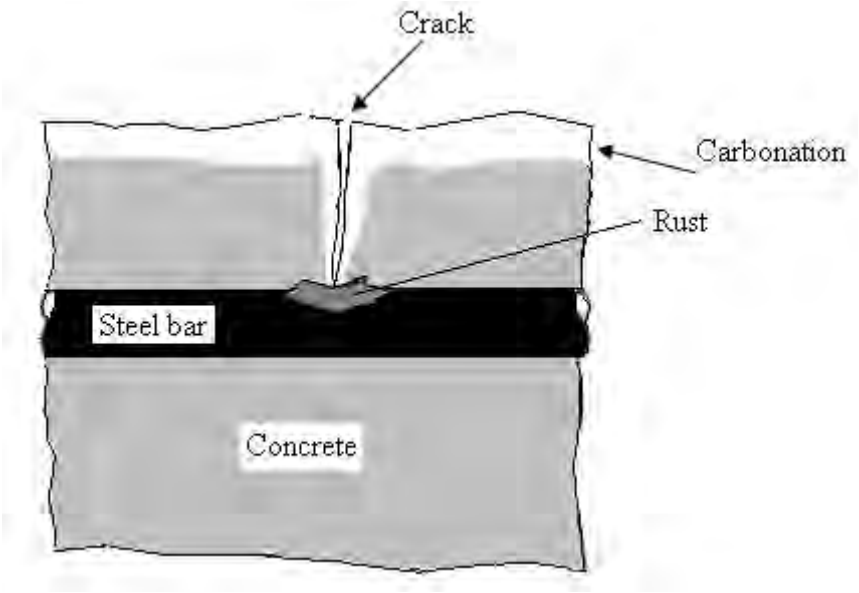

Figure 2-14 Initiation of localized corrosion in the carbonated cracked concrete

The cracks can be generated in concrete due to chemical reactions e.g. alkali aggregate reaction, shrinkage, freezing and thawing cycles, corrosion of steel bar and mechanical loading. When the tensile load exceeds the reinforcement tensile strength, cracks will also be initiated. These cracks considered to be small (<0.5 mm) will be transverse to the reinforcing steel. Some of these cracks will be self-healed and hence, reduce the diffusion rate of corrosive agents. However, the presence of wider cracks i.e. macro-cracks with widths of 0.5 mm or greater, will accelerate the corrosion process. Development of large cracks could be as a result of plastic shrinkage , thermal expansion, settlement or impact damage, etc. (Broomfield, 2007).

A study done by Suzuki et al. (1990) found that large cracks led to more active corrosion compared to minor cracks. This is attributed to a higher concentration of Cl^-, decrease of pH value and a higher depletion of oxygen. A short-accelerated and long-term exposure corrosion test of steel embedded in cracked concrete were carried out by Mohammed et al. (2003) and revealed that, the steel under cracked area acts as an anode and that other areas act as a cathode. Furthermore, the corrosion rate was found to be high under the cracked area compared to uncracked areas. This was attributed to a direct supply of aggressive agents and corrosion fuel through the crack "direct path" as illustrated in Figure 2-15. Some of the narrow cracks healed due to formation of ettringite, calcite and brucite in the crack. Therefore, the ingress of the aggressive agents was obstructed resulting a significantly reduced corrosion rate. It is suggested, however, that the crack frequency, concrete quality and cover depth are more important factors influencing the corrosion of steel reinforcing bar than crack width (BRE Digest 444, 2000).

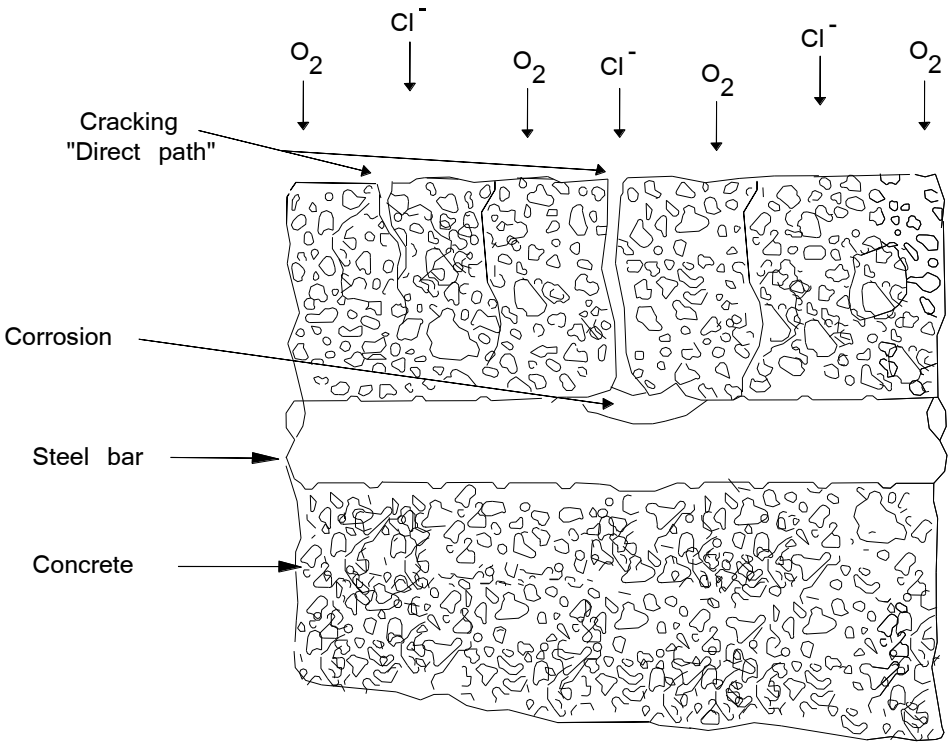

Figure 2-15 Shows the direct path of chloride ions in cracked concrete

2.1.5 Factors affecting corrosion of steel reinforcing bar embedded in concrete

2.1.5.1 External factors that affect corrosion of steel reinforcing bar

Most of the external factors that affect the corrosion progress of steel reinforcing bar embedded in concrete are attributed to environmental parameters. The presence of oxygen and the moisture content in concrete are necessary for the corrosion process to proceed. The degree of permeability of concrete will affect the oxygen diffusion rate. More permeable concrete will lead to the easy access of oxygen. Another dominant factor influencing oxygen diffusion in concrete is the moisture content of the concrete. The diffusion rate of oxygen is very low when the moisture content of the concrete is high. This is because of oxygen

diffuses more rapidly through pores that are filled by air (Hunkeler, 2005). Furthermore, the moisture content of concrete is a very important factor that determines the resistivity of concrete which in fact affects the corrosion behaviour of reinforcement.

When the pores in the concrete are completely filled by water, the ions can be transported easily whereas the mobility of gases is reduced. Increases in relative humidity within the range 80-100 % will decrease the carbonation of concrete. Diffusion of some acidic gases, for instance SO_2, rather than carbon dioxide will decrease the alkalinity of the concrete. Specific reduction of the pH value results in corrosion initiation of reinforcing steel, loss of passivity and hence catastrophic reinforcement corrosion (Ahmed, 2003). Besides that, a rise in exposure temperature may result in increase in the corrosion rate of the steel reinforcing bar as discussed in Chapter 6 part A.

The environment surrounding structures has an effect on the corrosion of the reinforcing steel. Structures in splash zones and areas that are subject to wet and dry cycles, will show more aggressive ions diffusion and hence, enhanced corrosion processes (Wilkins and Sharp, 1990).

2.1.5.2 Internal factors that affect corrosion of steel reinforcing bar

The internal factors affecting corrosion of reinforcing steel embedded in concrete are a combination of concrete and steel quality. A good quality concrete can be made by using a proper cement composition which will provide protection to the steel reinforcing bar against corrosion process by keeping a high alkaline environment around the steel surface, pH 11.5-14 (Page, 2007) as a result of the presence of $Ca(OH)_2$ and other alkaline compounds formed

in the hydration process of the cement. Another means of steel protection in concrete is by binding a considerable amount of chloride ions, either chemically or physically, due to the reaction with the C_3A and C_4AF content of the cement in the concrete. A more serious corrosion problem can occur by using contaminated aggregates, contaminated mixing and curing water and concrete admixtures that contain a reasonable portion of chloride leads to a rise in the level of chloride in the concrete and hence increased corrosion rates (Page, 2007). The permeability of the concrete is the factor most influencing the penetration of chloride ions and carbonation depth. The permeability of the concrete is a function of the water to cement ratio. The use of mineral admixtures in concrete is commonly used to improve the concretes' durability parameters such as impermeability (Bamforth, 2004).

In general, increases of water to cement ratio leads to an increase of the oxygen diffusion coefficient and reduces the carbonation resistance. The rate of carbonation has been found to be increased linearly as the w/c ratio increases (Ho and Lewis, 1987). High cement content results in a high binding capacity, and also increases the quantity of impermeable cement pastes and thus more durable concrete. To obtain a good quality concrete, the water to cement ratio should be maintained between 0.35 to 0.45. Also, a very dense concrete can be produced by using a low water to cement ratio, i.e. considerably less than 0.4, which will have a very low capillary porosity (Turkmen et al., 2008). In practice, the recommended water to cement ratio should be selected carefully depending on the class of exposure and the designed service life (BS 8500-1, 2006).

The use of adequate cement content has a significant effect on concrete strength and subsequently concrete durability. On the other hand, surface defects and honeycombs can be

formed due to the use of inadequate cement content in concrete mixes without proper consolidation. The penetration and diffusion of some aggressive substances may be enhanced in the presence of such defects and then create a suitable environment to initiate corrosion. A minimum of 340-380 kg of cement in a cubic meter of concrete is recommended for reinforced concrete structures exposed to a marine environment (BS 8500-1, 2006). Aggregate size and grading should be taken into account to produce a good quality impermeable concrete. In practice, a number of issues during the construction stage should be considered to avoid serious problems which may occur in the future. These involve washing aggregates to remove contaminating materials, avoiding the use of contaminated ingredients of concrete, sticking to recommended levels of water to cement ratio, cement content, cover thickness, etc., insuring proper compaction of freshly placed concrete and proper curing systems (Ahmed, 2003).

Concrete cover is another important factor that has a significant effect on corrosion of steel reinforcing bar in concrete due to chloride and carbonation penetration. A good cover is one of the first requirements to produce a highly durable concrete. A good concrete cover should be designed depending on the exposure environment and the intended designing life (BS 8500-1, 2006). The advantages of a low water to cement ratio and good concrete cover are to increase the time for chloride ions and carbonation of the concrete to reach the reinforcing steel and thuse increasing the time to initiate corrosion of reinforcement.

2.2 BAG HOUSE DUST AS CONCRETE ADDITIVE

Bag house dust (BHD) material, generated by one of Saudi Basic Industries Corporation (SABIC) plants, was utilized in this entire research. Details about BHD production and the

chemical composition of BHD are presented in the next sections. The retardation effect of incorporating EAFD in concrete is reviewed followed by an explanation of the possible retardation mechanism.

2.2.1 Production of BHD

During the steel making process, a number of dusts are generated including electric arc furnace dust (EAFD). EAFD is defined as "a very fine powder forming a major part of the smoke or fume from the furnace". These fumes are passed through cooling pipes and then filtered by specially designed bag filters. The collected dust is named as Bag House Dust (BHD). Therefore, the BHD is a by-product of Electric Arc Furnace steel making process. Up to 2003, the total estimated quantity of the BHD that was produced at steel making plants was more than 200,000 tons in Saudi Arabia. Recently, the annual rate has increased by 25,000 tons. Since the BHD is a waste by-product material, proper disposal is important as the disposal of such material is costly. For instance, the yearly cost of BHD disposal was estimated at around Saudi Riyals (SR) 5,000,000 (Al-yami et al., 2003). Therefore, the use of BHD in the concrete industry is a most effective way of BHD disposal to eliminate the environmental pollution, storage and handling problems (Al-Zaid et al., 1997).

2.2.2 Chemical composition of BHD

There are a number of factors that lead to a considerable variation in the chemical composition of the BHD. For instance, BHD sources could differ from one plant to another and from one melt to another, and also, type and amount of scrap material used in the electric arc furnace. To determine the BHD chemical composition, four different samples were

collected and analysed by the supplier. The oxides of Fe, Zn, Ca, Na, Si, Mg, Mn, K and Pb were found to be the main constituents of the BHD. BHD contains heavy metals such as Zn and Pb and therefore, it is classified as a hazardous material according to the European Waste Catalogue (EWC, 2002). The analysis of the BHD samples and their average are presented in Table 2-1, as received from the supplier. Note that, the received BHD for use in this research was analyzed by X-ray fluorescence technique for confirmation purposes and the analysis is presented in Chapter 3.

Table 2-1 Typical chemical composition of BHD (Al-Sugair et al., 1996)

	Analysis, % by mass				
Element	A	B	C	D	Average
Aluminium (Al)	0.71	0.66	0.69	0.74	0.7
Calcium (Ca)	9.41	9.28	9.3	9.56	9.34
Cadmium (Cd)	0.0004	0.0004	0.0004	0.0004	0.0004
Copper (Cu)	0.06	0.06	0.06	0.06	0.06
Iron (Fe)	33.5	33.3	33.7	33.9	33.6
Potassium (K)	1.73	1.6	1.68	1.77	1.7
Magnesium (Mg)	2.28	2.27	2.29	2.35	2.3
Manganese (Mn)	1.80	1.79	1.8	1.82	1.8
Sodium (Na)	2.48	2.63	2.62	2.54	2.57
Nickel (Ni)	0.01	0.01	0.01	0.01	0.01
Lead (Pb)	1.3	1.32	1.3	1.3	1.31
Phosphorus (P)	0.13	0.14	0.10	0.14	0.13
Silicon (Si)	2.43	2.34	2.32	2.41	2.38
Tin (Sn)	0.03	0.03	0.03	0.03	0.03
Sulfur (S)	0.59	0.58	0.56	0.56	0.57
Titanium (Ti)	0.09	0.08	0.08	0.09	0.09
Zinc (Zn)	10.7	10.8	10.7	10.7	10.7

2.2.3 Physical properties of BHD

The bulk density of the analysed BHD is 764.8 kg/m^3. The sieve analysis of BHD indicates that the BHD is a very fine material, 98 % of the BHD passed sieve no. 50 which has a diameter of 300 micrometer. Table 2-2 shows the sieve analysis of the BHD (Al-Sugair et al.,

1996). However, the analysis of the used BHD material in this research show that the laser diffraction measurements indicated that over 60% of the particles were smaller than 5 μm and the specific surface area of the BHD was found by nitrogen adsorption analysis (BET) to be 660 m^2/kg.

Table 2-2 Sieve analysis of BHD

Sieve Seize no.	Diameters, mm	% Passing
4	4.76	100
8	2.38	100
16	1.19	99.9
30	.595	99.7
50	0.297	98.7
100	0.149	96.4
200	0.074	9.0

2.2.4 Retardation effect of EAFD

The main drawback of using BHD material in concrete is its retardation effect. A comparative study between BHD concretes and Conplast RP 264 concretes was conducted by Al-Zaid et al. (1999). The Conplast RP 264 admixture is used as a retarder in the local market. The dosage of Conplast RP 264 used in their study was 0.6 litres per 100 kg of cement. It was concluded that the addition 2 % of BHD can be used as an efficient concrete set retarder. The BHD satisfied both British standard, BS 5075 Part 1 and US standard, ASTM C494 Type D to be classified as a set retarder (Al-Zaid et al., 1997). This increase of setting time in the BHD-concrete was attributed to the presence of zinc in the BHD (Al-Sugair et al., 1996).

Several studies utilizing EAFD revealed the same effect on setting times (Balderas et al., 2001, Castellote et al., 2004). Also de Vargas et al. (2006) found the addition of 5, 15 and 25

% EAFD in cement pastes delayed the initial and final setting times of the cement. A recent study conducted by Maslehuddin et al. (2011) verified that a replacement of only 2 % of cement by BHD resulted in an increase in both setting times. The corresponding initial and final setting times for control mix were 3hr:50min and 5hr:22min and for BHD concrete are 17hr:50min and 25hr:57min, respectively.

2.2.5 Retardation mechanism of EAFD

The presence of $Ca(OH)_2$ is evidence of the hydration process occurring since portlandite is one of the main cement hydration products. Work carried out studying the evolution of $Ca(OH)_2$ from a sample containing 10 % zinc metal waste by using DTA analysis showed that no formation of $Ca(OH)_2$ existed when the samples were hydrated for 28 days. Even after 90 days hydration the approximate $Ca(OH)_2$ detected was only 5 % (Asavapisit et al., 1997). The analysis of mortars containing EAFD was performed by Castellote et al., (2004) using X-ray diffraction. The $Ca(OH)_2$ peaks were less intensive in EAFD-mortar compared to mortars without EAFD. The results of de Vargas et al., (2006) confirmed the Castellote et al., (2004) finding. Also, from the de Vargas et al., (2006) study, the peaks of $Ca(OH)_2$ decreased as EAFD addition increased indicating the suppression of the cement hydration process.

Bag house dust (BHD) contains zinc ions and previous studies have found that the use of by-products that contain zinc and lead compounds can cause retardation in the setting time of hardened concrete (Arliguie et al., 1982, Brehm et al., 2004, Gervais and Ouki, 2000, Hooper et al., 2002, Lieber, 1968, Monosi et al., 2001, Morrison et al., 2003, Thomas et al., 1981, Weeks et al., 2008). It was found in a study of the retardation of cement by ZnO that ZnO

had a specific influence only on the hydration of the C_3S phase and depends on the specific surface area and on the C_3S content of the cement (Lieber, 1968).

Although numerous investigations have been carried out to understand and explain why the zinc hinders the cement hydration process, there is still disagreement about whether the process of cement hydration is inhibited because of the formation of zinc hydroxide which acts as a amorphous layer around cement grains or because of the consumption of calcium and hydroxide ions due to the formation of insoluble calcium hydroxy-zincate. According to Arliguie and Grandet (1990), Asavapisit et al., (1997) and (2005), Arliguie et al., (1982) and Lieber (1968) who investigated the cause of the retardation of cements containing zinc, the retardation is caused by the formation of an amorphous layer around the cement grains which acts as a coating that prevents/controls cement hydration, although in their studies there was no direct evidence of such a layer. The amorphous layer is believed to be in the form of a zinc hydroxide ($Zn(OH)_2$) compound. This layer is described as a very low permeability membrane (Asavapisit et al., 1997). It was suggested that, in the presence of high a concentration of free calcium and hydroxyl ions in the pore solution, the cement hydration will restart only after the transformation of formed zinc hydroxide to calcium hydroxy-zincate ($CaZn_2(OH)_6 \cdot 2H_2O$) has been started (Arliguie and Grandet, 1990).

Another hypothesis on the reason why the hydration process is obstructed in the presence of zinc is due the consumption of calcium and hydroxide ions due to the formation of insoluble calcium hydroxy-zincate and not because of the formation of an impermeable film around grains as discussed above. Peaks of calcium hydroxy-zincate were detected by Hamilton and Sammes (1999) and Castellote et al., (2004) in hardened cement pastes and mortars.

Dissolution of additional calcium ions in the solution will encourage the reaction of zinc oxide found in EAFD with hydration reaction products, mainly calcium hydroxide, to form calcium hydroxy-zincate (Castellote et al., 2004) according to this equation

$$2ZnO + Ca(OH)_2 + 4H_2O \rightarrow CaZn_2(OH)_6 \cdot 2H_2O \quad [2.15]$$

A research done recently by Weeks et al. (2008) to investigate the cause of the retardation of cement when it contains zinc using X-ray diffraction analysis showed no microstructural evidence of the formation of coatings around cement grains. Furthermore, it has been suggested by Weeks et al., (2008) that the retardation of setting time could be due to the formation of calcium-hydroxy-zincate rather than the formation of the gelatinous surface layer on cement grains. The initial consumption of calcium and hydroxide ions from the solution, by zinc to form calcium-hydroxy-zincate, delays the calcium hydroxide precipitation and development of calcium-silicate-hydrate gel.

2.2.6 Effect of EAFD on corrosion of reinforcement

Very limited research has been performed to investigate the effect of EAFD addition on corrosion of reinforcement embedded in concrete contaminated with EAFD (Al-Mutlaq and Chaudhary, 2007, Al-Sugair et al., 1996, Chaudhary et al., 2003, Maslehuddin et al., 2011). Based on the existing studies, the results show that improvement in the corrosion resistance of steel bars embedded in BHD-concrete compared to those bars embedded in plain concrete. Further discussion related to the role of EAFD on the corrosion process was discussed in more details in Chapter 4.

It can be seen from the research cited in section 2.2.5 that, the retardation mechanism is not yet fully understood and further research is required. Therefore, an investigation was carried out in an attempt to gain a better understanding of the retardation mechanism and to evaluate the potential for counteracting the retardation effect when high levels of BHD is utilized in concrete. Another important aspect in durability, which are not yet widely investigated, needs to be studied is that the influence of BHD material on the corrosion process of the reinforcement embedded in concrete containing various levels of BHD. To achieve the main objectives of this research, various testing programmes were performed as presented in Table 2-3.

Table 2-3 Testing programmes summary

Chap. No.	Chapter title	Test methods	Parameters			Test period
			Spc. type and mix proportion*	Additives, %*	Source of Chloride	
4A	Effect on the corrosion behaviour of steel bar embedded in mortar	Bars embedded in mortars. The corrosion behaviour was monitored by corrosion potential and corrosion rates measurements.	Mortars made with a W:C:S ratio of 0.5:1.0:2.0	0 or 2 BHD	Internal chloride equivalent to 0, 0.4 and 2.0* %	Up to 171
4B	Effect on pore solution chemistry	In situ leaching method	Mortars made with a W:C:S ratio of 0.5:1.0:2.25	0 or 2 BHD	Internal chloride equivalent to 0, 0.4 and 2.0* %	Preconditioning period of 30 days and then pore solution extraction after periods of 3, 7, 21 and 60 days
5A	Influence on cement paste porosity	Bulk density and coarse capillary porosity measurements for thin discs	Cement pastes prepared at w/c ratio of 0.4, 0.5 and 0.6	0, 2 and 3 BHD	NA	Cured for 2 weeks at ambient temp. and then at 38 ºC in 35 mM NaOH for 5 and 10 weeks
5B	Influence on chloride diffusion process into concrete	Estimating chloride diffusion coefficients and determining the depth at which chloride concentration is critical	Concrete mixes were prepared at w/c ratio of 0.5 and 0.6 and designed at constant C:FA:CA ratio of 1:1.5:2.5	0, 2 and 3 BHD	Immersed in a sealed vessel containing a 2.82 M solution of NaCl	Cured for 63 days and then immersed in 2.82 M solution of NaCl for 98 days
6A	Influence on chloride threshold value	Exposing mortar containing steel bar to two NaCl solutions associated with two temperatures of 20°C and 40°C and then removal of 2 mm annulus of mortar surrounding the rebar when depassivation occurred	Mortars made with a W:C:S ratio of 0.5:1:2.1	0, 2, and 3.5 BHD	Immersed in a 0.25 M NaCl solution	Cured for 7 days at 20 ºC and then subjected to wet and dry cycles up to 321 days

Table 2-3 Testing programmes summary. Continue

6B	Influence on bleeding of concrete	Collection of the bleed water from the concrete surface	Concrete mixes prepared with constant W:C:FA:CA ratio of 0.5:1:1.5:2.5	0, 2, and 3.5 BHD	NA	The accumulated water was collected at 10 min intervals for the first 40 min and then at 30 min intervals until no bleeding water was observed
7A	Effect of BHD addition on compressive strength	Crushing of 100 mm cubes	- Concrete mixes prepared at W:C:FA:CA ratio of 0.5:1:1.5:2.5 - First cured for 14 days at ambient temp. and then at 60 ^{o}C until the time of testing	0, 2, and 3.5 BHD	NA	Tested at 3, 7, 28 and 60 days
7B	Influence on concrete-steel bond strength	Pull-out tests	Concrete mixtures prepared with constant W:C:FA:CA ratio of 0.5:1:1.5:2.5	0, 2 and 3.5 BHD	NA	Tested at 28 and 60 days
8	Effectiveness of chloride-free concrete accelerators on the characteristic properties of concrete	Compressive strength and UPV measurements and thermal analysis studies	Cement paste prepared at a constant water/cement ratio of 0.4	0 and 8 % BHD and 0 and 3.5 % calcium nitrite and calcium formate	NA	Tested at 3, 7 and 28 days
		Slump, compressive strength and UPV measurements	Concrete mixes were prepared with a W:C:FA:CA ratio of 0.4:1:1.2:2.2	0 and 8 % BHD and 0 and 3.5 % calcium nitrite and calcium formate	NA	Tested at 3, 7 and 28 days
		Setting times measurements using a Vicat apparatus	mortar	0 and 8 % BHD and 0 and 3.5 % calcium nitrite and calcium formate	NA	Up to 24 hours

Chapter 3

MATERIALS USED AND EXPERIMENTAL TECNIQUES

3.1 MATERIALS

3.1.1 Cement

Saudi ordinary Portland cement (OPC-Type I), manufactured by Saudi Cement Company, was used for all mixtures. The chemical analysis and physical properties of the Saudi OPC provided by the manufacture are given in Table 3-1.

3.1.2 Bag House Dust

Bag house dust (BHD) was used throughout this research as an additional material as per cent by weight of cement. The chemical composition of BHD analysed by X-ray fluorescence spectrometry (XRF) is given in Table 3-2. The obtained chemical composition of the BHD material used in this research differs than that presented in Table 2-1 and this could be due to the change in type of the scrape and in the collection date. The material safety data sheet for BHD material is presented in Appendix A.

3.1.3 Water

Distilled water was used to prepare all the cement paste specimens, mortars and concrete mixes. Before pore liquids were analysed, see section 3.4, the samples were diluted by 18 Mμ deionised water, produced by an Elga UHQ instrument.

Table 3-1 Chemical analysis and physical properties of Saudi OPC (Type I)

Constituents	Weight (%)
Silicon dioxide (SiO_2)	21.52
Aluminum oxide (Al_2O_3)	4.64
Ferric oxide (Fe_2O_3)	3.09
Calcium oxide (CaO)	65.31
Magnesium oxide (MgO)	1.59
Sulfur trioxide (SO_3)	2.25
Tricalcium silicate (C_3S)	60.3
Dicalcium silicate (C_2S)	16.2
Tricalcium aluminate (C_3A)	7.1
Tetracalcium aluminoferrite (C_4AF)	9.4
LOI	1.12
Fineness, cm^2/gm	3540

Table 3-2 Chemical analysis of BHD

Element	Average weight (%)
Aluminum (Al)	0.17
Calcium (Ca)	5.79
Iron (Fe)	29.44
Magnesium (Mg)	2.5
Manganese (Mn)	1.52
Lead (Pb)	1.8
Silicon (Si)	1.31
Zinc (Zn)	18.78
Potassium (K)	3.24
Sodium (Na)	0.88
Chloride (Cl)	2.25
Sulphur (S)	0.46
Phosphorus (P)	0.13
Copper (Cu)	0.13

3.1.4 Aggregate

The fine aggregate used in preparing all the concrete mixes was siliceous. For mortar specimens clean quartize sand supplied by Tarmac Roadstone Ltd. was used. The coarse aggregate that was used in all the concrete mixtures was siliceous rounded river gravel with a maximum size of 14 mm. The sieve analysis data of fine and coarse aggregate, used in this study are shown in Table 3-3 and Table 3-4, respectively. Sieve grading of the aggregates was performed according to (BS 812-103.1, 1985). The limits specified in (BS EN 12620:2002+A1:2008, 2002) are also presented in the same table.

3.1.5 Chemicals

Two non-chloride accelerators were used in this research, namely calcium nitrite (CN) and calcium formate (CF) to investigate their effect on compressive strength development of the concrete prepared with different levels of BHD. Calcium nitrite was supplied by Wintersun Chemical Group. It contains a minimum of 94 % calcium nitrite with a maximum of 4.5 % calcium nitrate. Calcium formate of analytical reagent grade with 98 % purity was supplied by Fisher Scientific.

Sodium chloride of analytical reagent grade with 99 % purity was supplied by Fisher Scientific.

Table 3-3 Fine aggregates sieve analysis

Sieve size	Passing (%)	Limits (F grading)
10 mm	100	-
5 mm	96	-
2.36 mm	85.2	80-100
1.18 mm	78.9	70-100
600 µm	70	55-100
300 µm	35.6	5-70
150 µm	14.1	-

Table 3-4 Coarse aggregates sieve analysis.

Sieve size	Passing (%)
50	-
37.5	-
20	-
14	100
10	76.5
5	9.61
2.36	1.44

3.2 MIXING PROCEDURE

3.2.1 Cement paste and mortar mixing procedure

Prior to mixing, all the required constituents were prepared and the mixing procedure was carried out according to ASTM C 305 (1999). First, the BHD was introduced by mixing the required proportion of BHD with the cement powder. The BHD and cement were placed in a container and manual dry mixing was performed, to ensure adequate dispersion of BHD particles in the mix. Thereafter, to produce mortar specimens sand was added and mixed thoroughly. When using non-chloride accelerators, they were introduced to the mixture by

dissolving the required proportions in the mixing water. Distilled water plus additives was then added and all constituents were mixed together for 4-5 minutes manually until a uniform consistency was achieved. The mix was cast in its own mould corresponding to each experiment. The casting process was carried out in two layers. Each layer was table vibrated lightly to remove air and minimize segregation. The top surface of the specimen with the air bubbles was removed by using a straight edge and more fresh mixture was added to fill the mould. The vibration process and filling with fresh mixture was repeated as necessary.

3.2.2 Concrete specimens mixing procedure

The required proportions of BHD material, water, fine aggregates and coarse aggregates were weighed for each mix. The BHD was added to the cement powder and then mixed (hand dry mixing) to ensure proper dispersion of BHD particles with the cement powder. Thereafter, fine and coarse aggregates were added and mixed thoroughly. Distilled water was then added and all constituents were mixed together for 4-5 minutes. When non-chloride concrete accelerators were used, additions of CF and CN were introduced into the mixture by dissolving weighed amounts in the mixing water (referred to in Chapter 8). For each experiment, the concrete mixes were then cast in their own appropriate moulds and compacted using a vibrator table (ASTM C 192/C 192M, 2002). Before demoulding, the specimens were covered by wet burlap to minimise water evaporation. All the control concrete specimens were demoulded after 24 hours and those concretes made with various BHD levels were kept in their moulds for longer times due to the retardation effect of BHD.

3.3 ELECTROCHEMICAL MEASUREMENTS

3.3.1 Preparation of steel bar specimens

All of the steel bars are 100 mm long and with a diameter of 8 mm. The surfaces of the steel bar specimens were polished first using P600 and then P800 emery paper, to remove debris. The steel bars, after degreasing with acetone and ethanol, were stored in desiccators for a period of at least one week before casting to allow formation of the oxide layer. The end of each steel bar was heated prior to soldering the wires to ensure a strong bond between the solder and the steel. Before casting, all steel bars were masked as described below.

3.3.2 Masking steel bar specimens

The greatest practical problem that is associated with the type of specimens shown in Figure 3-1, is the initiation of crevice corrosion at the ends of the steel bar. The avoidance of crevice corrosion in the specimens is very difficult (Page and Treadaway, 1982). The method of masking the embedded steel bars and materials used, to avoid crevice defects, is illustrated here and described by Lambert et al. (1991). Both ends of each steel bar were masked with a duplex coating. This involves the application of two coatings: first a cement slurry coating and then followed by a two part epoxy adhesive coating. The aim of this application of cement paste is to provide an alkaline environment and hence reduce the risk of corrosion, especially crevice corrosion at the bar ends. The second coating, the epoxy resin layer, was applied to prevent ingress of chloride ions. The first coating of cement slurry was made by mixing cement with water and styrene-butadiene rubber emulsion (SBR). The quantities of water and SBR were equal in volume (50% water, 50% SBR). SBR has been used in repair

work due to its increased adhesion. The first coating was applied by dipping both ends of each steel bar in a container of cement paste and SBR. The coated steel bars were then left for 24 hours to dry. The second coating was made by mixing a two part epoxy adhesive. Immediately after mixing, a layer of the epoxy adhesive was applied to the cement paste coating. Figure 3-1 shows a typical steel bar used in the corrosion electrochemical measurements.

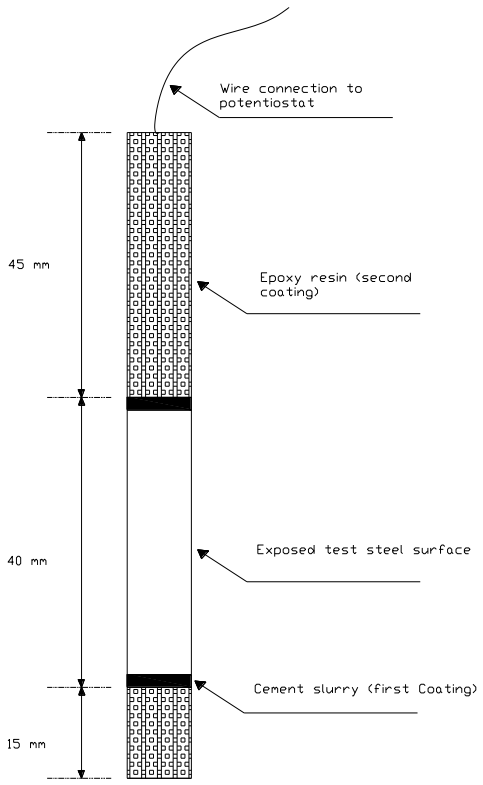

Figure 3-1 Diagram of the steel bar prepared for corrosion measurements

3.3.3 Interfacial defects

Plastic ties similar to those used in practice were used in some experiments to create interfacial detects at the vicinity of the steel bar. The principal objective of using plastic ties was to create regions with possible defects such as crevices, macroscopic voids filled with water or areas of high porosity behind or under the steel-defect-cement interface as demonstrated in Figure 3-2. This was thought to provide a means by which the influence of crevices of a kind that were representative of commonplace interfacial defects on reinforcing bars in actual concrete structures could be studied in a reproducible manner. These plastic ties were 2 mm thick. They were fixed at the middle-section of exposed surface of the steel electrode at regular spacing. A photo of the plastic ties wrapped around the steel surface is presented in Figure 3-3.

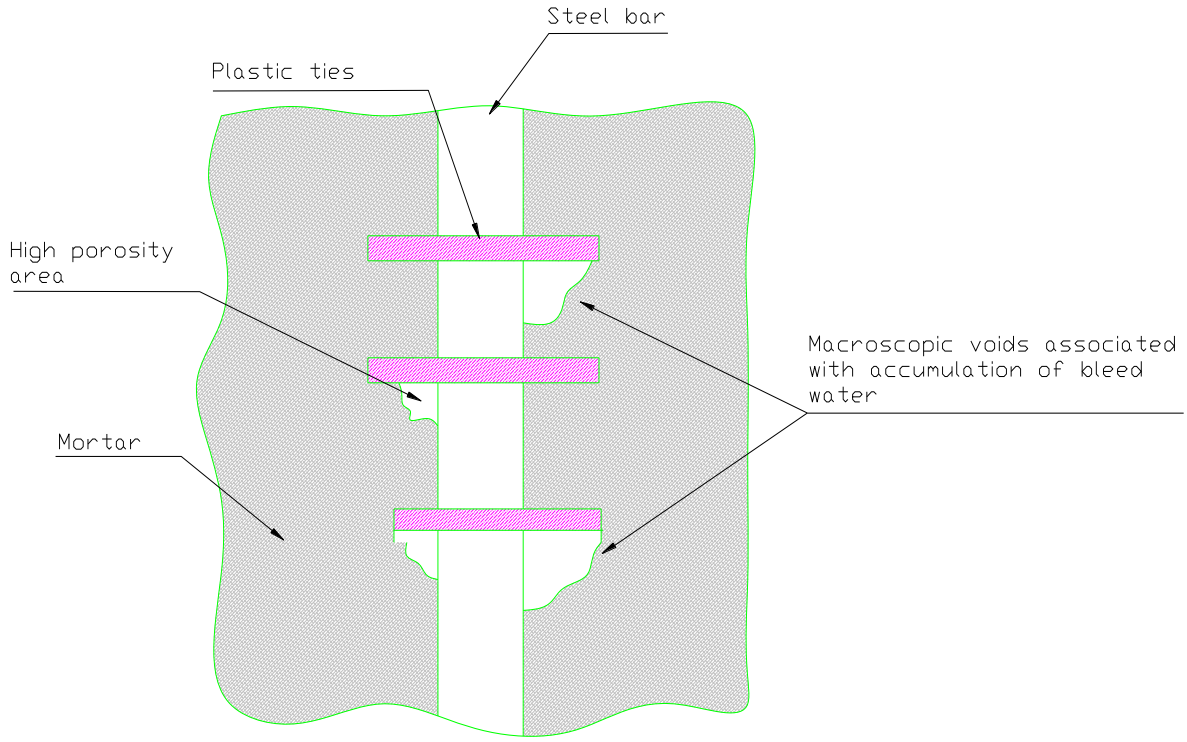

Figure 3-2 Illustration of expected interfacial defects associated with plastic ties at steel surface

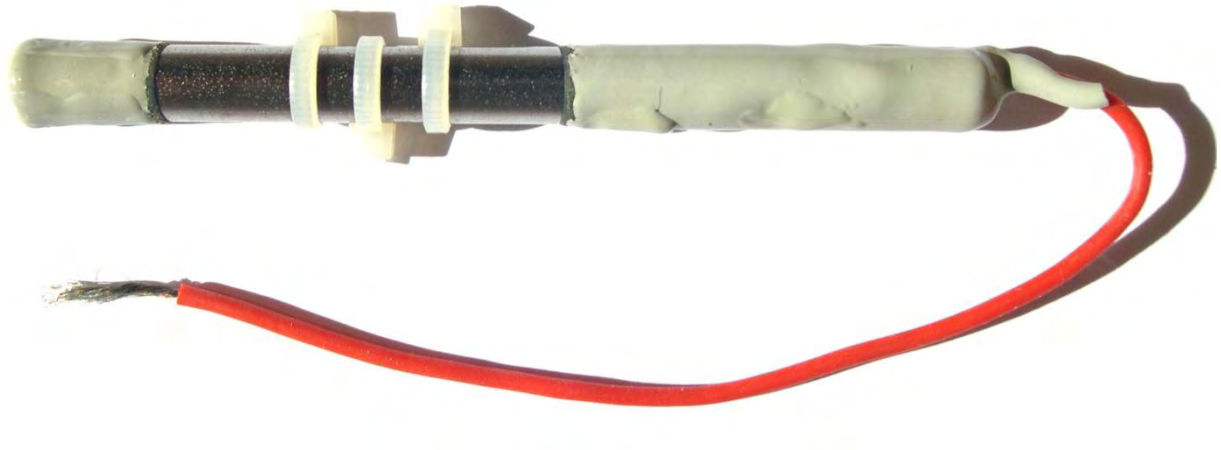

Figure 3-3 Steel bar wrapped with plastic ties used in some experiments

3.3.4 Preparation of gel bridges

Electrolyte gel bridges were made and inserted into the mortar/concrete specimens to provide contacts with an external reference electrode. They were made by mixing 3.3 % agar with 15 % potassium nitrate solution. The solution was heated to dissolve the agar and it was then injected into a plastic tube where it set and formed a gel. The ends of the gel bridges were kept in distilled water to prevent them from drying out before being cast in mortar specimens.

3.3.5 Electrochemical measurements

Instantaneous corrosion measurements have been carried out using the DC Linear Polarization Resistance (LPR) method described by (Stern and Geary, 1957) and (Stern and Weisert, 1959). The LPR method was employed in this research to monitor the corrosion of steel reinforcing bar embedded in the mortar because it is considered to be a non-destructive technique, to provide reliable information on the corrosion behaviour of the steel bar, and it is

fast and the most widely used technique for monitoring corrosion due to its simplicity (Rodriguez et al., 1994).

To measure the instantaneous corrosion rate, the steel bar embedded in mortar was polarized between + 10 mV and – 10 mV of the corrosion potential (E_{corr}). The E_{corr} of the steel embedded in mortar specimen was measured against a saturated calomel reference electrode. The embedded steel bar was polarized to ± 10 mV from Ecorr at a sweep rate of 10 mV/min. The response current density was measured. A plot of applied potential (ΔE) and measured current density (Δi) for a corroding specimen was constructed, and the linear polarization resistance, R_p, was calculated from the slope of that plot. The corrosion current density was calculated using the Stern-Geary equation;

$$I_{corr} = \frac{\beta_a * \beta_c}{2.3\,(\beta_a+\beta_c)} \quad \frac{(\Delta i)}{(\Delta E)} \qquad [3.1]$$

Where $B = \beta_a*\beta_c / 2.3\,(\beta_a+\beta_c)$, and $R_p = (\Delta E) / (\Delta i)$

Then,

$$I_{corr} = \frac{B}{R_p} \qquad [3.2]$$

From the above equations, I_{corr} is the corrosion current density ($\mu A/cm^2$), β_a and β_c are the anodic and cathodic Tafel constants, and R_p is the linear polarization resistance ($ohms \cdot cm^2$) (ASTM, 1995). From the Stern-Geary equation, corrosion current densities were calculated by assuming B = 26 mV, because it was found by Andrade and Gonzalez (1978) that in the

case of active corrosion, there was a good consistency between measured corrosion rates and weight losses of steel bars embedded in concrete.

3.3.6 Weight loss measurements procedure

The weight loss measurement of corroded steel bars has been used to evaluate the extent of the corrosion of reinforcing steel embedded in mortar. The weight loss measurement technique used in this research was similar to that used by Parrott (1994) and Ngala et al. (2002) to assess the extent of corrosion of the steel bar. The same steel bars used in electrochemical measurements were used to determine the weight losses of the embedded steel. On completion of electrochemical measurements, the steel bar was extracted from the mortar specimens by breaking the specimens carefully. The two ends of the steel bars which had been masked were cut off to determine the weight loss just of the exposed area. All large loosely adherent pieces of mortar and any debris were removed by abrading very lightly with a tooth brush, taking care not to damage the surface of the steel. The rebars were cleaned from the remaining cementitious debris and corrosion products by pickling the steel bars in "Clark's solution" (containing 50 g/l $SnCl_4$ and 20 g/l Sb_2O_3 in concentrated HCl 35 % w/v solution) for 5 min. The steel bars, were then removed and washed with distilled water. Care was taken during the cleaning to avoid any significant removal of the underlying steel. The cleaning process was repeated to make sure the steel bars were free of rust, as necessary.

The steel bars were then washed with distilled water, dried with tissue and degreased with acetone and ethanol. They were then kept in the oven at 105 ºC for 1 hour to ensure the complete removal of moisture from the steel. The steel bars were then transferred to

desiccators to cool to room temperature before being measured to calculate weight per unit area. Control specimens of uncorroded mild steel bars from the same patch were prepared with the same procedure applied on corroded specimens to determine the weight per unite area. The control specimens were cleaned with the same procedure to assess any loss in their weight before and after pickling the control specimens in "Clark's solution". The weight loss (mg/cm^2) was calculated by subtracting the weight of corroded cleaned steel bars from that of the control specimens.

3.4 ANALYSIS OF PORE LIQUIDS' IONIC CONCENTRATIONS

3.4.1 Determination of hydroxyl ion concentration

The hydroxyl ion concentration was assessed by titration of the pore solution with 0.001 M nitric acid with a mixture of bromocresol green/methyl red (BG/MR) solution used as an indicator. The main reason of using BG/MR was due to its ability to show a clear end point at pH 4.6 and to make sure that all the existing bicarbonate was neutralized (Cooper, 1941), as the pore solution became rapidly carbonated after extraction because of its small volume resulting in lowering of the pH. 0.05 ml of pore solution was placed in a conical flask and 1 or 2 drops of the (BG/MR) were added. The 0.001 M nitric acid was added to the beaker carefully, using a 25 ml burette, to neutralise the pore solution. Once the end point was reached, the amount of nitric acid used was measured. Thereafter, the hydroxyl ion concentration was determined by the following equation;

$$M_b = \frac{M_a \times V_a}{V_b} \qquad [3.3]$$

Where,

M_b is the molarity (mol/L) of the base, in this experiment hydroxyl ion concentration;

M_a is the molarity (mol/L) of the acid used to neutralise the base, in this case 0.001M HNO_3;

V_a is the volume (ml) of 0.001M nitric acid used to neutralise the solution, and

V_b is the volume (ml) of base used, in this experiment 0.05 ml.

3.4.2 Determination of free chloride ion concentration

Chloride analysis of pore liquids was carried out by a spectrophotometric method described by Vogel (1978). The pore liquids were diluted with deionised water to reduce the chloride concentration until it was within the range of a calibration curve constructed from standard chloride solutions, see Figure 3-4. For this purpose, 2 ml of the diluted pore liquids was placed in a conical flask with 2 ml of 0.25 M ammonium iron (III) sulfate [$Fe(NH_4)(SO_4)_2.12H_2O$] in 9M-nitric acid, followed by 2 ml of a saturated solution of mercury (II) thiocyanate in ethanol. The solution was kept for 20 minutes before the absorbance reading at 460 nm was taken. From a constructed calibration curve, the chloride concentration in the solution corresponding to the absorbance reading was determined.

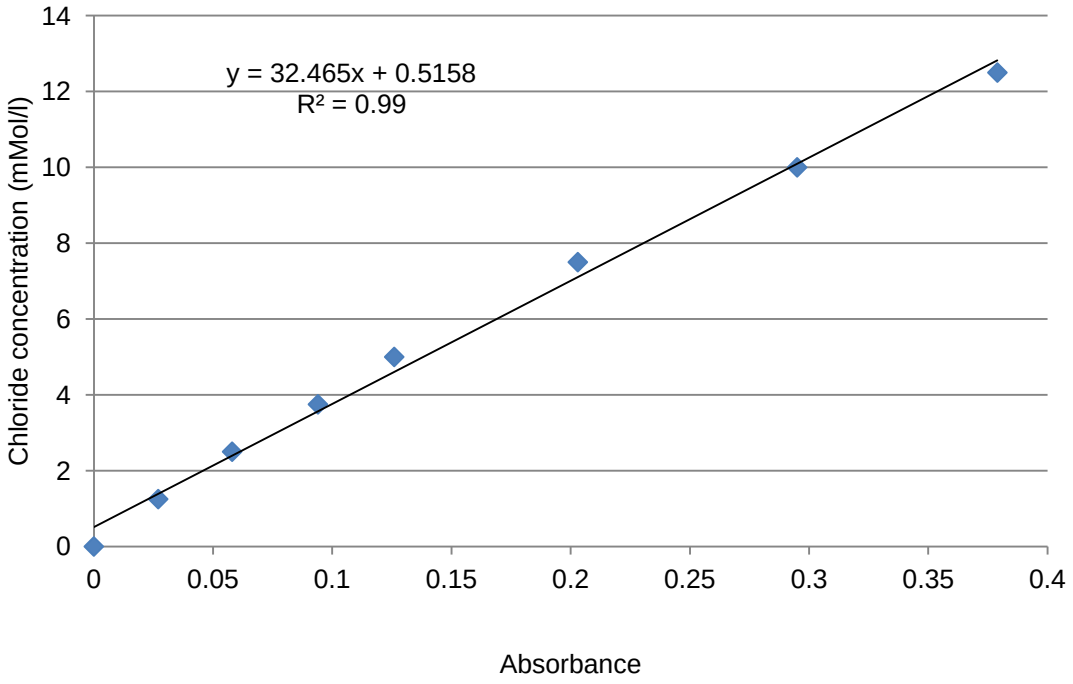

Figure 3-4 Calibration curve used to estimate chloride concentration in pore solutions

3.5 DETERMINATION OF TOTAL CHLORIDE

To determine the total chloride, the obtained sample was ground until it is passed through a 150 µm sieve and dried at 105 – 110 ºC for a period of 24 hours. A titration procedure was used to determine the total chloride content from the obtained sample as described by Rilem TC 178-TMC (2002). This involved weighing 1g of the ground powder and adding 50 cm^3 of HNO_3 (1:2). Following this, the solution was heated until it boiled for one minute, then 5 cm^3 of the 0.05 M $AgNO_3$ was added and the solution heated again until it boiled for another minute. The solution was cooled to room temperature and filtered. Subsequently, HNO_3 (1:100) was added to the filtrate until it had reached about 200 cm^3. This was done to make sure all the chloride was washed from the beaker, filter paper and the funnel to the flask. Twenty drops of the $NH_4Fe\ (SO_4)_2.12H_2O$ were added as an indicator and the contents of the

flask were titrated with 0.05 M NH_4SCN solution until they became slightly reddish brown in colour. The titrated volume of 0.05 M NH_4SCN was recorded as V_1. A blank test was run using the procedure described above with the same reagent but without the sample. The titrated volume (V_2) of 0.05 M NH_4SCN solution was again recorded.

$$\text{The percentage of chloride content, \% Cl} = \frac{3.5453\ V_{Ag}M_{Ag}\ (V_2 - V_1)}{m\ V_2} \qquad [3.4]$$

Where

V_{Ag} is the volume of $AgNO_3$ added (cm^3);

M_{Ag} is the molarity of the $AgNO_3$;

V_1 and V_2 is the volume of added NH_4SCN (cm^3);

m is the mass of the sample (g).

3.6 LOSS ON IGNITION

To determine the chloride threshold value as a % by weight of cement in each individual specimen, the collected materials were analyzed to determine the calcium content using XRF. The obtained material was ground until it is passed through a 150μm sieve. Prior to XRF analysis, 1 gm of the collected powders was placed into a pre-weighed crucible, covered, and then placed in the furnace. The temperature of the furnace was increased slowly until it reached 925 ± 25 ºC and left for 5 mins. The cover was removed and the crucible and its contents were left for further a 30 minutes at the same temperature. The crucible was placed in the desiccator with silica gel and left to cool down to room temperature and then weighed. A repetition of the ignition, cooling and weighing of the crucible and its contents were carried

out until the difference in mass was less than 0.0005 gm (BS 1881-124:1988). The ignited samples were then used for the calcium content analysis.

3.7 X-RAY FLUORESCENCE SPECTROMETRY TECHNIQUE

For the purposes of studying the elemental composition of materials, X-ray fluorescence spectrometry (XRF) was utilized. The XRF technique is a non-destructive method which allows a direct analysis of each element and its concentration in the sample provided. XRF is an easy measuring technique which can deal with a variety of samples. The sample can be either in liquid, powder or solid form. XRF instruments consist of a high intensity 4 kW Rhodium X-ray tube, two collimators and five analyzer crystals.

Each prepared sample was placed in an individual cup. The sample was bombarded with a primary X-ray beam causing excitation in the sample to generate X-ray fluorescence. The primary X-rays resulted in ejecting electrons from the inner atomic shells leaving vacancies. These vacancies are filled by electrons dropped from higher to lower energy atomic shells. The excess energy was then released as X-ray fluorescence radiation which was collected by a detector. From the collected radiation, each element can be identified by its characteristic wavelength. The intensity of the radiation determines the concentration of the element.

3.7.1 XRF analysis procedure

The elemental concentration of the materials were determined using S8 Tiger X-ray fluorescence spectrometer supplied by BRUKER. The medium to analysis the sample was Helium gas. The samples were ground and sieved to pass 150 µm size. For BHD material analysis, before the sample was analysed, it was dried in an oven at about 105 ºC for 24 hours. Three representative samples were analysed.

Chapter 4

EFFECT OF BHD ADDITION ON CORROSION BEHAVIOUR

PART A: EFFECT ON THE CORROSION BEHAVIOUR OF STEEL BAR EMBEDDED IN MORTAR

4.1 INTRODUCTION

For those reinforced concrete structures that are exposed to a marine environment, the chloride-induced corrosion will be the main cause of deterioration of those structures, as reviewed in Chapter 2. When chloride ions are available in sufficient concentration in the pore solution, they are likely to destroy the passive layer and induce corrosion. Therefore, the addition of BHD in concrete may have an effect in the pore solution chemistry particularly on chloride ions concentration since some of the chlorides that are available in the BHD, see Table 3-2 , may leach from the BHD when added into the concrete. A higher chloride ion concentration in the pore solution suggests a higher corrosion risk probability. This signifies the importance of the assessment of the consequences of the addition of BHD on the corrosion process.

Previous work by Chaudhary et al. (2003) and Maslehuddin et al. (2011) has investigated the effect of BHD addition on the corrosion behaviour of steel bar embedded in concrete. These studies remain very limited, however, which emphasises the importance of performing further research for two main reasons (i) to confirm and understand the effect of BHD addition on the corrosion behaviour of steel bar embedded in mortar and (ii) to study the change in the pore solution chemistry due to the addition of BHD. In order to achieve this, three experiments

were conducted. First, to assess the corrosion performance of steel bars embedded in mortar (see part A), the behaviour of embedded steel bars was monitored electrochemically by measuring corrosion current density using a DC Linear Polarization Resistance (LPR) method with ohmic drop compensation. The linear polarization resistance method has been developed since 1950s (Stern and Geary, 1957) and used for steel in concrete since the 1970s (Andrade and Gonzalez, 1978). In the second experiment, pore solutions were extracted and analysed to investigate whether the addition of BHD has an effect on pore solution chemistry utilizing an in situ leaching method, see Part B. This provides a reliable technique for determining the chloride concentration and pH in concrete pore water. In the third experiment, chloride leaching behaviour tests were performed, see Part C. The experimental work related to the first part followed by results analysis and discussions are presented in the next sections.

4.2 EXPERIMENTAL PROCEDURE

4.2.1 Mortar specimen preparation for electrochemical measurements

Mortars with a W:C:S ratio of 0.5 : 1.0 : 2.0 by weight and with 0 or 2 % BHD were mixed in the same way described in subsection 3.2.1. Additions of chloride (equivalent to 0, 0.4 and 2.0 % by weight of cement) were made by dissolving the required quantities of AR grade NaCl in the mixing water. Triplicate specimens of each mix were cast in plastic containers 85 mm height and with a diameter increasing from 45.5 mm at the bottom to 65 mm at the top. The steel bars, gel bridges and stainless steel meshes were inserted, and fixed by the PVC lid, in plastic containers as shown in Figure 4-1. After 24 hours, the mortars were demoulded and

kept in a fog chamber at 20 ± 2 ºC for one week. Before casting, the gel bridges and steel bars were prepared and masked as described in subsection 3.3.4, 3.3.1 and 3.3.2, respectively.

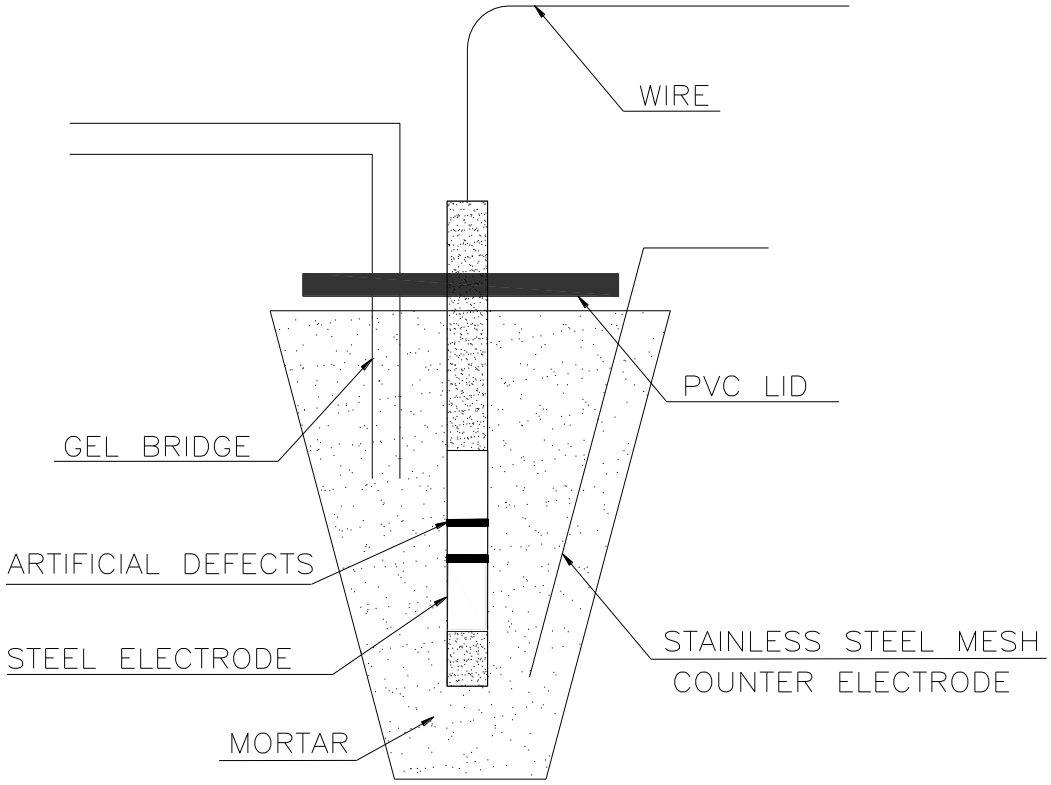

Figure 4-1 Diagram of the mortar specimens used for corrosion measurements

4.2.2 Testing procedure

After one of week curing, corrosion potentials and corrosion rate measurements were made. The mortar specimens were then subjected to weekly wet and dry cycles involving immersion in tap water for four days followed by drying in air at room temperature for three days. At the

end of the third day and before immersion again, corrosion potential and corrosion rates were measured. This weekly regime was repeated for the whole duration of the experiment.

During the testing period, for each mortar specimen, potential measurements and corrosion rate measurements were carried out with a cell arrangement shown in Figure 4-2. The corrosion cell consisted of an external reference electrode, a working electrode and a counter electrode. A saturated calomel reference electrode (SCE) was used as the external reference electrode. One end of a gel bridge was embedded in the mortar specimen and positioned close to steel bar surface and the other end was placed in 2 M potassium nitrate solution. The reference electrode was also, placed in the potassium nitrate solution during the reading. For potential measurements, the reference electrode and steel bar were both connected to a high impedance voltmeter. The corrosion rate measurements were carried out using the LPR technique. The instantaneous corrosion rate measurements were performed as described in subsection 3.3.5.

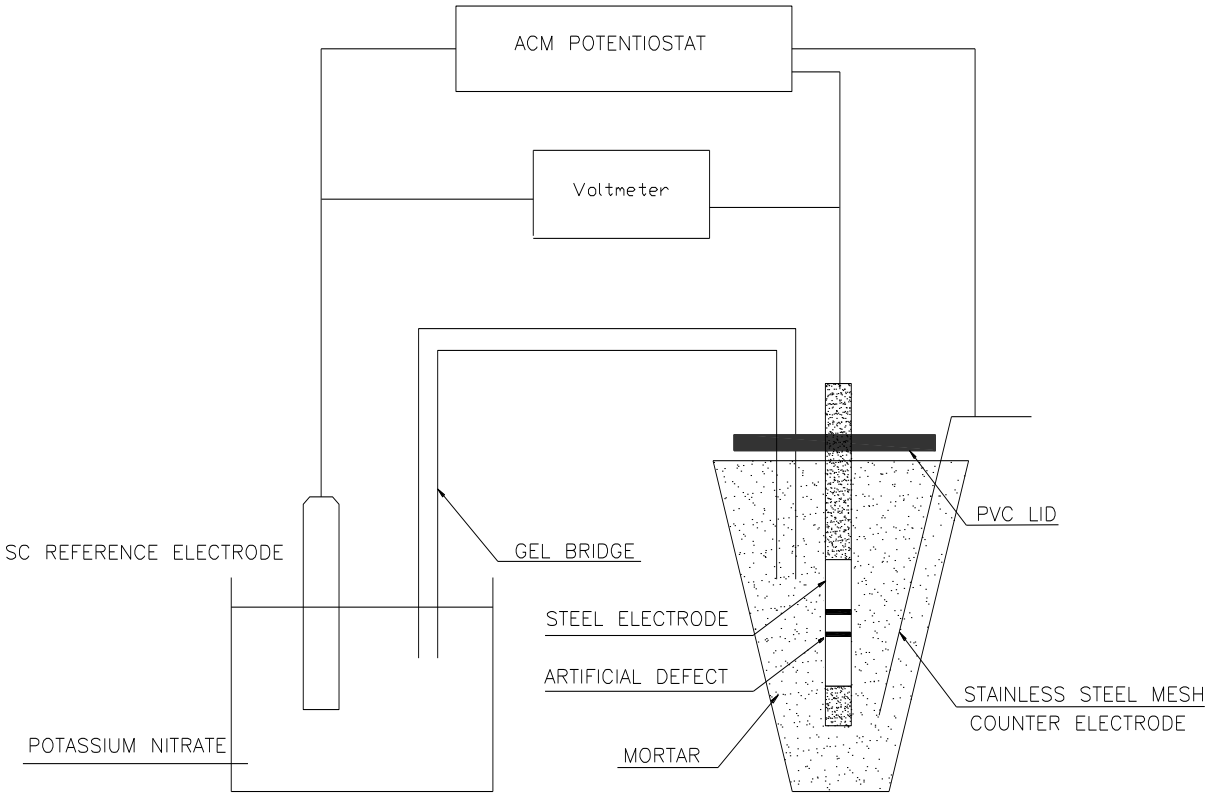

Figure 4-2 Schematic diagram of the electrochemical monitoring process for corrosion specimens

4.3 RESULTS ANALYSIS AND DISCUSSION

4.3.1 Corrosion current density data

The results of corrosion current density (I_{corr}) measurements for steel bars embedded in control mortars (0 % BHD and 0 % chloride) and in BHD mortars containing various levels of chlorides were plotted against the period of exposure in Figure 4-3 to 4-5. All the results presented in the graphs represent average values obtained from triplicate specimens in this experiment.

In the case of mortars made without any addition of sodium chloride and incorporating 2 % BHD as addition by weight of cement, some fluctuations in the I_{corr} values were observed particularly in the last part of the exposure period, from day 143 and afterwards, indicating an unstable oxide film. The reason for fluctuations in the I_{corr} values is not fully understood. If the corrosion rate is under anodic control, then more negative potentials combined with higher corrosion rates for the steel bars will be observed. For corrosion under cathodic control, the steel potentials will tend to move to more negative values when a reduction in the corrosion rates occurs as the flux of oxygen is restricted. Therefore, the observed fluctuation in I_{corr} values cannot be attributed to oxygen diffusion "cathodic control" because, in fact, the corrosion process when BHD was added into the concrete was subject to anodic control as discussed in subsection 4.3.2.

Also, the addition of 2 % BHD resulted in higher I_{corr} values compared to the control specimen. This increase in the I_{corr} values was expected due to the significant increase in the free chloride ion concentration found in the pore solution, extracted from BHD mortar, compared to that in the control specimens after 7 and 21 days of curing, as discussed in section 4.8.1. In the absence of chlorides, the I_{corr} values of the steel bar embedded in control mortars were more stable than those bars embedded in the BHD mortars during the whole test period. However, it can be noticed from Figure 4-3 that, the I_{corr} values in both control and BHD mortars with nil chloride addition, were much less than 0.1 $\mu A/cm^2$ and this indicates the steel bars embedded in both control and BHD mortars were in the passive condition region (Andrade et al., 1990) during the whole of the monitoring period. This was expected, since the $[Cl^-/OH^-]$ ratios found in pore liquids extracted from control and BHD mortars and both containing no chloride varies between 0.01 and 0.03 for control and BHD mortars during all

the hydration times as discussed in the next Part. This was far lower than the threshold value of 0.6 which was suggested by Hausmann (1967) if this criterion is assumed to control this behaviour.

I_{corr} values obtained from plain (0 % BHD) and 2 % BHD mortar containing 0.4 per cent chloride by weight of cement are shown in Figure 4-4. At the beginning of exposure, the I_{corr} value in plain mortar containing 0.4 % chloride was as high as 0.11 $\mu A/cm^2$, whereas the I_{corr} value of steel bar embedded in BHD mortar containing the same level of chloride was 0.07 $\mu A/cm^2$. In both cases, after day-7 and until day-17 of exposure, the I_{corr} values declined gradually, which suggested a tendency of repassivation of the steel bar. As curing time increased, it was found that I_{corr} values obtained from steel bars embedded in plain and BHD mortars increased gradually, which suggest depassivation of the steel bars. Such behaviour could be tentatively explained by the changes in the pore solution chemistry obtained from the mortars. This increase in I_{corr} values was associated with a gradual increase in the concentration of free chloride ion found in the pore solutions extracted after 3, 7, 21 and 60 days of curing.

The I_{corr} value that was obtained from the steel bar embedded in mortar containing 0.4 % chloride and cast without BHD crossed the threshold value of 0.1 $\mu A/cm^2$ towards the active corrosion region after aproxmately115 days of exposure, whereas the I_{corr} value on steel bar embedded in mortar with same level of chloride e.g. 0.4 % and with 2 % BHD took a longer period to cross the threshold value, taking until 150 days after casting.

Mortars made with 2 % addition of chloride by weight of cement, showed higher I_{corr} values that increased gradually during the whole period of the experiment, as shown in Figure 4-5. At the beginning of the exposure and until day 52, as can be seen in Figure 4-5, the steel bar embedded in 2 % BHD mortar exhibited higher corrosion rates compared to other steel bars embedded in nil BHD mortar. Since some of the chlorides will be taken up by the cement hydration products and as BHD is known to be a retarder which slows down the hydration process of the cement leading to higher free chloride at early ages, that additional chloride is available in the pore solution to enhance the corrosion rate.

In both mortars containing 2 % chloride and made with and without BHD, the I_{corr} values were higher than the threshold value of 0.1 $\mu A/cm^2$ from the beginning of the exposure indicating active corrosion took place. This behaviour of both sets of mortars was explained as high levels of free chloride ion concentration were found in the pore solution extracted after 3, 7, 21 and 60 days of curing, leading to higher $[Cl^-/OH^-]$ ratios. After 52 days of exposure, the I_{corr} value obtained from steel bar embedded in mortar mixed with 2 % BHD and 2 % chloride exhibited slightly lower values than that in mortar containing the same level of chloride, but made without BHD addition. A similar effect for BHD was observed in a study carried out by Al-Sugair et al. (1996) indicated that the corrosion rate of steel bar embedded in BHD concrete was high compared to control specimens during the first 126 days of immersion. However, after 277 days and onwards, this situation changed as lower corrosion rates were noticed in the BHD specimens. Another investigation on the effect of BHD on the corrosion behaviour of steel embedded in concrete was carried out by Chaudhary et al. (2003). They found the overall average corrosion rate of steel reinforcing bar embedded in slabs cast with 2 % BHD and contaminated with 1 % chloride by weight of cement was 60 % lower than that in

control slabs after 12 months of exposure. They attributed the reduction in the corrosion rate as due to a refined pore structure and/or the presence of ZnO in the BHD. Furthermore, this reduction in the corrosion rate could be related to the enhancement in [OH^-] concentration found in the pore solution and to the reduction in the coarse capillary porosity, as discussed in section 4.8.2 and section 5.4, respectively.

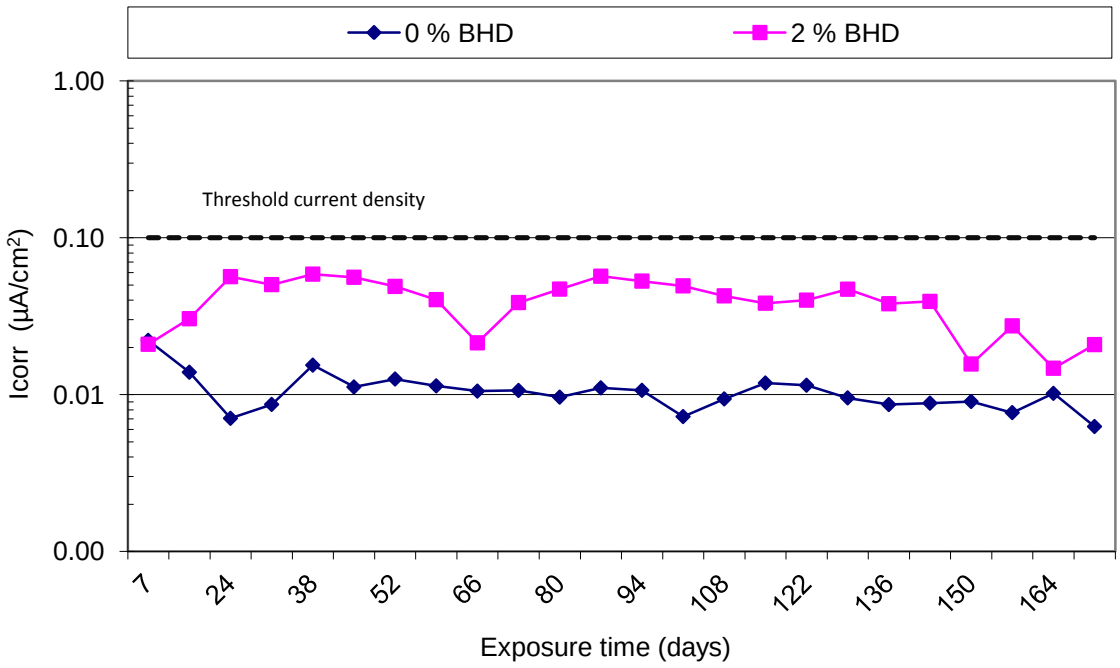

Figure 4-3 Corrosion current densities of steel bars embedded in mortars without addition of sodium chloride

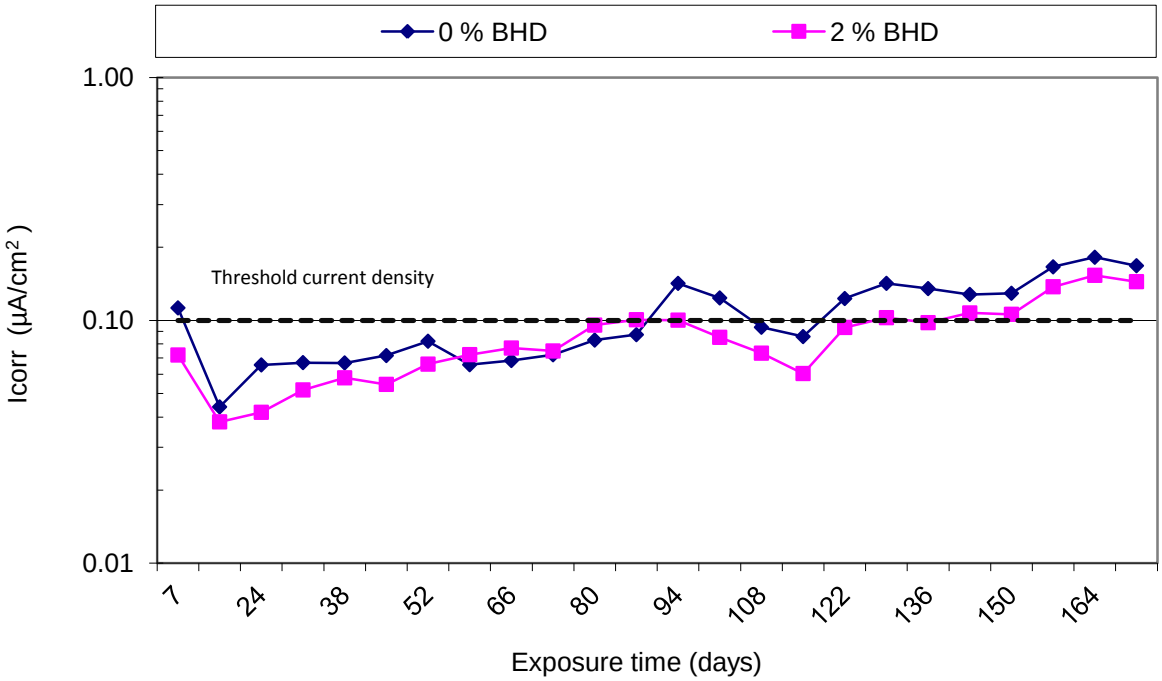

Figure 4-4 Corrosion current densities of steel bars embedded in mortars with 0.4 per cent addition of chloride by weight of cement

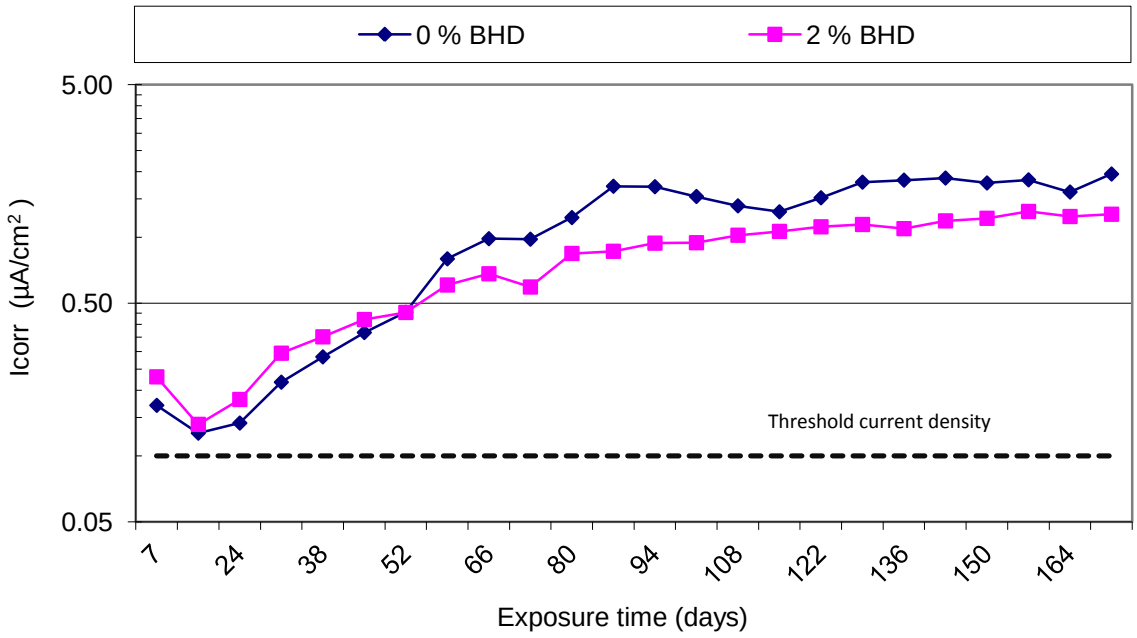

Figure 4-5 Corrosion current densities of steel bars embedded in mortars with 2.0 per cent addition of chloride by weight of cement

The additions of different levels of chlorides to mortar made with and without a 2 % addition of BHD resulted in higher I_{corr} values compared to mortar made without chloride, as shown in the above figures. This effect was due to the increase in chloride levels from 0.4 to 2 % by weight of cement.

4.3.2 Corrosion potentials

The results of corrosion potentials (E_{corr}) as a function of the exposure period obtained from both steel bars embedded in mortars containing various levels of chloride and mixed with and without 2 % BHD addition by weight of cement are presented in Figure 4-6 to 4-8. Each individual data point represents an average of three values obtained from replicate specimens.

Figure 4-6 demonstrates the influence of BHD addition on the corrosion behaviour of steel bar embedded in mortar made without addition of chloride. This figure indicates that the addition of BHD causes a fluctuation in the corrosion potentials compared to those in the control specimens from the beginning of the exposure, which implies that the addition of BHD does not help to stabilize the passive film. In addition, during the first 38 days of curing, the steel bar embedded in BHD mortar exhibited more negative E_{corr} values, more negative than the corrosion potential threshold value of -270 mV (versus SCE) which suggested a 90 percent chance of corrosion (ASTM C876, 1999). However, after this period of exposure, the E_{corr} values decreased gradually and crossed the corrosion potential threshold value toward the passive state region. The E_{corr} values continued to move toward less negative values and exhibited less negative potentials for steel bar embedded in BHD mortar compared to E_{corr} values of those steel bars embedded in control specimens and this potential

stayed stable between days 108 and 150 of curing. After that, the corrosion potentials in the steel bar embedded in BHD mortar started to diminish as exposure time increased and reached a value of -123 mV at day 171. In the case of the control specimens, the E_{corr} values were less negative than the corrosion potential threshold value from the beginning and exhibited stable E_{corr} values to the end of the experiment, the measured potential at day 171 was recorded as -195 mV.

In the case of 0.4 per cent chloride addition, both mortars mixed with and without BHD initially exhibited more negative E_{corr} values which then moved sharply in a positive direction (during a period of approx. 2 to 3 weeks) indicating a re-passivation of the steel bar. After this period of exposure, the corrosion potentials more or less stayed border-line, -270 mV (SCE), until day 157 as seen in Figure 4-7. Afterwards, both steel bars embedded in mortar mixed with and without BHD and both contaminated with 0.4 % chloride started to reveal more negative potentials (towards active corrosion region) where the E_{corr} values became more negative gradually as exposure time increased indicating that active corrosion of the steel bar took place until the end of the experiment. In general, there were no significant differences between the electrochemical response of the steel bars embedded in control and BHD mortars both containing 0.4 % chloride, as shown in Figure 4-4 and Figure 4-7.

In Figure 4-8, the steel bar embedded in mortar containing 2 per cent chloride and mixed with and without BHD addition experienced corrosion potentials more negative than -270 mV (SCE) throughout the whole experiment span. At around day 80, however, the steel bar embedded in BHD mortar started to reveal less negative corrosion potentials compared to those bars embedded in mortars containing the same level of chloride and made without BHD

addition. A similar trend of corrosion resistance was noticed on the same steel bars, where I_{corr} values were less compared to those I_{corr} values obtained from steel bars embedded in mortar cast without BHD, see Figure 4-5. This could presumably be attributed to the higher level of $[OH^-]$ concentration found in the pore solution extracted from BHD mortar compared to that in mortar made without BHD addition, as seen in Figure 4-20. This could be supported by the finding of the work conducted by Gouda (1970) and Goñi and Andrade (1990) that showed an increase of E_{corr} values (less negative) as pH values increases.

Chaudhary et al. (2003) studied the effect of 2 % BHD addition on the corrosion of steel bar embedded in concrete slabs that were mixed with and without 1 % chloride by weight of cement. The corrosion potentials were less negative in BHD concrete mixed with and without chloride compared to concrete slabs that were cast without BHD and containing the same level of chloride. Al-Sugair et al. (1996) carried out an investigation on the effect of 2 and 3 % BHD as cement replacement on the corrosion behaviour of the steel bar embedded in concrete. The concrete specimens were placed in a tank filled by 3.5 % sodium chloride solution. They found the corrosion potentials in BHD concrete to be less negative than that in the control specimens.

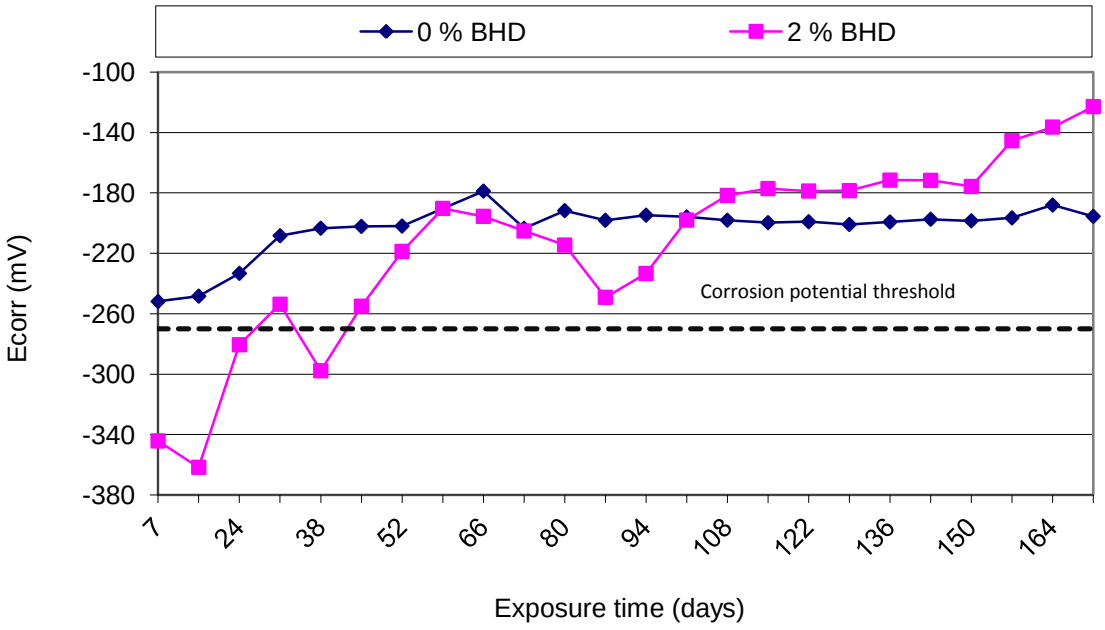

Figure 4-6 Corrosion potentials of steel bars embedded in the control and BHD mortar specimens without any addition of sodium chloride

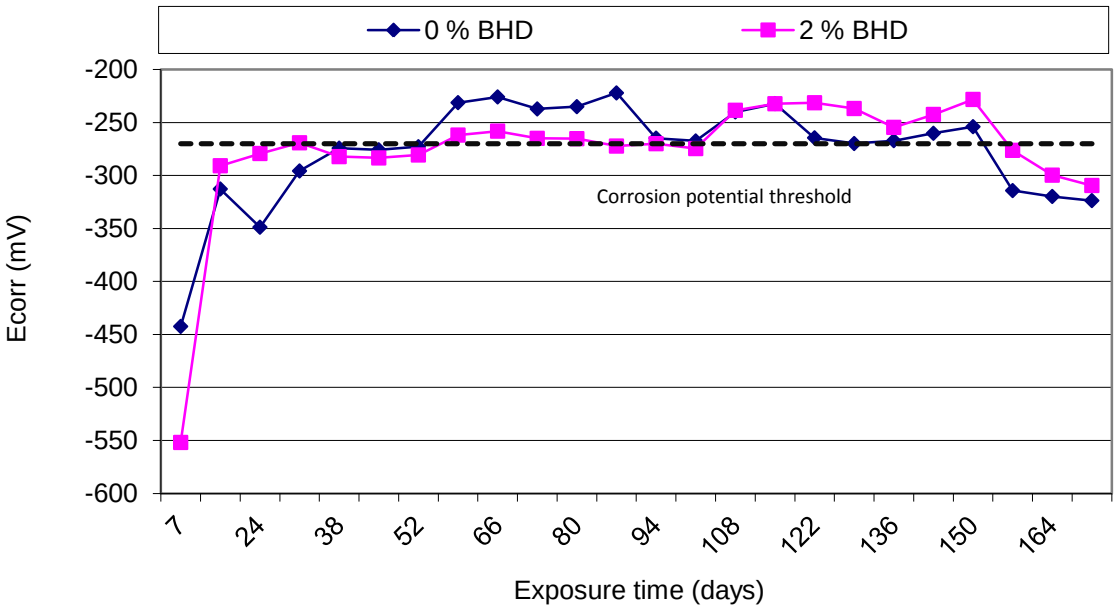

Figure 4-7 Corrosion potentials of steel bars embedded in the control and BHD mortar specimens containing 0.4 per cent chloride by weight of cement

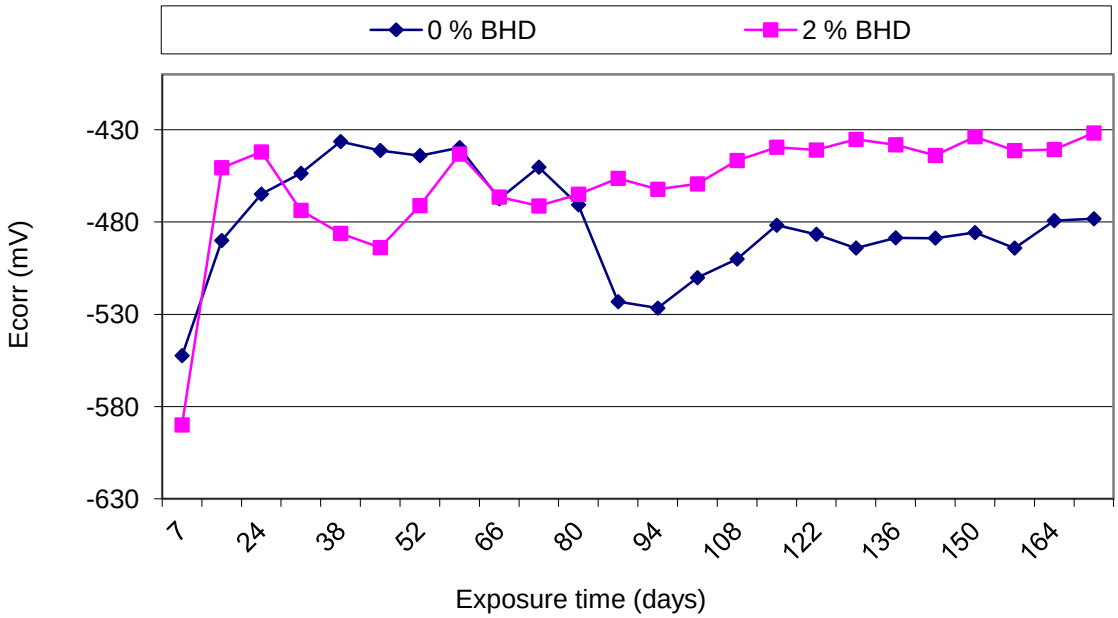

Figure 4-8 Corrosion potentials of steel bars embedded in the control and BHD mortar specimens containing 2.0 per cent chloride by weight of cement

The corrosion rate of steel bar embedded in concrete is controlled by several factors including diffusion of oxygen, resistivity of the concrete and the composition of the pore solution (Goñi and Andrade, 1990). The important implication is that the addition of BHD into mortar does not accelerate the corrosion rate of the steel bar in the presence of chloride, as shown in Figure 4-4 and Figure 4-5, despite BHD containing an additional amount of chlorides as can be seen from the BHD chemical composition in Table 3-2. This suggests that there are other factors that influence the propagation of the corrosion process on steel bars embedded in BHD mortars. One of the main reasons responsible for the corrosion process in steel bar embedded in concrete is the pore solution which is in contact with embedded steel. Therefore, the corrosion behaviour of steel bar embedded in BHD mortar is likely to be attributed partly to the pore solution composition and partly to the physical properties of concrete. The

magnitude of the corrosion process is also mainly affected by the composition of pore solutions and/or by the physical properties of the concrete such as the porosity. Consequently, the changes in the pore solution chemistry over time were studied to investigate the aggressiveness of the pore solutions (as discussed in Part B of this Chapter) and the porosity of cement pastes which were responsible for providing access routes for the corrosive media/agents were also investigated in Chapter 5 part A.

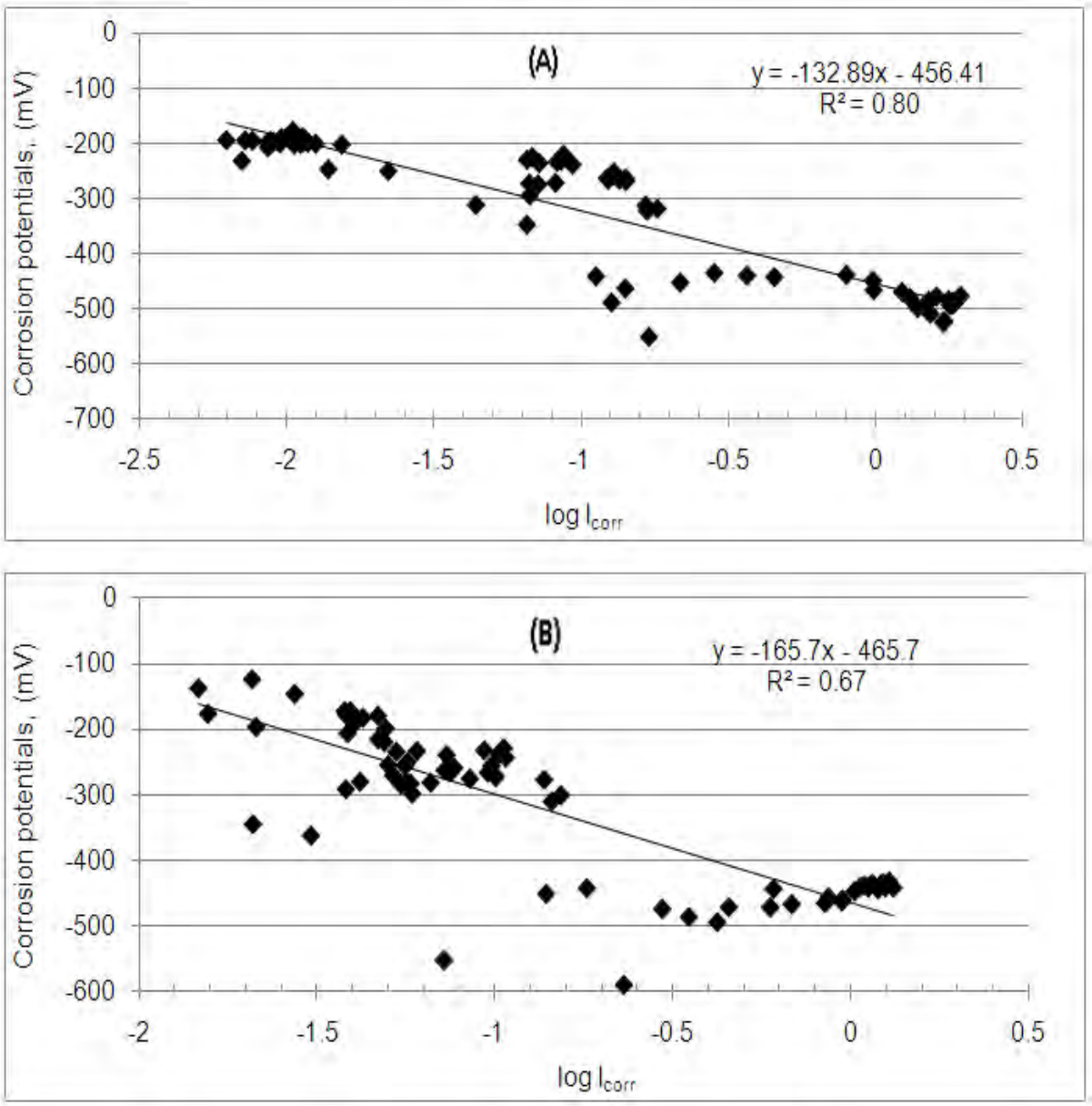

Figure 4-9 Best-fit straight-line plots of corrosion potentials versus log corrosion current density for steel bar embedded in mortar incorporated with BHD additions of A) 0 and B) 2 and both mixed with 0, 0.4 and 2 % chloride

Table 4-1 Statistical data from regression analysis

Figure No.	B (mv)	R^2
Figure 4-9 (A)	-133	0.80
Figure 4-9 (B)	-166	0.67

In general, Figure 4-9 (A) and (B) show that, the I_{corr} values increase with increasingly negative values of E_{corr}, which suggests that the process of corrosion is controlled by the anodic reaction e.g. iron dissolution from steel bars embedded in plain and in BHD-mortars.

4.3.3 Gravimetric corrosion analysis

In order to validate the electrochemical measurements of I_{corr} values, and to obtain a clearer picture of the effect of the BHD addition on the corrosion behaviour of steel bar, the corrosion weight losses per unit area (mg/cm^2) were measured as described in subsection 3.3.6. From the same steel bars used for electrochemical measurements, weight losses compared to control specimen (0 BHD and 0 % chloride) were measured and the equivalent weight losses were calculated from I_{corr} values showing a reasonable agreement as illustrated in Figure 4-10. Each column in the chart represents an average value of three steel bars' weight losses embedded in replicate mortar specimens. In the absence of added chloride, the weight losses of steel bars embedded in 2 % BHD mortars were found to be slightly higher than those in control specimens although more noble values of E_{corr} were found in BHD mortar compared to control specimens after 101 days of exposure and onwards. However, this result is in agreement with I_{corr} values obtained from the same steel bars where the I_{corr} values were found to be higher in BHD mortar compared to control specimens. The addition of 2 % BHD into mortar containing 0.4 and 2 % chloride reduced the corrosion rate slightly compared to specimens made without BHD and containing the same level of chlorides. This was confirmed by weight loss measurements that were obtained from the corresponding steel bars. The addition of chloride i.e. 0.4 and 2 % accelerated the corrosion of the steel bars that were embedded in 0 and 2 % BHD mortar which was confirmed by gravimetric analysis, see Figure

4-10. The results obtained from gravimetric analysis are in line with the values of the electrochemical measurements which validate the measured values of I_{corr} obtained during electrochemical monitoring. An example of how I_{corr} values were converted to weight losses using Faraday's law is illustrated in Appendix B.

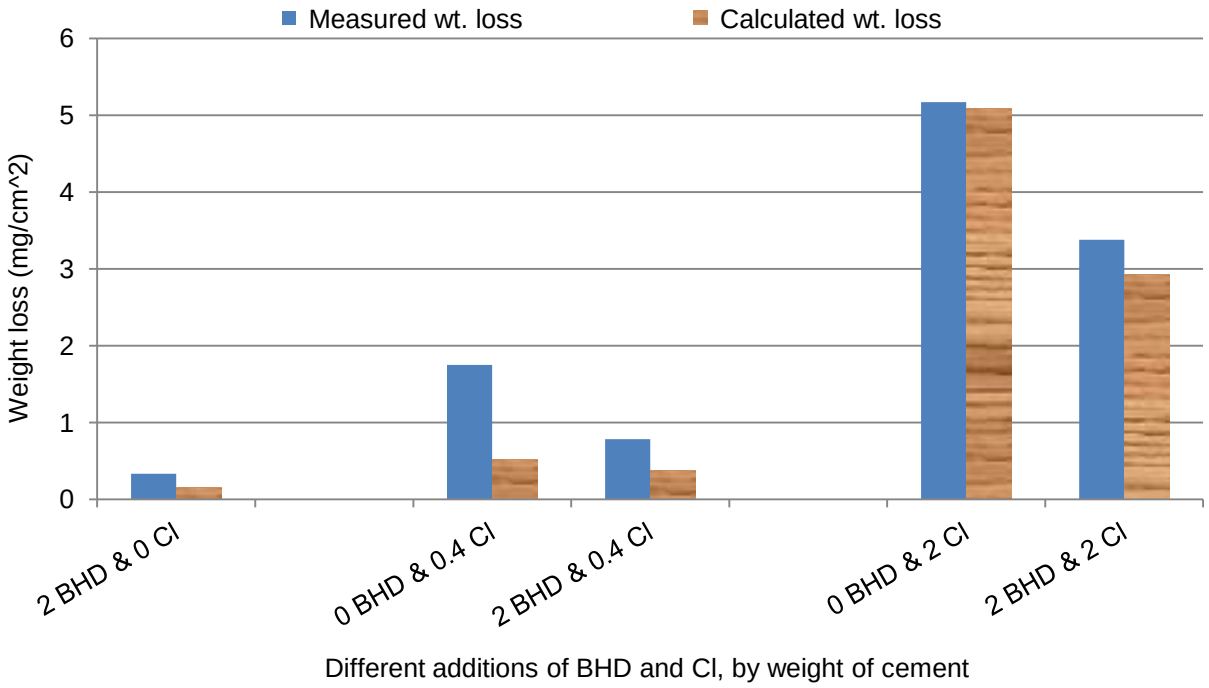

Figure 4-10 Calculated and gravimetric weight losses obtained from steel bars embedded in mortar mixed with and without BHD addition and containing 0.4 and 2 per cent chloride

4.3.4 Visual observation

In this experiment, plastic ties were used to simulate one aspect of the site defects as explained in subsection 3.3.3. Another reason for using these plastic ties was to provide a suitable environment to initiate and accelerate corrosion due to the short time of this experiment. The extent of rust on steel bars embedded in mortar contaminated with different levels of chloride and incorporating 0 and 2 % BHD by weight of cement is illustrated in

Figure 4-11. This figure shows that, most of the corrosion took place just under the plastic ties which shows that the use of plastic ties as a defect is reproducible in providing a suitable environment and conditions at the steel-concrete interface to initiate corrosion preferentially. For illustration purposes, the numbering system that appears in the figure can be demonstrated as follows;

For instance, specimen no. 0-0.4-1;

Where,

0 is the percentage of BHD added into the mix by weight of cement,

0.4 is the percentage of chloride added into the mix by weight of cement,

1 is the specimen replication number.

The extent of rust on steel bars embedded in mortar increased, as can be observed in Figure 4-11, with increasing chloride levels in the mixes. In addition to this, the addition of 2 % chloride into mortar led to more severe corrosion compared to that on all other specimens. In the case of mortars mixed with 2 % BHD and containing nil chloride, there was a sign of corrosion (red spots under the plastic spaces, see specimens no. 2-0-1 and 2-0-2 in Figure 4-11) whereas there was no sign of corrosion in steel bar embedded in mortar made without BHD addition and with nil chloride, (see specimens no. 0-0-1, 0-0-2 and 0-0-3 in Figure 4-11). This is consistent with the fact that the weight losses obtained from steel bars embedded in 2 % BHD mortars were higher compared to those found in control specimens, see Figure 4-10. This type of corrosion on the steel bars is most probably crevice attack associated with the area of low level of oxygen under the artificial defect. Pitting corrosion

was also observed in some corroded bars which was probably due to the formation of macro defects at the steel bar-defect-concrete interface. Such defects are more likely to occur if there is a possibility of settlement or water bleeding. This initiated the idea to investigate the effect of BHD addition on the water bleeding process, see Part B of Chapter 6.

The rebar embedded in mortar mixed with 2 % BHD and containing 0.4 % chloride exhibited less corrosion than that in mortar made without BHD addition and containing the same addition of chloride. More severe corrosion was observed on steel bars embedded in mortar made without BHD and containing 2 % chloride compared to steel bar embedded in mortar mixed with 2 % BHD and containing the same level of chloride. For example, the rebar was severely corroded through its length, see specimen 0-2-1, whereas the extent of corrosion was limited to the area under the plastic spaces as seen on specimen no. 2-2-1, 2-2-2 and 2-2-3.

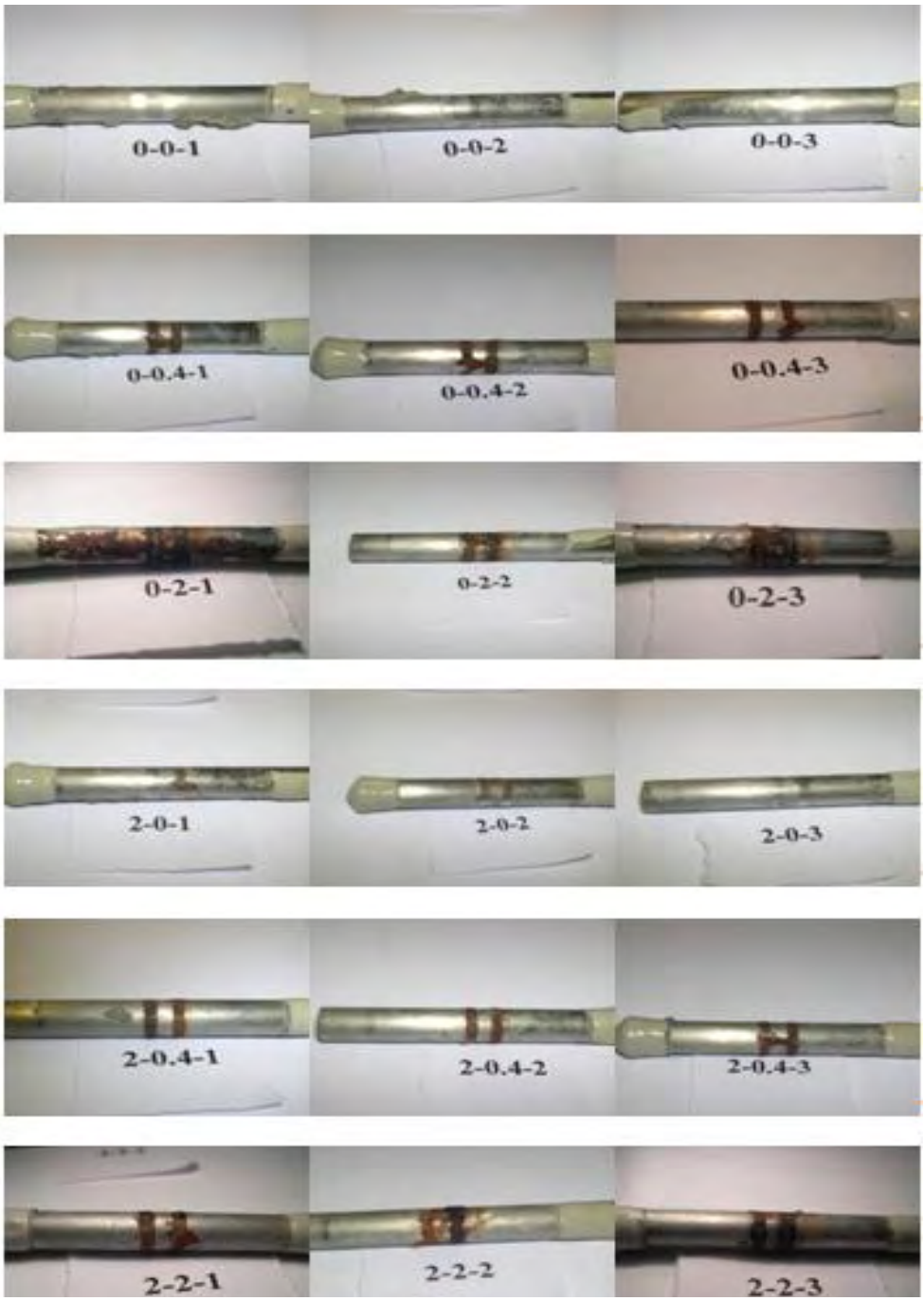

Figure 4-11 The extent of rust in steel bar extracted from mortar containing different levels of chloride and containing 0 and 2 per cent BHD

4.4 CONCLUSIONS

In this experiment, the corrosion potentials and corrosion current densities were measured to assess the effectiveness of BHD addition in the mitigation of steel bar corrosion in mortar specimens, prepared with various levels of chlorides. The addition of BHD into mortar containing 0, 0.4 and 2 % chloride by weight of cement resulted in slightly less negative corrosion potentials accompanied with lower corrosion current densities compared to mortar made without BHD and containing the same level of chlorides. The only exception to this was for steel bar embedded in BHD mortar and made with no chloride addition that exhibited higher I_{corr} values compared to the steel bar embedded in control mortar (0 % BHD and 0 % chloride).

This reduction in I_{corr} values accompanied with less negative E_{corr} values in BHD mortar could be attributed partly to the composition of the pore solutions extracted from the BHD mortars where higher OH^- concentrations were found in most of the BHD mortars at different ages compared to those in mortars without BHD. Furthermore, this improvement in corrosion resistance could also be partly due to the influence of the BHD particles in improving the physical properties of the BHD-specimen such as porosity.

PART B: EFFECT ON PORE SOLUTION CHEMISTRY

4.5 INTRODUCTION

Steel bar embedded in concrete is normally protected against corrosion by the high alkalinity of concrete pore solution that maintains the protective passive layer on the metal surface. As reviewed in Chapter 2, some chloride salts when they penetrate into concrete from the external environment or when introduced into the mix, will be bound by cement hydration products (Page, 2007). This depends on several factors such as cement type, water/cement ratio and total chloride content (Arya et al., 1990, Page et al., 1986). However, not all the chlorides will be bound but some will remain free. The unbound chloride (free chloride) that remains in the pore solution is believed to be the main ion that can destroy the passivity of the steel bar (Kayyali and Haque, 1995, Suryavanshi et al., 1998). Therefore, concrete that has a higher binding capacity for chloride should provide a greater protection from the corrosion process to the steel bar embedded in it.

Reduced alkalinity (hydroxyl ion concentration) in the pore solution is another significant factor that can cause depassivation of the steel bar when it is reduced to a critical pH value of less than 11.5 (Gouda, 1970). In fact, the relative concentrations of chloride ions and hydroxyl ions in the pore solution provide an indication of the aggressivity of the pore solution towards embedded steel. Therefore, it is very important to study the effect of BHD addition into the concrete on the pore solution chemistry and for this purpose it was necessary to establish a simple method, which could be set up with the facilities available in the School of Civil Engineering at the University of Birmingham. An account of this simple in situ

leaching method is presented in the next section, followed by experimental details and the result analysis and discussion sections.

4.6 IN SITU LEACHING METHOD BACKGROUND

The in situ leaching method employed in this research to study the effect of BHD addition on pore liquid phases was as described by Caseres et al. (2005). This method was first developed to determine the pH of the concrete and mortar pore water (Sagues et al., 1997). After that, it was used to measure the concentration of nitrite in concrete pore water (Li et al., 1999). Further study was carried out by Caseres et al. (2005) to demonstrate the applicability of the use of the in situ leaching method in determining the chloride ion concentration and pH value in concrete pore water. They found that, the chloride concentration and pH values obtained using the in situ leaching method were in agreement with those results obtained by using the well-established pore expression technique (Longuet et al., 1973). The only limitation of the in situ leaching method is the loss of pore water so that the cavity becomes empty. This could be overcome by minimizing the number of openings of the cavity and by sufficient water saturation during preconditioning. The in situ leaching method is simple to implement, safe and not expensive to conduct in comparison with other techniques for the extraction of pore liquids such as the method devised by Longuet et al. (1973) which is destructive and requires safety precautions since high pressure is applied during the expression process and involves a complete crushing of the specimen.

4.7 EXPERIMENTAL PROCEDURE

4.7.1 Preparation procedure for pore liquid studies

Two groups of mixes were prepared to study the behaviour of pore liquids in mortars. All these mixtures were prepared with different levels of chlorides and BHD. The mix proportions used for group (1) and group (2) are given in Table 4-2. The chloride was introduced to the mixture by dissolving the required quantities of NaCl in the mixing water. Six specimens were cast from each mix.

The mortar mix had a W:C:S ratio of 0.5:1.0:2.25 by weight and the mixing procedure was carried out as described in subsection 3.2.1. Each mix was cast in a plastic cylinder mould, 70 mm long and 100 mm in diameter. After 24 hours, the cylinders were demoulded and kept in a closed container. The bottom of the container was kept filled with water at all times and the samples were also covered by wet burlap to maintain a relative humidity of approximately 100 % for 30 days. The surfaces of the mortars were mist sprayed by distilled water during a preconditioning period of 30 days. Soda lime was placed inside the container to adsorb any CO_2 gas and the containers were covered by their caps.

Table 4-2 Mix proportions used for pore liquid studies

Group No.	BHD, %	Chloride, %
(1)	0	0, 0.4 and 2
(2)	2	0, 0.4 and 2

4.7.2 Test procedure

At the end of the preconditioning period, 3 cavities 20 mm apart were drilled perpendicular to the surface of each mortar. Each cavity was 5 mm in diameter and 35 mm in depth. Next, all cavities were carefully cleaned to remove dust. Around each cavity opening, a plexiglas cap was fixed with epoxy adhesive. A fixed volume of distilled water was injected into each cavity (Vw = 0.5 cm^3). Then, specimens were returned to the sealed container at 100 % relative humidity and kept at 20 ± 2 °C until the time of extraction. Figure 4-12 shows the schematic diagram of the mortar used for the pore liquid studies.

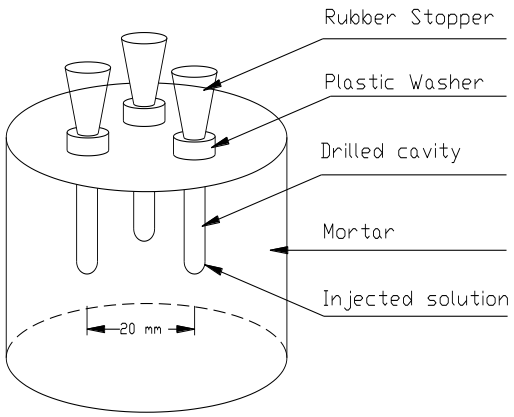

Figure 4-12 Schematic diagram of mortar used for pore liquid analysis

The pore liquids were extracted from mortar specimens and analyzed to obtain free chloride and hydroxide ion concentration after 3, 7, 21 and 60 days of curing. The hydroxyl ion

concentration was assessed by titration, as described in subsection 3.4.1. The chloride analysis procedure is presented in subsection 3.4.2.

4.8 RESULTS ANALYSIS AND DISCUSSION

4.8.1 Influence on chloride ion concentration

The free chloride ion concentration in the pore solutions, extracted from plain specimens containing different level of chlorides, against curing periods is plotted in Figure 4-13. It can be observed from Figure 4-13 that, the addition of different levels of chloride, 0.4 and 2 % by weight of cement, resulted in a simultaneous increase in the free chloride ion concentration in the pore solution as chloride levels (in the form of sodium chloride) increased. A similar trend in the results was noticed in free chloride ion concentration in the pore solution extracted from 2 % BHD mortar that containing the same levels of chloride, see Figure 4-14.

The effects of nil and 2 % BHD addition on the pore solution chemistry evolution containing different levels of chloride are shown in Figure 4-15 through Figure 4-17. In the case of chloride free mortars, the free chloride ion concentration in the pore solution extracted from 3, 7 and 21-days-old specimens was higher in BHD specimens compared with control specimens (0 % Cl and 0 % BHD) as demonstrated in Figure 4-15. Surprisingly, after the hydration process proceeded further, this value in BHD specimens was less than the value in control specimens after 60 days curing. It is difficult to explain this result, but it might be related to the ability of cement to remove of some of the chloride due to the formation of cement hydration products since the strength of 2 % BHD concrete was found to be higher than that

in control specimen, see section 7.3. All the free chloride ion concentration analysis data is presented in Appendix C.

In 0.4 per cent chloride addition specimens, see Figure 4-16, the addition of 2 per cent BHD into the mortar caused an increase in the free chloride ion concentration in the pore solution compared to the control specimens. The concentration of free chloride ion in the pore solution extracted from mortar that contained 2 % BHD addition and 2 % chloride was less than that in the control specimen when the pore solution was extracted after 3 days of curing suggesting that the ability of chloride removal in the control specimens depends on chloride content. Page et al., (1991) found that at higher levels of chloride (i.e. 1 %) the capability of cement to bind chloride was reduced and resulted in a substantial proportion of chlorides remaining free in solution. Again, the free chloride concentration found in pore water extracted after 7, 21 and 60 days curing remained high for 2 % BHD-mortar compared to specimens made without BHD and both prepared with 2 % chloride, as shown in Figure 4-17. These results, in most of the specimens, indicated that the addition of BHD into mortar caused an increase in the free chloride ion concentration in the pore solution compared to the chloride concentration found in mortars cast without BHD.

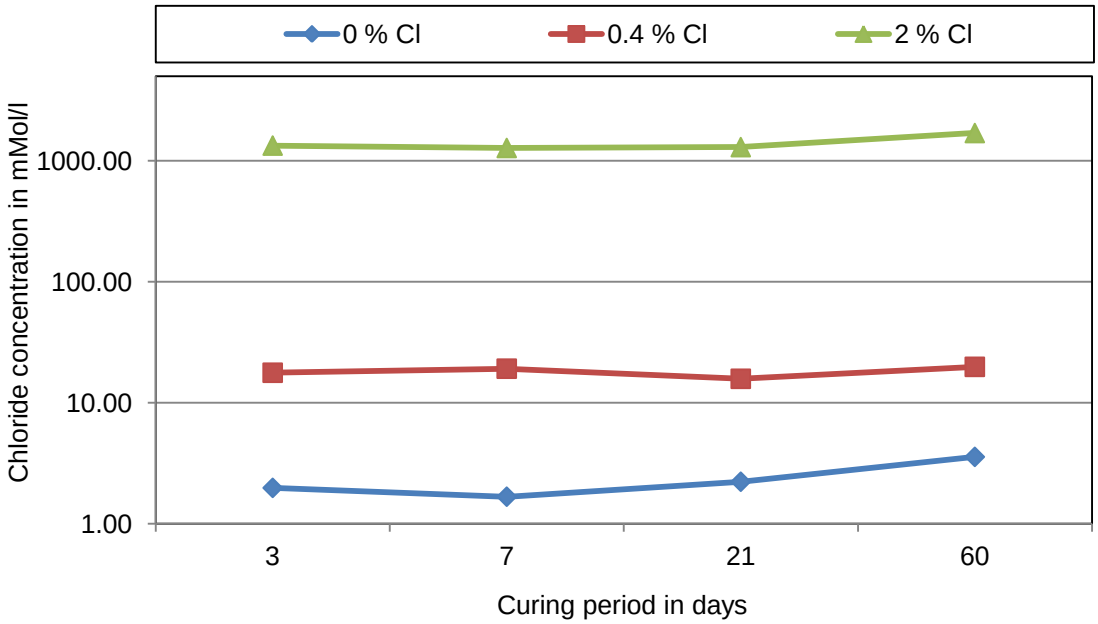

Figure 4-13 Effect of different levels of chloride on the free chloride ion concentration in the pore solution extract from mortars cast without BHD addition

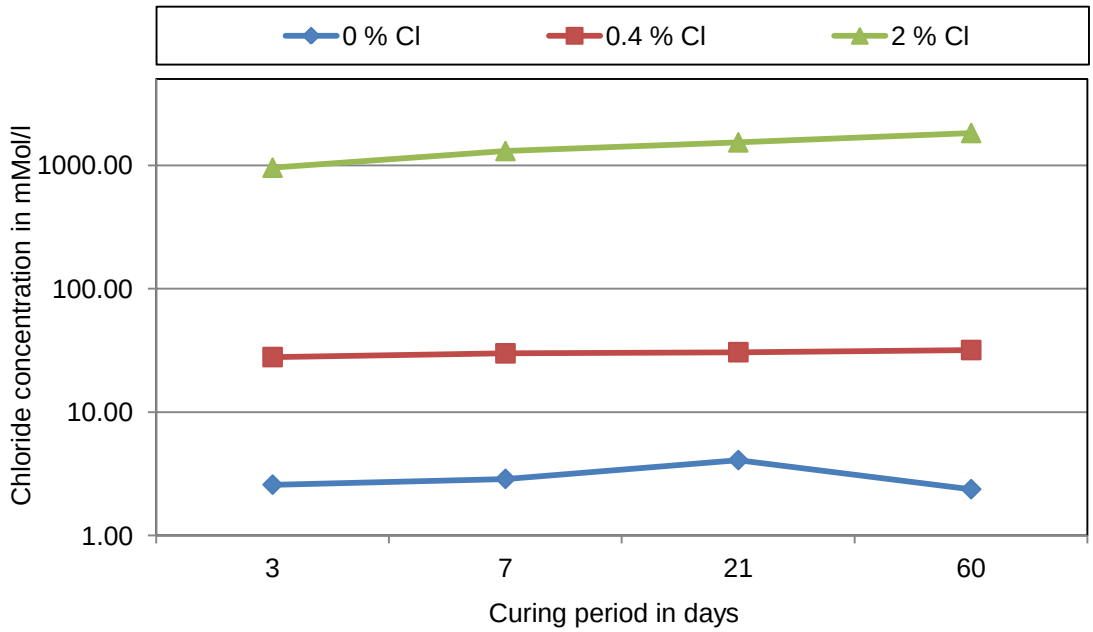

Figure 4-14 Effect of different levels of chloride on the free chloride ion concentration in the pore solution extract from mortars cast with 2 per cent BHD addition

The chemical composition of the BHD indicates that 2.25 per cent chloride existed in the BHD, as shown in Table 3-2. In the present work, 2 percent of BHD was used as addition by weight of cement which suggests that the mixture will be contaminated with 0.045 per cent chloride by weight of cement when 2 percent of BHD is added. If some of the chloride is considered to be soluble in water, this high free chloride concentration found in the BHD mortar may attributed to the dissolved chloride in the pore solution that is available from the BHD added. To confirm this, more efforts were spent trying to understand the behaviour of the chloride that existed in BHD material when mixed with different leaching solutions. More details about the results of chloride leaching tests from BHD materials are presented in Part C of this Chapter.

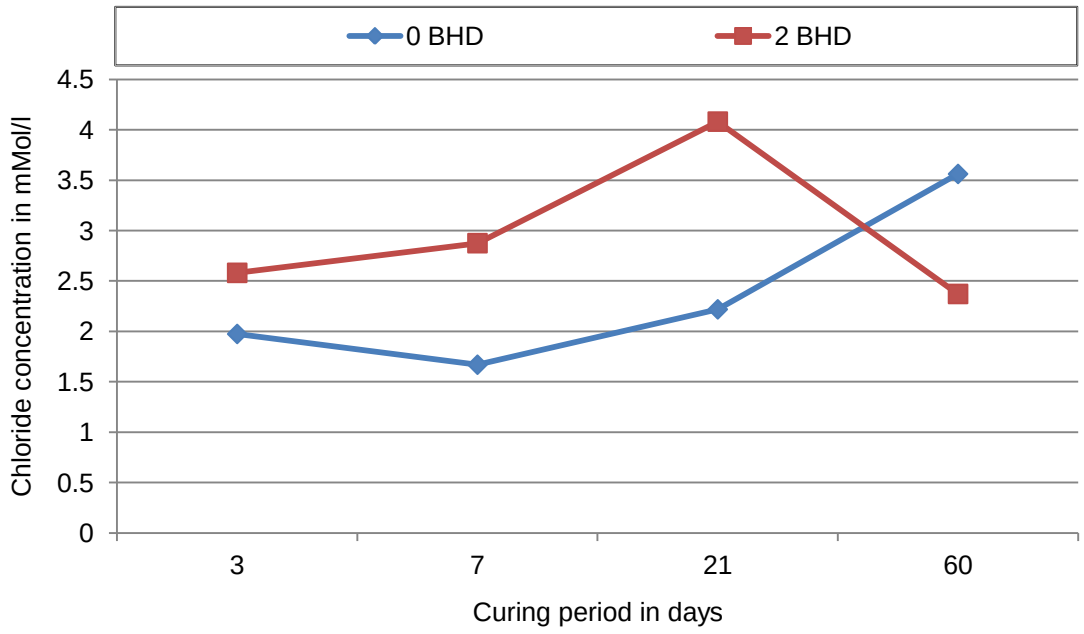

Figure 4-15 Chloride ion concentration in pore liquids extracted from control (0 BHD) and BHD mortar specimens without chloride addition at different ages

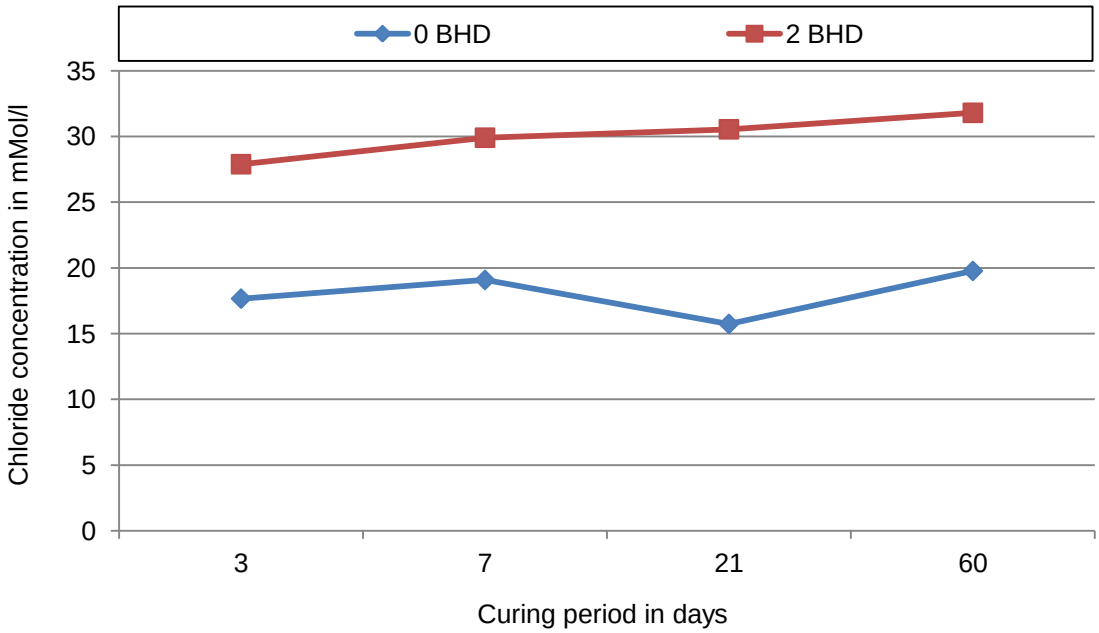

Figure 4-16 Chloride ion concentration in pore liquids extracted from control (0 BHD) and BHD mortar specimens with 0.4 per cent chloride addition at different ages

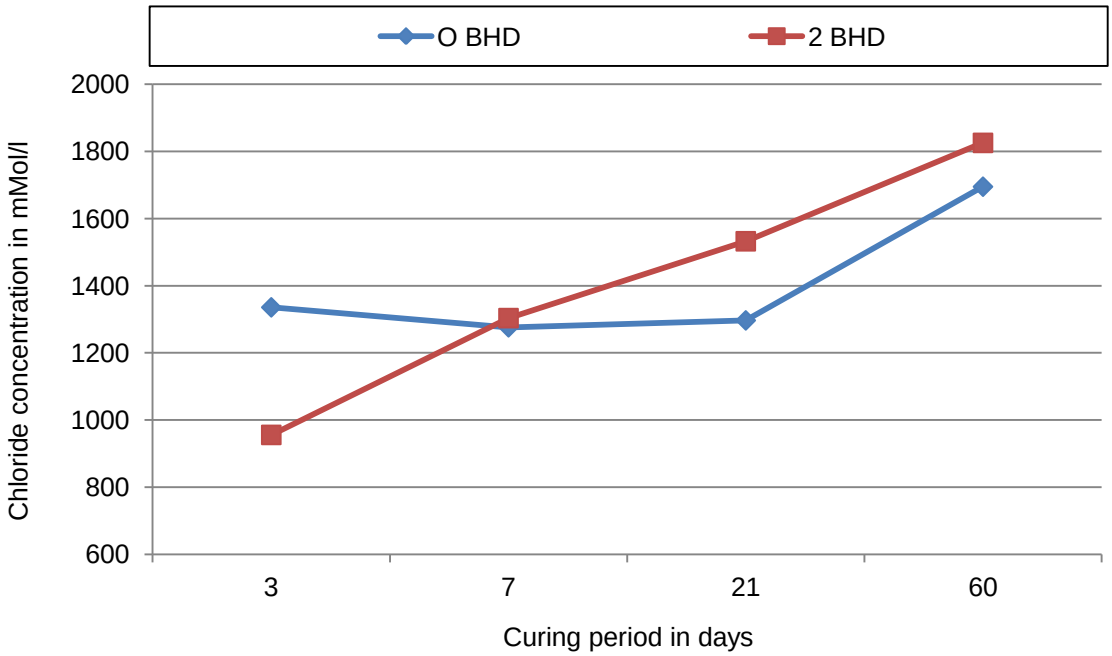

Figure 4-17 Chloride ion concentration in pore liquids extracted from control (0 BHD) and BHD mortar specimens with 2.0 per cent chloride addition at different ages

The influence of hydroxyl ion concentration in the pore solution of hardened cement paste on chloride binding was studied by Tritthart (1989). It was found that, the chloride concentration depends on the composition of the pore liquids and particularly on the hydroxyl ion concentration; the chloride ion concentration increased as the pH of the storage solution increases from 12.5 to 13.7. This increase of the free chloride ion concentration in the pore solution was attributed by Tritthart (1989) to the competition between hydroxyl ions and chloride ions for adsorption sites on the hydrated cement surface. It was found from pore liquid analysis that, as discussed in section 4.8.2, the hydroxide ion concentrations of BHD mortars were higher than those of control specimens. Since the addition of BHD raises the hydroxyl ion concentration in the pore solution, this increase in the chloride concentration in the pore solution extracted from BHD mortar could be explained tentatively by suggesting that all the adsorption sites on the hydrated cement surface are occupied by hydroxyl ions that were available in excess in the pore solution due to the addition of BHD. The chloride ions will be then adsorbed (bound) if the adsorbed hydroxyl ions are released/removed from the surface of the hydrated cement.

If this is the case, then a higher degree of competition between hydroxyl ions and chloride ions in the pore solution for the adsorption sites may occur, consequently high concentration of free chloride ions (because most of the adsorption sites are occupied by OH^-) combined with high hydroxyl ions will be available in the pore solution due the addition of BHD. According to Roberts (1962), when the alkalinity of the solution increases the solubility of the calcium chloro aluminate is increased and hence more free chloride ions are also released.

There are different mechanisms by which some of the chloride ions could be bound. Roberts (1962) found that the free chloride ion concentration was less for sulphate-resisting Portland cement than for ordinary Portland cement and this was attributed to the C_3A component in the cement which will enhance binding capacity due to the formation of Friedel's salt. Similarly, Holden et al., (1983) reported that the free chloride concentration in various cement pastes of constant w/c with 0.4 % added chloride was in the following order;

SRPC >> OPC (A) > OPC (B)

The major difference between these cements was C_3A content of the cement, where SRPC contained 1.9 %, OPC (A) contained 7.7 % and OPC (B) contained 14.3 %. They attributed this increase in the free chloride ion concentration as illustrated above to the lower component of the C_3A in SRPC which may result in decreasing the ability of the SRPC to form Friedel's salt ($3CaO.Al_2O_3.CaCl_2.10H_2O$). The effect of tricalcium aluminate content of cement on corrosion of reinforcing steel in concrete was also investigated by Rasheeduzzafar et al., (1990) which showed that the concentration of free water-soluble chloride ions decreased significantly as the C_3A content of the cement increased from 2, 9, 11 to 14 %. This reduction in the free chloride ions was attributed to the ability of the high C_3A content cement to bind the free chloride ions by the formation of insoluble calcium chloro aluminate compound. From the above, it can be observed that some of the chlorides will be bound due to the formation of Friedel's salt. Therefore, the formation of Friedel's salt could be inhibited during the hydration of cement due to the retardation effect of the BHD, thus resulting in reducing the consumption of the free chloride ions that are available in the pore solution.

4.8.2 Influence on hydroxyl ion concentration

The effect of 2 per cent BHD addition on the alkalinity of the pore liquids extracted from mortars containing different levels of chlorides versus hydration times is shown in Figure 4-18 to Figure 4-20. In the absence of chlorides, Figure 4-18 indicates that the addition of BHD has an effect on the concentration of OH^- ion in the pore solution extracted from these mortars. The addition of 2 % BHD causes an increase in the OH^- concentration compared to that in control specimens at all hydration ages. A study of the effect of 2 % BHD addition in cement paste pore solution chemistry reported by Al-Mutlaq and Chaudhary (2007) showed a raising of OH^- concentration in the pore solution that is extracted from BHD cement paste compared to control specimens (0 % BHD addition), where these results are in line with the results of present work. The differences between OH^- concentration in BHD mortars and control specimens decreased as hydration times increased.

The concentration of OH^- in the pore solution extracted from mortar cast with 2 % BHD addition and containing 0.4 % chloride addition by weight of cement is more than that in mortar containing the same level of chlorides but without BHD addition at all hydration periods, as shown in Figure 4-19. In both cases, the OH^- concentration decreased as hydration time increased from 3 days to 7-days and then increased as curing time increased from 7 days to 60 days.

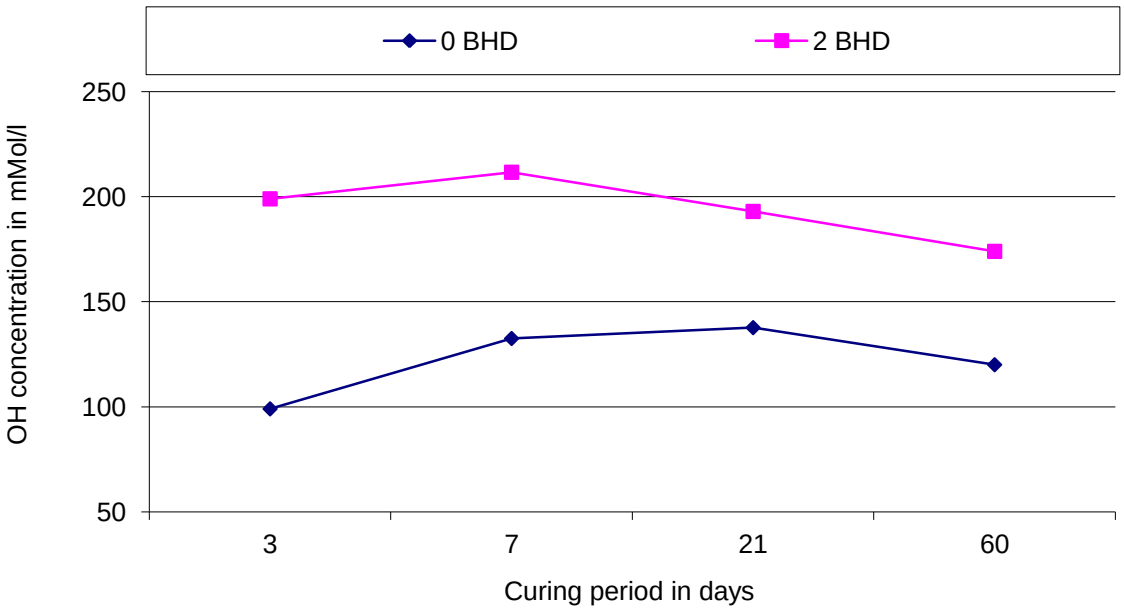

Figure 4-18 Effect of BHD addition on OH^- concentration of mortar specimens cast without any addition of chloride at different ages

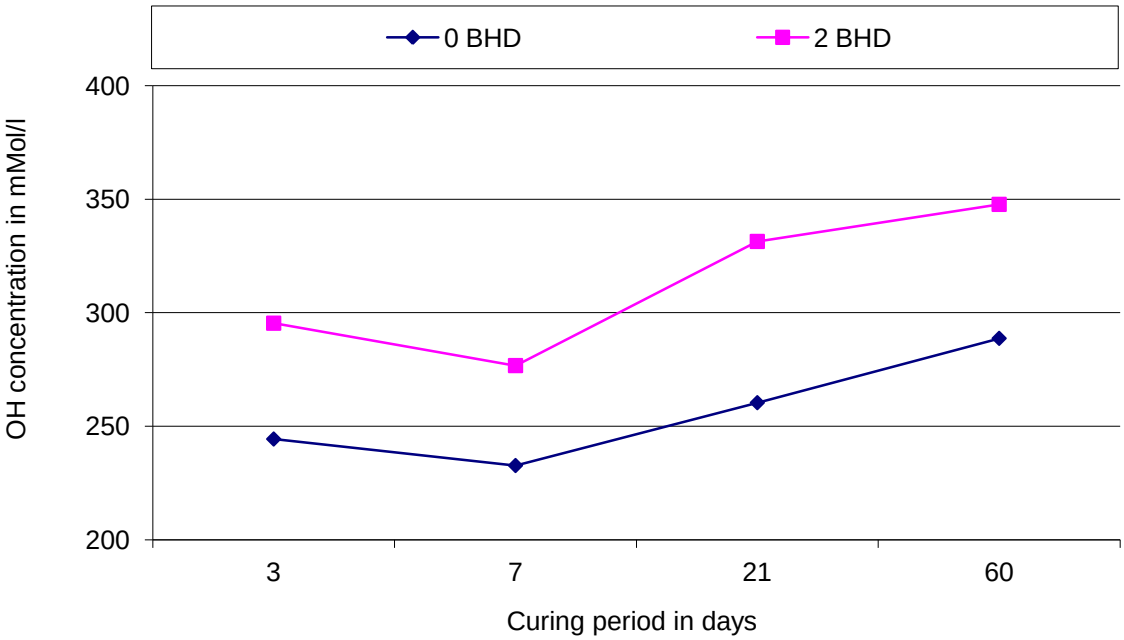

Figure 4-19 Effect of BHD addition on OH^- concentration of mortar specimens containing 0.4 per cent addition of chloride at different ages

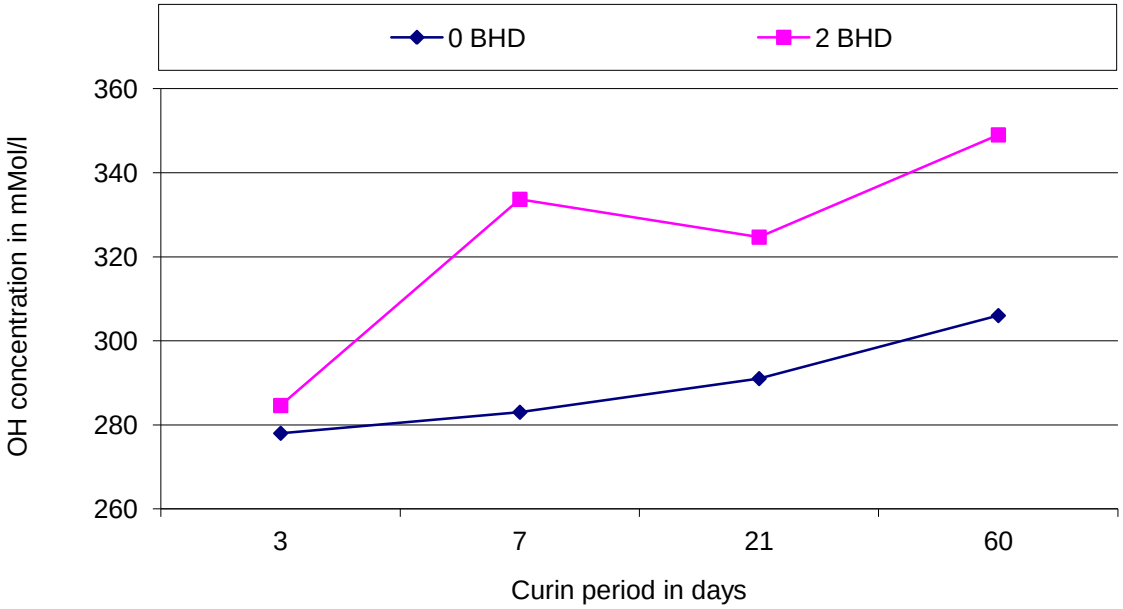

Figure 4-20 Effect of BHD addition on OH^- concentration of mortar specimens containing 2.0 per cent addition of chloride at different ages

Figure 4-20 indicates that the OH^- concentration in the pore solution extracted from 2 % BHD mortar and containing higher chloride level (2 %) is higher than those found in mortars that contained 2 % chloride and were made with no BHD addition. This higher OH^- concentration in BHD specimens was found at all hydration times. Furthermore, the OH^- concentration in the pore solution extracted from both mortar groups (0 and 2 % BHD addition) increased gradually as curing times increased as illustrated in Figure 4-20. All the OH^- concentration data are presented in appendix A. The work done by Al-Sugair et al. (1996) in the use of electric-arc furnace by-products in concrete revealed that higher pH values were obtained immediately after mixing (1-10 minutes) when 2 and 3 % of cement was replaced by BHD compared to control specimens (without BHD replacement), whereas after 7 days they found the pH values were higher in the control specimens compared to BHD specimens.

Figure 4-21 and Figure 4-22, show the effects of sodium chloride on the concentration of OH^- in the pore liquids extracted from mortar mixed with and without 2 % of BHD and containing different levels of sodium chlorides (nil, 0.4 and 2 % by weight of cement). It is clear from these results that the addition of sodium chloride has an effect on the OH^- concentration in the pore solution. From these figures, it is notable that the OH^- concentration increased significantly in pore solutions extracted from mortar containing 0.4 and 2 % chloride and made with and without 2 % BHD compared to OH^- in pore solutions extracted from mortar containing nil chloride and made with and without BHD addition. The influences of chloride and sulphate ions on durability was investigated by Holden et al., (1983). The results of this study support their findings as they reported that for two types of ordinary Portland cements, the concentration of OH^- in the pore liquids increased as the addition of chloride increased from 0 to 0.4 per cent by weight of cement in both cements. As indicated by Byfors et al., (1986) the addition of 1.0 percent sodium chloride by weight of cement increased the concentration of OH^- in the pore solutions. Similarly, the addition of 0.4, 1 and 2 % chloride as sodium chloride caused an enhancement of the OH^- concentration in the pore liquids as reported by Lambert et al., (1991). Similar findings were reported by Hansson et al., (1985). The results of this study are in line with others' findings.

According to Gouda (1970) greater alkalinity, pH more than 11.5, is required to maintain a stable passive film on steel bars. Therefore, sufficient alkalinity in the concrete is required to form and maintain the passive layer on the surface of steel bar embedded in the concrete and hence prevent corrosion attack (Page and Treadaway, 1982). It is important to point out however, this high alkalinity of the pore solution offered by BHD could increase the risk of alkali silica reactions if reactive aggregates are used (Domone, 2010).

This increase of OH^- concentration in BHD specimens is partly attributed to the addition of BHD. This result may be explained by the presence of some alkalies in the BHD material, as discussed later in Part C. Another possible explanation for this is because of added sodium chloride. Some authors such as (Yonezawa et al., 1989) have speculated that when sodium chloride is added to cement it will react with $Ca(OH)_2$ to form $CaCl_2$ while Na^+ and OH^- are released into the pore liquid and hence increase its alkalinity.

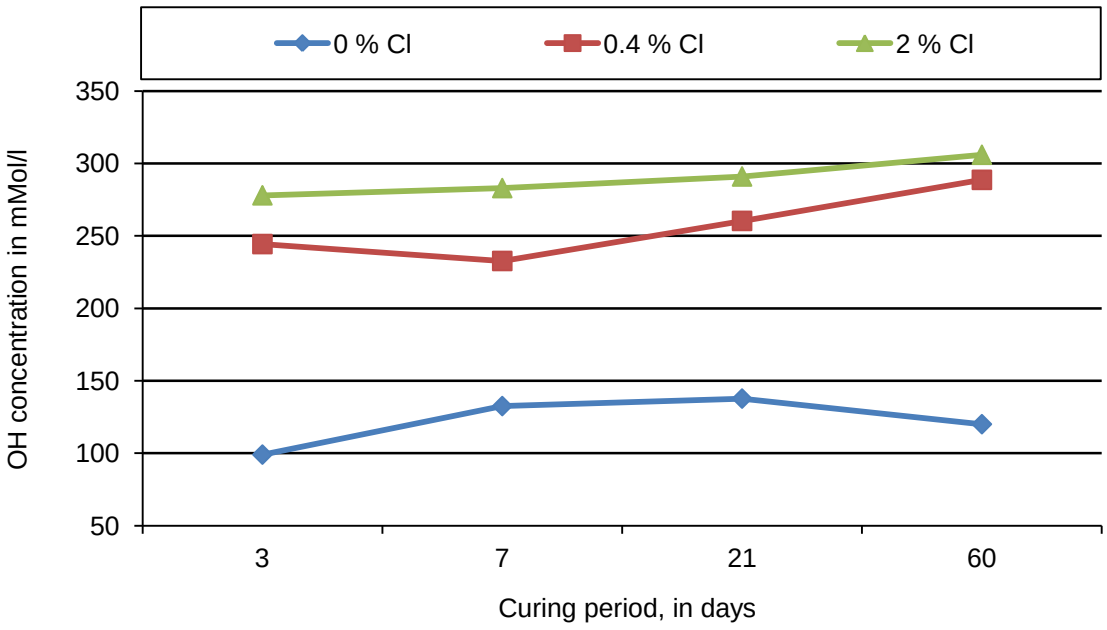

Figure 4-21 Effects of different levels of sodium chloride on OH^- concentration in pore liquids extracted from mortar made without BHD addition

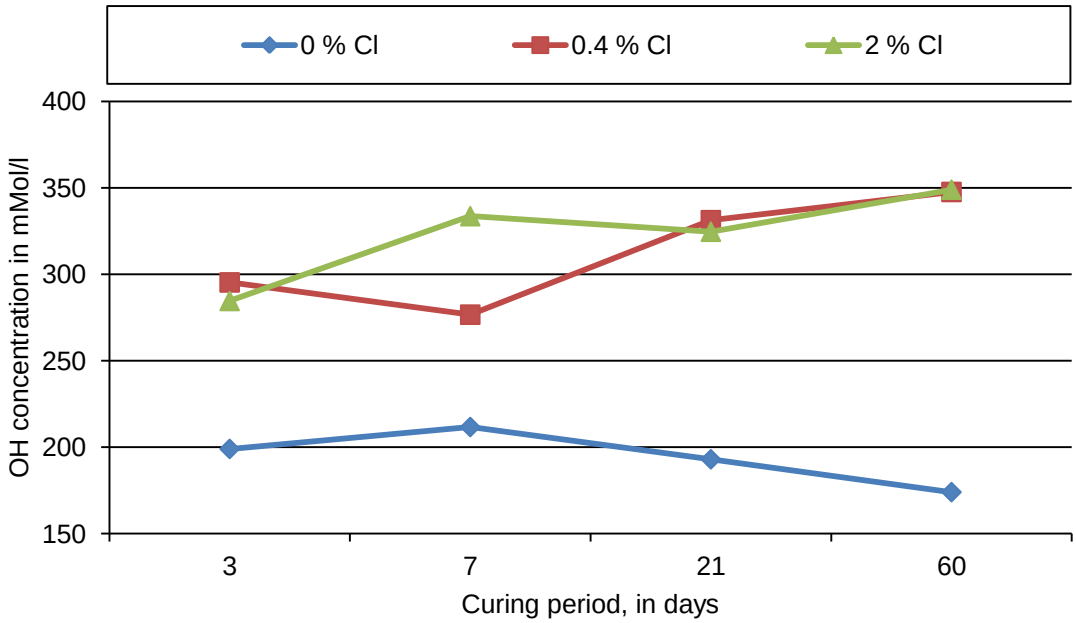

Figure 4-22 Effects of different levels of sodium chloride on OH^- concentration in pore liquids extracted from mortar made with 2 per cent BHD addition

The addition of BHD to mortar resulted in increased free chloride concentrations in the pore solutions, which suggests that the steel bars embedded in BHD mortar should have experienced higher corrosion than those bars embedded in mortar made without BHD addition. However, there were no major differences in corrosion resistance between the steel embedded in mortars made with and without BHD and 0.4 % chloride while a better corrosion resistance was observed in case of the steel bar embedded in BHD mortar compared to control mortar and both containing 2 % chloride, see section 4.3.1, in spite of the fact that BHD mortar has a significantly higher chloride free ion concentration in the pore liquid than that in mortar made without BHD. The steel bar embedded in concrete is normally protected by a passive layer against corrosion initiation and this is due to the high alkalinity of the pore solution in concrete. This corrosion protection mechanism that involves the passivity of steel is influenced by hydroxyl ions (Page and Treadaway, 1982). Hence, higher levels of OH^- ions

will help to maintain the passivity of the steel bar for a longer period suggesting that this high alkalinity could be one of the main factors that control corrosion processes in the BHD mortar. It was found by Hausmann (1967) that, there was no corrosion development when steel bar was immersed in a sodium hydroxide solution with pH value of 13.2 and containing 0.25 sodium chloride.

4.9 CONCLUSIONS

The effect of 2 % BHD on the anions present in the pore solution extracted from mortar made with and without chloride addition was investigated. It can be concluded that, in most specimens, the BHD has a significant influence on the chloride concentration in the pore water. The results indicated that the addition of BHD into mortar resulted in high free chloride ion concentrations compared to that in control specimens at all chloride addition levels (nil, 0.4 and 2 percent). This was true except for 60-day-old specimens cast without chloride (see Figure 4-15) and for 3-days-old specimens cast with 2 % chloride, see Figure 4-17 where the free chloride ion concentration in specimens made without BHD was found to be higher than that in specimens made with 2 % BHD addition. The increase of free chloride ion concentration due to the addition of BHD could be partly attributed to the presence of chloride in the BHD material where some of the chloride will dissolve in the pore water, partly due to an increase of the alkalinity of pore solution offered by BHD and possibly due to the effect of BHD in inhibiting the formation of Friedel's salt.

The addition of BHD plays a significant role in determining the hydroxyl ion concentration found in the pore solution. At all chloride addition levels, the hydroxyl ion concentration in

the pore solution extracted from BHD mortars was found to be higher compared to specimens made without BHD addition at all curing periods. This increase in the alkalinity in the BHD mortar could be attributed to the alkali content such as potassium oxide and sodium oxide that is available in the BHD material, as discussed in the next part.

The addition of sodium chloride led to an increase in the OH^- concentration in the pore solution extracted from both nil and 2 per cent BHD specimens compared to specimens cast without sodium chloride addition and this could be attributed to the release of Na^+ and OH^- in the pore solution due the reaction of sodium chloride with $Ca(OH)_2$ to form $CaCl_2$.

PART C: CHLORIDE LEACHING TESTS

4.10 TEST PROCEDURE

The main objective of this experiment was to evaluate the degree of chloride solubility in BHD material. A representative BHD sample was selected to determine the chloride concentration in the eluates. This representative sample was then dried at 105 ºC for 24 hours. A 5 gm sample of dried BHD was mixed with 50 ml of 0.2 M sodium hydroxide solution. The solution was rotated end-over-end for 24 hours. The solution was then filtered through a filter paper. The eluates were analysed to determine the chloride concentration. This procedure was repeated to determine the solubility of chloride and the pH value of another representative BHD sample mixed with distilled water (DW).

The chloride ion concentrations were determined using the procedure described in subsection 3.4.2. For pH measurement, the hydroxyl ion concentration in the solution was determined by titration as described in subsection 3.4.1. The pH value was then determined using the following equation:

$$pH = \log(OH^-) + 14 \qquad [4.1]$$

For the distilled water a SevenGp pH meter was used to measure the pH value.

4.11 RESULTS ANALYSIS AND DISCUSSION

The concentration of the chloride analysed from the leached solution is presented in Table 4-3 indicating a leaching of some of the chlorides present in BHD. Work on determining the concentration of chloride ion in EAFD sample that leached in water was carried out by Delalio et al. (1998). They reported that more than 96 % of chloride that exists in EAFD dissolved into the eluate. Sofili and Rastovan-Mio (2004) examined eluates prepared by mixing and shaking EAFD with redistilled water. The concentration of chloride was determined after 1, 10 and 30 days. They found concentrations of some anions such as chloride in the leached water that were constant over time.

However, a study carried out by Li and Tsai (1993) found that the chloride in EAFD could be present in a different form such $ZnCl_2 \cdot 4Zn(OH)_2 \cdot H_2O$. In their study, leaching tests, using distilled water and reagent-grade HCl solution at different concentrations, were performed. The results indicated that the $ZnCl_2 \cdot 4Zn(OH)_2 \cdot H_2O$ did not leach out when distilled water was used as leaching solution, whilst the $ZnCl_2 \cdot 4Zn(OH)_2 \cdot H_2O$ dissolved completely when the leaching solution was HCl and the concentration of the solution was greater than 0.5 M.

Table 4-3 Chloride concentration obtained from different leached solutions

Leaching solution	Sample #	mMol/l	Average
DW	1	51.08	57.45
	2	61.33	
	3	55.29	
	4	60.78	
	5	58.77	
0.2 NaOH	1	44.85	51.85
	2	52.72	
	3	54.92	
	4	55.11	
	5	51.63	

The degree of chloride solubility seems to be slightly affected by the pH of the solution. The leachability of chloride is noticed to increase as pH decreases. Table 4-4 illustrates the measured pH values obtained from different leached solutions in the presence of BHD and without. The addition of BHD increased the pH of the DW leached solution compared to the same leached solution but without addition of BHD (as control). The corresponding pH value of the BHD-DW leached solution was 13.17 and 6.34 for control leached solution indicating the effect of BHD incorporation on the pH of the leached solution.

The higher alkalinity of pore solution in the concrete depends on the amounts of alkali in the mixture. The dominant alkalis in the binder are potassium oxide (K_2O) and sodium oxide (Na_2O). These oxides are soluble in the water (Neville, 1995) and (Taylor, 1997). In the presence of water, they dissolve in water resulting in potassium hydroxide (KOH) and sodium hydroxide (NaOH) which will lead to a pore solution of high alkalinity reaching a value of pH in excess of 13 after few hours of hydration. In this study, it could be noticed from the BHD chemical composition (Table 3-2) that the BHD material contains a considerable amount of

potassium (K^+) and some sodium (Na^+) as high as 3.24 and 0.88 % by mass of BHD respectively. The addition of 2 percent BHD therefore significantly increases the alkali content in the mixture. The K_2O and Na_2O is rapidly soluble in water (Taylor, 1997) where this may allow for an excess of the KOH and NaOH in the pore water resulting in high alkaline solutions.

Table 4-4 Titrated pH values measured from different leached solutions

Dust	Leaching solution	Sample #	pH	Average
0	DW (Control)	1	6.27	6.34
		2	6.31	
		3	6.35	
		4	6.36	
		5	6.39	
	0.2NaOH	1	13.32	13.32
		2	13.32	
		3	13.33	
		4	13.32	
		5	13.32	
BHD	DW	1	13.14	13.17
		2	13.16	
		3	13.18	
		4	13.18	
		5	13.20	
	0.2NaOH	1	13.54	13.54
		2	13.54	
		3	13.53	
		4	13.55	
		5	13.54	

4.12 CONCLUSIONS

It can be concluded that some of the existing chloride in BHD material leached out confirming that the higher chloride ion concentration in the pore solution extracted from mortar mixed with BHD did originate from the BHD material. The solubility of chloride present in BHD was slightly affected by the pH of the leaching solution where more chloride leaches when the pH of leaching solution is reduced.

The results of this part confirm the effect of BHD on the pH of the pore water. The pH value in BHD-DW leached solution was higher than that in control DW leached solution indicating this increase in pH was due to the addition of BHD.

Chapter 5

EFFECT OF BHD ADDITION ON POROSITY AND CHLORIDE DIFFUSION

PART A: INFLUENCE ON CEMENT PASTE POROSITY

5.1 INTRODUCTION

The rate of deterioration of concrete structures is normally affected by the rate at which harmful substances can penetrate into the concrete. The rate of chloride penetration into concrete has been found to depend on many factors including the porosity and permeability of concrete as discussed in the next Part. Accordingly, concrete porosity is one of the most important parameters that influences the durability of concrete (Aitcin, 1994). Therefore, improving the engineering properties such as porosity will ensure good durable concrete that is essential when concrete structures are subjected to the penetration of aggressive substances. A low porosity material will not only result in low permeability concrete but will also enhance its strength (Domone, 2010). As the diffusivity of aggressive ions such as chloride is a major concern, producing a low porosity medium by using additives and a low w/c ratio is beneficial.

5.2 EFFECTS OF SCM ON POROSITY

Page et al., (1981) investigated the influence of blended cements by studying pore size distribution in cement pastes that were made with 0 % additive, 65 % ground granulated blast-furnace slag (BFS) and 30 % pulverized fuel ash (PFA) by means of mercury intrusion

porosimetry (MIP). The results showed that the BFS-cement pastes had the finest pore size distribution compared to PFA and control specimens whilst PFA cement-pastes were more porous than both the other materials (plain and BFS cement pastes) indicating different relationships between the porosity of cement pastes and their chloride diffusion resistances.

A set of results for the pore size distribution of blended cements (silica fume and fly ash) reported in a study carried out by Mehta and Gjørv (1982) showed that a higher pore size distribution was found in fly ash cement pastes than that in control specimens. After 90 days curing, however, the volume of large pores (>0.1 μm) in fly ash pastes was similar to that in control specimens and this was attributed to the slow progress of the pozzolanic reaction. In the case of silica fume-cement paste, the volume of large pores was less than that of the control specimens at all hydration periods (7, 28 and 90 days).

It is believed that the decrease in pore size in the blended cements is attributed to the transformation of calcium hydroxide that is produced during cement hydration to C-S-H which has a fine pore structure (Feldman, 1984). In work done by Kumar et al., (1987) it was shown that a decrease in mobility of Cl^- ions in Portland cement blended with silica fume, fly ash and blast-furnace slag was observed compared to control specimens. It was suggested that this decrease in the mobility is due to the finer pores of the blended cements which in turn increases the tortuous path for chloride ion migration from one point to another. Furthermore, Ngala et al., (1995) investigated the effect of 30 % fly ash (FA) cement pastes, on the total and capillary porosity and chloride diffusion rate. It was found that, the FA pastes have higher total porosity compared to OPC pastes whereas the capillary porosity in the FA pastes

was lower than OPC specimens made with the same w/s ratio. The effective chloride diffusion coefficients obtained from FA pastes were also found to be significantly lower than those in OPC pastes of the same w/s ratio. This suggests that the capillary porosity in OPC cement pastes has a higher continuity than that in FA-cement pastes (Ngala et al., 1995).

The quantity and characteristics of various types and size of pores in the cement paste play a major role in durability of concrete because they influence not only physical properties but also the mechanical properties of concrete. For instance, compressive strength is one of the most important concrete properties which is governed by the porosity of cement paste (Rostásy et al., 1980). Furthermore, the volume of all voids in concrete (entrapped air, capillary pores, gel pores and entrained air) has a direct influence on the strength of concrete. Replacement of cement by fly ash and silica fume was utilized to develop high performance mortar. The highest strength was noticed in all of the fly ash replacements (20, 30 and 40 % by weight of cement) that were prepared together with 8–12 % SF addition which also had the lowest porosity (Khan, 2003). A high-strength (100 MPa) concrete can be achieved by incorporation of SF (FIP, 1988) where the strength development was attributed to improvement in the bond between aggregate-cement paste and the corresponding smaller porous interfacial zone (Khan et al., 2000).

Further studies of the use of mixtures of high and low surface-area pozzolans, such as silica fume and fly ash, have shown improvement in strength of concretes compared to control specimens. This improvement in strength could be related to the transformation of free lime resulting in more C-S-H formation and to the pore size distribution of cement pastes. Furthermore, the progress of the pozzolanic reaction, in the case of blended cements, led to a

reduction in the volume of large pores (>0.1 μm). It was concluded that higher strength values were associated with the reduction in large pore volumes of cement pastes (Mehta and Gjørv, 1982).

Clearly, the use of certain supplementary cementitious materials has been found to have a positive effect on the coarse capillary porosity which in turn reduces the permeability to harmful agents. For comparison purposes and better understanding of the influence of various additions of BHD on some of the engineering properties, the effect of different levels of BHD addition on the capillary porosity was investigated in the following section.

5.3 EXPERIMENTAL PROCEDURE

5.3.1 Preparation of cement paste specimens

Two groups of specimens, A and B were made with 0, 2 and 3 % BHD addition by weight of cement. Each group was prepared at 0.4, 0.5 and 0.6 water to cement ratio. The cement paste mixing procedure was performed in the same way described in subsection 3.2.1. A sealable plastic container (cylindrical plastic mould with 29 mm diameter by 82 mm height) was filled with cement paste and vibrated for 2-4 minutes until the entrapped air bubbles were removed to the surface. The top of the cement paste with any air bubbles was removed by using a straight edge and more fresh cement paste was added to fill the container. Further vibrations, repeating the same process were carried out as necessary. After that, the container was covered by a polythene sheet and then sealed with its cap. The container was placed in an end-over-end rotating machine for at least 24 hours at 8 rpm to minimize bleeding and

segregation. After 24 hours rotation, all specimens were kept at 100 percent relative humidity curing in a fog chamber at temperature of 22 ± 2 ºC for two weeks. Then, all the specimens were demoulded and immersed in a 35 mM NaOH solution and stored in a room at temperature of 38 ± 2 ºC for 5 weeks for group A and, in case of group B the specimens, were immersed in the same solution and stored in a room at temperature of 38 ± 2 ºC for 10 weeks to ensure a high level of hydration was achieved since the BHD is regarded as a retarder (Ngala, 1995).

After completing the required period of curing, thin discs were cut from the central regions of the specimens for porosity measurements. This process was carried out using a tile saw with the blade lubricated by distilled water. Thicknesses of the obtained discs were 4 mm approximately. Thereafter, the specimen surfaces were ground with grade 600 emery paper, rinsed with distilled water and then dried with tissue paper before starting porosity measurements.

5.3.2 Test procedure

After completing the specimen preparation process, all discs were tested for coarse capillary porosity as described by Ngala (1995). Before the capillary porosity measurements, the obtained discs must be in a saturated surface dry condition. This can be achieved by immersing the discs in 35 mM NaOH solution and monitoring the weight change every 24 hours. The discs were then removed from the solution for the porosity measurements when a constant weight was achieved. To obtain the coarse capillary porosity, the saturated surface dry cement paste specimen was exposed to an atmosphere at a relative humidity (RH) of 90.7

% until a near-constant weight was achieved. A saturated salt solution of hydrated barium chloride ($BaCl_2.2H_2O$) was placed in airtight vacuum desiccators to achieve the RH of 90.7 %. Fresh air, which had been passed through two jars containing silica gel and soda lime to absorb any CO_2 to minimize the carbonation, was injected into the desiccators after each weighing of the discs. When a constant weight was achieved, the loss of weight on drying is due to the evaporation of water from the large capillary pores and this is known as coarse capillary porosity. The use of this particular type of capillary porosity measurement, which corresponds to pores wider than about 30 nm (Parrott, 1992), was adopted in this investigation mainly because of following reasons;

a) The procedure avoids unrealistic drying, which may cause porosity artefacts (Parrott, 1987),
b) This simple measurement of capillary porosity correlates with the rate of water absorption (Parrott, 1992).
c) The use of other techniques such as oven-drying techniques can result in damage to the pore structure (Gallé, 2001).
d) The use of mercury intrusion porosimetry (MIP) could result in rupture of the pore structure due to the high pressures used (Cheng-yi and Feldman, 1985).
e) Another limitation of using MIP is that it may result in incorrect pore sizes which are related to the "ink bottle" effect where the mercury should intrude successively to reach inside the specimen and fill all the pores (the large and small dia. pore) without any restriction in the path (Diamond, 2000).

f) Most of the gel pores and closed pores remain non-intruded when MIP technique is applied, resulting in inaccurate pore system characterisation (Kumar and Bhattacharjee, 2003).

5.3.3 Determination of bulk density

The durability of concrete structure that vulnerable to corrosion of reinforcement is clearly related to its density. The cement paste that has a high density will provide a high resistance against penetration of any harmful agents into the concrete. Also, major variations between replicate specimens can be assessed by bulk density measurements; therefore, bulk density measurements were conducted on all cement paste specimens that were used for porosity measurements as described by Ngala (1995).

To obtain the bulk density, the weight of cement paste specimen immersed in water was measured and recorded as "W_1". Thereafter, the specimen was removed from the water and wiped with tissue to achieve a saturated surface dry condition. The weight of specimen in air and with the saturated surface dry condition was recorded as "W_2". The bulk density is the weight of specimen in air divided by the loss of specimen weight in water and this can be determined according to Archimedes' principle;

$$\text{Bulk density} = \frac{W_2}{W_2 - W_1} \left(\frac{g}{cm^3}\right) \qquad [5.4]$$

5.3.4 Determination of coarse capillary porosity

After bulk density measurements and determining weights of "W_1" and "W_2", the cement paste specimens were exposed to an atmosphere of 90.7 % RH at a constant temperature of 22 ºC until a near constant-weight achieved and this was recorded as "W_3". More details in the experimental procedure can be found in subsection 5.3.2. Since water has a density of 1 g/cm^3, the void volume was calculated by weighing the specimen with saturated surface dry condition "W_2" and then drying the specimen till a constant weight was achieved "W_3", the loss in weight (W_2-W_3) represents the void volume. The ratio of the void volume to the total volume is the porosity. The total volume was measured by subtracting the weight of specimen in water "W_1" from the weight of specimen in air "W_2". The coarse capillary porosity can be then calculated using the following equation;

$$\text{Coarse capillary porosity } (\%) = \frac{(W_2 - W_3)}{(W_2 - W_1)} \times 100 \qquad [5.5]$$

5.4 RESULTS ANALYSIS AND DISCUSSION

Table 5-1 to Table 5-6 presents the bulk density and coarse capillary porosity for cement pastes of group A and group B that were both prepared at different w/c ratios of 0.4, 0.5 and 0.6 and containing 0, 2 and 3 % BHD.

For both groups, as was expected, the capillary porosity increased as the water content increased indicating the increased availability of water-filled space. Also, the results of the capillary porosity measurements for group B that had been hydrated for 10 weeks show that the capillary porosity was less in plain and all BHD-mixes that were prepared at various w/c

ratios compared to group A mixes. This reduction in capillary pore volume is due to the higher degree of hydration, hence more deposition of C-S-H gel. For instance, at w/c ratio of 0.5, the calculated capillary porosity percentage measured for plain cement paste is 6.99 for group B, while in group A at the same w/c ratio the calculated percentage of capillary porosity for plain cement paste is 9.58.

Table 5-1 Individual bulk density and coarse capillary porosity measurements obtained from plain cement pastes prepared at various w/c ratios and cured for 5 weeks

Spc. No.	w/c ratio	Bulk density (g/cm^3)	Coarse capillary porosity (%)
1	0.4	1.64	3.95
2		1.62	4.34
3		1.56	4.28
4		1.59	4.51
5		1.60	4.87
Avg.		**1.60**	**4.39**
1	0.5	1.47	9.26
2		1.46	9.04
3		1.52	9.75
4		1.46	9.71
5		1.50	10.12
Avg.		**1.48**	**9.58**
1	0.6	1.48	16.94
2		1.45	15.14
3		1.45	14.50
4		1.47	15.13
5		1.43	15.35
Avg.		**1.46**	**15.41**

Table 5-2 Individual bulk density and coarse capillary porosity measurements obtained from 2 % BHD-cement pastes prepared at various w/c ratios and cured for 5 weeks

Spc. No.	w/c ratio	Bulk density (g/cm^3)	Coarse capillary porosity (%)
1	0.4	1.64	2.51
2		1.66	2.74
3		1.65	2.69
4		1.65	2.94
5		1.61	2.65
Avg.		**1.64**	**2.71**
1	0.5	1.54	8.08
2		1.51	7.69
3		1.53	7.75
4		1.54	7.98
5		1.53	7.46
Avg.		**1.53**	**7.79**
1	0.6	1.43	13.45
2		1.43	12.38
3		1.46	12.64
4		1.46	12.42
5		1.45	13.67
Avg.		**1.45**	**12.91**

Table 5-3 Individual bulk density and coarse capillary porosity measurements obtained from 3 % BHD-cement pastes prepared at various w/c ratios and cured for 5 weeks

Spc. No.	w/c ratio	Bulk density (g/cm^3)	Coarse capillary porosity (%)
1	0.4	1.71	3.02
2		1.67	2.73
3		1.67	2.63
4		1.65	2.72
5		1.70	2.82
Avg.		**1.68**	**2.79**
1	0.5	1.63	6.83
2		1.55	6.62
3		1.50	6.48
4		1.53	7.36
5		1.53	6.51
Avg.		**1.55**	**6.76**
1	0.6	1.44	13.37
2		1.42	12.60
3		1.47	13.43
4		1.45	12.90
5		1.47	14.31
Avg.		**1.45**	**13.32**

Table 5-4 Individual bulk density and coarse capillary porosity measurements obtained from plain cement pastes prepared at various w/c ratios and cured for 10 weeks

Spc. No.	w/c ratio	Bulk density (g/cm^3)	Coarse capillary porosity (%)
1	0.4	1.67	3.83
2		1.64	3.79
3		1.68	3.03
4		1.64	3.33
5		1.66	3.47
Avg.		**1.66**	**3.49**
1	0.5	1.53	6.99
2		1.54	7.09
3		1.54	7.06
4		1.54	6.59
5		1.51	7.23
Avg.		**1.53**	**6.99**
1	0.6	1.45	13.34
2		1.45	13.70
3		1.41	13.33
4		1.43	13.80
5		1.42	12.29
Avg.		**1.43**	**13.29**

Table 5-5 Individual bulk density and coarse capillary porosity measurements obtained from 2 % BHD-cement pastes prepared at various w/c ratios and cured for 10 weeks

Spc. No.	w/c ratio	Bulk density (g/cm^3)	Coarse capillary porosity (%)
1	0.4	1.66	2.37
2		1.65	2.49
3		1.68	2.40
4		1.67	2.05
5		1.64	2.42
Avg.		**1.66**	**2.35**
1	0.5	1.55	4.10
2		1.54	4.43
3		1.54	4.51
4		1.51	4.35
5		1.55	4.52
Avg.		**1.54**	**4.38**
1	0.6	1.43	10.02
2		1.46	9.94
3		1.45	10.07
4		1.46	9.94
5		1.44	9.94
Avg.		**1.45**	**9.98**

Table 5-6 Individual bulk density and coarse capillary porosity measurements obtained from 3 % BHD-cement pastes prepared at various w/c ratios and cured for 10 weeks

Spc. No.	w/c ratio	Bulk density (g/cm^3)	Coarse capillary porosity (%)
1	0.4	1.63	2.97
2		1.62	2.71
3		1.63	2.88
4		1.66	3.02
5		1.65	2.68
Avg.		**1.64**	**2.85**
1	0.5	1.53	4.62
2		1.57	4.21
3		1.58	4.23
4		1.58	4.65
5		1.58	4.45
Avg.		**1.57**	**4.43**
1	0.6	1.46	9.51
2		1.48	9.96
3		1.46	9.39
4		1.49	9.38
5		1.47	8.94
Avg.		**1.47**	**9.44**

The capillary porosity measurements obtained from group A cement paste specimens made with 0, 2 and 3 % BHD and prepared at different w/c ratios are illustrated in Figure 5-1. Figure 5-2 demonstrates the capillary porosity measurements for group B (10 weeks hydration period) prepared with same mixing proportions as group A. All the presented values in these figures are averaged values for 5 discs obtained from each specimen.

The results of coarse capillary porosity measurements indicated a reduction in capillary pore volume due to the incorporation of 2 and 3 % BHD into cement pastes compared to plain cement paste specimens at all w/c ratios, as can be observed in Figure 5-1 and Figure 5-2. The reduction in capillary porosity due to addition of BHD is more pronounced when longer time was allowed for hydration (group B) as shown in Figure 5-2. When considering different levels of BHD, there is no significant effect on the coarse capillary porosity that was obtained

from 3 % BHD-specimens when compared to that in 2 % BHD-cement paste specimens. This indicates that 2 % is the optimum level of BHD addition and more than that will not cause significant reduction in the capillary pore volume.

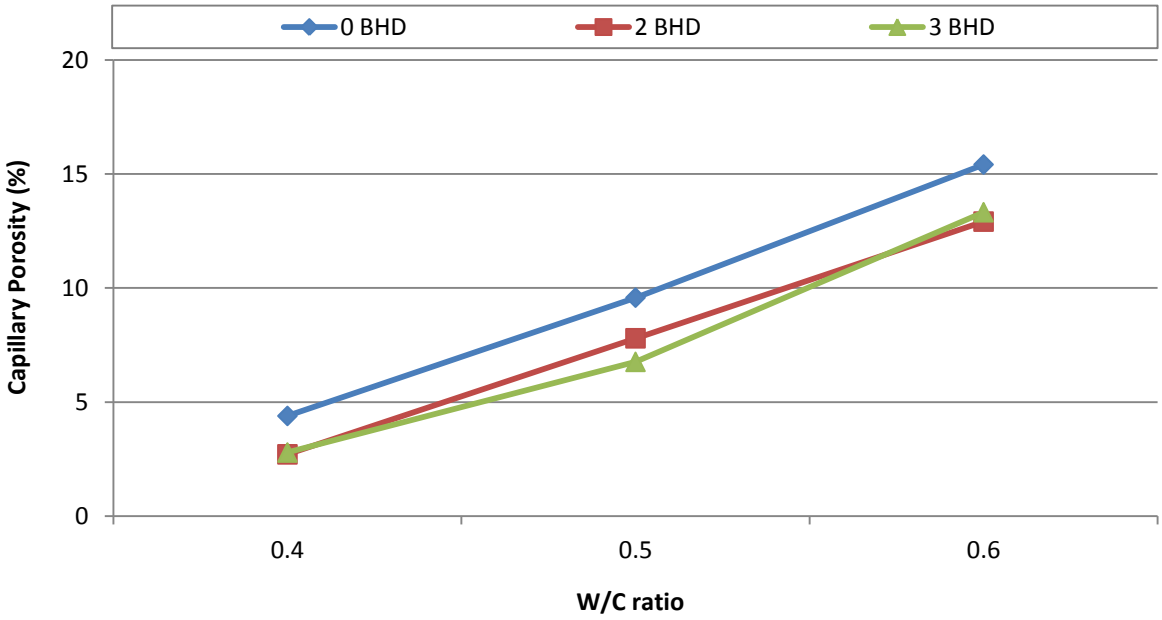

Figure 5-1 Capillary porosity measurements obtained from cement paste specimens contaminated with nil, 2 and 3 % BHD and prepared at various w/c ratios and hydrated for 5 weeks

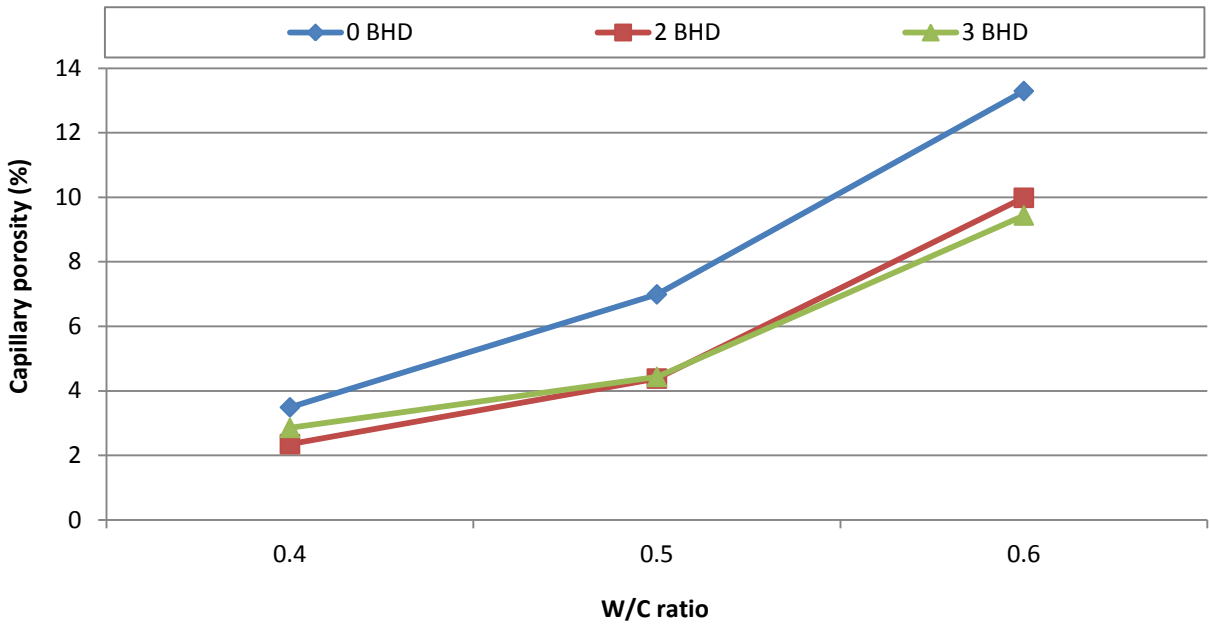

Figure 5-2 Capillary porosity measurements obtained from cement paste specimens contaminated with nil, 2 and 3 % BHD and prepared at various w/c ratios and hydrated for 10 weeks

The reduction of the capillary porosity volume due to addition of BHD is not yet fully understood and, since the BHD is not substantially composed of silica or alumino-silicates, it cannot be attributed to a pozzolanic reaction. ZnO is one of the main compounds in the BHD material so the reaction of ZnO with OH^- in the presence Ca^{++} could result in a precipitate of $Ca(Zn(OH)_3)_2 . 2H_2O$ within the concrete which may help in reducing the capillary porosity in the BHD-cement paste (Troconis de Rincón et al., 2002). Another possible hypothesis is that the finest size of BHD particles (≈ 1 µm) (Stegemann et al., 2000) may act as a filler and improve the particle packing. If this is the case, then chloride ions will not find a way to easily penetrate through the cement matrix due to tortuosity and/or non connectivity of capillary pores. Therefore, the addition of BHD into concrete may be beneficial in improving the concrete resistance to aggressive substances penetration and for this reason further work in

the next part was performed to assess the chloride penetration rate in concrete containing various levels of BHD.

5.5 CONCLUSIONS

Addition of BHD materials, 2 and 3 % by weight of cement, reduced the coarse capillary porosity effectively in both groups A and B. The effectiveness of BHD in reducing the coarse capillary porosity was more evident in samples hydrated for 10 weeks (Group B). This reduction in capillary porosities could be due to filling and packing of the available voids with the BHD particles resulting in pore refinement of the structure, hence causing more tortuosity and/or non connectivity in the pore microstructure. As expected, the capillary porosities were also found to be increased as the water/cement ratio increased.

PART B: INFLUENCE ON CHLORIDE DIFFUSION PROCESS INTO CONCRETE

5.6 INTRODUCTION

In some environments where aggressive substances such as chloride ions are available, concrete structures may be subjected to deterioration due to the corrosion of the reinforcing steel. The main cause of such deterioration is penetration of chloride ions through the concrete cover and at high enough concentrations of chlorides at the steel surface corrosion may be initiated. Therefore, producing a durable concrete to control/delay the diffusion of the aggressive ions into the concrete structure is fundamental. The use of certain supplementary cementitious materials (SCMs) in concrete can improve its durability due to refinement of the microstructure, which reduces the rate of chloride penetration through the concrete cover and thus extends the service life.

Chloride diffusion into concrete is considered a major factor that influences the durability of concrete. There is a tendency to use various "chloride diffusivity parameters" in concrete design criteria if durable concrete is required (Ahmad et al., 2008). Furthermore, if durability assessment is required, it is very important to determine the diffusivity of chloride ions into concrete particularly for reinforced concrete structures which are located in an aggressive marine environment (Zheng and Xinzhu, 2008). For that reason, the chloride diffusivity is a very important durability parameter since it may play a major role in accelerating deterioration and thus reducing the service life of structure.

The main objective of this part is to assess whether BHD affects the rate of penetration of chloride into concrete by means of a standard diffusion test.

5.7 CHLORIDE DIFFUSION PROCESS IN CONCRETE

Aggressive substances can move into concrete by different transport mechanisms. The main transport mechanisms that could promote the deterioration of concrete structures are diffusion, permeation, capillary absorption and migration. When the concrete structures are subjected to aggressive environments such as marine environments the primary transport mechanism of chloride ion ingress is often diffusion. Diffusion is the random transport of ions, atoms, or molecules in a mixture or solution from a high concentration area to an area with lower concentration (Kropp et al., 1995).

In practice, the diffusion of substances normally occurs under non-steady-state conditions. This indicates a build-up of the diffused substance within the concrete during the diffusion process. The local concentration of the diffused substances as a function of penetration depth and time is often represented by Fick's second law of diffusion (Equation 5-1) although for ions such as chloride this is an oversimplification, as discussed for example by Page (2007).

$$\frac{\partial c}{\partial t} = D \frac{\partial^2 c}{\partial x^2} \qquad [5.1]$$

In concrete, the diffusion process is commonly assumed to take place in a unidirectional way into a semi-infinite medium that is subjected to a constant concentration of chloride solution.

A solution of Fick's second law that is often used to determine the chloride diffusion coefficient (ASTM 1556, 2004) can be expressed as:

$$c\ (x,t) = \ Cs - (Cs - Ci)\ erf\ \frac{x}{\sqrt{4\ D\ t}} \qquad [5.2]$$

Where;

C (x, t) the concentration of chloride ion at depth x and time t, mass %

C_s the chloride concentration at surface, mass %,

C_i the initial chloride concentration, mass %,

x distance from surface to midpoint of the layer, m,

D_{app} apparent chloride diffusion coefficient, m^2/s

t the exposure time, s

erf error function.

Despite the fundamental objections that can be raised to the approach, apparent diffusion coefficients obtained from equation [5-2] have been widely used in the literature for many years to characterise the resistances of different types of concrete to chloride penetration. It was therefore decide to compare the performance of concrete with and without BHD additions by this means according to ASTM 1556 (2004).

In this study Microsoft Excel solver command was utilized to estimate the D_{app} values. After determining the chloride ion concentration profiles, the chloride concentration data were inserted in the Excel sheet with the corresponding depth values to obtain the best-fit curve from regression analysis. Initially, before running the regression analysis, D_{app} and C_s values

should be reasonably assumed. After inserting the chloride concentration data with their corresponding depths, measured C_i, exposure time and by assuming D_{app} and C_s values, the regression analysis can be run by using the Excel solver command to obtain the best-fit diffusion curve and calculate C_s and D_{app} values.

5.8 EFFECTS OF SCM ON CHLORIDE DIFFUSION COEFFICIENTS

Apparent chloride diffusion coefficients can be used to compare the resistance of different concrete compositions to chloride ingress. Many researchers utilised this technique to estimate D_{app} values in concrete made with different SCMs and/or prepared at various w/c ratios. The rate of chloride diffusion into concrete depends on many parameters. It has been reported in many studies that the use of supplementary cementitious materials in concrete plays a major role in controlling diffusivity of chloride ion into the concrete. A different degree of improvement in concrete resistance to chloride ion penetration was noticed when SCMs such as fly ash, slag and silica fume were incorporated into the concrete (Baghabra et al., 2009, Bentz et al., 1996, Cabrera and Claisse, 1990, Domone, 2010, Gjørv and Vennesland, 1979, Mangat et al., 1994, McPolin et al., 2005, Thomas et al., 1999).

A reduction in water content also resulted in an increase of the chloride penetration resistance into the concrete (Baghabra et al., 2009). In addition cement type, aggregate content, quality of concrete, binding capacity, ion exchange capacity, exposure environments and ambient temperature have been found to have a significant effect on the chloride diffusion rate into concrete (Buenfeld and Okundi, 1998, Costa and Appleton, 1999, de Rincón et al., 2004, Gjørv and Vennesland, 1979, Oh and Jang, 2007).

In the case of BHD none of the existing studies carried out on the effect of EAFD/BHD on the resistance of concrete to chloride ion penetration were performed under a standard diffusion test method. Nevertheless, it has been reported by Castellote et al., (2004) that incorporation of EAFD into concrete improve the chloride diffusion resistance. The rapid chloride permeability test, (ASTM C 1202-94, 1994), was carried out by Maslehuddin et al., (2011) to investigate durability characteristics of the EAFD concrete. In their study, 2% of cement was replaced by EAFD. Their results indicate a reduction of 52% in the chloride penetration due to the incorporation of EAFD when compared to plain concrete, which agrees with Castellote's et al., (2004) findings.

Since the chloride diffusion process is often the primary factor that affects the durability of the concrete structures that are exposed to a marine environment, as discussed in section 5.7, the effectiveness of using BHD in controlling chloride diffusion rates into concrete was investigated in this part by estimating chloride diffusion coefficients and also by determining the depth at which chloride concentration is critical. Experimental work and the implications of the results are also analysed and discussed in following sections.

5.9 EXPERIMENTAL PROCEDURE

5.9.1 Concrete specimens preparation

Three concrete mixes were prepared by incorporating three levels of BHD. These were 0 (control mix), 2 and 3 % BHD addition. The concrete mixes were prepared at w/c ratio of 0.5 and 0.6 and designed at constant C:FA:CA ratio of 1:1.5:2.5. The concrete mixing procedure

used was similar to that presented in subsection 3.2.2. The prepared mixture was then cast in three 100 mm cubes, which were compacted using a vibrator table. All the concrete specimens were cured in a 100 % RH fog chamber at a temperature of 22 ± 2 ºC for 63 days prior to diffusion testing.

5.9.2 Preparation of test specimens for exposure in NaCl solution

After curing, the test specimens were prepared according to ASTM 1556 (2004). A specimen ready for test is shown in Figure 5-3.

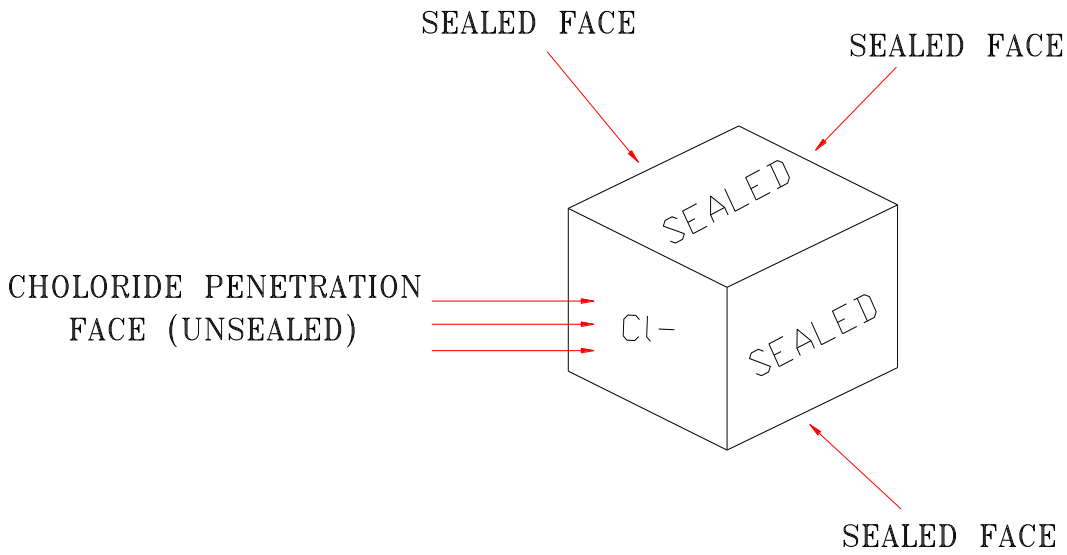

Figure 5-3 Sealed concrete specimen prepared for chloride diffusion process

5.9.3 Test procedure

After sample preparation, the sealed test specimens were removed from the saturated calcium hydroxide water bath, then immediately rinsed with tap water. The sealed specimens were then immersed in a sealed vessel containing a 2.82 M solution of NaCl (165 g ± 1 g NaCl per litre), as shown in Figure 5-4. The exposed surface area to exposure liquid volume ratio was maintained within the range of 50 ± 30 cm^2/l. The vessel was completely filled by the sodium chloride solution and closed tightly to prevent evaporation. The solution temperature was maintained at 22 ± 2 ºC. The test specimens were kept immersed in this solution for 98 days.

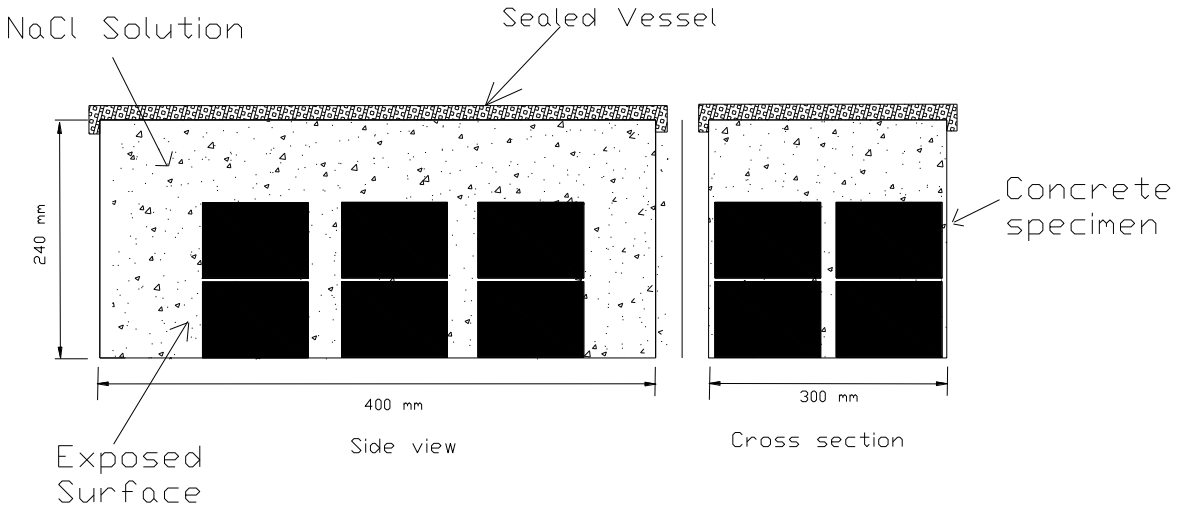

Figure 5-4 Schematic diagram of the exposed concrete specimens in the vessel

After this period of exposure, the test specimens were removed from the solution and rinsed with tap water. The test specimens were left for at least 24 hours to dry at a maintained temperature of approximately 22 ± 2 º C and with 50 ± 3% RH. Before beginning to grind off the exposed face of the test specimen, the coated area which surrounded the exposed face was completely removed. In detail, a 5 mm thick area of the specimen from the edge of the exposed face to appropriate depth (arrowed as the cleaned area in Figure 5-5) was removed.

This was to make sure that no coating would be mixed with the dust obtained during the profile grinding process; if any had been, it might have affected the chloride analysis. Figure 5-5 shows the coated area removed from all the faces surrounding the exposed surface of the test specimen, when the test specimen was prepared for the grinding process. The dried specimen was ground off in layers starting from the exposed surface. The distance from the exposed surface to the mid-depth of each layer was measured and used in obtaining the calculated chloride content. In the mid stage of the grinding process, a breakdown of the lathe was reported. A remedial technique with the facility of the Civil Engineering Laboratory was immediately adopted. The remaining part of the specimen was cut into slices using a tile saw with the blade lubricated by distilled water. The slices were then ground to determine the chloride content as described in section 3.5.

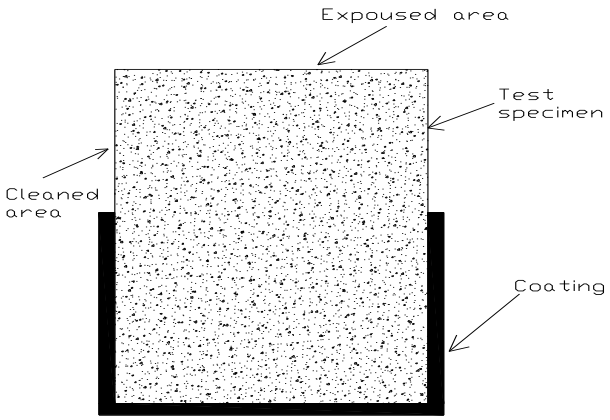

Figure 5-5 Test specimen ready for grinding off process

5.9.4 Determination of the initial chloride content of the test specimen

From the second part of the concrete specimen, a slice at least 20 mm in thickness was cut and ground. The ground powder was used to measure the initial chloride (C_i) content of the test specimen. The collected dusts were analysed to determine the total chloride content as described in section 3.5.

5.10 RESULTS ANALYSIS AND DISCUSSION

The effect of BHD incorporation on chloride penetration into concrete was evaluated on the basis of (i) chloride diffusion coefficient (D_{app}) and (ii) the depth at which chloride content reached a significant value of 0.4 % by weight of cement.

The chloride diffusion coefficient (D_{app}) and the surface chloride concentration (C_s) were determined, using equation [5.2] described in section 5.7, from different concrete specimens containing 0, 2 and 3 % BHD additions and prepared at two different w/c ratios of 0.5 and 0.6. For each specimen, the chloride concentration against the depth was plotted. A typical chloride diffusion profile together with the best-fitted curve is illustrated in Figure 5-6 . For all other specimens, the chloride concentration profile data and the best-fitted curves are presented in Appendix D.

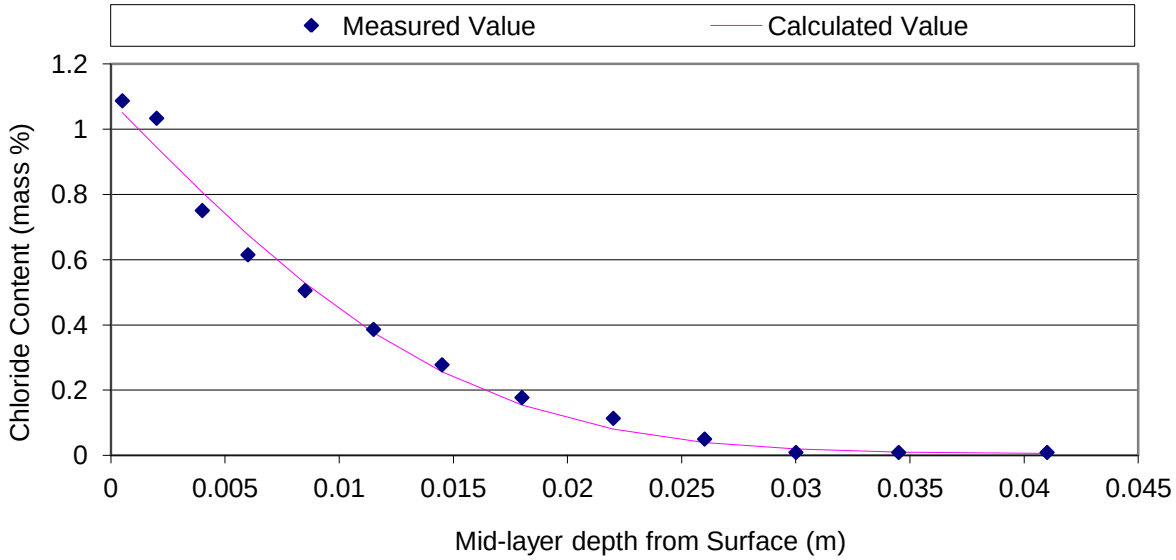

Figure 5-6 A typical chloride diffusion profile together with the best-fitted curve for plain concrete prepared at w/c ratio of 0.5 (specimen no. 1)

The obtained D_{app} values are summarised in Table 5-7. Some of the presented D_{app} values, however show a considerably high diffusion coefficient although these samples (marked with * sign) have low chloride concentrations at the surface (C_s). This situation has been noticed only in the BHD concretes. It appears either there was human error involved during the experimental work or it was due to the addition of BHD material. Also, in some of the presented D_{app} values a high scatter was observed. This could be due to unexpected reasons such as breakdown of the lathe during the profile grinding process.

Table 5-7 Chloride concentrations at concrete surface and average D_{app} values

Sample #	W/C ratio	BHD, %	Cs, %	D_{app}(10E-12), m^2/s
A01	0.5	0	1.09	8.70
A02			1.05	9.89
A03			1.00	12.30
A21		2	0.99	9.90
A22*			0.60	18.36
A23			0.98	9.44
A31		3	0.70	9.46
A35			0.95	9.40
A36*			0.64	11.15
B01	0.6	0	1.26	8.32
B02			1.25	16.11
B03			1.19	9.92
B21		2	1.18	9.62
B22			1.14	4.38
B23*			0.57	21.77
B31*		3	0.66	26.47
B32			1.37	5.32
B33			0.84	9.70

Because of the above reasons, it was impossible to establish the effect of BHD addition on the chloride penetration rate into concrete based on the estimated chloride diffusion coefficients and therefore it was decided to try an alternative approach. The influence of BHD material on chloride penetration into various concrete specimens was evaluated by estimating the chloride penetration depth for each specimen at which the chloride content is critical i.e. 0.4 % by weight of cement (assuming the calcium content is uniform for a given mix). The 0.4 % chloride by weight of cement was selected as an arbitrary chloride content because, in practice, it is the maximum allowable limit in reinforced concrete structures (BS EN 206-1, 2000). Also at higher values the risk of corrosion initiation in steel bar embedded in concrete is likely to be high (Vassie, 1984).

To estimate the depth, equations of a best-fit curve for each specimen were obtained together with coefficients of determination (R^2). Values between 0.92 and 0.99 for R^2 were found. The equation was then selected on the basis of the highest R^2. A typical example of a best-fit curve together with experimental results are shown in Figure 5-7.

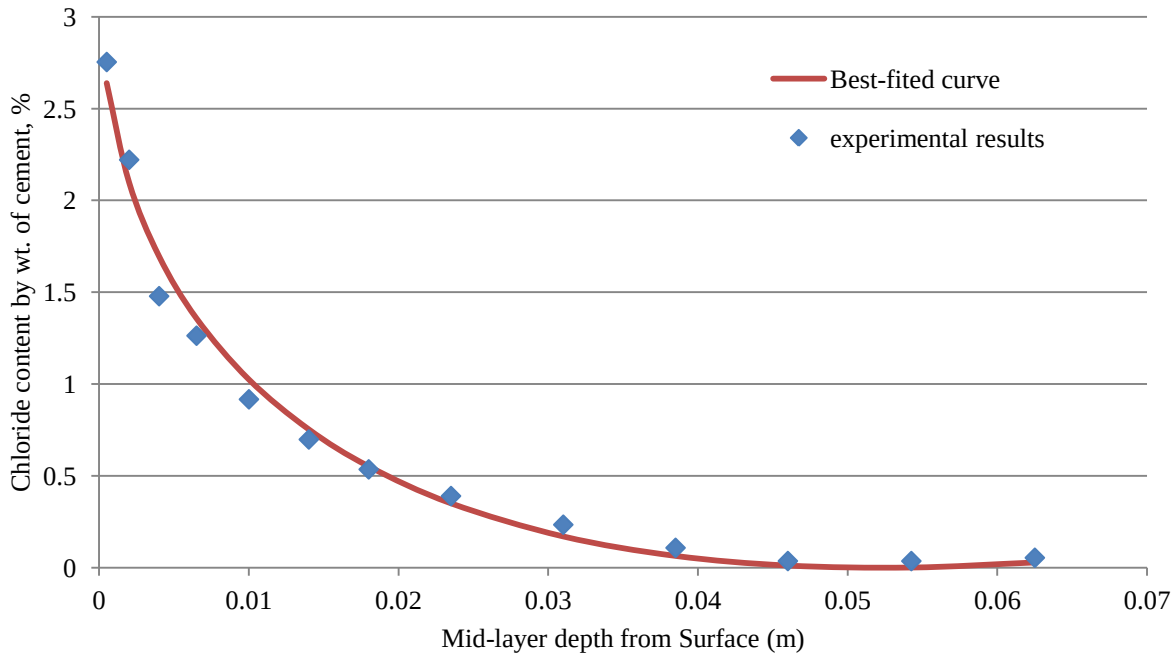

Figure 5-7 A typical example of the best-fited curve for a particular specimen used for 0.4 % chloride depth estimation

The equation from the above curve is expressed as follows:

$$\text{Chloride content by weight of cement (\%)} = (a+bx^{0.5})^2 \qquad [5.3]$$

Where,

a and b are constants determined by the non-linear regression analysis of experimental results for each individual specimen. X is the depth of the penetrated chloride, in this study at which the chloride content is 0.4 % by weight of cement, in mm.

The estimated depths of chloride penetration into various concrete specimens containing 0, 2 and 3 % BHD additions and prepared at w/c ratios of 0.5 and 0.6 are presented in Table 5-8.

Table 5-8 Average depths of chloride penetration into concrete specimens containing various level of BHD and prepared at two w/c ratios at which chloride content was 0.4 % by weight of cement

Sample #	W/C ratio	BHD %	Depth in mm	Avg.
A01	0.5	0	18.50	20
A02			19.81	
A03			20.99	
A21		2	18.99	19
A22			17.76	
A23			19.51	
A31		3	16.70	18
A35			21.40	
A36			15.91	
B01	0.6	0	21.94	24
B02			29.80	
B03			20.71	
B21		2	23.36	21
B22			21.36	
B23			19.66	
B31		3	22.26	21
B32			22.46	
B33			19.04	

Using this alternative approach resulted in lowering the scatter to some extent in the estimated depths of chloride penetration into concrete. However, in view of the small numbers of specimens tested, it is unclear whether the inclusion of BHD into concrete prepared with w/c ratio of 0.5 and 0.6 has resulted in any significant improvement in the resistance to chloride ingress compared to those specimens made without BHD.

5.11 CONCLUSION

The small numbers of the specimens tested in this experiment for each mix together with the high scatter in the results does not help to draw a convincing conclusion. Due the restriction in time and material it was not possible to repeat this experiment. However, a general conclusion that can be drawn from this part is that the addition of various levels of BHD does not have an adverse effect on the resistance to chloride ingress into concrete.

Chapter 6

EFFECT OF BHD ADDITION ON CHLORIDE THRESHOLD AND BLEEDING CAPACITY OF CONCRETE

PART A: INFLUENCE ON CHLORIDE THRESHOLD VALUE

6.1 INTRODUCTION

When a critical amount of chloride ions around a steel surface is achieved, corrosion of the steel reinforcing bar will be initiated. This particular amount of the chloride, which leads to the corrosion initiation, is called the chloride "threshold" value. The determination of the chloride "threshold" value is important since it has been used to predict the service life of concrete structures when the failure mechanism is mainly due to chloride-induced corrosion.

This chloride threshold value required for corrosion initiation is controversial, because this value changes depending on several factors including change in the surrounding environment such as temperature (Benjamin and Sykes, 1990), quality of concrete such as cement type (Hussain et al., 1996, Rasheeduzzafar et al., 1990) and the use of blended materials (Thomas, 1996).

The main objective of this part was to study the effect of BHD addition on chloride "threshold" value. In addition to this, the influence of temperature on corrosion initiation was also investigated. The effects of SCMs on the chloride threshold value are reviewed in the next section, followed by experimental work and then results analysis and discussion.

6.2 EFFECT OF SCM ON THE CHLORIDE THRESHOLD VALUE

Ambient temperate is one important factor which has a vital effect on the required chloride concentration "threshold value" to initiate corrosion. Schiessl and Raupach (1990) who investigated the influence of concrete composition and microclimate on the critical chloride content in concrete concluded that one of the influencing factors on the corrosion rate and critical chloride content which should not be underestimated is temperature. It was found, in research reported by Benjamin and Sykes, (1990), that the critical chloride concentration needed for pitting, decreases with increasing temperature.

The use of blended cements in the Middle East where some concrete structures are subjected to aggressive environments such as chloride bearing soils and ground water could be advantageous. Numerous researches (Diamond, 1986, Goñi and Andrade, 1990, Gouda, 1970, Hausmann, 1967, Hope and Alan, 1987, Hussain et al., 1995, Oh et al., 2003, Page et al., 1986) have been carried out experimentally to establish critical chloride content and/or the $[Cl^-]/[OH^-]$ ratio that is required to cause the onset of corrosion in steel bar. However, most of the research cited above was performed by (a) simulating the concrete pore solution or (b) performed on plain or on blended cements where chlorides were introduced by dissolving the chlorides into the mixing water.

Nevertheless, there are still some studies that have been performed on the blended cements where the chlorides were allowed to penetrate from external sources. For instance, Hansson and Sorensen, (1988) investigated the influence of several factors on the critical chloride content necessary to initiate corrosion of reinforcement steel embedded in concrete. Their study focused on the effect of cement type. The results of their study revealed that the

replacement of Danish standard cement with 3 and 22 % fly ash has only a slight effect on the critical chloride content. However, the time to initiate corrosion in fly ash mortars was increased markedly and this was attributed to the low porosity of fly ash mortar.

Also Thomas, (1996) prepared concrete specimens made with 0, 15, 30, and 50 % fly ash as cement replacement. These concrete specimens were the exposed to a marine environment. Results indicated that the chloride threshold concentration decreased as fly ash replacement increased. The corresponding chloride threshold values estimated from different fly ash levels were 0.7, 0.65, 0.5 and 0.2 % by weight of cement, respectively. However, it was found that the mass losses of steel bars embedded in fly ash concrete were less than that in control specimens. The reduction of corrosion rates in fly ash concrete were attributed to the high resistance of fly concrete to chloride ion penetration.

A ten-year result that was obtained from concrete made with 15, 30, and 50 % fly ash mass and subject to marine environment for 10 years also indicated that replacements of fly ash led to a reduction in chloride threshold value as fly ash contents increased as reported by Thomas and Matthews (2004). They also, however, found that the replacement of fly ash resulted in a reduction in the weight losses and chloride penetration into concrete. Also, Ryou and Ann (2008) found in blended cement concretes, in which chlorides were allowed to penetrate from the external environment, the critical chloride concentration necessary to initiate corrosion in concrete mixed with 30 % pfa was in the range of 0.22 to 0.35 % while for OPC concrete it varied between 0.48 to 1.52 % indicating a reduction of chloride threshold value due the pfa replacement. In the same study, the chloride threshold value for 60 % ground granulated blast-furnace slag (ggbs) replacement was between 0.43 and 0.71 % and, for 10 % silica fume

concrete, it was in the range of 0.46 and 1.13 %. However, in both blended concretes, the chloride diffusion coefficients were found to be lower than that in the plain OPC concrete. A similar finding was found in a study carried out by Hansson and Sorensen (1988) who concluded that a reduction in the critical chloride value needed to initiate corrosion in 10 % silica fume cement compared to plain Portland cement was approximately one third.

Incorporation of supplementary cementitious materials into concrete does not appear to help in reducing the chloride threshold values despite the fact that chloride diffusion coefficients and corrosion rates may be less when compared to those of concrete made with plain cements.

These differences between the obtained chloride threshold values indicate the difficulty in predicting a consistent chloride "threshold" value under different circumstances. Another main reason for the variety of critical chloride contents required to initiate corrosion is disruption of the integrity of the layer of hydration products deposited at the steel-concrete interface (Lambert et al., 1991). Furthermore, it is very difficult to find and perform a reliable rapid laboratory test to predict chloride threshold value, Page (2009).

A number of researches have been carried out to study the possibility of the use of BHD material in the concrete industry (Al-Mutlaq and Chaudhary, 2007, Al-Sugair et al., 1996, Al-Zaid et al., 1997, Chaudhary et al., 2003, Maslehuddin et al., 2011), but these researches remain very limited and none of these researches investigated the influence of BHD material on the chloride threshold value. The BHD material will be utilised mainly in Saudi Arabia, where concrete structures are subjected to an aggressive environment involving high humidities combined with high temperature (typically 20-40 ºC) variation during the day.

Therefore, in this research particularly, it was aimed to assess the effect on the chloride threshold value of steel in concrete with 0, 2 and 3.5 % levels of addition of BHD at two different temperatures.

6.3 EXPERIMENTAL PROCEDURE

6.3.1 Steel bar preparation

Thirty six steel bars were utilized in this experiment, which were prepared for electrochemical measurements according to the procedure described in subsection 3.3.1. Before casting, all steel bars were masked, see subsection 3.3.2 for masking procedure. The working electrode surface area exposed to the corrosive action of the mortar was 10.1 cm^2.

6.3.2 Mortar specimen preparation and casting procedure

Four groups of mixtures were prepared for the chloride threshold value experiment. Each group was cast with the same levels of BHD but exposed to a different range of temperatures, 20°C (as a reference temperature) and 40°C, being an average temperature in Saudi Arabia.

The first group (A1) and second group (A2) were prepared by casting mortars with 0, 2, and 3.5% BHD and exposed to two solutions associated with two temperatures of 20°C and 40°C, respectively. Groups (A1) and (A2) were cast without artificial crevices; for more details see subsection 3.3.3, on the steel bars. Group three (B1) and four (B2) were cast with the same proportions of BHD as used in group (A1) and (A2) and exposed to the same solution as

group (A1) and (A2), except that the steel bars in group (B1) and (B2) had artificial crevices at the surface where such defects may be expected to reduce the protection level of steel bar, afforded by surrounded layer of cement hydration products, due to disruption of integrity of the formed layer (Lambert et al., 1991). If so, then the corrosion initiation in these specimens will be accelerated. Experimental conditions and number of steel bars used in each group are summarized in Table 6-1.

Table 6-1 Experimental conditions and number of steel bars used in chloride threshold studies

	Without artificial defects (Group A1 & A2)		**With artificial defects (Group B1 & B2)**	
BHD %	**20 °C**	**40 °C**	**20 °C**	**40 °C**
0	3	3	3	3
2	3	3	3	3
3.5	3	3	3	3
Total	**36**			

The mortar mix was prepared with fixed proportions of W:C:S ratio of 0.5:1:2.1 by weight of cement and mixed by the same procedure described in subsection 3.2.1. The prepared mix was cast in plastic containers 85 mm in height and with a diameter of 49 mm. Before casting, each bar was inserted in the middle of the plastic container which was fixed by its cap lid. The casting process was carried out in two layers. Each layer was table vibrated for one minute or less to minimize segregation. The cover of each mortar specimen was maintained at 20.5 mm. Triplicate samples were cast from each mix. After demoulding, all the mortar specimens were cured in a fog chamber at 20 ± 2 ºC for seven days before being subjecting to exposure testing as described below. Figure 6-1 illustrates a typical mortar specimen with embedded steel bar used in this research.

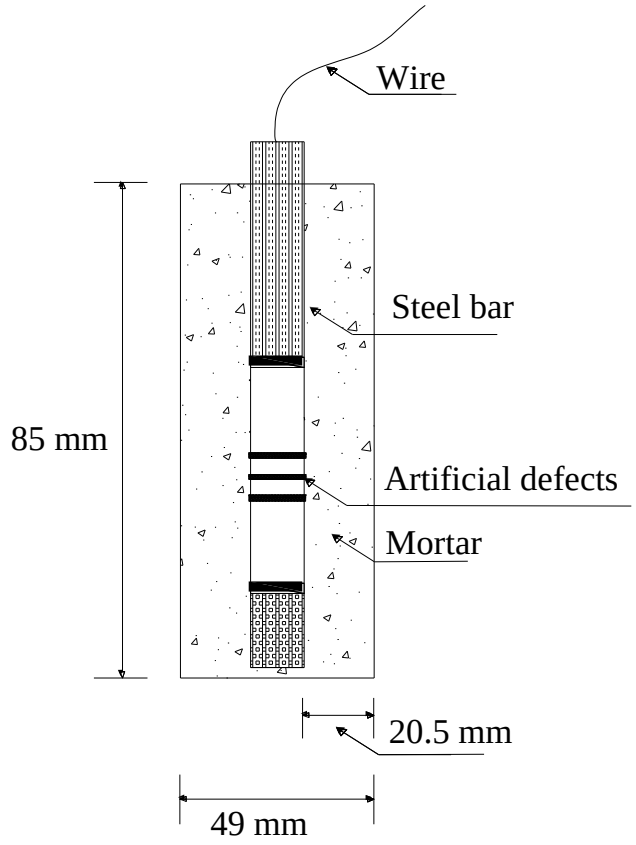

Figure 6-1 Schematic diagram of steel bar immersed in mortar

6.3.3 Exposure tests

Prior to commencement of the exposure tests, the electrochemical condition of the steel bars in each of the specimens was assessed by corrosion potential (E_{corr}) and corrosion rate (I_{corr}) measurements. The mortar specimens were then subjected to wet and dry cycles to accelerate the corrosion process. All the mortar specimens were immersed in 0.25 M NaCl solution to the top of the specimens for five days. After that, they were removed from the solution and kept to dry in air at their specified controlled temperature for two days to complete one cycle. At the end of the drying period and before the immersion again, E_{corr} and I_{corr} were measured. The corrosion potentials and corrosion rates were measured on a weekly basis for the whole

duration of the test period. The NaCl solution was replaced with a new solution every two weeks.

The exposure test and the electrochemical measurements were terminated as soon as depassivation (active corrosion) of the given specimen was observed. It was noticed by Andrade et al. (1990) that there are no corrosion products that may be detected or the corrosion is insignificant when measured I_{corr} values are below 0.1 to 0.2 $\mu A/cm^2$. However, the corrosion products may be observed when the corrosion rate exceeds 0.2 $\mu A/cm^2$. In this study, the detection of the onset of steel bar corrosion (depassivation) was determined by a substantial jump in corrosion current density to a value more than 0.2 $\mu A/cm^2$. The depassivation state of the steel bar was further confirmed by a sudden decrease in corrosion potential to a more negative value.

During the test period, for a given specimen, the electrochemical measurements were conducted using the cell arrangement shown in Figure 6-2. The corrosion cell consists of an external reference electrode, working electrode and an external counter electrode. The external reference electrode was placed on the top of the mortar specimen surface and perpendicular to the embedded steel bar. Wet sponge was used between the external reference electrode and the surface of the mortar to ensure good electrolytic contact. For potential measurements, the reference electrode and steel bar were both connected to a high impedance voltmeter. Subsequently, the corrosion rate measurements were carried out using a potentiostat. The working electrode is the steel bar, which is embedded in the mortar specimen. The external counter electrode is a stainless steel plate, which was placed under the mortar specimen surface and parallel to the embedded steel bar. Wet sponge was used

between the external counter electrode and the surface of the mortar. To perform corrosion measurements, the external reference electrode, the working electrode and the external counter electrode were all connected to the potentiostat. The corrosion measurement was performed as described in subsection 3.3.5.

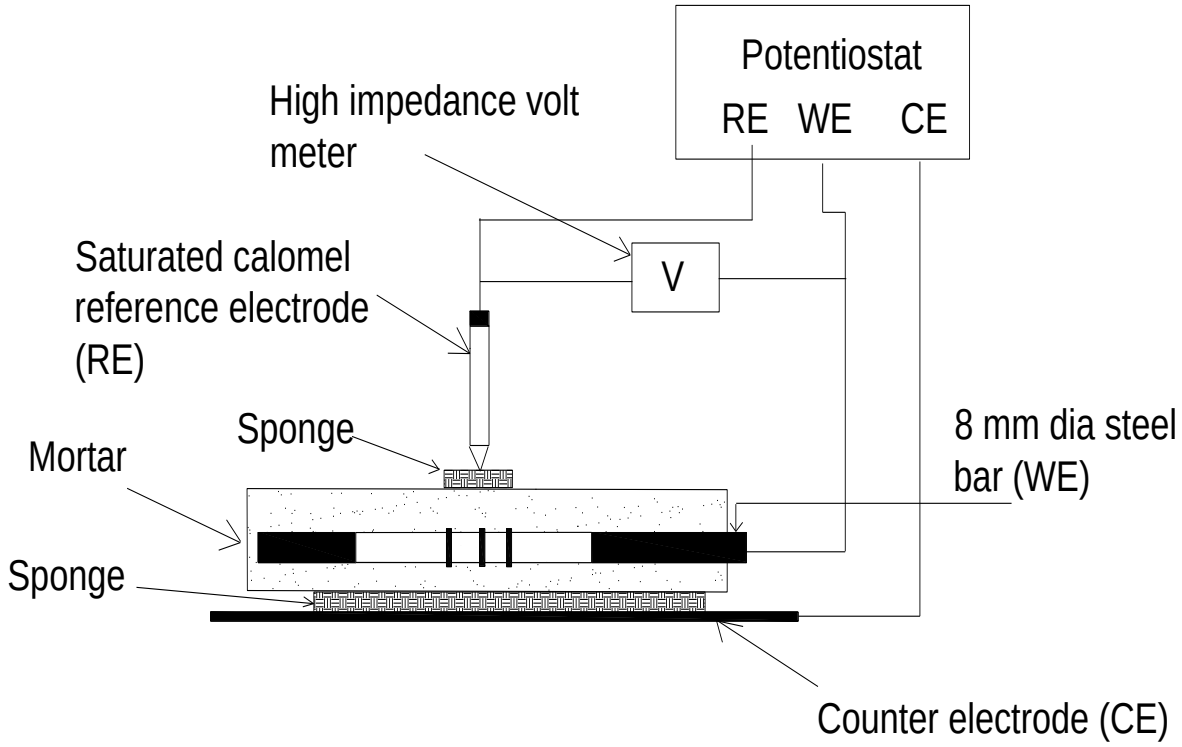

Figure 6-2 Schematic drawing of the mortar specimens used for electrochemical measurements

6.3.4 Determination of critical chloride levels

To estimate the critical chloride levels in specimens for which depassivation of the embedded steel was observed, the mortars were spilt longitudinally so that the 8 mm steel bars could be removed. The 2 mm annulus of mortar surrounding the exposed surface area of the steel was

then immediately removed as a dust sample. This was done by inserting a drill of 12 mm diameter into the hole left after extracting the steel bar. The dusts were analyzed to determine chloride content, see section 3.5 for the chloride analysis procedure. To present the chloride content for each specimen in percent by weight of cement, some of the extracted dusts were firstly ignited as in section 3.6 and then analysed to determine the calcium contents by XRF as described in subsection 3.7.1.

6.4 RESULTS ANALYSIS AND DISCUSSION

The critical chloride content that is necessary to initiate corrosion can be specified by the content of the free chloride, $[Cl^-]/[OH^-]$ ratio or by the total chloride content (Glass and Buenfeld, 1997). In the field, the extraction of the pore solution and determination of pH value at the level of reinforcement is very difficult. Therefore, the risk of the corrosion can be more conveniently indicated by the total chloride content by weight of cement rather than by the ratio of chloride to hydroxyl ion concentration (Hussain et al., 1996). Furthermore, Glass and Buenfeld (1997) concluded that the best presentation of the chloride threshold value in concrete is by expressing the total chloride content by weight of cement. Therefore, the critical chloride content "threshold value" in this study was expressed as the total chloride content percentage by weight of cement.

Prior to the extraction of mortar powder for chloride analysis, the initiation of active corrosion was determined as illustrated in section 6.3.3. An example of detection of active corrosion initiation due to a substantial change in I_{corr} and E_{corr} values in steel bar embedded in mortar is illustrated in Figure 6-3. The chloride threshold values with time to initiate corrosion in steel

bar embedded in mortar and subjected to two different temperatures are presented in Table 6-2 and Table 6-3. The corrosion current and corrosion potential data obtained from steel bars used in the determination of the chloride threshold values are presented in Appendix E.

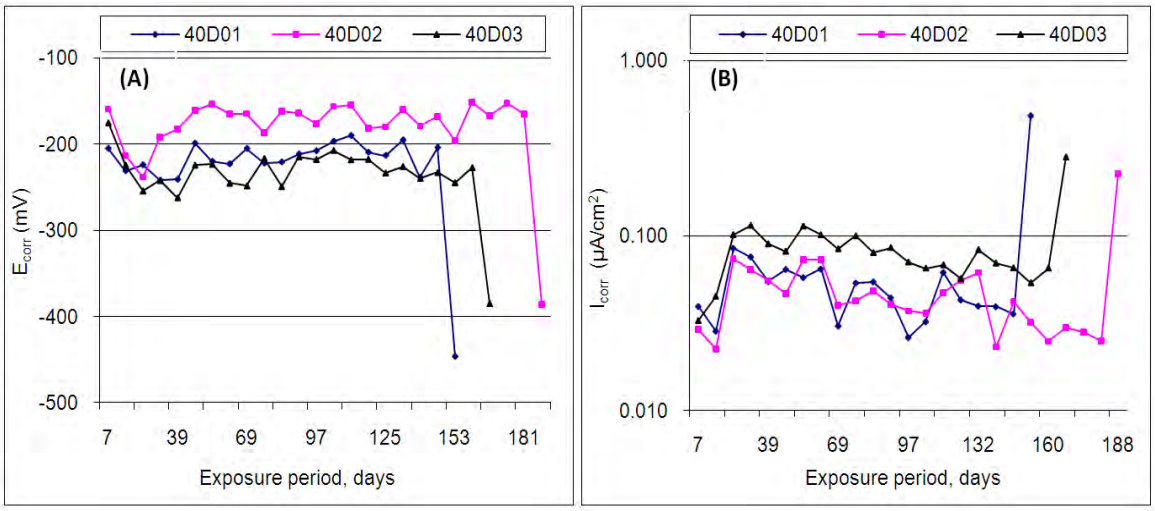

Figure 6-3 A sudden change in (A) corrosion potentials and (B) corrosion current density in the steel bar embedded in mortar without BHD addition and subjected to 40 ^{0}C temperature

From Table 6-2, in the absence of steel bar surface artificial defect it can be clearly observed that there was no corrosion detected on any of the steel bars that were embedded in mortar exposed at 20 ºC temperature. However, corrosion initiation was detected on all the control (0 % BHD addition) specimens subjected to 20 ºC and this faster corrosion onset was associated with the presence of interfacial defects, indicating that the protection level of steel bar embedded in mortar was reduced. The critical chloride content that led to depassivation of the steel was in the range 0.28-0.48 % by weight of cement, which is reasonably similar to the 'threshold chloride' levels that have often been associated with a significant risk of corrosion in reinforced concrete structures exposed to chloride ingress (Vassie, 1984). The effect of artificial defects at the steel bar surface in accelerating corrosion initiation was even

more clear in mortars subjected to 40 ºC temperature, see Table 6-3, where all the steel bars embedded in mortars incorporating different levels of BHD were corroded within the time-frame of this experiment indicating the success of this method in accelerating the corrosion process. The influence of the interfacial defects (crevices) was in line with expectations since they disrupt the integrity of the buffering layer of cement hydration products that is believed to play an important role in restraining pit growth on embedded steel (Page, 2009).

From data presented in Table 6-3 it can be seen that all the specimens, when subjected to 40 ºC and in the presence of the interfacial defects, were corroded providing a complete set of results that can be utilized to study the effect of different levels of BHD material on chloride threshold value required to initiate corrosion in steel bars embedded in mortar. Incorporation of 2 and 3.5 % BHD resulted in high chloride content necessary to initiate corrosion at the level of steel bar surface compared to mortar made without BHD addition. Furthermore, higher chloride threshold values were observed in 3.5 % BHD-mortar. The corresponding averaged chloride threshold content was 0.39, 0.89 and 1.19 % by weight of cement for mortars containing 0, 2 and 3.5 % BHD, respectively. The minimum time (days) required to initiate corrosion was also less in plain mortar when compared to 2 and 3.5 % BHD-mortar, see column no. 5 in Table 6-3 . It should be recognized that these chloride threshold values found in this study are tentative and a confirmative study is necessary.

Table 6-2 Time to initiate corrosion and chloride threshold values of the steel bars embedded in mortars made with various level of BHD and treated at 20 ºC

Sample No.	Tem. ºC	Defect	BHD	Time to initiate corrosion (days)	Cl % (by wt. of cement)	Avg. Cl %
20C01	20	No	0.00	NC*	NC	-
20C02				NC	NC	
20C03				NC	NC	
20C21			2.00	NC	NC	-
20C22				NC	NC	
20C23				NC	NC	
20C31			3.50	NC	NC	-
20C32				NC	NC	
20C33				NC	NC	
20D01		Yes	0.00	132	0.28	0.35
20D02				153	0.28	
20D03				272	0.48	
20D21			2.00	NC	NC	-
20D22				NC	NC	
20D23				NC	NC	
20D31			3.50	NC	NC	-
20D32				286	1.20	
20D33				279	1.27	

*NC: Not corroded (I_{corr} on steel bar was less than the corrosion threshold value of 0.2 μA/cm^2 until the end of experiment, e.g. 321 days)

Table 6-3 Time to initiate corrosion and chloride threshold values of the steel bar embedded in mortar that obtained with various level of BHD and treated at 40 ºC

Sample No.	Tem. ºC	Defect	BHD	Time to initiate corrosion (days)	Cl % (by wt. of cement)	Avg. Cl %
40C01	40	No	0.00	NC*	NC	-
40C02				NC	NC	
40C03				NC	NC	
40C21			2.00	265	1.00	-
40C22				NC	NC	
40C23				286	2.17	
40C31			3.50	300	2.10	-
40C32				NC	NC	
40C33				NC	NC	
40D01		Yes	0.00	153	0.36	0.39
40D02				188	0.45	
40D03				167	0.34	
40D21			2.00	244	0.89	0.89
40D22				209	0.91	
40D23				188	0.87	
40D31			3.50	251	0.99	1.19
40D32				244	1.23	
40D33				195	1.35	

*NC: Not corroded (I_{corr} on steel bar was less than the corrosion threshold value of 0.2 µA/cm^2 until the end of experiment, e.g. 321 days)

This increase in the critical chloride content needed to cause the onset of the corrosion in steel bar embedded in BHD-mortar could be attributed to many factors. As discussed in subsection 4.8.2, the hydroxyl ion concentration was enhanced due to the incorporation of BHD in mortar. This high hydroxyl concentration in the pore solution extracted from BHD-mortar could help in maintaining the steel bar in a passive condition state for longer times (Page and

Treadaway, 1982). In other words, a higher [OH^-] concentration may help in maintaining a lower [Cl^-]/[OH^-] ratio.

Alternatively, however, it could be linked to the effect of BHD on the bleeding capacity of the fresh mortar. Tests on fresh concretes were performed and the results show that, the bleeding capacity of fresh concrete was reduced significantly when various levels of BHD used, as discussed in section 6.8. The effect of created macroscopic voids, because of accumulation of the excessive bleed water, on the corrosion initiation of steel bar will be discussed in section 6.6. The effect of reduction in the bleeding may therefore be to maintain a compact layer of cement hydration products on the steel in the vicinity of the plastic ties, thereby enhancing the local buffering capacity and reducing the disruption of regions surrounding embedded steel bar.

6.5 CONCLUSIONS

The effect of two levels of BHD addition on the chloride threshold value was investigated. Incorporation of 2 and 3.5 % BHD resulted in enhancement in chloride threshold values required to initiate corrosion at the level of steel bar surface. The critical chloride contents necessary to initiate corrosion at 40 ºC increased as BHD addition level was increased. The corresponding averaged chloride threshold content was 0.39, 0.89 and 1.19 % by weight of cement for mortars that contained 0, 2 and 3.5 % BHD, respectively. This increase in the chloride threshold values due to the addition of BHD materials could be due to enhancement in hydroxyl ion concentration in the pore solutions and partly due to reduction in bleeding capacity and capillary porosity.

Exposure temperature has an effect on corrosion resistance. Increase of exposure temperature from 20 to 40 ºC decreases corrosion resistance and this could be due to increase in the chloride penetration rate and corrosion reaction

The use of plastic ties to create interfacial defects at the vicinity of steel bar surface helps to provide suitable conditions (crevices) to initiate and accelerate the corrosion.

PART B: INFLUENCE ON BLEEDING OF CONCRETE

6.6 INTRODUCTION

Bleeding of concrete is defined as the tendency of a portion of mixing water to accumulate (by rising up) on the top surface due to segregation (settlement) of some solids in freshly mixed concrete (Neville, 1995). This implies that concrete that has a deep section and/or longer setting times before the stiffening stage is more vulnerable to bleeding. If excessive bleeding occurs then a weak zone at the top of the concrete may be formed causing surface delamination (Kosmatka, 1994). However, some minor bleeding is not detrimental since a serious problem in some hot countries is the development of plastic shrinkage cracking when the evaporation rate of the water on top of the concrete surface is faster than the bleeding rate (Lerch, 1957).

Hoshino (1989) investigated the effect of bleeding on compressive strength. His study found a reduction of the compressive strength as the bleeding rate of water increases. It was concluded by Hoshino (1989) that the effect of bleeding rate on strength of the lower part of the specimen is much less compared to that in the upper part. The increase of bleed water in a particular element of the structure will result in an increase of the water to cement ratio in the top part of the element and so affect the strength (Kosmatka, 1994, Neville, 1995). Khayat (1998) stated that the variation of the water to cement ratio across the element height affects the in situ porosity and mechanical properties of the concrete which supports the same hypothesis reported by (Kosmatka, 1994).

The resistance of concrete to aggressive substances, such as chlorides, is directly related to the water to cement ratio and permeability of the concrete. Furthermore, the permeability of the concrete may be increased because the bleed water will leave behind empty pockets leading to the formation of air voids (Neville, 1995). The increase of both water to cement ratio and permeability due to excessive bleeding would reduce resistance of the concrete and thus allow the aggressive substances to penetrate more easily (Kosmatka, 1994).

Corrosion of reinforcement is considered to be the most common reason that leads to deterioration in reinforced concrete structures as seen in the literature review Chapter 2. The active corrosion is characterised by the presence of macroscopic voids at the steel-concrete interface (Lambert et al., 1991). The formation of such voids beneath the horizontal steel bar is mainly due to the rising of bleed water in freshly mixed concrete. In research carried out by Soylev and François (2003) it was found that the existence of bleeding water, at the steel-concrete interface, enhances the corrosion process in the presence of chloride. It follows that the bleed water will also cause a region characterised by open-textured zones (Page, 2009) and at such region and in the presence of chloride ions the corrosion will be initiated (Page and Treadaway, 1982).

Many factors are found to have an effect on the bleeding of concrete including cement properties, fine aggregates and the use of fine materials such as fly ash and silica fume. For instance, the addition of fly ash and silica fume produced lower bleeding in fresh mortar compared with a control mortar made without additives as reported by SchiessI et al. (1990). It is not known if BHD has any effect on the bleeding of fresh concrete. Addition of small amounts of BHD, e.g. 2 % by weight of cement increased the setting times (Al-Zaid et al.,

1999). Also, further additions of BHD caused a severe retardation in the setting times as discussed in subsection 8.4.2, which may then increase the risk of segregation and so increase the chance of water bleeding.

It can be seen from the above that the effects of bleeding on the durability of concrete can be important. It was therefore decided to investigate the effect of two levels of BHD addition on bleeding in freshly mixed concrete. Experimental work and the analysis and discussion of the results are presented in the following sections.

6.7 EXPERIMENTAL PROCEDURE

6.7.1 Concrete specimens preparation

Two levels of BHD, 2 and 3.5% by weight of cement, were used to prepare concrete mixes with constant W:C:FA:CA ratio of 0.5:1:1.5:2.5 by weight of cement. The concrete mixing was performed according to the procedure described in subsection 3.2.2. The mixed concrete was poured immediately in a specific mould for bleeding evaluation as described in the next section.

6.7.2 Determination of bleeding water

The bleeding of freshly mixed concrete was determined according to BS EN 480-4 (2005). The vessel used was a rigid cylinder with a diameter of 250 ± 10 mm and a height of 280 mm ± 10 mm. The prepared concrete mix was poured into the vessel in three layers. Each layer

was compacted with 25 strokes of a tamper. After compaction of the third layer, the excess concrete was removed carefully with a float leaving the top of the concrete with a reasonably smooth surface. The weight of the sample was then determined. The filled vessel was placed on a level floor and covered with a lid. During the first 40 min, the accumulated water from the concrete surface was collected by means of a pipette at 10 min intervals. After the completion of the first 40 min, the bleeding water was collected at 30 min intervals until no more bleeding water was observed.

Two minutes before the water collection, the vessel was tilted carefully to facilitate easy collection. After drawing off the bleed water, the vessel was returned to its original place without any jarring. After each water collection, the bleed water was transferred to a measuring cylinder and the weight of accumulated water was recorded. At the end of experiment, the bleeding water was determined as follows:

$$\text{Bleeding water (B) , \%} = \frac{m_w}{w \times m_s} \times 100 \qquad [6.1]$$

Where

B is the bleed water as percentage of the total water

M_w is the bleed water mass, in gm

M_s is the sample mass, in gm

w is the water proportion in the fresh concrete by mass.

6.8 RESULTS ANALYSIS AND DISCUSSION

In Figure 6-4 the effect of 2 and 3.5 % BHD addition by weight of cement on the bleeding of fresh concrete is shown. Each column represents an average value for three specimens. It was noticed that, the bleeding water decreases as BHD level increases. More reduction in the quantity of water bleeding from fresh concrete was observed when 3.5 % BHD was added to the concrete. This was not expected since the addition of BHD cause delays in the setting of concrete significantly. Nevertheless, the reduction in the bleeding water could be attributable to the fineness of BHD. The fineness of BHD materials (high surface area) may cause enhanced adsorption of some of the mixing water resulting in a lower free water content and consequently less bleeding of fresh concrete.

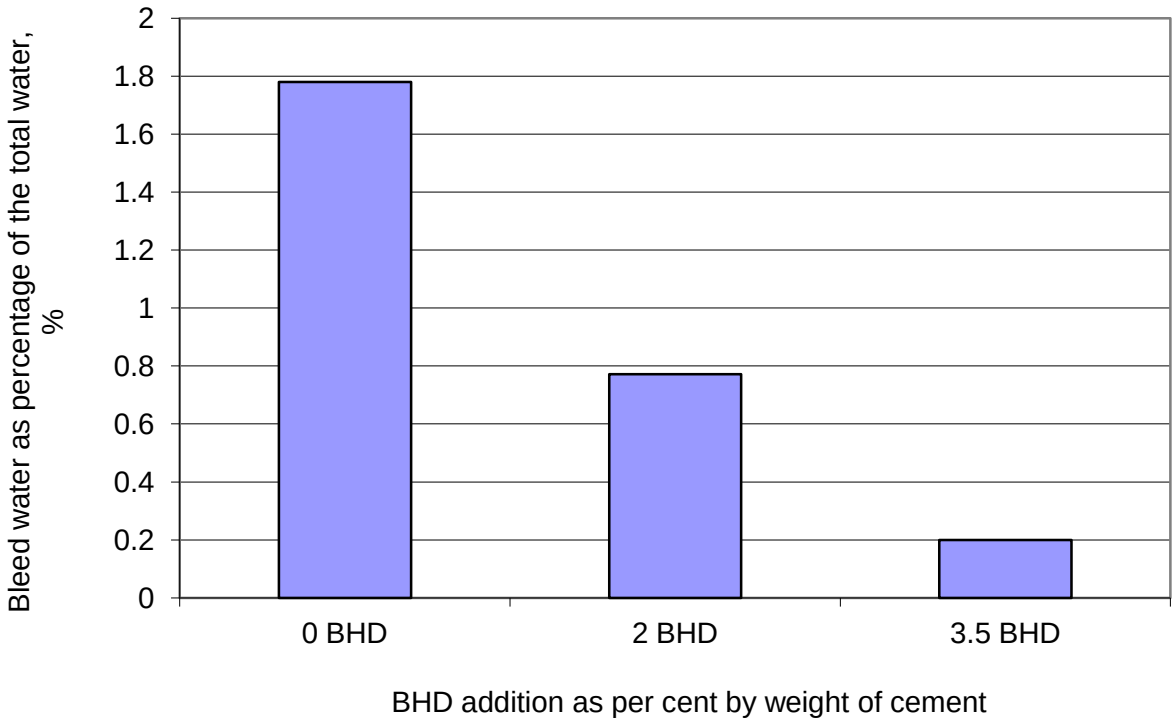

Figure 6-4 Effect of different levels of BHD addition on bleeding of fresh concrete specimens

6.9 CONCLUSIONS

It can be concluded from the above results that the incorporation of BHD into concrete reduced the bleeding of freshly mixed concrete at a given water to cement ratio. This reduction in bleeding could be partly attributed to the high specific surface area of BHD. It is suggested that this may be a factor in explaining the beneficial effect of BHD on the threshold chloride level for corrosion of steel in concrete for reasons discussed in Part A of this chapter.

Chapter 7

EFFECT OF BHD ADDITION ON COMPRESSIVE AND CONCRETE-STEEL BOND STRENGTH

PART A: EFFECT OF BHD ADDITION ON COMPRESSIVE STRENGTH

7.1 INTRODUCTION

Temperature of the air, relative humidity, solar radiation and wind velocity are the main components of hot climate that affect the properties of fresh and hardened concrete. Saudi Arabia is classified as having hot-dry climatic conditions during the day (Al-Gahtani et al., 1998). In such an environment, during the mixing and placing stage, increases in water demand and in the rate of water evaporation of mixing water and also from the surface of the concrete result in slump loss and accelerated setting times (Neville, 1995).

Furthermore, in a high temperature climate, the loss of strength in a concrete structure is one of the most common problems that can occur and this is because of the increase in water demand and inadequate curing at the higher temperatures (Mustafa and Yusof, 1991). The influence of a hot climate on the hardening properties of concrete was investigated by Abbasi et al. (1992). In their study, 52 reinforced concrete beams were prepared and cured in hot weather (outside the laboratory). The results indicated that there was a reduction in strength by as much as 25 %. Also, Sawan (1992) stated that when concrete is subjected to high temperature corresponding with low humidity, the concrete will suffer a reduction in strength at later ages due to the high rate of evaporation followed by an excessive loss of water from

the concrete which affects the hydration process. This is because the hydrated cement paste structure has a direct influence on strength. This reduction in strength could also be due to the rapid hydration process that will result in a formation of non-uniform hydration products and more porous physical structure (Neville, 1995). The effect of severe hot-dry climate conditions on the compressive strength of concrete was also studied by Alsyed (1997). His results indicated that this type of climate adversely affected the strength of concrete and may reduce it by more than 15 percent. Research conducted by Al-Gahtani et al. (1998) to investigate the effect of hot-weather conditions on the compressive strength of concrete showed a 16 % reduction in the compressive strength of concrete prepared at normal laboratory temperature and then cured in hot weather compared to concrete specimens prepared and cured in normal laboratory conditions.

To avoid undesirable properties such as a loss in strength, that may occur in hot climatic regions, procedures such as reducing the time between placing and the start of curing to a minimum should be considered. Starting to cure the concrete as soon as possible by applying the appropriate curing methods, reducing the wind velocity over the concrete surface to minimize the rate of moisture loss and, if needed, shading the concrete surface from direct sunlight to control the temperate of the surface can also be helpful (Lerch, 1957).

The mechanical behaviour of different BHD concretes, which were subjected to high temperature, was therefore studied by measuring compressive strength development after specific periods of hydration to help quantify the influence of temperature.

7.2 EXPRIMENTAL PROCEDURE

7.2.1 Concrete specimen preparation

Concrete mixes were prepared by incorporating different levels of BHD addition. Two levels of BHD, i.e. 2 and 3.5% were utilized in this study. The concrete mixes were prepared at W:C:FA:CA ratio of 0.5:1:1.5:2.5 by following the procedure described in subsection 3.2.2. The prepared mix was then cast in twelve 100 mm cubes, which were compacted using a vibrating table. After demoulding, they were cured in the way described in the next section.

7.2.2 Testing procedure

Both control and BHD compressive strength specimens, initially, were cured under water at room temperature for a period of 14 days to ensure a formation of uniform hydration products. In practice, the minimum curing period according to SABIC engineering standard is 14 days (Sabic, 2001). Then they were continuously cured in a water bath at a controlled temperature of 60 ± 3 ºC until the time of testing. Three concrete cubes from each mix were crushed for compressive strengths measurements at each designated curing period, i.e. 3, 7, 28 and 60 days. The compressive strength tests were performed according to BS EN 12390-3 (2009).

7.3 RESULTS ANALYSIS AND DISCUSSION

The adverse effect of a high temperature on the compressive strength, as discussed in section 7.1, was avoided by mixing, placing and then curing the concrete specimens under water at normal laboratory conditions for 14 days after casting. This process divides the experiment/study into two stages. Stage I, studies the effect of lower levels of 2 and 3.5 % BHD addition on strength development of the concrete at the early stage of hydration without exposure to a hot environment and so avoiding any adverse effect on the hydration process. The specimens in stage I were tested 3 and 7 days after casting. Whilst in stage II, the specimens were cured under two conditions as described in subsection 7.2.2 and tested after 28 and 60 days curing to investigate the long-term effect of the hot environmental exposure on concrete strength development.

The results of the compressive strength measurements obtained in this study for stage I and II are provided in Figure 7-1. The data from stage I revealed that, the compressive strength of concrete containing 2 % BHD and tested after 3 days from casing, exhibited a higher strength compared to that of control specimens. As expected, higher additions of BHD, 3.5 %, showed a lower strength compared to the controls and 2 % BHD-concrete specimens, this reduction in strength being due to the action of BHD as a retarder. However, after 7 days curing, the compressive strength of concrete specimens containing 2 and 3.5 % BHD were 52.7 MPa and 51.8 MPa respectively, while the compressive strength of concrete made without BHD addition was 40.3 MPa.

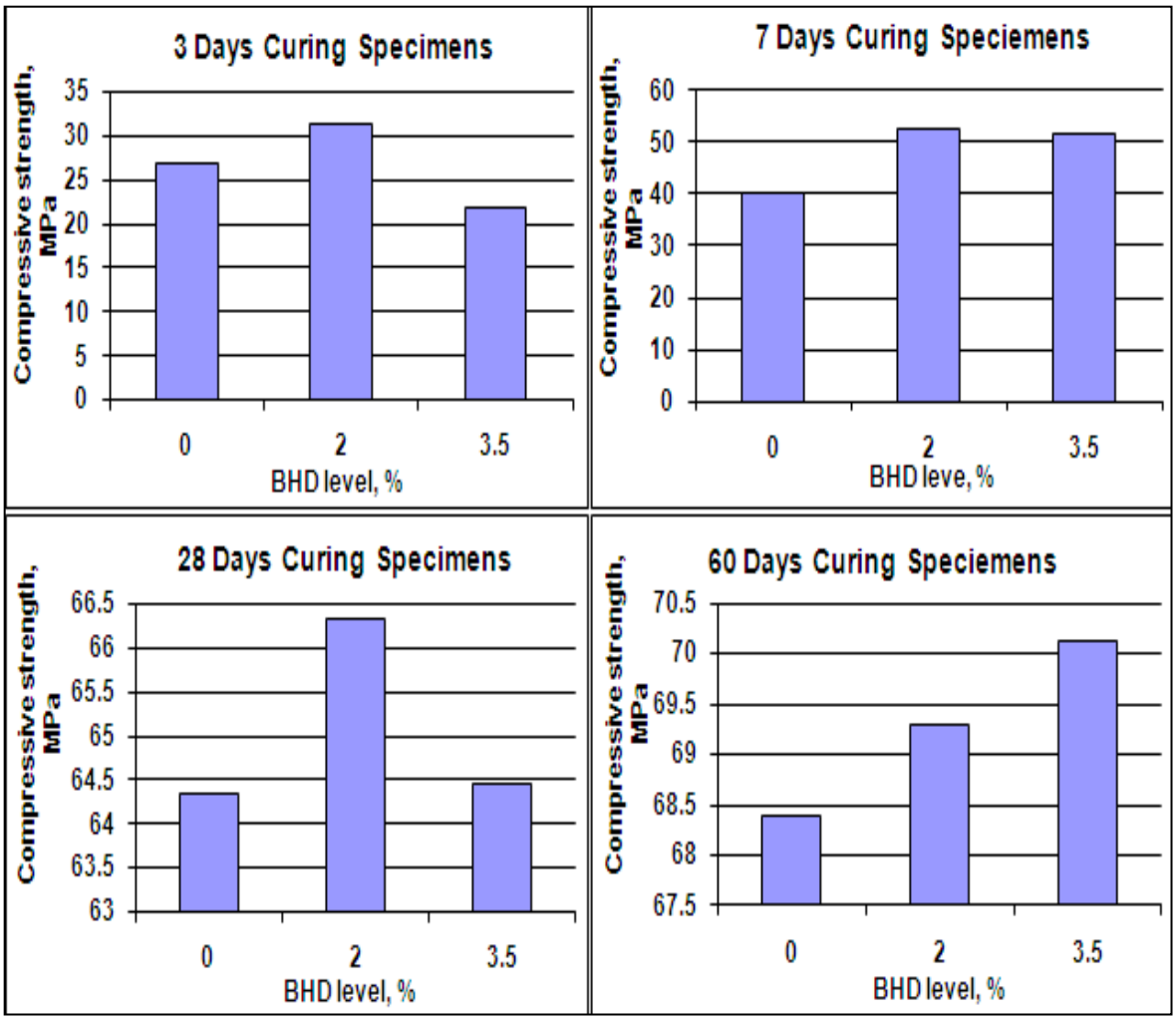

Figure 7-1 Compressive strength results of stage I and II for concrete speciemns made with different levels of BHD

The findings of the current study are consistent with those of Maslehuddin et al. (2010) and Al-Zaid et al. (1997) who investigated low levels of BHD. Al-Zaid (1997) and co-workers investigated the effect of 2 and 3 percent BHD replacement by weight of cement on compressive strength development. They reported that, at all ages i.e. 3, 7, 28, 90 and 210 days, the strength in BHD-concretes exhibited higher values compared to controls. A recent work was carried out by Maslehuddin et al. (2010) who concluded that a beneficial gain in compressive strength was achieved, when 2 percent of BHD was added into the mixture when compared to control samples.

In stage II, where all the concrete specimens were exposed to a hot climate condition, the concrete specimens were tested after 28 and 60 days from casting. The compressive strength obtained from 2 % BHD-concrete was higher than that of the controls tested at ages of 28 and 60 days. The compressive strength of 3.5 % BHD-concrete was more than that in the control specimens when tested 28 and 60 days after casting showing achieved strength values for 3.5 % BHD-concrete specimens of 64.5 and 70.1 MPa, respectively. For control specimens, the achieved strengths were 64.3 and 68.4 MPa, respectively. The highest compressive strength among all BHD-concretes was achieved in concrete containing 3.5 % BHD addition tested after 60 days.

The effect of porosity on strength was discussed by many authors as cited above in section 5.2 where the strength of blended cements was improved due to the reduction in porosity. This indicates that the improvement in compressive strength of BHD concrete could be related to the improvement in porosity (refer to section 5.4) and partly to the reduction in consistence, see section 8.4.1, and not due to the pozzolanic characteristics of BHD as suggested by Al-Zaid et al., (1997).

7.4 CONCLUSIONS

Incorporation of more than 2 % BHD into concrete adversely affects the early hardening of concrete e.g. during the first 3 days after casting. After a longer hydration period, the addition of BHD improved the compressive strength of concrete specimens and this could be linked to the effects of BHD on the cohesiveness and porosity. Exposing concrete specimens to hot climate conditions did not adversely affect the compressive strength of BHD-concrete.

PART B: INFLUENCE ON CONCRETE-STEEL BOND STRENGTH

7.5 INTRODUCTION

The bond strength between concrete and embedded steel bars plays a major role in the functioning of reinforced concrete structures. The strength of the concrete is a very important parameter found to affect the bond strength at the concrete-steel interface (Fédération Internationale du Béton (fib), 2000). The use of BHD as an addition to concrete results in a delay in the setting time and consequently reduces the hardening rate at early ages as discussed in the previous part and Chapter 8. This reduction in the early age strength development rate could be detrimental because the early removal of formwork may lead to a substantial loss of bond strength if the hardening of the concrete around the steel bar is not fully achieved due to the retardation effect of BHD addition. This puts emphasis on the importance of a study into the effect of BHD addition on the steel bar to concrete bond strength. Experimental work together with the results analysis and discussion are presented in the following sections.

7.6 EXPERIMENTAL PROCEDURE

7.6.1 Steel bar preparation

Eighteen plain round steel bars 10 mm in diameter were prepared for bond strength assessment by rinsing with acetone then ethanol and exposing them to air for 24 hours before

casting to ensure dry, clean and free from any contamination such as oil, grease or loose particles.

7.6.2 Specimen preparation and mix proportion

To determine the bond strength between steel and concrete containing various levels of BHD, pull out tests were performed. 150 mm cube moulds (Figure 7-2) were used for making the specimens. A single steel bar was incorporated into each concrete cube at the central axis. The location of steel bar was selected based on a study carried out by Williamson (1999) that signifies that the location of plain rebar has little effect on the bond strength. The effective bond length of the bar was 15 times the diameter of the bar (15d) (Walker et al., 1997). During the placing and vibrating of the fresh concrete, the bar was kept in a horizontal position along the axis of the mould, as shown in Figure 7-3.

Concrete mixtures were prepared by addition of 0, 2 and 3.5 % BHD with constant W:C:FA:CA ratio of 0.5:1:1.5:2.5 and mixed according the procedure described in subsection 3.2.2. The mixture was then cast in six moulds made specifically for the purpose of this experiment, and compacted using a vibrating table. After demoulding, the concrete specimens were covered by damp burlap plus a polyethylene sheet at a temperature of 22 ± 2 ^{o}C until the appropriate hydration period was achieved. The pull out test was performed after hydration periods of 28 and 60 days.

7.6.3 Testing procedure

To facilitate the pull-out test, the concrete specimen was set up as shown in Figure 7-4, and horizontal axial force was applied to the steel bar. The load was measured with a calibrated load cell, as showing in Figure 7-4. Before applying any force and to measure the free end slip, a dial gauge was installed at the opposite end of the steel bar. The main purpose of readings of the displacement was to indicate the occurrence of the failure. In each specimen, the steel bar was loaded until a maximum load was achieved where a sign of surface cracking started to appear around the steel at the concrete surface followed by free movement of the steel bar indicating the failure of the specimen. The maximum load achieved was then recorded for a given specimen.

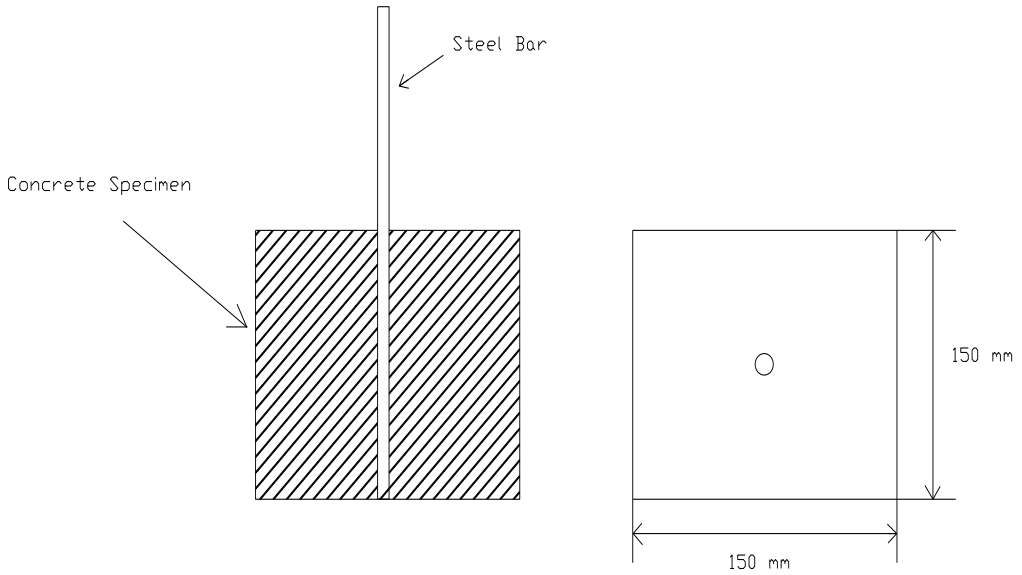

Figure 7-2 Dimensions of pull out test specimen

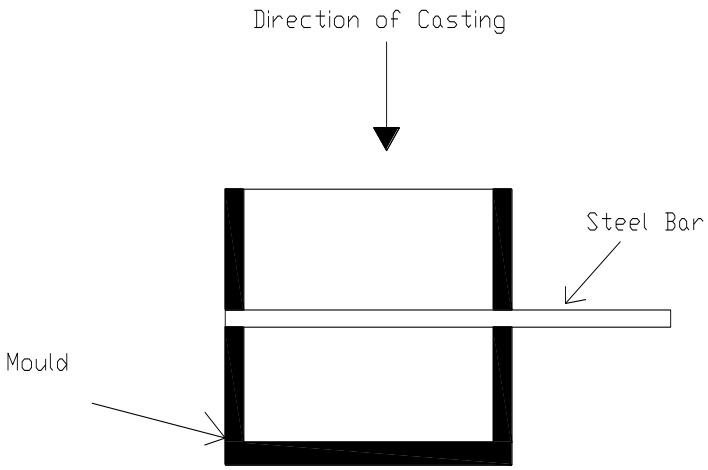

Figure 7-3 Sketch of the mould and casting process

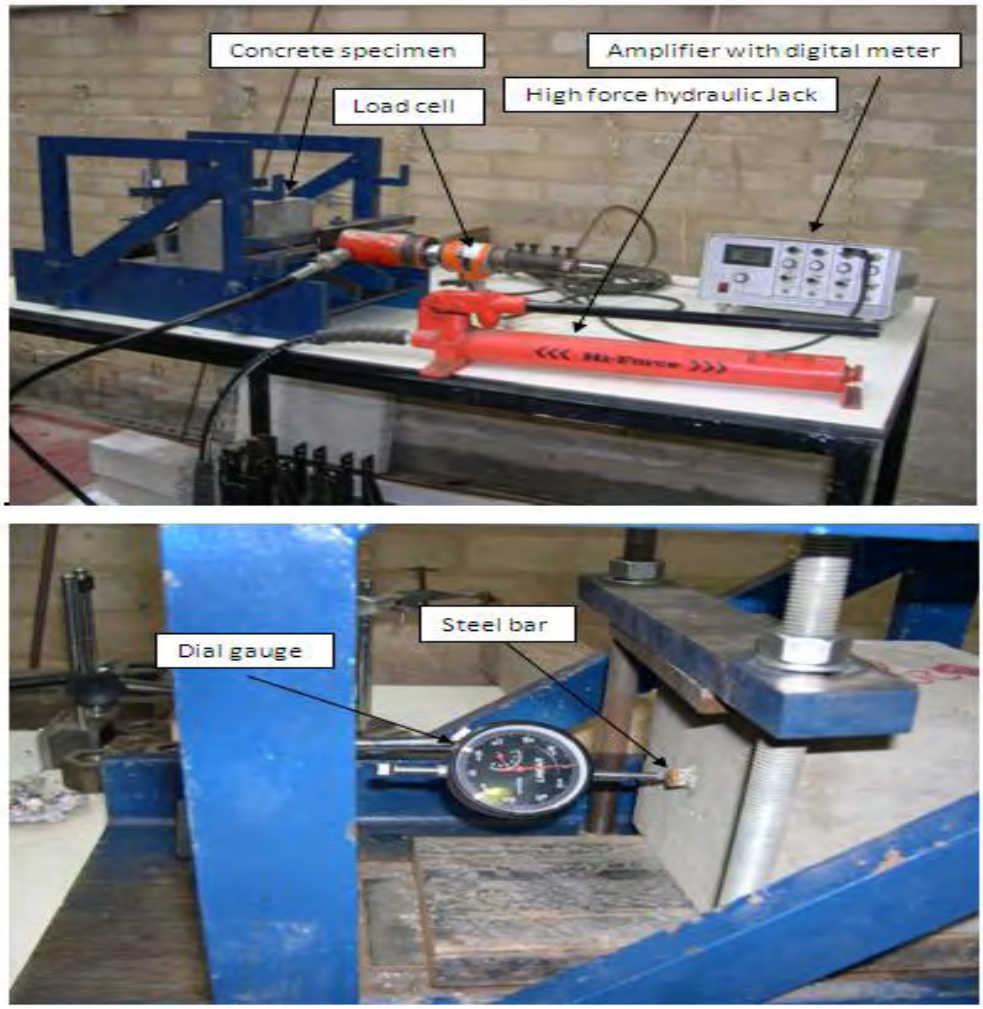

Figure 7-4 Pullout test measurement setup used for bond strength evaluation

7.7 RESULTS ANALYSIS AND DISCUSSION

The formation of voids beneath the horizontal surface of the steel bar is largely related to the bleeding capacity and/or settlement of the fresh concrete. The risk of formation of some defects which are associated with bleed water could be low since no adverse effect of the incorporation of BHD into concrete on bleeding was found, see part B of Chapter 6. However, concrete that has a long setting time may be vulnerable to progressive settlement. This in turn affects the quality of the cement paste at the concrete-steel interface and weakens the bond strength between the embedded steel bar and the concrete.

Experimental bond strengths can be obtained from maximum experimental pullout forces using the following equation:

$$f_{b,max} = \frac{P_{max}}{\pi dl} \qquad [7.1]$$

Where $f_{b,max}$ is experimental bond strength, P_{max} is maximum experimental pullout force, d is diameter of reinforcement bar, l is embedment length of reinforcement bar (Gorst and Clark, 2003).

The effect of the different levels of BHD additions on bond strength obtained from concrete specimens cured for 28 and 60 days can be seen in Figure 7-5. Each point represents an averaged value from thee specimens. All the bond strength results are summarized in Table 7-1. The maximum bond strength (in N/mm^2) is the achieved value where the failure of the

specimen occurred. In this study, the bond strength of control specimens corroborate the findings reported by (Williamson, 1999).

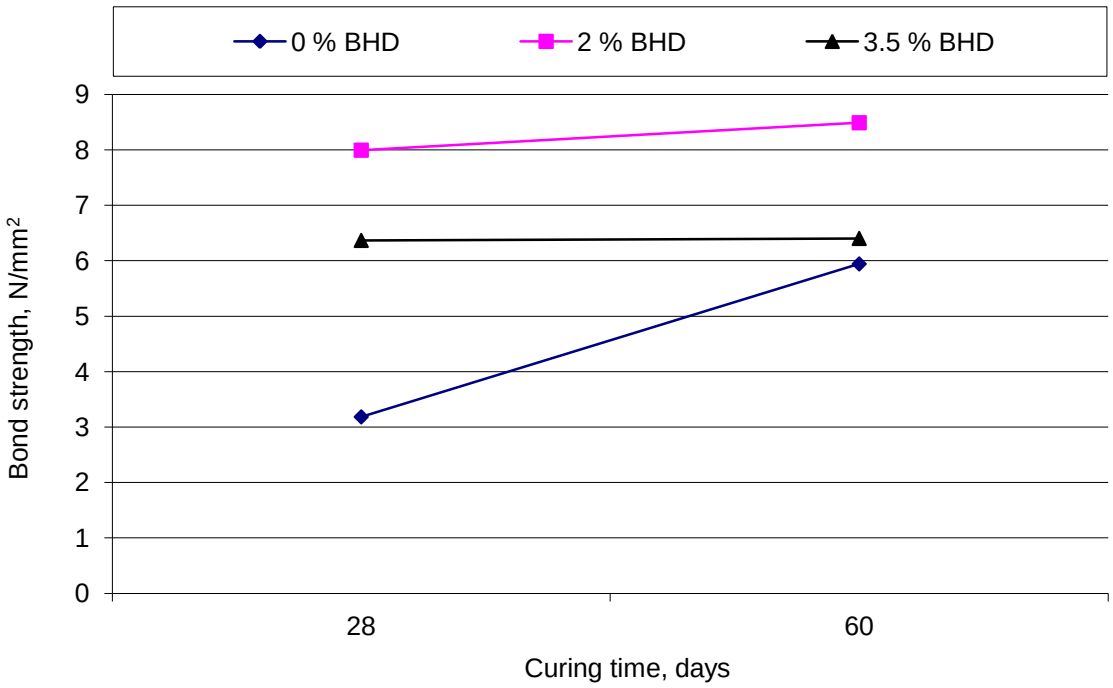

Figure 7-5 Average bond strength obtained from concrete prepared with various levels of BHD and cured for 28 and 60 days

The bond strength between the steel bar and concrete containing 2 % BHD and cured for 28 and 60 days was higher to some extent compared to that in control specimens. Considering curing time, the bond strength values increased as hydration period increased.

For BHD addition of 3.5 % by weight of cement, it can be seen from the above figure that all the specimens produced values of bond strength higher than the bond strength in control specimens at all ages. The variation of bond strength with age for 2 and 3.5 % BHD-concrete was small.

Table 7-1 Bond strength results

BHD %	Curing time, days	Max. bond strength (N/mm^2)	Bond strength avg. (N/mm^2)
0	28	3.6	3.2
		2.8	
		3.2	
	60	5.5	5.9
		4.7	
		7.6	
2	28	7.0	8.0
		7.6	
		9.3	
	60	8.7	8.5
		8.3	
		8.5	
3.5	28	6.6	6.4
		6.4	
		6.2	
	60	6.4	6.4
		6.2	
		6.7	

There are many factors that may play a role in improvement of bond strength between concrete and steel reinforcing bar such as the workability and compressive strength of the concrete (Lachemi et al., 2009). According to BS 8110-1 (1997) the design ultimate anchorage bond stress is directly proportional to the square root of characteristic concrete cube strength. Gjorv et al.,(1990) investigated the effect of silica fume on the bond strength. They concluded that the improvement of bond strength is associated with improvement with the compressive strength of the concrete. It follows that, the improvement of bond strength could be due to the improvement in BHD-concrete compressive strength and porosity of BHD-cement pastes as discussed in the previous part and section 5.4, respectively thus may affect the microstructure and morphology of the concrete-steel interfacial zone. Also, the bleed water, associated with the segregation of aggregates, was found to be reduced by the addition of BHD material which implies that the accumulation of free water beneath the steel

bar may also be reduced and so reduces microscopic voids in the vicinity of the steel bar, hence leading to higher bond strength.

7.8 CONCLUSIONS

The addition of BHD material to concrete does not have an adverse effect on bond strength between steel reinforcing bar and concrete. These results are provisional given that the number of specimens for a given mix was only three.

Chapter 8

EFFECTIVENESS OF CHLORIDE-FREE CONCRETE ACCELERATORS ON THE CHARACTERISTIC PROPERTIES OF CONCRETE

8.1 INTRODUCTION

Concrete accelerating admixtures involve a range of chemicals which may affect cement hydration rate, thus resulting in reducing the setting time and in many cases enhancing early strength development rate. The concrete accelerating admixtures can be divided mainly into i) rapid set accelerators and ii) setting and hardening accelerators. They are acids or salts of acids such as calcium nitrite and calcium formate (Edmeades and Hewlett, 2003). A concrete hardening accelerating admixture can be defined as "material that can be added to concrete during the mixing in a quantity not more than 5% by mass of cement content of the concrete to increase the early strength development rate with or without affecting the setting time" (BS EN 934-2, 2009). According to ASTM C494/C494M -10a (2010) the accelerating admixture is defined as "an admixture that accelerates the setting and early strength development of concrete". The main advantages in using concrete accelerating admixtures are allowing early strength development, allowing a reduction in the curing period and allowing a reduction in the forms removal period (Domone, 2010).

Historically, calcium chloride was broadly regarded as the cheapest and most effective accelerator of Portland cement hydration (Ramachandran, 1976) and it was used as a concrete accelerator admixture since 1885 (Rixom and Mailvaganam, 1986). However, in 1977 the use

of calcium chloride in concrete as an accelerator admixture was banned in the UK in instances where steel reinforcement or any metal is embedded in concrete. This was due to the tendency of the calcium chloride to increase the rate of corrosion of embedded metals (Page, 2007). Therefore it was decided to use non-chloride accelerators such as calcium nitrite and calcium formate in this study.

Calcium nitrite (CN) is known as an anodic corrosion inhibitor due to its corrosion inhibitive characteristics to the embedded steel bar when added into concrete as reported by many researchers (Berke et al., 1993, Berke and Rosenberg, 1989, El Jazairi and Berke, 1990, Rosenberg et al., 1977, Tomosawa et al., 1990) and as a hardening accelerator of Portland cement concrete. Calcium nitrite complies with the requirements of the ASTM specification C494 standard as a concrete accelerator (El-Jazairi et al., 1990, Rosenberg et al., 1977). Similarly calcium formate (CF) is an admixture which, has been found to improve the early strength development of the concrete without causing any threat to the corrosion of embedded reinforcement, which is the case with some concrete accelerators, such as calcium chloride due to the introduction of chloride ions. CF is a popular commercial chemical admixture (Lohtia and Joshi, 1995) and its incorporation into concrete improves the 28-day strength.

The use of higher levels of BHD in concrete causes severe retardation of both setting and hardening. For this reason, the quantity of BHD that can be added into concrete has been restricted. The maximum allowable level of BHD to be used in the concrete in Saudi Arabia is approximately between 2 and 3% by weight of cement (Al-Sugair et al., 1996). To utilize higher percentages in concrete the retardation effect of BHD must be overcome. Therefore, an attempt was made to investigate the effect of using non-chloride accelerators, namely

calcium nitrite and calcium formate, on the characteristics of BHD-concrete hydration (hardening) with a view to gaining a better understanding of hydration mechanism of BHD concrete in the presence of hardening accelerators. A literature review of the effect of these non-chloride accelerators, CN and CF, on the fresh and hardening properties of concrete was also conducted.

8.2 LITERATURE REVIEW

8.2.1 Effect of calcium nitrite on hardening of concrete

8.2.1.1 Influence on compressive strength development

The use of calcium nitrite in concrete structures will not only inhibit the corrosion process on the steel reinforcement but will also have favourable effects on some of the hardening properties of the concrete, such as early compressive strength development.

A considerable amount of literature has been published on the effect of calcium nitrite on early strength development. These studies have shown an improvement in compressive strength at early stages when calcium nitrite is added into the concrete mixture. A study carried out by Rosenberg et al. (1977) to investigate the effect of introducing various levels of calcium nitrite on concrete compressive strength development after 1, 7 and 28 days of curing showed that the concrete compressive strength increases as CN increased throughout all ages. After 28 days of curing, the incorporation of 2, 3, 4 and 5% calcium nitrite by weight of cement into concrete led to a higher compressive strength than that in control specimens by

13.9%, 17.4%, 26.8% and 29%, respectively. A major technical review conducted by Berke and Rosenberg (1989) regarding the use of calcium nitrite as a chemical admixture concluded that, the additions of calcium nitrite into concrete resulted in compressive strength improvement. The 3 days compressive strengths for concretes that were prepared at a w/c ratio of 0.56 and with 1 and 2% of calcium nitrite were higher than that of the plain concrete by 3 and 26%, respectively.

Furthermore, Brown et al. (2001) reported that an addition of 15 l/m^3 of calcium nitrite into concrete raised the strength of the control concrete by 26.2%, 38%, 20.6% and 16.3% when tested after 3, 7, 28 and 365 days, respectively. The effect of 2% and 4% calcium nitrite by weight of cement on compressive strength of concrete prepared with a w/c ratio of 0.45 was evaluated by Al-Amoudi et al. (2003). The calcium nitrite used in their study was in the liquid form, which contains of 30% calcium nitrite solid content by weight. This study revealed that the compressive strength of concrete made with 2% and 4% calcium nitrite was higher (approx. 27.7 MPa and 28.2 MPa, respectively) when compared to control specimens, which achieved a value of 25.7 MPa approximately after a curing period of 28 days. The addition of 4% calcium nitrite produced only a slight increase in compressive strength compared to 2% calcium nitrite concrete at 28 days curing.

The effectiveness of CN on strength development in concrete with different qualities (high or low w/c ratio concrete) has been investigated by many researchers. In research reported by Tomosawa et al. (1990) the development of compressive strength was higher in concrete that was prepared with 0.5 w/c ratio, compared to concrete prepared with 0.6 w/c ratio, when both contained the same dosages of calcium nitrite (10, 20 and 30 l/m^3 of solution containing 33%

CN solid content). At 28 days, the gain of strength in concrete of 0.5 w/c ratio incorporating 10, 20 and 30 l/m^3 calcium nitrite was higher than that in the control specimen by 15.4%, 14% and 13.4%, respectively. For a 0.6 w/c ratio concrete containing the same dosages of calcium nitrite, strength development was higher by 0.7, 4.8 and 7% compared to plain concrete, respectively.

A study carried out by Berke et al. (1993) showed an increase in concrete strength (two mixes were prepared with a w/c ratio of 0.4 and 0.5) by 31% and 11% after 7 days and 48% and 39% after 28 days of curing, respectively, due to the incorporation of 15 l/cm^3 of 30% CN solution, indicating that the lower w/c ratio concrete had the higher strength development. Another study was conducted by Mulheron and Nwaubani (1999) to investigate the effect of calcium nitrite in three types of concrete. These were: high quality concrete prepared with w/c of 0.3, good quality concrete prepared with w/c of 0.45 and poor quality concrete prepared with w/c of 0.6. It was found that in all the concrete mixes, which incorporated 4% calcium nitrite (anal. grade) by weight of cement, the compressive strengths were higher by 12 ± 1% compared to other mixes that had been prepared with the same mix proportions but without calcium nitrite. Troconis de Rincón et al. (2002) prepared concrete mixes at different w/c ratios (0.45, 0.5 and 0.6) and with 2%, 3% and 4% CN solution by weight of cement and found that the 28 days compressive strength increases as CN addition increases depending on the w/c ratio.

In addition to the above studies, Montes et al. (2005) compared the compressive strength development of concrete prepared at w/c ratio of 0.29, 0.37 and 0.45 and containing 0, 12.5 and 25 l/m^3 calcium nitrite (in the form of liquid containing a minimum of 30% calcium

nitrite solid content), with concrete that was prepared without calcium nitrite as a control mix. It was found that the mean strengths of calcium nitrite concretes were higher in all cases when compared to control specimens, after a curing period of 28 days. It was also noted that the 28 days compressive strength of concrete prepared with 0.37 and 0.45 w/c ratio increased gradually as calcium nitrite addition increased from 12.5 l/m^3 to 25 l/m^3, while the compressive strength development of concrete that was prepared with a lower w/c ratio of 0.29 decreased when the addition of calcium nitrite increased from 12.5 l/m^3 to 25 l/m^3. Table 8-1 presents the increases of compressive strength development in percentages for concrete prepared at different w/c ratios and made with 3 levels of calcium nitrite.

Table 8-1 The percentage of concrete compressive strength development made with different levels of calcium nitrite and prepared at various w/c ratios

W/C	CN, l/m^3	Strength development*, %
0.29	0	-
	12.5	14.2
	25	8.1
0.37	0	-
	12.5	16.1
	25	21.5
0.45	0	-
	12.5	14.5
	25	32.7

* Compared to control

The highest enhancement in compressive strength development reported by Montes et al., (2005) was noticed in the concrete that was prepared with a w/c ratio of 0.45 and with 25 l/m^3 of calcium nitrite, as can be seen from Table 8-1.

However, some of the data obtained by other workers regarding the performance of calcium nitrite on the concrete compressive strength is contradictory. In some research where a low addition of calcium nitrite was used, e.g. 5 l/m^3 as 30% calcium nitrite solution, the calcium-nitrite-concrete contributed a 10.4% higher strength than that of reference concrete at 3 days while no significant strength change was noticed between CN-concrete and reference concrete at 28 days, as reported by De Schutter and Luo (2004).

The inclusion of CN in concrete is found to be effective in improving the early compressive strength as cited by all the above researches. For this particular reason, it was decided to use CN in this study as an accelerator admixture.

8.2.2 Effect of calcium nitrite on fresh properties of concrete

8.2.2.1 Influence on workability

The durability and the hardened properties of concrete can be influenced by the workability of the concrete. For instance, the strength of concrete is seriously affected by the compaction degree and to reach the maximum density of compaction, the concrete must have sufficient workability. A sufficient workability of concrete is necessary so that the concrete can be transported, placed, compacted and finished easily without segregation. The workability of concrete can be influenced by many factors, including water content, size of aggregate and grading, shape and texture of aggregate (Neville, 1995) and the use of chemical admixtures.

In early work performed by Rosenberg et al. (1977) it was found that the incorporation of calcium nitrite into concrete had little effect on slump value. According to Tomosawa et al. (1990), adding calcium nitrite (11.8 l/m^3 as 30% CN solution) into concrete led to a slight increase in the slump value, e.g. from 180 mm to 190 mm. Another study carried out by Berke and Sundberg (1990) on calcium nitrite as a corrosion inhibitor showed that an increase in slump value (from 66 mm to 91 mm) was observed when 2% calcium nitrite by mass of cement was incorporated into the mixture.

The effect of two types of cement on the properties of fresh concrete were evaluated by De Schutter and Luo (2004). The first type was Portland cement CEM I 42.5 R and the second type was blast furnace slag cement (BFS). It was found that the addition of calcium nitrite (5 l/m^3 as 30% CN based solution) enhanced the consistence of the fresh concrete by 27% and 67% in Portland cement and BFS cement, respectively. The enhancement in consistence of the concrete was more pronounced in the case of BFS cement. Table 8-2 illustrates slump values measured from two different concretes and the percentage of improvement in the slump due to the addition of CN.

Table 8-2 Slump tests measurements obtained from plain and BFS concrete made with and without CN addition

Mix Name	Slump, mm	percentage of improvement*, %
Portland cement	75	-
Portland cement + CN	95	27
BFS cement	55	-
BFS cement + CN	90	64

* compared to mixture made without CN.

From Table 8-2, it was observed that the use of BFS cement reduces the consistence from 75 mm as in plain concrete to a value of 55 mm. Incorporation of calcium nitrite into concrete made with BFS cement increases consistence by 64 % compared to that in BFS-concrete made without CN. This finding indicates that the calcium nitrite improves the consistence of the fresh concrete in both cements, plain and blended cements and more significant influence was noticed in the blended cement.

It would appear from the available literature that calcium nitrite enhances the workability of concrete.

8.2.2.2 Influence on setting time

One of the major purposes of introducing calcium nitrite into concrete is due to its characteristics in accelerating the concrete compressive strength development rate at early hydration ages. In the majority of cases, also, the addition of calcium nitrite resulted in shorter setting times when compared with reference concrete. In 1977, Rosenberg et al. carried out a study of the use of calcium nitrite in concrete which showed that addition of calcium nitrite accelerated the setting time of the concrete. Furthermore, it was found that, initial and final setting times were both accelerated by more than 2 hrs compared with those of the reference mixture when 1% of calcium nitrite by weight of cement was incorporated. In the case of 2% calcium nitrite addition, the setting times were accelerated significantly. The corresponding initial and final setting times were accelerated by more than 5 hours compared with the reference mixture.

8.2.3 Effect of calcium formate on hardening of concrete

8.2.3.1 Influence on compressive strength development

The other non-chloride concrete accelerator chemical admixture used in this investigation was calcium formate (CF). Commonly, CF has been used as an alternative non-chloride concrete accelerator admixture (Domone, 2010). CF is an organic chemical admixture with a formula of $Ca(HCOO)_2$. It is a by-product that results from manufacture of the polyhydric alcohols (Rixom and Mailvaganam, 1986).

CF has a US patent number of 3,210,207 as a non-corrosive accelerator for the setting of cements (Dodson et al., 1965). According to Dodson et al., the results of 2% CF addition revealed that the CF improves the compressive strength of concrete. Another study was carried out by Rosskopf et al. (1975) adding CF at rates of 0.5, 1.0, 1.5 and 2.0% by weight of cement. The results indicated that the addition of CF accelerates the strength development rates. The addition of 2% CF increased the strength by 20.3% and 7.8% compared with that in the control when tested after 7 and 28 days, respectively. In another study, the strength results revealed that the development rate in CF-concrete containing 2% CF addition was higher compared to plain concrete in the first 24 hours and the 4% CF-concrete was higher in strength compared to 2% CF-concrete (Ramachandran, 1995).

The strength development of concrete may be influenced by the cement composition when CF is used as admixtures. Gebler (1983) evaluated the effectiveness of CF as a non-chloride concrete accelerator admixture. The levels of CF that were investigated in his work were 1, 2, 3 and 4% by weight of cement. All the 28-days compressive strengths improved due to the

incorporation of CF at all CF levels. However, the results indicated that the strength improvement was influenced by the sulfate content in the cement. In detail, the development of the strength of the concrete when CF was incorporated was more effective when the C_3A to SO_3 ratio in the cement was higher than 4. Also, in Gebler's (1983) study it was reported that the addition of 2 and 3% CF by weight of cement is the optimum level to accelerate compressive strength development.

Further study was carried out by Heikal (2004), to examine the effect of CF addition on the mechanical properties of cement paste. Various dosages of CF of 0, 0.25, 0.5 and 0.75 by weight of cement were incorporated in the mixtures. The results of Heikal's (2004) work indicated that the addition of all dosages improved the compressive strength of cement cured for only 3 days and up to 365 days.

Recently, however, an evaluative study on the consequences of CF as a concrete accelerator on the fresh and hardening properties of cement mortars was conducted by Felekoglu et al. (2011) and this showed there was a reduction in compressive strength in samples that were tested after 1, 7 and 28 days curing. The CF was used as a liquid containing 14.6% CF solid content. The CF dosages were 0.4 and 1 and 1.6% CF by weight of cement. This reduction in compressive strength could be attributed to the low level of CF solid content (14.6%), which implies that the CF content in the solution was not sufficient enough to improve the strength.

8.2.3.2 Acceleration mechanism

The acceleration mechanism by which CF accelerates compressive strength development is unclear. The use of hardening accelerators which are either acids or salts of acids are believed to affect mainly C_3S phase to enhance strength development rate at early ages by aiding the dissolution of lime (Edmeades and Hewlett, 2003). Incorporation of CF accelerates the reaction rate for calcium silicate phases (C_3S and C_2S) (Rixom and Mailvaganam, 1986) where these silicates are responsible for producing the main hydration products; calcium silicate hydrate (C-S-H) and calcium hydroxide (CH). The C-S-H is the main component that contributes to most of the strength at an early stages of hydration (Neville, 1995). The quantity of the $Ca(OH)_2$ formed is more than double, due to the hydration of C_3S when compared to C_2S hydration. Consequently, the formation level of $Ca(OH)_2$ could be used as an indication of the hydration reaction progress and to evaluate the extent of C_3S hydration. A study was carried out by Ramachandran (1982) to investigate the effects of chemical admixtures on cement hydration. The rate of hydration was evaluated by measuring the $Ca(OH)_2$ which formed at various times. The results that were obtained in this work revealed that a higher amount of $Ca(OH)_2$ was formed in the presence of CF, indicating that the rate of hydration of tricalcium silicate was accelerated. A further study to evaluate the influence of CF on the C_3S hydration was carried out by Singh and Abha (1983). The hydration rate of the C_3S at different hydration times with range of levels (0-6%) of CF was measured by determination of free $Ca(OH)_2$ and non-evaporable water content. The hydration degree with various amounts of CF is presented in Table 8-3.

The results shown in Table 8-3, revealed that the addition of CF accelerated the hydration rate of C_3S at all times, which resulted in a high degree of hydration compared to the control specimens. It was found that there was no significant effect of more than 2% CF addition on the rate of hydration of C_3S and this can be seen more clearly by comparing the degree of hydration during the 24 hour period when a variety of CF dosages were incorporated. This was attributed to the completed adsorption of the calcium formate at the C_3S surface, while any excess of CF will not accelerate the hydration process.

Table 8-3 Hydration degree of cement contaminated with various levels of CF as reported by Singh and Abha (1983)

% CF	Time, hrs.	% Degree of hydration
0	4	12.73
	8	39.36
	16	50.15
	24	59.95
0.5	8	46.08
	24	68.08
1.0	8	52.85
	24	69.78
2.0	4	45.24
	8	68.08
	16	76.11
	24	80.33
4.0	4	42.71
	16	80.00
	24	82.88
6.0	4	44.86
	16	80.38
	24	82.71

Furthermore, a reduction in the pH value of the solution could be another factor that accelerates the hydration reaction. The incorporation of calcium formate caused a slight reduction in the pH of the solution as reported by Singh and Abha (1983), which aids the acceleration of the hydration of cement. Consequently, more formation of $Ca(OH)_2$ occurs and the excess of the formed $Ca(OH)_2$ will precipitate, followed by further reduction in the pH of the solution (Singh and Abha, 1983) and hence more dissolution of calcium silicates.

8.2.4 Effect of calcium formate on properties of fresh concrete

8.2.4.1 Influence on workability

Workability tests were performed for different concrete mixes by Dodson et al. (1965). CF was incorporated into five different mixes of concrete and the workability for most of the mixes increased. Research reported by Gebler (1983), however, showed that the inclusion of CF into mortar mixture had an adverse affect on the workability of mortar. The result revealed that there was a reduction of 32.7% in slump as CF increased from 0% to 6% CF by weight of cement. There was no technical explanation given by Gebler (1983) for this reduction in the workability. Rixom and Mailvaganam (1986) stated that the addition of CF as an accelerating admixture in concrete has no significant effect on workability. Another study carried out by Felekoglu et al. (2011) who studied the effect of various levels of CF (0.4, 1 and 1.6% by weight of cement) on consistence by measuring the flow, showed that the addition of CF has no effect on the workability of cement mortar. CF was added in the form of solution containing 14.6% CF solid content.

8.2.4.2 Influence on setting time

The setting times can be influenced by many factors such as water content, cement fineness, the ambient temperature, C_3A content (Neville, 1995) and might be by hardening accelerator admixtures. The principal aim of using a non–chloride hardening accelerator admixture such as CF is to accelerate early strength development, as discussed in subsection 8.2.3.1. Also, incorporation of CF into concrete was found to reduce the setting time. Rosskopf et al. (1975) investigated the influence of different levels of CF on setting time development. Four levels of CF, 0.5, 1, 1.5 and 2% by weight of cement, were evaluated. The final setting time was lower by 18%, 23%, 30% and 38% in the concrete made with these four levels of CF respectively, compared to that of the control specimen. A 51% and 59% reduction in initial and final setting time was achieved, respectively when 5% CF by weight of cement used in the concrete compared to plain concrete as reported by Bensted (1978). By adding 2% of CF by weight of cement, Bensted (1980) confirmed the action of CF as an accelerator of setting. Bensted (1980) attributed the acceleration in setting times to the early formation of C-S-H. In addition, Bensted (1980) found that the formation of ettringite was accelerated by the addition of CF. Data from a study carried out by Heikal (2004) reveals that cement pastes made with 0.25, 0.5 and 0.75% CF by weight of cement exhibited shorter setting times and the final setting time was reduced from 270 mins in the control specimen to 210, 200 and 180 mins as CF addition was increased from 0.25, 0.5 to 0.75%, respectively. Heikal (2004) attributed this reduction in the setting time in CF cement paste to the amount of ettringite formed and its crystalline shape.

In a recent study performed by Felekoglu et al. (2011), however, it was reported that the addition of CF had no considerable effect on the reduction of the setting time. This failure of

CF in accelerating the setting process was attributed to three reasons: (1) the low solubility of CF, (2) low dosage of CF and (3) the C_3A/SO_3 ratio of the cement was less than 4 since a higher value is required to accelerate the setting effectively as claimed by Gebler (1983).

The above cited studies have shown clearly addition of both of CN and CF accelerated the compressive strength development of the Portland cement concrete. For the purpose of this Chapter, experiments were conducted to examine the possibility of overcoming the excessive concrete retardation when high levels of BHD are used by incorporating CN and CF as non-chloride concrete hardening accelerators.

8.3 EXPERIMENTAL PROCEDURES

8.3.1 Sample preparation

8.3.1.1 Cement paste specimens

For compressive strength, UPV and thermal analysis studies, cement paste specimens were prepared at a constant water/cement ratio of 0.4, using the various additions of BHD and accelerators by weight of cement indicated in Table 8-4 and mixed as described in subsection 3.2.1. The 8 % BHD addition was chosen based on the results of the work curried out by Hamilton and Sammes (1999) that show the addition of 5 % EAFD into concrete did not reduce the 7-days compressive strength significantly while the addition of 10 % EAFD caused a sever retardation. The mixed cement pastes were then cast in 50 mm cube moulds. 18 cubes were cast from each mix. They were cured at room temperature in the moulds for the first 3

days and then in a sealed container filled with water-saturated, CO_2-free air until required for testing. After a specific period of hydration, ultrasonic pulse velocity (UPV) and compressive strength tests were carried out for each specimen. For TG/DSC studies, one specimen was selected from each mix. The selected specimens were ground using mortar and pestle until they passed through a 0.5 mm sieve. To stop further hydration of the cement, acetone was added to the ground material with stirring and then slowly evaporated (Traetteberg et al., 1974). Note: this technique for stopping hydration was used as other researchers have found that it does not significantly modify the composition of hydrated cement paste (Collier et al., 2008). Prior to the application of TG/DSC analysis, the dried samples were stored in a vacuum desiccator over silica gel and soda lime before being ground to pass a 63 µm sieve. For more details of thermal analysis technique and testing procedure see subsection 8.3.6 and 8.3.6.1, respectively.

Table 8-4 Mix design proportions for TG/DSC studies.

Mix No.	BHD, %	Non-chloride accelerator, %
1	0	0
2	8	0
3	8	3.5 per cent of CF
4	8	3.5 per cent of CN

8.3.1.2 Concrete specimens

Several concrete mixes were prepared with a W:C:FA:CA ratio of 0.4:1:1.2:2.2 by weight of cement. The required quantity of BHD material by weight of cement was weighed and mixed in the same way described in subsection 3.2.2. The concrete specimens were then cured in a

fog chamber where the temperature was maintained at 22 ± 2 ºC and with a relative humidity of 100 per cent until the appropriate hydration times were achieved. Table 8-5 gives a summary of the mix variables.

Table 8-5 Summary of BHD and non-chloride accelerators proportions evaluated in this study

Mix No.	BHD, %	Non-chloride accelerator, %
1	0	0
2	8	0
3	0 and 8	3.5 per cent of CF
4	0 and 8	3.5 per cent of CN

8.3.2 Determination of consistence of concrete

Slump tests were performed for all mixes prepared with different proportions of BHD and different dosages of non-chloride accelerators to evaluate the effect of the combination of BHD additive and concrete accelerators on the consistence of concrete. The tests were carried out in according to BS EN 12350-2 (2000).

8.3.3 Determination of ultrasonic pulse velocity

Ultrasonic pulse velocity measurements were carried out using a PUNDIT 7 Ultrasonic Pulse Velocity (UPV) Tester. Resonant frequencies of 54 KHz were used. UPV tests were performed according to BS EN 12504-4 (2004) for all concrete cubes just before the compressive strength measurements.

8.3.4 Determination of compressive strength

To study the effectiveness of CF and CN accelerators on the compressive strength development of concrete containing elevated levels of BHD, cement pastes and concrete mixes were prepared as described in subsection 8.3.1.1 and 8.3.1.2, respectively. Cement pastes and concrete cubes from each mix were crushed for compressive strengths measurements after a curing period of 3, 7 and 28 days. The compressive strength tests were performed according to BS EN 12390-3 (2009).

8.3.5 Determination of setting time

Setting times of mortar were determined using a Vicat apparatus. The Vicat apparatus consists mainly of a plunger with a needle attached at the end and a mould provided with a glass base plate. Before filling, the mould was placed on the greased base plate to prevent water leaks from the bottom of the mould. The mould was then filled with a mortar which was prepared as described in subsection 3.2.1. After filling, the excess mortar was removed carefully with a straight edge leaving the mould with a flat surface and the initial and final setting times determination were conducted according to BS EN 480-2 (2006).

8.3.6 Thermal Analysis Technique

For the purposes of studying the effects of CN and CF addition on hydration in BHD-cement pastes, thermal analysis was utilized. The extent of the cement hydration process can be evaluated by comparing the quantity of the hydration products formed at specific ages. There are multiple thermal analysis techniques available, the most widely used of which are thermogravimetry (TG), differential thermal analysis (DTA) and differential scanning

calorimetry (DSC). DSC is a simple technique for identifying various materials that undergo physical or chemical transformations with associated energy changes which can be measured when a gradual heating programme is applied.

The sample to be tested is placed in one cavity and a thermally inactive reference material (alumina) is placed in the second cavity. Both, the specimen to be tested and the reference are subjected to a uniform heating rate. The temperature difference (ΔT) between the sample (Ts) and reference (Tr) were maintained throughout controlled temperature program ($\Delta T = Ts - Tr = 0$). The resulting difference of heat flow (ΔQ) i.e. amount of energy, between the materials was recorded as a function of temperature and/or time, where ΔQ depends on the exo- or endothermal character of the transformation occurring in the test sample. For instance, in the case of a decomposition process , the observed ΔQ may be positive indicating an endothermal process (Brown, 2001). In the case of specimens of hydrated cement, hydration products that undergo thermal decomposition at particular ranges of temperature are also identifiable by their endothermal ΔQ peaks on the DSC trace.

In this research, TG was also used to measure the changes in the weight of the sample when a constant heating programme was applied which caused the removal of bound water from all the hydration products. The first derivative of the mass-change (TG) curve will result in a DTG curve which can be used to resolve overlapping processes. This (TG) technique is a useful method particularly to quantify the calcium hydroxide present in hydrated cement samples as the thermal decomposition of calcium hydroxide to calcium oxide and water produces clear endothermal DTG peaks and mass changes over a limited range of temperatures in the region of 500 ºC.

8.3.6.1 TG/DSC studies procedure

In the present work, a NETZSCH STA 449 C thermal analyzer was used to provide simultaneous TG and DSC measurements over the temperature range from room temperature to 800°C with a heating rate of 10°C per minute. The TG/DSC studies were carried out in an argon atmosphere. The reference standard sample in this study was alumina, Al_2O_3. The size of the specimen used for TG/DSC studies was between 20 and 40 mg.

8.4 RESULTS ANALYSIS AND DISCUSSION

8.4.1 Effect of Calcium Nitrite and Calcium Formate on Consistence

Although there has been limited work carried out on the effect of BHD on properties of fresh concrete, the work that has been done previously has focused on utilizing BHD in small quantities. For instance, Al-Sugair et al. (1996) and Al-Zaid et al. (1999) investigated the influence of 2 and 3% of BHD by weight of cement on some of the properties of fresh concrete, whereas in this current study the addition of BHD was 8% by weight of cement.

Table 8-6 shows the slump measurements, which were obtained according to (BS EN 12350-2, 2000), for concrete mixes containing different levels of BHD, made with and without concrete accelerators. It is clear from Table 8-6 that the addition of BHD severely reduced the consistence of the concrete, which exhibited practically zero slump as shown in Figure 8-1. A reduction in the workability of the concrete containing EAFD was also reported by Castellote et al. (2004). This reduction could probably be related to the high specific surface of EAFD as the material is composed of very fine spherical particles which are smaller than 5

µm in size (Flores-Velez and Dominguez, 2002, Machado et al., 2006, Stegemann et al., 2000). The explanation of this is that the finer particles require more water to lubricate the larger surface area.

Table 8-6 Effects of CN, CF and BHD additions on slump data

Sample	Slump (mm)
Control	43
8% BHD only	0
3.5% CN only	90
3.5% CF only	74
8% BHD + 3.5% CN	60
8% BHD + 3.5% CF	130

Figure 8-1 Actual concrete slump for 8 per cent addition made without concrete accelerators

As expected, based on previous studies (Berke and Sundberg, 1990, Dodson et al., 1965, Tomosawa et al., 1990), additions of CN and CF increased the workability of the control concrete, see Table 8-6. Also the consistence of the BHD concretes effectively improved when CN or CF was used as an additive and showed consistences in the S2 and S3 classes, respectively as defined by BS EN 206-1 (2000). The mechanisms of these effects are not yet understood but they are thought to be dependent on the ability of the two admixtures to deflocculate aqueous dispersions of BHD/cement powder, releasing water trapped within clusters of particles and so facilitating flow of the fresh paste.

8.4.2 Effect of calcium nitrite and calcium formate on setting times

On the basis of previous studies reviewed in subsection 2.2.4, BHD increases the setting time considerably when introduced into concrete. Such behaviour is not acceptable practically and it is believed to be a drawback of using high levels of BHD in concrete construction industry, therefore the use of concrete accelerators may be beneficial.

Table 8-7 presents the initial and final setting times for different mortars made with and without the BHD addition and non-chloride accelerators, where incorporation of BHD material into mortar had a strongly retarding effect on setting times. This delay in setting times of BHD-mortars obtained in the current research could attributed to the consumption of the dissolved calcium and hydroxide ions in the solution due to the formation of calcium hydroxy-zincate resulting in delay of calcium hydroxide precipitation and formation of calcium-silicate-hydrate gel (Weeks et al., 2008) where further related discussion is presented in subsection 2.2.5.

Table 8-7 Effects of CN, CF and BHD additions on setting times of mortars

Sample	Initial setting time	Final setting time
Control	4 hrs 10 mins	5 hrs 55 mins
3.5 CN only	3 hrs 0 mins	3 hrs 54 mins
3.5 CF only	4 hrs 0 mins	4 hrs 55 mins
8% BHD	12 hrs 40 mins	17 hrs 10 mins
8% BHD + 3.5% CN	18 hrs 38 mins	23 hrs 50 mins
8% BHD + 3.5% CF	20 hrs 40 mins	24 hrs 54 mins

To utilize higher levels of BHD, the setting time needs to be improved and for this reason, the retardation effect of BHD was compensated by using CN and CF as concrete accelerator. The setting times of OPC mortars containing 3.5% CN and 3.5% CF addition by weight of cement were reduced compared to those in the control specimen confirming the effectiveness of these accelerators on setting times.

The mortars contaminated with 8% BHD by weight of cement were treated by addition of either 3.5% CN or 3.5% CF by weight of cement trying to overcome the retardation effect of BHD. In both cases, the improvement in setting times was not achieved and even more delay in setting was noticed when CN or CF was used. This failure in reducing the setting time in the 8% BHD-mortar treated with 3.5% CN and 3.5% CF addition may be related to the changes in consistence described in the previous section but again the detailed mechanisms remain to be resolved.

It was found that the addition of 3.5% CN and 3.5% CF improved the strength development rate in both of cement pastes and concretes, as discussed in section 8.4.4.1 and 8.4.4.2,

respectively, containing 8% BHD after 3 days curing compared to those concretes made with the same level of BHD but without concrete accelerators. These results indicate that the CN and CF did not improve the setting of BHD mortar but rather improved the hardening characteristics of the BHD concrete. Consequently, these accelerating admixtures, namely calcium nitrite and calcium formate, act as hardening accelerators and not as setting accelerators in the presence of BHD material and the Saudi Portland cement used in this research.

8.4.3 The relationship between UPV and compressive strength

In order to evaluate the possible effect of non-chloride accelerators on the hardening of cement pastes, which were prepared with a water/cement ratio of 0.4 as described in section 8.3.1.1, made with elevated level of BHD a number of tests (UPV, compressive strength and TG/DSC studies) were performed to gain a better understanding of the retardation mechanism when BHD is added into cement. Due to the time concerns involved and the limited amount of the Saudi OPC available, this study was limited to 8 % BHD addition.

The UPV technique was adopted in this study for three main reasons: (a) UPV test provides a good indication of the mechanical properties of development during the hardening/stiffening of concrete (Komlos et al., 1996) and (Grosse and Reinhardt, 2003); (b) UPV values can be used to predict the strength of hardened concrete when a good relationship between strength and UPV is obtained for a particular mix (Lin et al., 2007); (c) it is considered a non-destructive technique where a number of tests can be repeated on the same concrete specimen without causing any damage (Bungey et al., 2006).

In this study, 8 % BHD was added into the cement paste and treated with CN or CF. In order to compensate, the main drawback effect of BHD, the influence of these non-chloride accelerators on compressive strength development rate in the BHD-cement paste was assessed after a hydration period of 3, 7 and 28 days.

The relationship between the mean cement paste compressive strength (f_c) results and mean ultrasonic pulse velocity (V) values, which were obtained from the same paste specimens prepared with 0 and 8 % BHD and treated with 0 and 3.5 % CN and CF by weight of cement is plotted in Figure 8-2. From Figure 8-2, it was found that a reasonably consistent relationship between the paste compressive strength and the ultrasonic pulse velocity was obtained, which followed the expected exponential form of curve (Bungey et al., 2006):

$$f_c = Ae^{BV} \qquad [8\text{-}1]$$

where:

f_c is the paste compressive strength, MPa;

V is ultrasonic pulse velocity, m/s:

A and B are constant.

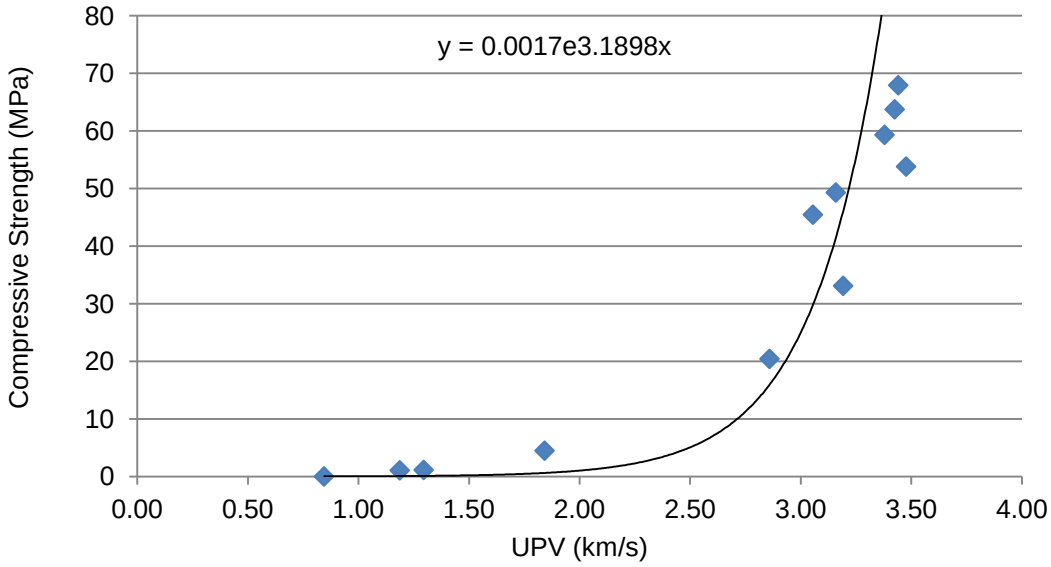

Figure 8-2 Relationship between compressive strength (fc) and ultrasonic pulse velocity (V) for cement pastes

8.4.4 Effect of calcium nitrite and calcium formate on hardening

8.4.4.1 Hardening of cement paste specimens

Compressive strength results were obtained from cement pastes prepared with 0 and 8 % of BHD, a 3.5 % dosage of CN and CF and hydrated for 3, 7 and 28 days are presented in Table 8-8. The corresponding UPV values are presented in Table 8-9 .

From Table 8-8 and Table 8-9, it can be observed that within 3 days all the control specimens (0 BHD and 0 CN/CF) attained an average strength value of 20.4 MPa with a UPV higher than 2.8 km/s. In the presence of BHD, however, the obtained UPV results and strengths failed to achieve comparable values to those in control specimens during the first 3-days. Actually, the hardening of the cement pastes was effectively suppressed for a period of at

least 7 days by the addition of 8% BHD to the control mix. However, for 28 day-specimens, the strength gained was higher than that in the control specimens as shown in Figure 8-3. The corresponding achieved strengths after 28 days of curing in BHD-concrete was 59.3 MPa whereas for the control specimens a value of 53.8 MPa was recorded at this age.

This severe retardation in the compressive strength development of the concrete containing BHD indicates that there was a significant delay in the cement hydration reactions caused by the BHD when more than 2 percent was added into the mixture. Besides that, the low rate of the hydration of 8% BHD-cement paste specimen was confirmed by TG/DTG curves where there were very small or negligible endothermal peaks due to decomposition of the $Ca(OH)_2$ and C-S-H formed during a hydration period of 3 and 7 days (see section 8.4.5).

A clear improvement was observed in the strength development of BHD-concretes treated with CN and CF, and this showed the effectiveness of CN and CF in recovering the hardening characteristics of the BHD-concretes. At early ages, i.e. 3 days hydration, the inclusion of either 3.5% CN or 3.5% CF in the specimens containing 8% BHD was not able to improve the strength. On the other hand, after allowing more time for hydration, all specimens containing either 3.5% addition of CN or CF and mixed with 8 % BHD attained higher compressive strength values when compared to control specimens at 7 and 28 days. Thus the two accelerators were both found to be effective not only in counteracting the excessive retardation of strength development associated with the BHD but actually led to improvements in strength at 7 and 28 days as demonstrated in Figure 8-3.

Table 8-9 presents the UPV development for specimens containing 3.5 % CN and 3.5 % CF and made with 8 % BHD addition. It can be seen that, the UPV values for CN/CF specimens mixed with and without 8 % BHD increases with an increase in the hydration times. Also, the trend of results is in line with compressive strength development obtained from the same specimens, as shown in Figure 8-3.

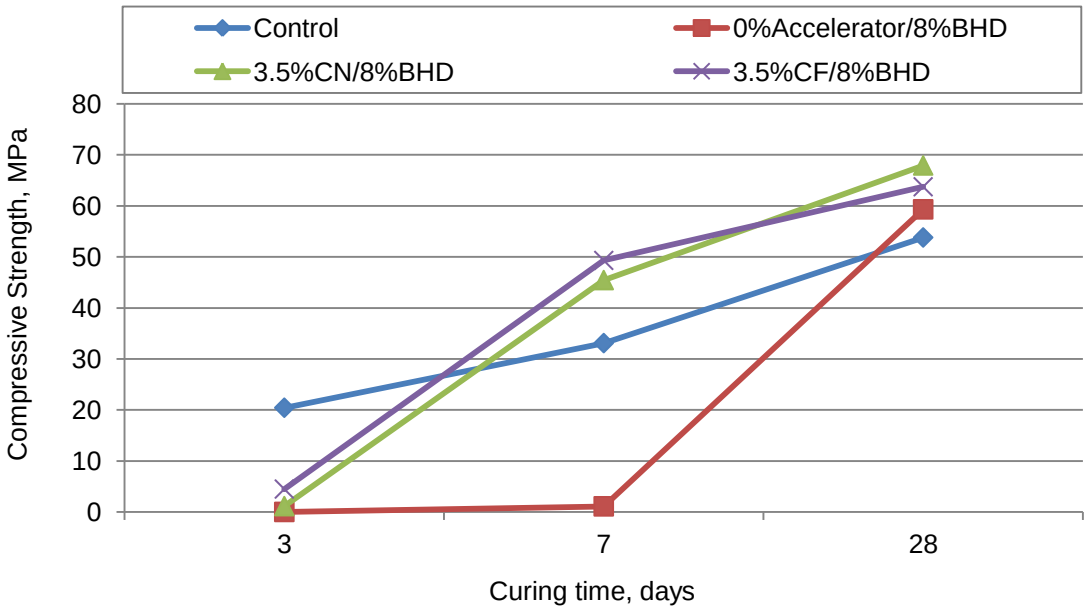

Figure 8-3 Effects of curing time and accelerating admixtures on compressive strengths of cement paste made with or without 8% addition of BHD

Table 8-8 Compressive strength results (in MPa) of cement paste made with nil and 8 per cent BHD addition and containing 3.5 % of CN and CF

Curing (days)	3				7				28			
BHD (%)	0	8	8	8	0	8	8	8	0	8	8	8
Accelerator (%)	0	0	3.5 CN	3.5 CF	0	0	3.5 CN	3.5 CF	0	0	3.5 CN	3.5 CF
Cube 1	20.5	0.0	1.1	4.5	33.7	1.0	46.4	50.6	54.2	59.0	68.6	67.4
Cube 2	21.2	0.0	1.1	5.0	32.8	1.1	47.7	49.6	53.4	54.3	68.7	69.0
Cube 3	21.2	0.0	1.2	4.3	32.9	1.0	46.9	50.1	53.5	60.7	70.2	59.8
Cube 4	20.2	0.0	1.1	4.4	31.4	1.1	44.5	50.0	52.8	62.5	67.2	62.8
Cube 5	20.0	0.0	1.2	4.5	35.0	1.1	44.0	47.8	55.1	59.4	68.9	64.0
Cube 6	19.4	0.0	1.2	4.3	32.9	1.1	43.2	47.7	53.9	60.1	64.0	59.4
Mean	20.4	0.0	1.1	4.5	33.1	1.1	45.5	49.3	53.8	59.3	67.9	63.7
SD	0.7	0.0	0.0	0.3	1.2	0.0	1.8	1.2	0.8	2.8	2.1	3.9

Table 8-9 UPV measurements (in Km/s) for cement paste made with nil and 8 per cent BHD addition and containing 3.5 % of CN and CF

Curing (days)	3				7				28			
BHD (%)	0	8	8	8	0	8	8	8	0	8	8	8
Accelerator (%)	0	0	3.5 CN	3.5 CF	0	0	3.5 CN	3.5 CF	0	0	3.5 CN	3.5 CF
Cube 1	2.86	0.83	1.32	1.83	3.27	1.23	3.01	3.13	3.46	3.33	3.42	3.42
Cube 2	2.87	0.85	1.29	1.85	3.21	1.16	3.03	3.23	3.42	3.31	3.36	3.42
Cube 3	2.86	0.84	1.30	1.85	3.23	1.18	3.06	3.18	3.45	3.40	3.45	3.40
Cube 4	2.84	0.86	1.32	1.84	3.16	1.20	3.09	3.21	3.50	3.40	3.47	3.45
Cube 5	2.87	0.85	1.30	1.82	3.23	1.18	3.03	3.11	3.45	3.38	3.50	3.40
Cube 6	2.86	0.83	1.27	1.84	3.18	1.17	3.05	3.16	3.50	3.45	3.45	3.45
Mean	2.86	0.84	1.30	1.84	3.21	1.19	3.05	3.17	3.46	3.38	3.44	3.42

8.4.4.2 Hardening of Concrete specimens

Owing to restricted availability of the cement that was imported from Saudi Arabia for this work, it was possible to undertake only a limited amount of work on concrete. Therefore, the concrete specimens were prepared with 0 and 8 % BHD and mixed with 0 and with either 3.5 % CN or 3.5 % CF addition. The strength development of concrete specimens made with 3.5% CN and 3.5 % CF addition were plotted against hydration times in Figure 8-4. The

achieved strengths associated with the addition of either 3.5% CN or 3.5% CF were higher than the corresponding values of the control specimens verifying the main action of CN and CF as concrete hardening accelerators. These findings further support the earlier studies which showed that the effectiveness of CN and CF on the early hardening development rate as discussed in section 8.2.1.1 and 8.2.3.1, respectively. Again, the concrete specimens made with 8% BHD produced broadly similar results to those obtained from cement pastes, showing no measurable compressive strength development during the first 7 days as indicated in Figure 8-5. The effect was counteracted by both accelerators, 3.5% CN additions being apparently more effective than 3.5% CF additions in this respect.

These results indicate the beneficial effects of using either 3.5 % of CN or CF as concrete accelerators to overcome the retardation effect of BHD on the hardening of concrete. This increase in compressive strength when concrete treated with the proposed levels of CF was attributed to improvement in hydration of C_2S and C_3S in the concrete which resulted in more hydration products, as reported by Ramachandran (1995) and Singh and Abha (1983). Supporting this hypothesis, the increase in the formation of hydration products such as CH and C-S-H that were associated with the addition of CN or CF was observed as discussed in subsection 8.4.5. The size of formate ion is 0.45 nm (Edmeades and Hewlett, 2003).

For a hardening accelerator to be effective, it should be soluble and ionised in the mixing water. Also, it should have sufficient ion mobility to penetrate into silicate phases and then accelerate lime dissolution. Therefore, the size of ion plays a major role. The size of nitrite ion is small as 0.34 nm. Also, CN is reasonably high in solubility when mixed with water (50g/100g) (Edmeades and Hewlett, 2003). Then, the acceleration characteristics of CN could

be attributed partly to its high solubility and due to the mobility of nitrite ions, which may promote the penetrability of nitrite ions into silicate phases and accelerate the dissolution of lime.

It can be said that the addition of either CN or CF into BHD concrete improves the compressive strength significantly, and makes it possible effectively to overcome the retardation effect caused by BHD, up to 8 per cent by weight of cement.

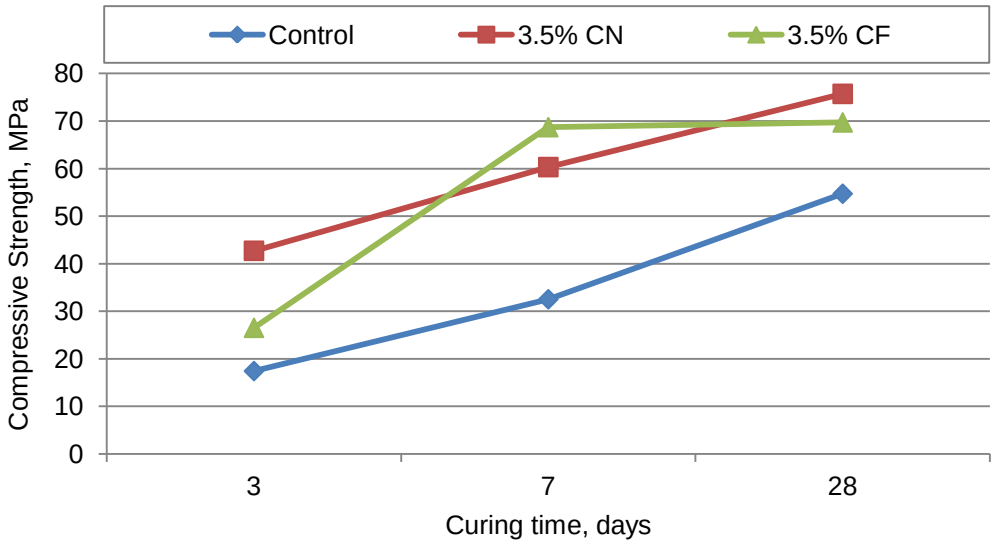

Figure 8-4 Effects of curing time and accelerating admixtures on compressive strengths of concrete cubes made without addition of BHD

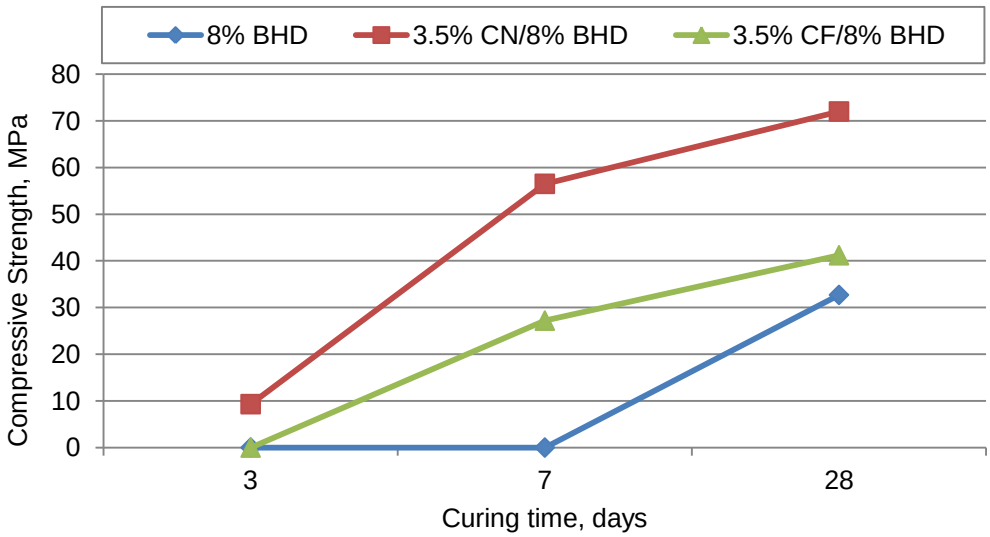

Figure 8-5 Effects of curing time and accelerating admixtures on compressive strengths of concrete cubes made with 8% addition of BHD

8.4.5 Thermal Analysis

Confirmatory evidence regarding the action of BHD as a retarder of cement hydration was provided by thermal analysis of the cement pastes. TG/DSC analyses were conducted on plain cement paste as a control specimen and on samples treated with 3.5% CN and 3.5% CF which were both containing 8% BHD as additive and cured for 3, 7 and 28 days; TG/DTG curves are presented in Figure 8-6 through Figure 8-9.

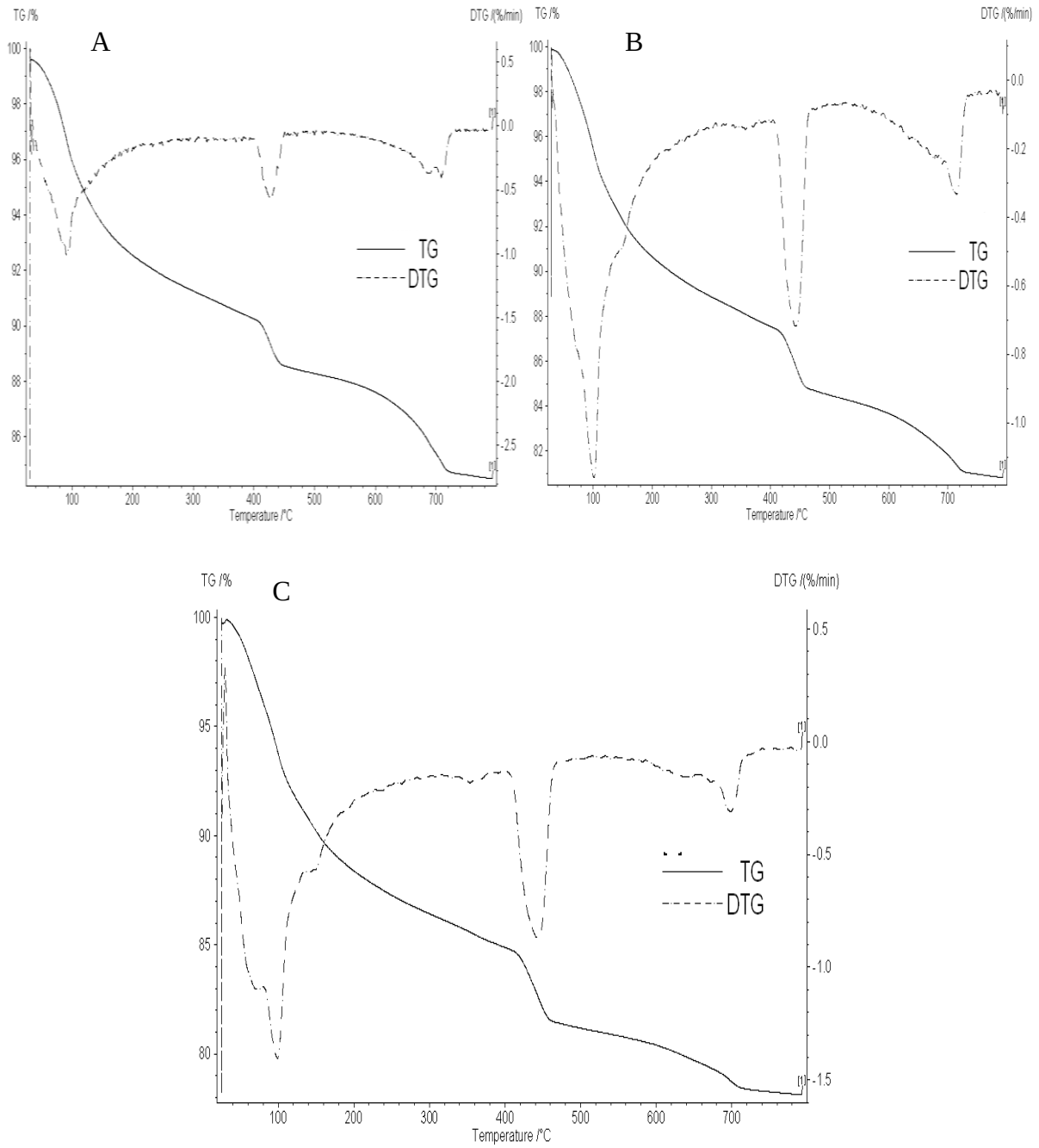

Figure 8-6 TG and DTG curves for plain cement paste specimens hydrated for periods of: A: 3 days, B: 7 days and C: 28 days

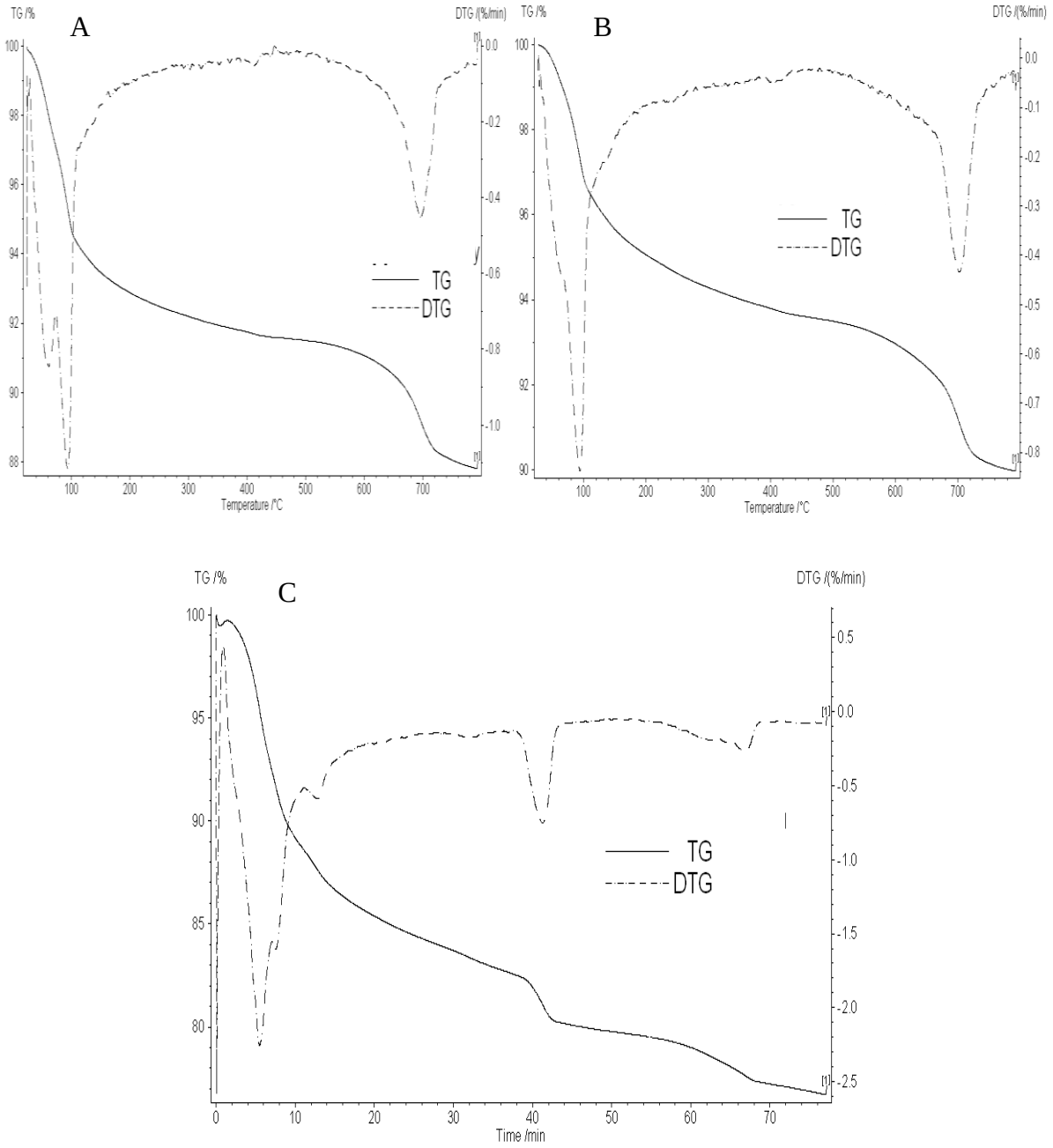

Figure 8-7 TG and DTG curves for cement paste specimens contaminated with 8% BHD and hydrated for periods of; A: 3 days, B: 7 days and C: 28 days

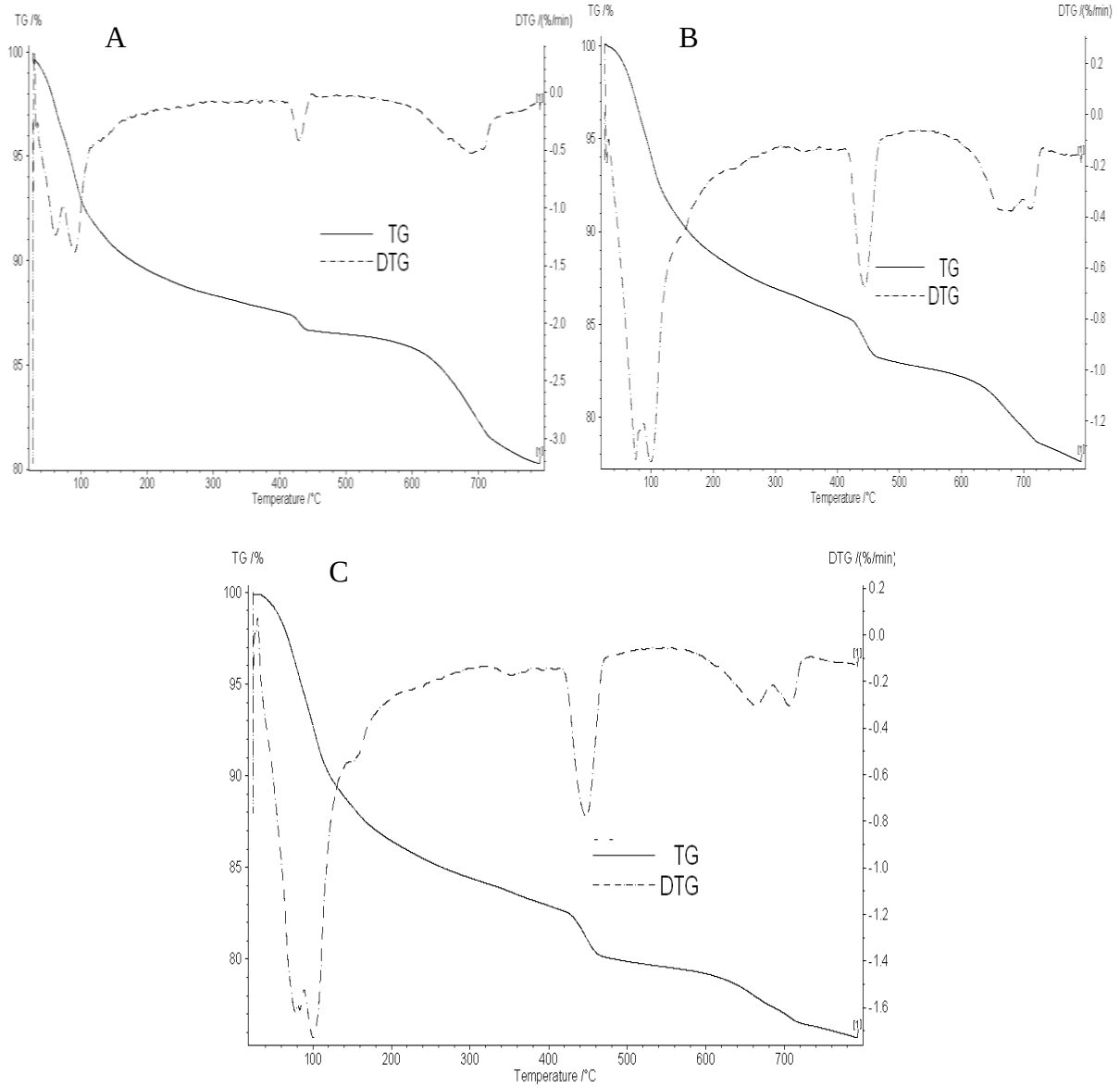

Figure 8-8 TG and DTG curves for cement paste specimens contaminated with 8% BHD and incorporated with 3.5% CF by weight of cement and hydrated for periods of; A: 3 days, B: 7 days and C: 28 days

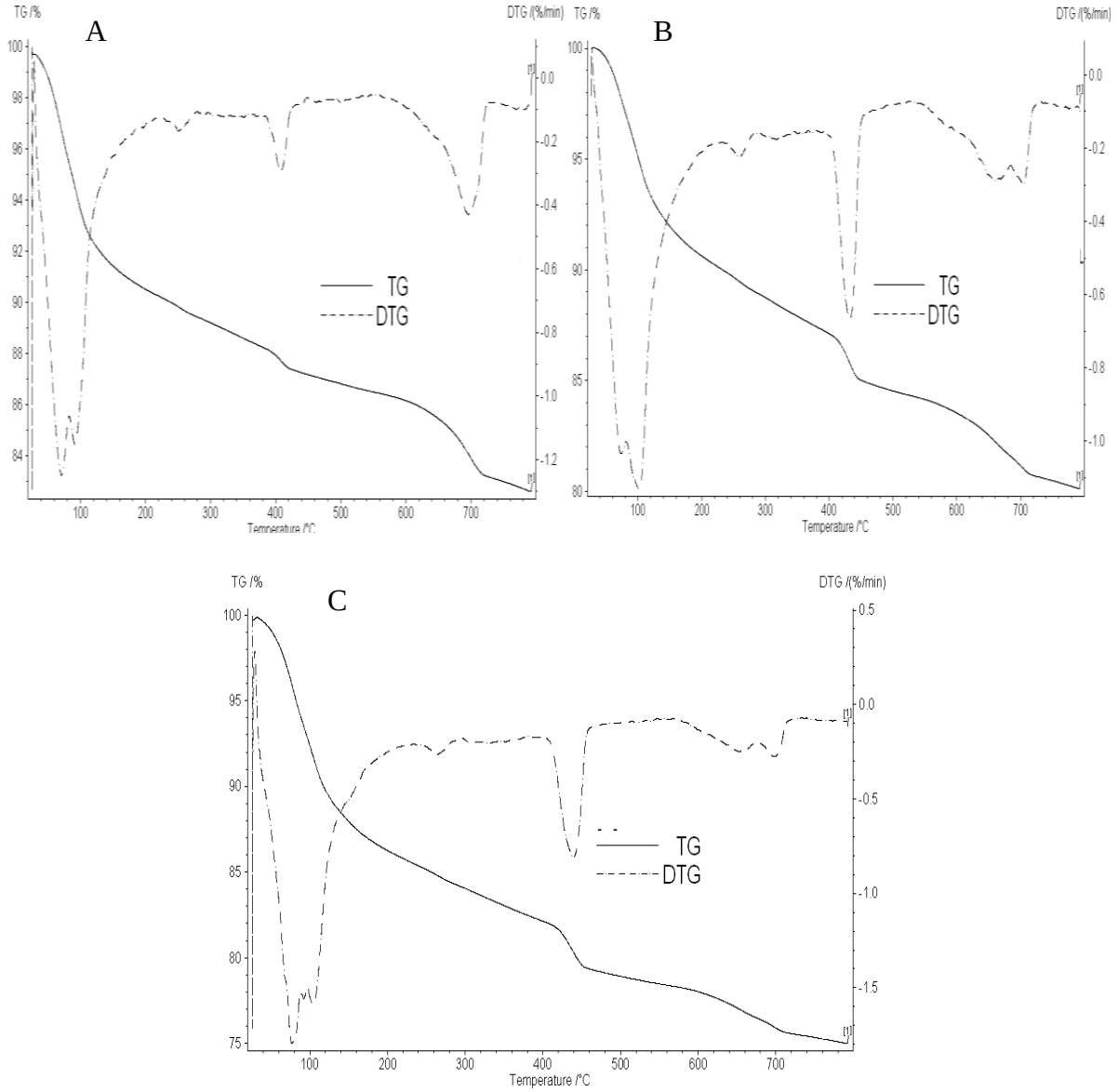

Figure 8-9 TG and DTG curves for cement paste specimens contaminated with 8% BHD and incorporated with 3.5% CN by weight of cement and hydrated for periods of; A: 3 days, B: 7 days and C: 28 days

In the case of control specimens, **Error! Reference source not found.**, the DTG curves xhibit a broad endothermal response over the temperature range 100-200^{o}C corresponding to the loss of bound water at about 115-125^{o}C from C-S-H, the principal hydration product of C_3S, which accounts for most of the strength development at early ages, and to decomposition of other hydrates, such as ettringite and the AFm phases (Taylor, 1997). At approximately 400

– 500°C a clearly defined endothermal peak can be observed, which signifies the thermal decomposition of the other hydration product of C_3S, namely Portlandite. A simple measure of the quantity of portlandite in the sample is thus provided by the magnitude of the associated step in the TG response which represents the weight loss associated with the reaction:

$$Ca(OH)_2 \rightarrow CaO + H_2O \quad [8.2]$$

The content of the calcium hydroxide formed during hydration was estimated using the following formula:

$$\text{Percentage of } Ca(OH)_2 \text{ content} = \frac{MW_{Ca(OH)_2}}{MW_{H_2O}} \; WL_{Ca(OH)_2} \quad [8.3]$$

Where;

$MW_{Ca(H)_2}$ is calcium hydroxide molecular weight; g/mol,

MW_{H2O} is water molecular weight; g/mol,

$WL_{Ca(H)_2}$ is weight loss due the decomposition of calcium hydroxide in %,

From DSC studies, The hydration degree can be also estimated by measuring enthalpy change (ΔH) values that represent the formation of $Ca(OH)_2$. ΔH is the amount of energy absorbed (heat transferred to the sample) due to the decomposition of hydration products. The ΔH is related to the area under the endothermal peak. The area under the peak can be obtained by integration using available software packages (Haines, 2002). In this study, ΔH was calculated using Proteus Analysis – Thermal Analysis version 4.8.3 software package. The

estimated portlandite and the obtained ΔH values are presented in Table 8-10. For validation purposes, A good linear consistent relationship between the estimated portlandite contents obtained by TG measurements and the ΔH values was observed with a very high coefficient of determination (R^2 = 0.98) as demonstrated in Figure 8-10.

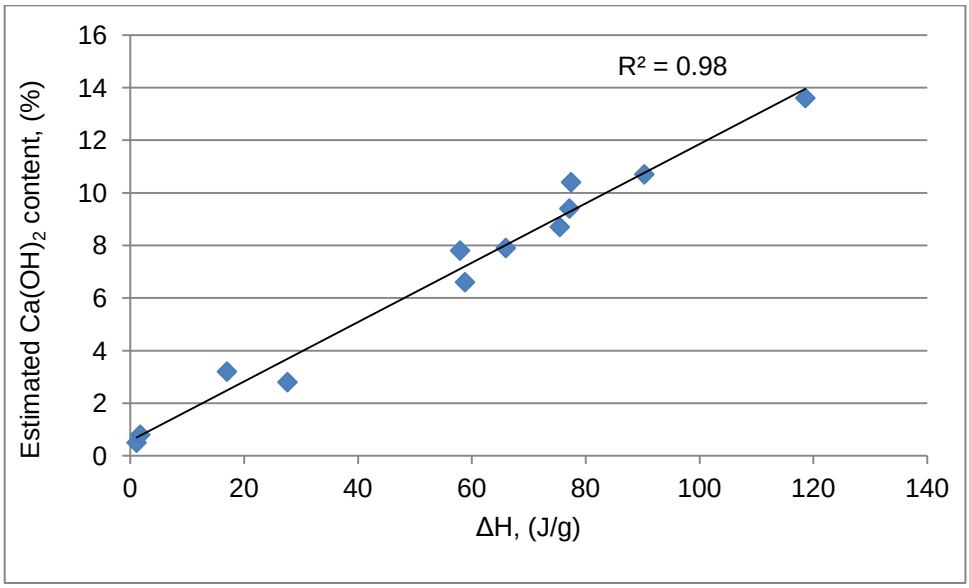

Figure 8-10 Relationship between the percentages of the estimated portlandite and enthalpy changes

The DTG curves in Figure 8-7 (A) and (B) show very small or negligible endothermal peaks at approx. 410 ºC in specimens made with 8% BHD, as evidence of very little formation of portlandite, confirming that hydration of C_3S had been almost completely blocked throughout the first 7 days of curing. A higher endothermal peak was detected for 28 day hydrated specimens indicating the start of the hydration reaction. It can be observed, however, that the incorporation of 3.5% CF or CN with 8% BHD specimens resulted in major endothermal peaks at all stages of hydration, which can be seen in the DTG/TG curves presented in Figure

8-8 and Figure 8-9 respectively. They provide evidence of the hydration products of C_3S. From the same specimens, appreciable quantities of portlandite were found even after 3 days indicating a higher degree of hydration, as presented in Table 8-10.

Although the mechanism of retardation of cement hydration by zinc and lead compounds remains incompletely understood, the evidence reported here seems consistent with the view that delayed precipitation of calcium hydroxide and C-S-H may be associated with the prior formation of calcium hydroxy-zincate or plumbate species which consume Ca^{2+} and OH^- from the pore solution (Weeks et al., 2008). As sources of additional Ca^{2+}, the CN and CF may thus reduce the time required to achieve supersaturation of the solution with respect to $Ca(OH)_2$. The continuing availability of CN after 3 days of curing is indicated by the small endothermal peak at about 250^{o}C in Figure 8-9. At this temperature, the calcium nitrite decomposes into calcium oxide and a mixture of nitrogen dioxides (Laue et al., 1988) according to following equation:

$$Ca(NO_2)_2 \rightarrow CaO + NO + NO_2 \qquad [8.4]$$

The endothermal peaks at temperatures in the range 650-800^{o}C, which were exhibited by all the specimens, signified the presence of calcium carbonate (Biffen, 1956), up to 5% limestone being a permitted constituent of Type 1 cements conforming to ASTM C150/C150M-09.

Table 8-10 Estimated calcium hydroxide content and ΔH values measured due to decomposition of CH

Sample	Age (Days)	Wt. Loss (%) for $Ca(OH)_2$	$Ca(OH)_2$ content (%)	ΔH (J/g) for CH
Control	3	1.6	6.6	58.8
	7	2.59	10.7	90.31
	28	3.3	13.6	118.6
8%BHD only	3	0.12	0.5	1.102
	7	0.19	0.8	1.742
	28	2.12	8.7	75.45
8%BHD/3.5%CF	3	0.67	2.8	27.61
	7	1.93	7.9	65.97
	28	2.28	9.4	77.14
8%BHD/3.5%CN	3	0.78	3.2	16.98
	7	1.9	7.8	57.94
	28	2.52	10.4	77.43

In this chapter, numerous tests were performed on different types of specimens to gain better understanding of the retardation mechanism and to examine the possibility of overcoming the retardation effect caused by BHD when added into concrete at high levels. Cement paste specimens were prepared using various additions of BHD and calcium nitrite and calcium formate as described in subsection 8.3.1.1 for compressive strength and UPV measurements and for thermal analysis studies. Also, the consistence of the concrete mixes prepared with different levels of BHD and calcium nitrite and calcium formate, see subsection 8.3.1.2 for the mix proportions and procedure, was evaluated using slump test and the compressive strength development rate was assessed by UPV measurements and then by crushing concrete cubes. Stiffing of different mortars prepared with additions of BHD and accelerators was assessed by setting times measurements using a Vicat apparatus. The conclusions of these results are summarized in the following section.

8.5 ONCLUSIONS

The main conclusions of the work in this chapter were as follows:

1. The incorporation of BHD into plain concrete at an addition level of 8% by weight of cement drastically reduced the workability of the material and increased the setting time of the cement substantially; it also delayed the onset of hardening by more than 7 days and caused serious reduction in the 28 strength of the material.
2. The use of CN or CF as admixtures at levels of 3.5% by weight of cement was effective in improving the workability of fresh concrete containing 8% BHD by weight of cement.
3. Neither admixture was effective in reducing the setting time of the cement in specimens containing 8% BHD but both admixtures caused major improvements in the rate of hardening of the material.
4. The retardation of cement hydration caused by 8% BHD additions was associated with the presence of a high level of zinc and, to a lesser extent, lead in the material which caused hydration of the C_3S component of the cement to be effectively blocked for several days.
5. The acceleration of hardening caused by 3.5% dosages of CN or CF was associated with the ability of these admixtures to counteract the long delay, caused by the presence of BHD, in formation of the hydration products of the C_3S component of the cement.

6. Further work is needed to resolve the detailed mechanisms of the retardation and acceleration effects observed in this research and to evaluate their practical implications.

Chapter 9

CONCLUSIONS AND RECOMMENDATIONS FOR FURTHER RESEARCH

In this Chapter all the general conclusions derived from each experimental study together with recommendations for future research are expressed.

9.1 CONCLUSIONS

Effect of BHD addition on corrosion behaviour of steel bars

In this investigation, the aim was to assess the effectiveness of 2 % BHD addition on the mitigation of the corrosion of steel bars embedded in mortar containing 0, 0.4 and 2 % chloride by weight of cement. On the basis of the results, steel bars embedded in BHD mortar made with no chloride addition exhibited higher corrosion rates compared to those bars embedded in control mortar (no BHD). On the other hand, the corrosion resistance of steel bars embedded in mortar containing different percentages of chloride was enhanced due to the addition of BHD. This improvement was linked to changes in characteristics of the pore solution chemistry.

Effect of BHD addition on hydroxyl ion concentrations

There is a significant influence on the hydroxyl ion concentration in the pore solution when BHD is incorporated. At all chloride addition levels, the hydroxyl ion concentration in the

pore solution extracted from BHD mortars was found to be higher compared to those specimens made without BHD addition at all curing periods.

Effect of BHD addition on free chloride ion concentrations

The addition of BHD led to an increase in the free chloride ion concentration in the pore water compared to that in control specimens at all chloride addition levels indicating a more aggressive pore water condition in the presence of BHD.

Chloride leaching tests

Some of the existing chloride in BHD leached out confirming that the higher chloride ion concentration found in the pore solution extracted from BHD mortar did originate from BHD. In addition to that, the incorporation of 2 % BHD has generally significant effect on pH value of the leached solution. The pH value of the control leached solution was 6.34 and the corresponding pH value for BHD-DW leached solution was 13.17. Also, it was found that the pH of the leaching solution has a slight effect on the solubility of chloride present in BHD where more chloride leaches when the pH of the leaching solution is reduced.

Effect of BHD addition on cement paste porosity

The addition of BHD caused a significant reduction in coarse capillary porosity. The reduction in coarse capillary porosity obtained from group B (10 weeks hydration period) cement paste specimens made with 2 % BHD and prepared at 0.4, 0.5 and 0.6 w/c ratios were 32.7, 37.3 and 24.9 % compared to control specimens prepared at the same w/c ratios. The reduction in the coarse capillary porosity is more pronounced in samples that hydrated for longer period i.e. group B. Incorporation of BHD led to a refinement of the pore structure due

to the packing and filling action. A higher water to cement ratio resulted in higher capillary porosities.

Effect of BHD addition on chloride ion diffusion

The objective of this investigation was to study the ability of the concrete to resist chloride ion penetration in the presence of BHD. This was achieved by determining the chloride diffusion coefficients and the depth from the surface at which chloride content is critical. The limitation of this study was that the scatter in the results was relatively high. However, this study has found that generally the BHD-concrete exhibited a comparable chloride ingress resistance performance to that in concrete made without BHD.

Effect of BHD addition on chloride threshold value

Portland cement blended with BHD resulted in enhancement in chloride-induced corrosion tolerance. The corresponding averaged chloride threshold content was 0.39, 0.89 and 1.19 % by weight of cement for mortars containing 0, 2 and 3.5 % BHD, respectively. This improvement could be associated with the formation of a compacted layer of cement hydration products on the steel in the vicinity of the plastic ties, enhancement in hydroxyl ion concentration in the pore solutions and a remarkable reduction in coarse capillary porosity.

The exposure temperature had a substantial effect on promoting the corrosion process. It was found that the steel bars subjected to higher temperatures corroded faster than those steel bars exposed to lower temperature.

The use of plastic ties played a dominant role in creating crevices at the interfacial zone thereby accelerating the corrosion process of the reinforcement.

Effect of BHD addition on bleeding of concrete

This study set out to examine the influence of various BHD additions on the bleeding capacity of the fresh concrete. The results of bleeding tests showed that inclusion of BHD into concrete reduced the bleeding of fresh concrete at a given water to cement ratio. Also, higher BHD additions led to a subsequent decrease in the bleeding capacity of concrete. The reduction in the bleeding capacity of the fresh concrete made with 2 and 3.5 % BHD were 56.7 and 88.8 %, respectively compared to concrete prepared without BHD addition.

Effect of BHD addition on concrete compressive strength development

The incorporation of 3.5 % BHD reduced the first 3 days early strength development rate whilst the 2 % BHD-concrete achieved higher strength values compared to that in a plain concrete specimen. At later ages, BHD-concretes of all levels exhibited higher strengths compared with that of plain concrete. Exposing the BHD-concrete specimens to higher temperature does not seem to have a detrimental effect on compressive strength development rate.

Effect of BHD addition on bond strength at steel-concrete interface

This study has found that there was no adverse effect on the bond strength between steel reinforcing bar and concrete when various percentages of BHD were incorporated.

In the light of experimental investigations mentioned above, it was found that the use of 2 and 3.5 % BHD addition by weight of cement improve the corrosion resistance of reinforcement. In addition to this, the additions of BHD have significantly reduced the coarse capillary porosity and increased the chloride threshold value. This improvement could be attributed partly to higher OH^- concentrations found in most of the BHD mortars and partly probably to the physical properties of the BHD mortar.

Effects of non-chloride accelerators on the characteristic properties of concrete containing BHD dust

The inclusion of 8% BHD in plain concrete drastically reduced the workability of the material and increased the setting time of the cement substantially; it also delayed the onset of hardening by more than 7 days and caused a serious reduction in the 28 day strength of the material.

Effective improvement in the workability of fresh concrete containing 8% BHD was observed when CN or CF were used as admixtures at levels of 3.5% by weight of cement.

The use of either admixture was not effective in reducing the setting time of the cement in specimens containing 8% BHD but both admixtures caused major improvements in the rate of hardening of the material.

The retardation of cement hydration caused by 8% BHD additions was associated with the presence of a high level of zinc and, to a lesser extent, lead in the BHD material which caused hydration of the C_3S component of the cement to be effectively blocked for several days.

The acceleration of hardening caused by 3.5% dosages of CN or CF was associated with the ability of these admixtures to counteract the long delay, caused by the presence of BHD, in formation of the hydration products of the C_3S component of the cement that is evident from thermal analysis studies.

9.2 RECOMMENDATIONS

Effect of BHD addition on free chloride ion concentrations

A surprising result was found in the free chloride ion concentration in the pore solution extracted from 60-days-old chloride-free-mortars, where a lower free chloride ion concentration was noticed in BHD specimens compared to that in control specimens. It is then highly recommended to study the chemistry of the pore water after allowing more time for the cement hydration process i.e. 120 days.

Leaching tests

Leaching tests were carried out by several workers such as Sofili and Rastovan-Mio (2004); Laforest and Duchesne (2007) and Salihoglu and Pinarli (2008) to investigate the influence of EAFD on the environment. The solubility of Zn ions was found to be reduced by increasing the alkalinity of the leachate solution (Salihoglu and Pinarli, 2008), (Salihoglu et al., 2007) and (Fernández-Olmo et al., 2007). This implies that the addition of BHD in concrete could minimize the leachability of toxic ions such as Zn to the environment due to the high alkalinity of the concrete caused by the BHD addition, which provides a basis for further work.

Effect of BHD addition on chloride diffusion coefficients

Due to the scatter in the D_{app} values and the small number of specimens for a given test, it was difficult to draw conclusions on whether the involvement of BHD in concrete will result in significant improvement in the resistance to chloride ingress or not. Therefore it is highly recommended to conduct more experiments. If the purpose of this experiment is to assess the

effectiveness of different additions of BHD into concrete on the chloride penetration resistance, then there is a definite need to increase the number of specimens, more than three from a given test, to reduce the scatter in the results. Also, in this study, some of the D_{app} values obtained from BHD-concrete specimens were found to be high despite the low chloride concentrations at the surface. This signifies the need for further work in the presence of BHD.

Effect of BHD addition on chloride threshold values

In chloride threshold experiments, the samples were subjected to constant wet/dry cycles and during the wet period, they were exposed to sodium chloride solution with a concentration of 0.25 M. The wet/dry regime was applied to accelerate the corrosion process; this regime may not happen in practice i.e. for submerged structures. It would be preferable if specimens were exposed outdoors to a saline soil, which represents the actual concentration of chloride and other ion species. This may require a longer time to obtain sufficient data.

One of the hypotheses discussed in section 6.4 that may play a part in enhancing the corrosion tolerance is formation of a compacted layer of cement hydration products on the steel vicinity due to low bleeding capacity of the fresh BHD-mortar. Further work is needed to assess this hypothesis.

Effect of BHD addition on bond strength at steel-concrete interface

Smooth steel bars, and not ribbed bars, were used to investigate the effect of additions of various levels of BHD on bond strength. Therefore further investigation in this regard using ribbed bars is desirable.

Effects of non-chloride accelerators on the characteristic properties of concrete containing BHD

Further work is needed to resolve the detailed mechanisms of the retardation and acceleration effects observed due the incorporation of CN and CF admixtures and to evaluate their practical implications.

An addition of either 3.5% CN or 3.5% CF in concrete containing 8% BHD resulted in an increase in setting times. Further research regarding the mechanisms of CN and CF in prolonging setting would be of great help.

Using a substantial level of BHD in concrete will lead to an increase in the chloride level which may accelerate the initiation and propagation phase. The use of CN in concrete may then compensate for the risk of added chloride due to the addition of BHD, since CN is known to be a corrosion inhibitor, and thereby reduce the risk of corrosion. There is, therefore, a definite need for future research to assess the behaviour of the corrosion process of the steel reinforcing bar embedded in concrete incorporating high levels of BHD and prepared with CN concrete accelerator.

Appendix A

Material Safety Data Sheet

MATERIAL SAFETY DATA SHEET g167

Electric Arc Furnace/
Argon Oxygen Desulfurization Flue Dust

Washington Steel Corporation
501 Western Avenue
Houston, PA 15342
(412) 222-8000

********** NO HMIS RATINGS **********

********** NFPA RATINGS **********
Health: 2 Fire: 0 Reactivity: 0 Specific Hazard: N/A

SECTION I PRODUCT IDENTITY

Product/Trade Name(s): EAF/AOD Flue Dust
Part Number: Not Applicable
MSDS Date: 04/03/96
CAS #: Not Applicable
Category: Not Applicable
Distributor: Not Applicable
Chemical Name: Not Applicable
Formula: Not Applicable
Brief Description: Mixture of various metals and additives associated with flue dust

SECTION II HAZARDOUS INGREDIENTS & EXPOSURE LIMITS

CHEMICAL NAME	CAS #	CONTENT[a] (%)	EXPOSURE LIMIT VALUES	
Calcium Oxide	1305-78-8	0-5	PEL	5 mg/m³
Chromium	7440-47-3	10-15	PEL PEL	0.5 mg/m³ as Cr(II) & Cr(III) 1 mg/m³ as Cr
Iron	1309-37-1	20-25	PEL	10 mg/m³
Lead	7439-92-1	1-3	PEL	see 29 CFR 1910.1025
Magnesium Oxide	1309-48-4	2-3	PEL	15 mg/m³ total particulate
Manganese	7439-96-5	4-5	PEL PEL	(C) 5 mg/m³ as Mn compounds (C) 5 mg/m³ as Mn fume
Nickel	7440-02-0	3-4	PEL PEL	1 mg/m³ metal & insol. comp. 1 mg/m³ soluble compounds
Silica	7631-86-9	8-9	N/A	
Zinc	7440-66-6	7-8	N/A	

[a]Variable composition; reported values represent maximum expected range of composition.

SECTION III PHYSICAL/CHEMICAL CHARACTERISTICS

Boiling Point:	Not Applicable
Vapor Pressure (mm Hg):	Not Applicable
Vapor Density (Air = 1):	Not Applicable
Solubility in Water:	Insoluble
% Volatile/Volume:	Not Applicable
Appearance and Odor:	Brown, granular or powder; no odor
pH:	11-12
Specific Gravity (H_2O = 1):	0.9-1.1
Miscellaneous Information:	Finely divided airborne material represents a potential respiratory hazard.

SECTION IV FIRE AND EXPLOSION HAZARD DATA

Flash Point:	Not Applicable
Flammable Limits:	Not Applicable
Lower Explosive Limit (LEL):	Not Applicable
Upper Explosive Limit (UEL):	Not Applicable
Extinguishing Media:	Use dry chemical, foam, or Class D extinguishing agents as appropriate for surrounding flammable materials.
Special Fire Fighting Procedures:	Self-Contained Breathing Apparatus (SCBA) must be worn with full turn-out gear, as appropriate for surrounding flammable materials.
Unusual Fire and Explosion Hazards:	None

SECTION V REACTIVITY DATA

Stable:	Yes
Hazardous Polymerization May Occur:	Will not occur
Conditions to Avoid:	This material is stable.
Incompatibility (Material to Avoid):	Strong mineral acids, calcium hypochlorite, performic acid, finely divided aluminum, ethylene oxide, and bromine pentafluoride
Hazardous Decomposition or Byproducts:	Lead, cadmium and zinc boil off at high temperatures.

SECTION VI HEALTH HAZARD DATA

Effects on Eyes: Irritations may occur from exposure to dust.

Effects on Skin: Skin exposure may result in dermatitis and skin lesions.

Effects Due to Ingestion: Injury may occur to esophagus and/or digestive system.

Effects Due to Inhalation: Acute exposure to airborne dust may cause irritation to the mucous membranes and upper respiratory tract. Chronic health effects associated with inhalation of the elements contained in this material are listed as follows: Calcium Oxide (CaO) - inflammation of the respiratory tract, ulceration, and

perforation of the nasal septum, bronchitis, and pneumonia. Chromium (Cr) - divalent (Cr II) and trivalent (Cr III) chromium exhibits a low order of toxicity; however, hexavalent chromium (Cr VI) is carcinogenic, causing lung cancer in humans. The presence of significant Cr VI in this product is extremely unlikely. Iron (Fe) - respiratory changes and illnesses such as bronchitis. Lead (Pb) - adverse effects to the blood-forming, nervous, urinary and

SECTION VI HEALTH HAZARD DATA (cont.)

Effects Due to Inhalation (cont.)
reproductive systems. Magnesium Oxide (MgO) - increased white blood cell count. Manganese (Mn) - respiratory problems such as bronchitis and pneumonitis and possibly a lack of coordination and Parkinson's disease. Nickel (Ni) - listed by the National Toxicology Program (NTP) and the International Agency for Research on Cancer (IARC) as a known human carcinogen. silicon dioxide (SiO_2) - respiratory diseases such as silicosis; confirmed carcinogen. Zinc (Zn) - low toxicity but may cause pulmonary changes.

First Aid Procedures for Eyes: Flush well with running water for at least 15 minutes to remove particulate. Get medical attention.

First Aid Procedures for Skin: Brush or vacuum excess dust. Wash well with soap and water.

First Aid Procedures for Ingestion: Seek medical attention if necessary.
First Aid Procedures for Inhalation: For overexposure, remove to fresh air. Get medical attention.

SECTION VII PRECAUTIONS FOR SAFE HANDLING AND USE

Steps to be Taken in Case Material is Released or Spilled: Always wear proper protective equipment. Sweep spilled dust and place material into a sturdy container. Prevent run-off into storm water drains and waterways. If high wind causes the dust to become airborne, lightly wet the material.

Waste Disposal Method: Dispose of in accordance to Federal, State and Local regulations.

Precautions to be Taken in Handling and Storing: Always wear proper protective equipment. Handling of the material must be conducted in well-ventilated areas. All containers storing the dust must be in good condition, properly labeled, and be kept covered.

Other Precautions: Store material in approved container.

SECTION VIII CONTROL MEASURES

Local Exhaust: Local exhaust is the preferable method in keeping exposures to a minimum.

Mechanical (General): Use general ventilation if local exhaust is insufficient or not practical.

Special Ventilation: Not Applicable

Other Ventilation: Not Applicable

Protective Gloves: Wear impermeable gloves when handling material.

Eye Protection: Wear approved safety glasses with side shields/goggles.

Other Protective Clothing or Equipment: Protective outerwear should be worn when handling material to avoid contamination of clothing.

SECTION VIII CONTROL MEASURES (cont.)

Work/Hygienic Practices: Use good housekeeping practices to prevent accumulations of dust and to minimize airborne dust concentrations.

Respiratory Protection: A properly fitted, NIOSH-approved, dust respirator should be worn whenever airborne concentrations of dust exceed the OSHA Permissible Exposure Limits (PELs) or other recommended limits. Refer to the OSHA Respiratory Protection Standard (29 CFR 1910.134) for more information.

SECTION IX ADDITIONAL INFORMATION

Additional Information

This product contains toxic chemicals subject to the reporting requirements of Section 313 of Title III of the Superfund Amendments and Reauthorization Act of 1986 and 40 CFR part 372. The chemicals are listed below:

Chromium	7440-47-3
Lead	7439-92-1
Manganese	7439-96-5
Nickel	7440-02-0
Zinc	7440-66-6

This material is also a RCRA-listed Hazardous Waste K061 and is to be managed in accordance to RCRA Federal and State regulations.

All information, recommendations, and suggestions contained herein are based upon data believed to be correct. However, no guarantee or warranty of any kind, expressed or implied, is made by Washington Steel Corporation with respect to the information provided.

Employers should use this information only as a supplement to other information gathered by them. Since the actual use of this product is beyond our control, and it is each employer's responsibility to assure the safety and health of their employees, Washington Steel Corporation will not assume liability rising out of the use of this product by others.

Appendix B

Example on calculation of weight loss

- Faraday's law states that one Faraday (96486.7 coulombs) is needed to corrode 28 gm of Fe.
- From the sample contained 2 % BHD and mixed with 2 % Cl., the average of measured I_{corr} was 1.01 μA/cm^2 for 116 days.

Then: the calculated weight loss = 1.01 * 10^{-6} (coulombs/cm^2/second) * 116 (days) * 24 (hour/day) * 3600 (second/hour) * 28 g (iron) * 10^3 (mg/g) / 96486.7 coulombs

= 2.93 mg Fe/cm^2

Appendix C

Pore solution analysis data

Table 1 Chloride free concentration analysis data

BHD %	Cl %	3 Days			7 Days			21 Days			60 Days		
		Cl^- mMol/l (3 specimens)			Cl^- mMol/l (3 specimens)			Cl^- mMol/l (3 specimens)			Cl^- mMol/l (3 specimens)		
	0	1.9	1.6	2.4	1.7	1.8	1.5	1.8	1.7	3.1	5.5	3.4	1.8
0	0.4	17.9	17.4	17.7	18.5	19.7	19.1	16.3	15.6	15.3	20.0	19.6	20.4
	2	1303.4	1372.0	1330.8	1289.6	1262.2	328.1	1234.7	1358.3	1275.9	1729.2	1660.5	1619.3
	0	2.4	1.5	3.8	3.2	2.6	2.9	5.4	5.4	1.5	2.2	2.6	2.2
2	0.4	27.7	27.8	28.1	31.5	28.3	29.9	29.9	29.2	32.5	32.5	31.7	31.2
	2	973.7	891.3	1001.2	1330.8	1275.9	1303.4	1605.5	1509.4	1481.9	1894.0	1715.4	1866.5

Table 2 Hydroxyl ion concentration analysis data

BHD %	Cl %	3 Days			7 Days			21 Days			60 Days		
		OH^- mMol/l (3 specimens)			OH^- mMol/l (3 specimens)			OH^- mMol/l (3 specimens)			OH^- mMol/l (3 specimens)		
	0	100	100	97	133	136	129	137	136	140	121	136	103
0	0.4	260	257	216	223	235	240	261	260	260	287	291	288
	2	282	272	280	286	279	284	353	295	346	311	289	318
	0	215	171	211	218	206	211	196	179	204	159	174	189
2	0.4	300	305	281	266	285	279	331	334	329	350	350	343
	2	280	286.8	287	333	336	332	331	319	324	348	339	360

Appendix D

Diffusion Data

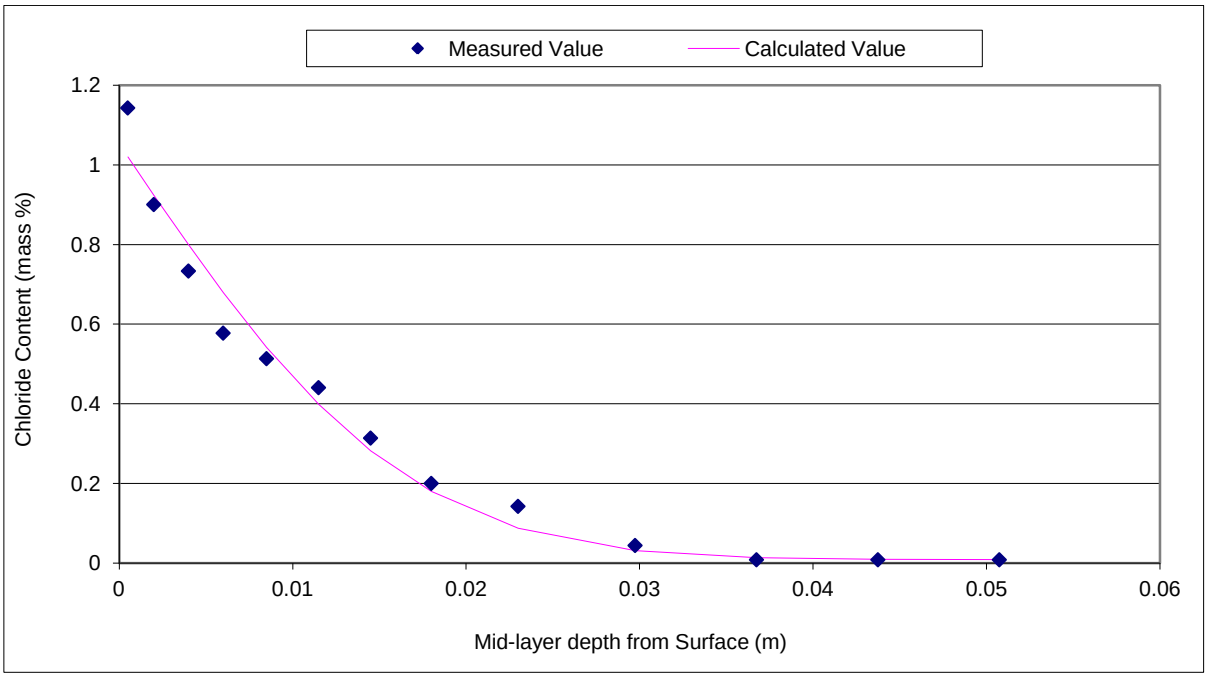

Chloride diffusion profile with best-fitted curve obtained from plain concrete prepared at w/c ratio of 0.5 (specimen no. 2)

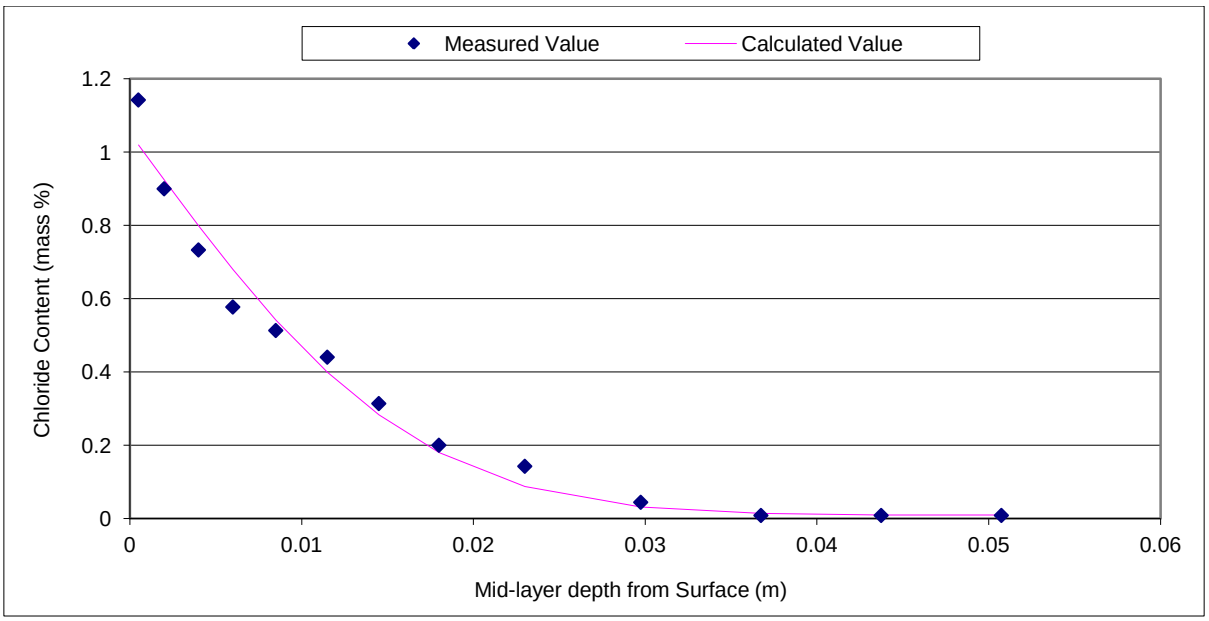

Chloride diffusion profile with best-fitted curve obtained from plain concrete prepared at w/c ratio of 0.5 (specimen no. 3)

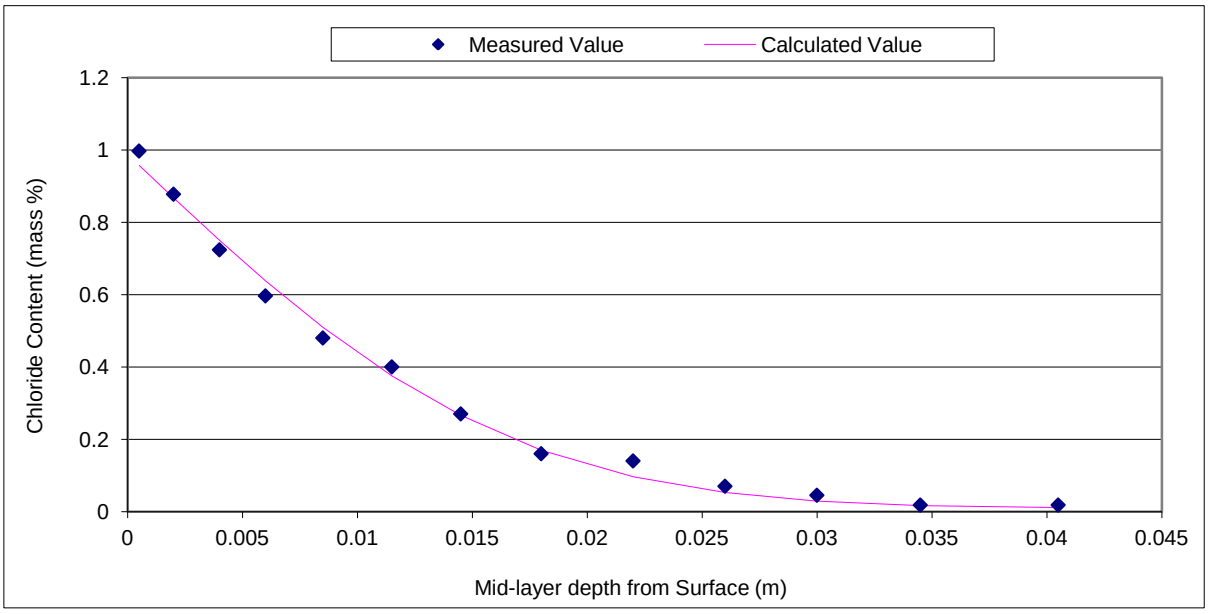

Chloride diffusion profile with best-fitted curve obtained from containing 2 % BHD by weight of cement and prepared at w/c ratio of 0.5 (specimen no. 1)

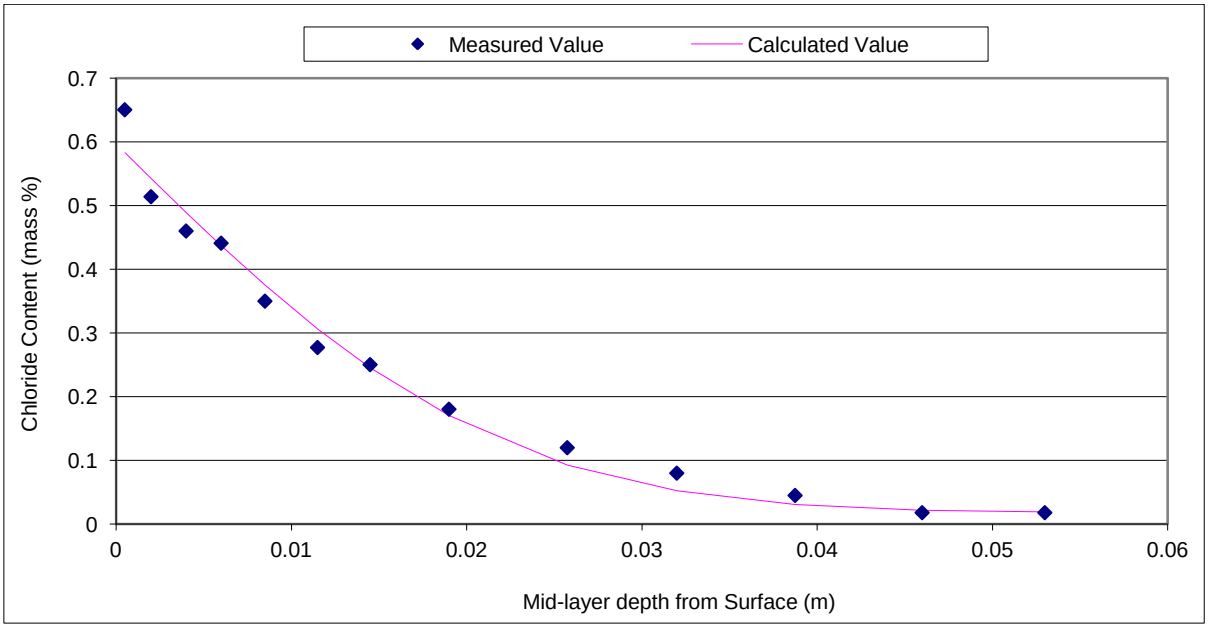

Chloride diffusion profile with best-fitted curve obtained from concrete containing 2 % BHD by weight of cement and prepared at w/c ratio of 0.5 (specimen no. 2)

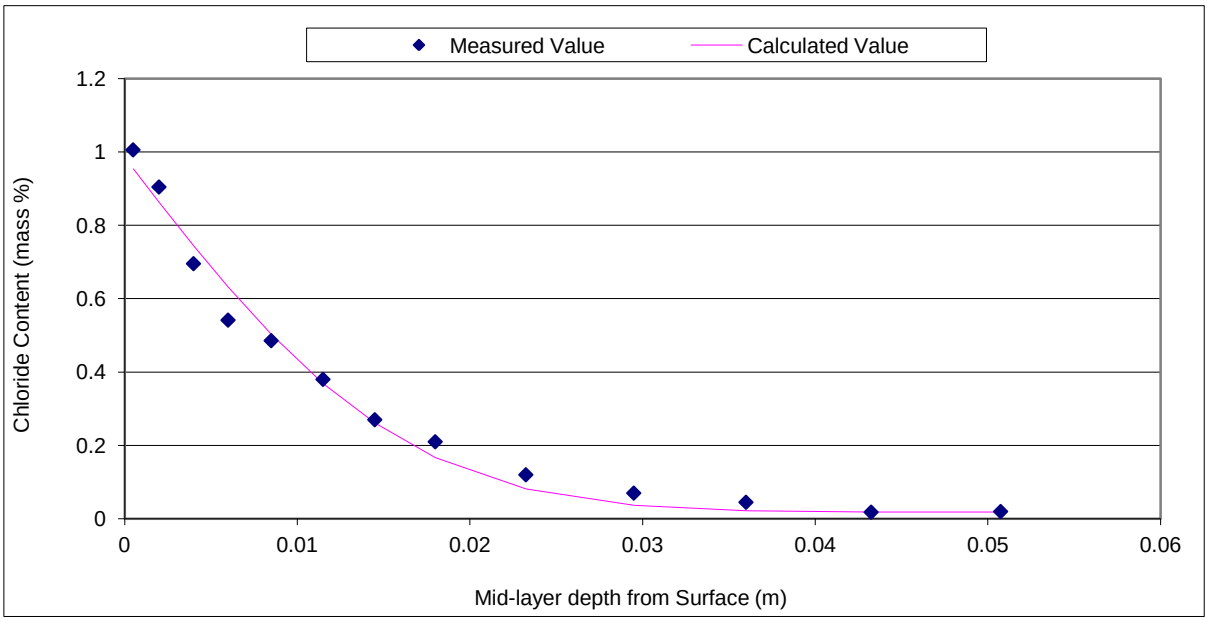

Chloride diffusion profile with best-fitted curve obtained from concrete containing 2 % BHD by weight of cement and prepared at w/c ratio of 0.5 (specimen no. 3)

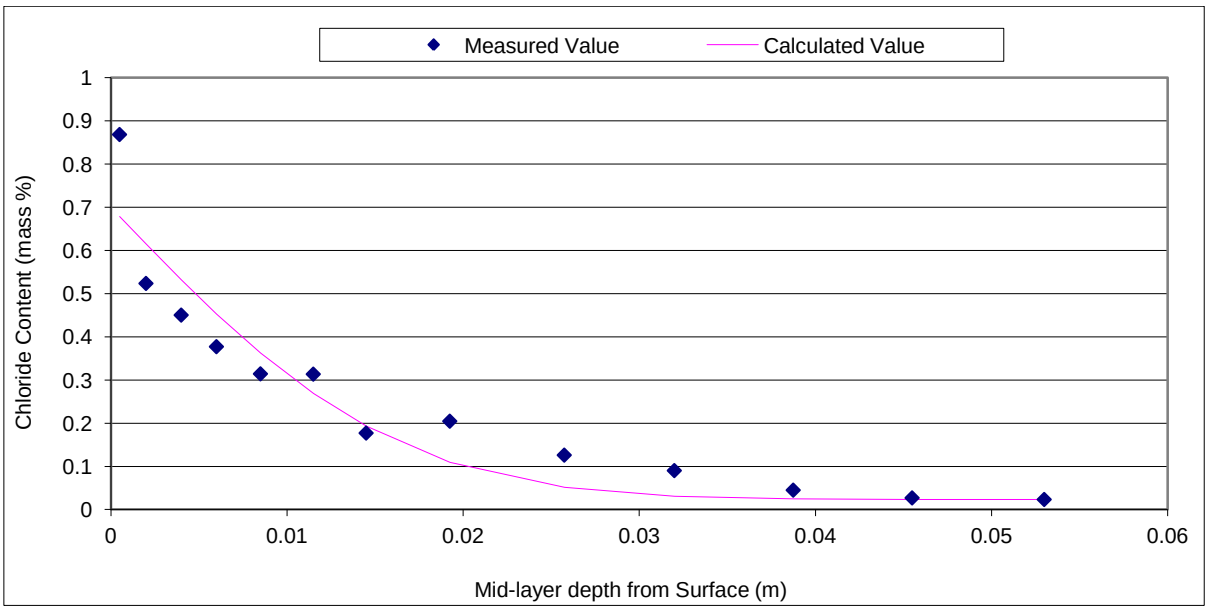

Chloride diffusion profile with best-fitted curve obtained from concrete containing 3 % BHD by weight of cement and prepared at w/c ratio of 0.5 (specimen no. 1)

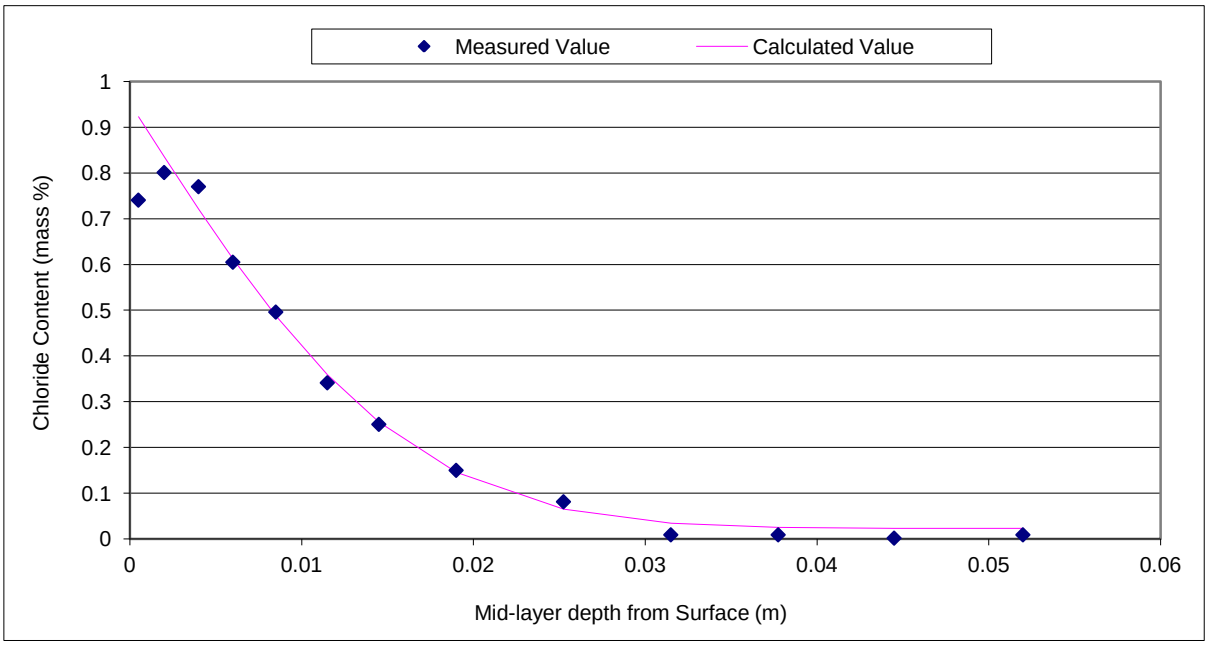

Chloride diffusion profile with best-fitted curve obtained from concrete containing 3 % BHD by weight of cement and prepared at w/c ratio of 0.5 (specimen no. 2)

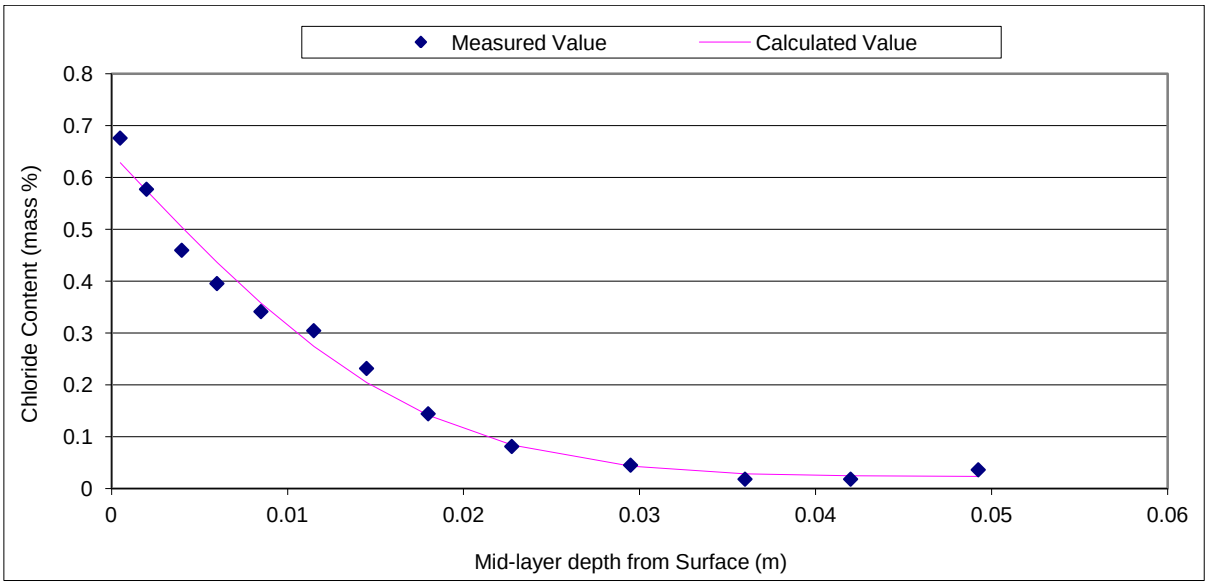

Chloride diffusion profile with best-fitted curve obtained from concrete containing 3 % BHD by weight of cement and prepared at w/c ratio of 0.5 (specimen no. 3)

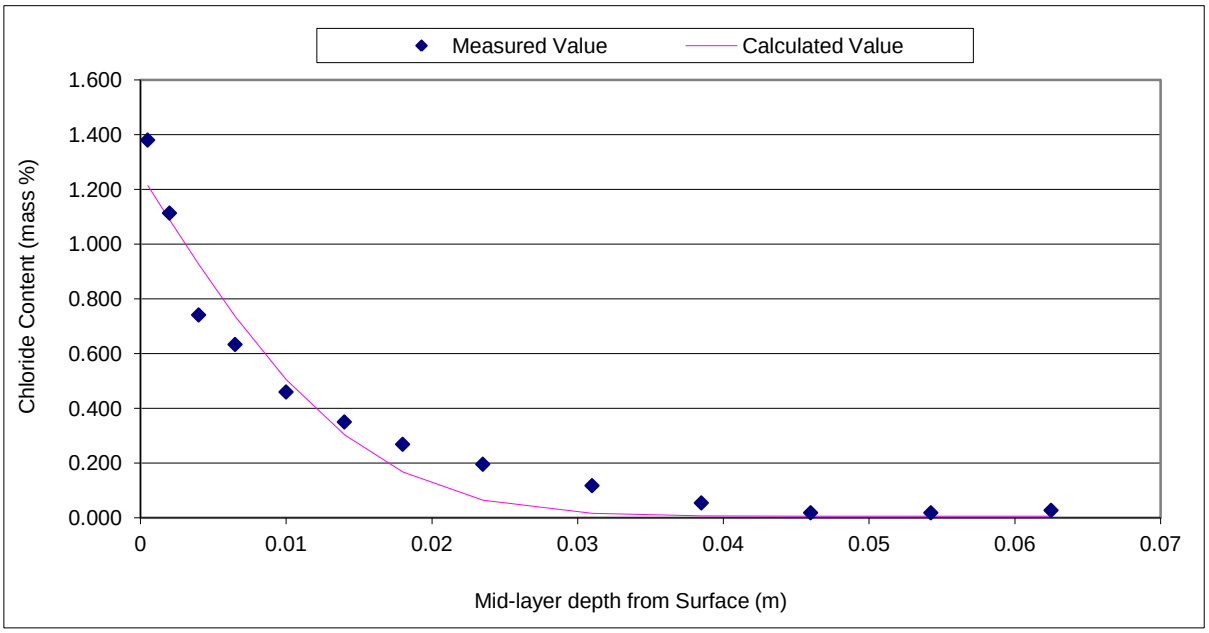

Chloride diffusion profile with best-fitted curve obtained from plain concrete and prepared at w/c ratio of 0.6 (specimen no. 1)

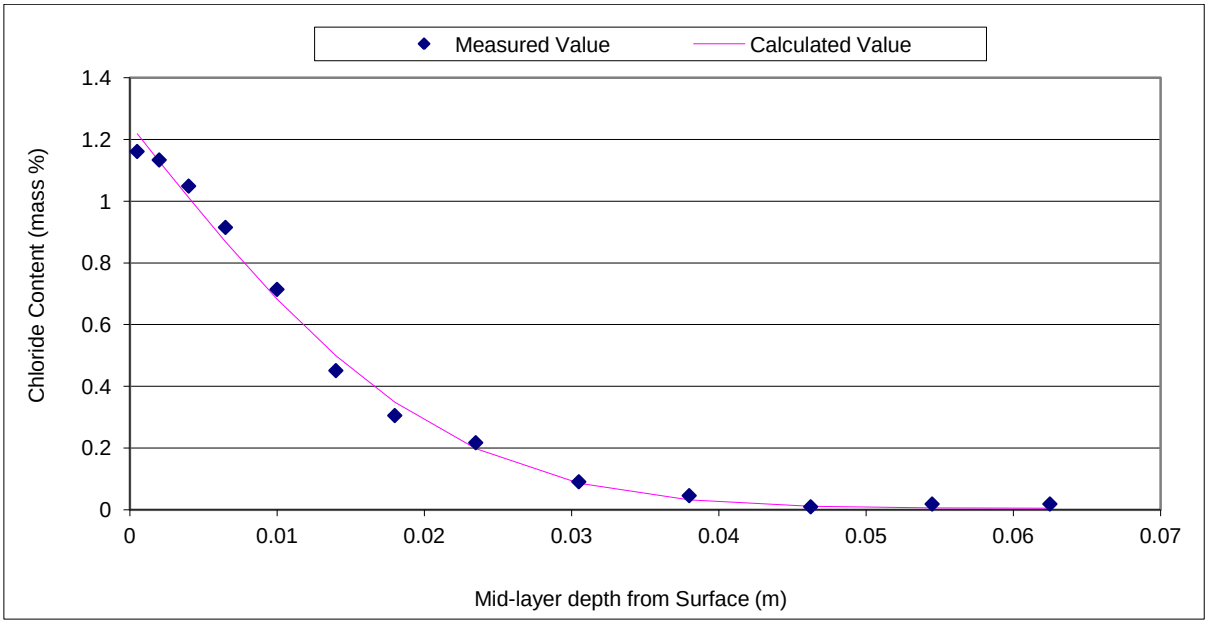

Chloride diffusion profile with best-fitted curve obtained from plain concrete and prepared at w/c ratio of 0.6 (specimen no. 2)

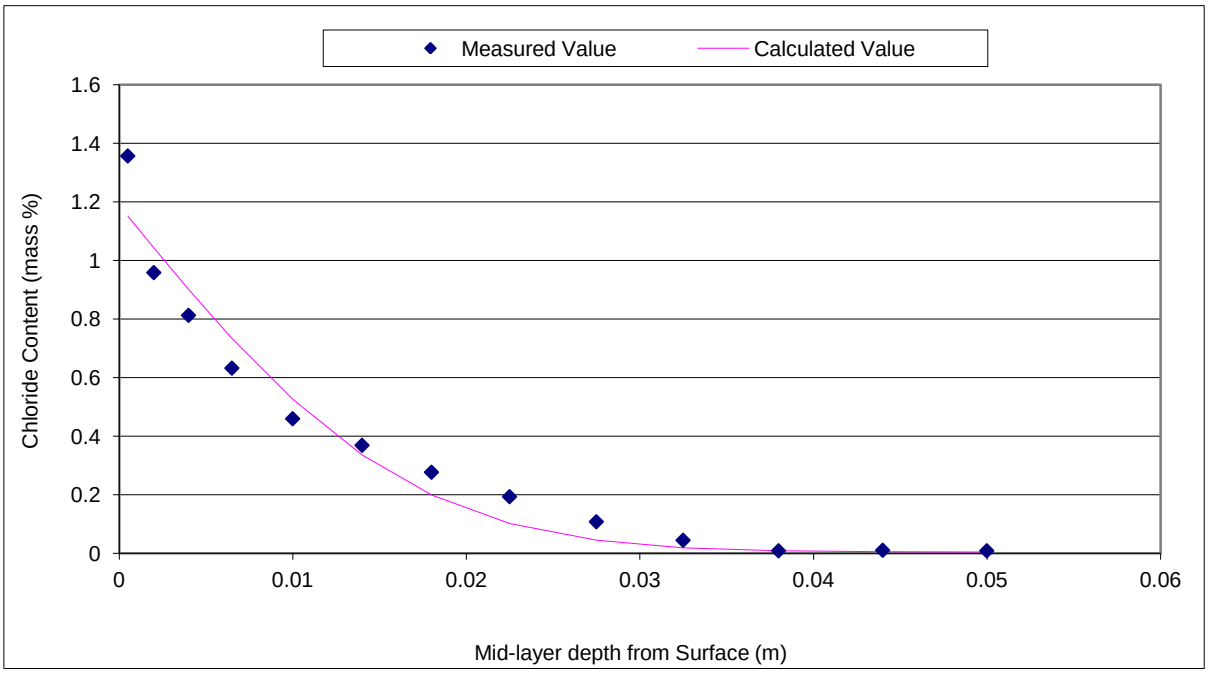

Chloride diffusion profile with best-fitted curve obtained from plain concrete and prepared at w/c ratio of 0.6 (specimen no. 3)

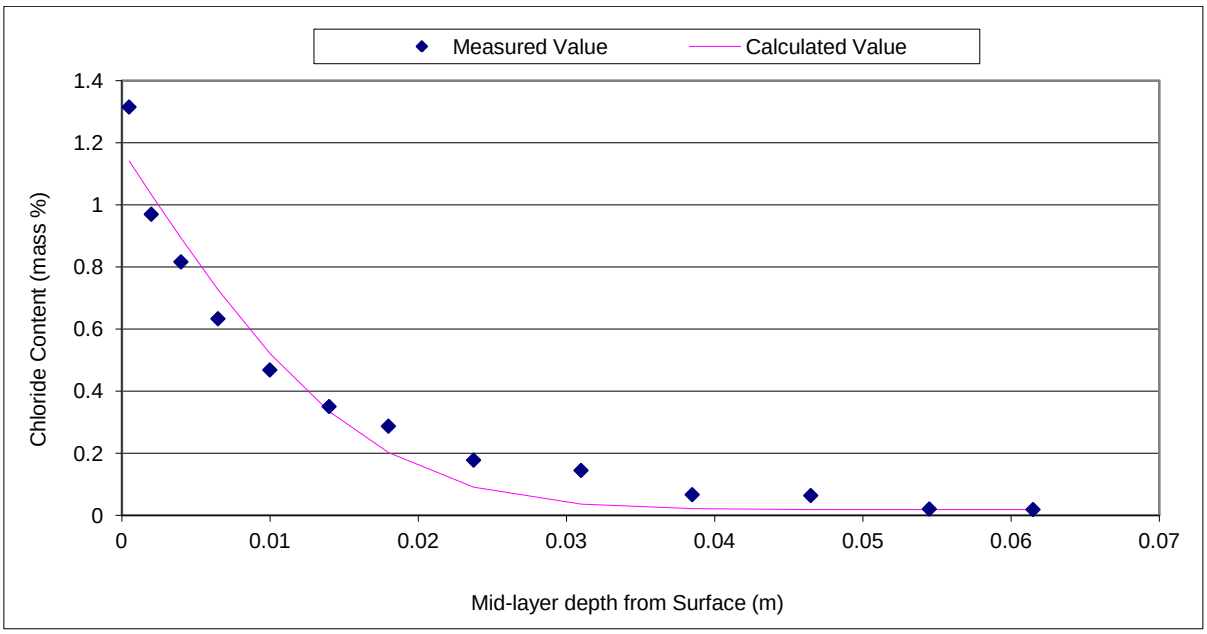

Chloride diffusion profile with best-fitted curve obtained from concrete containing 2 % BHD by weight of cement and prepared at w/c ratio of 0.6 (specimen no. 1)

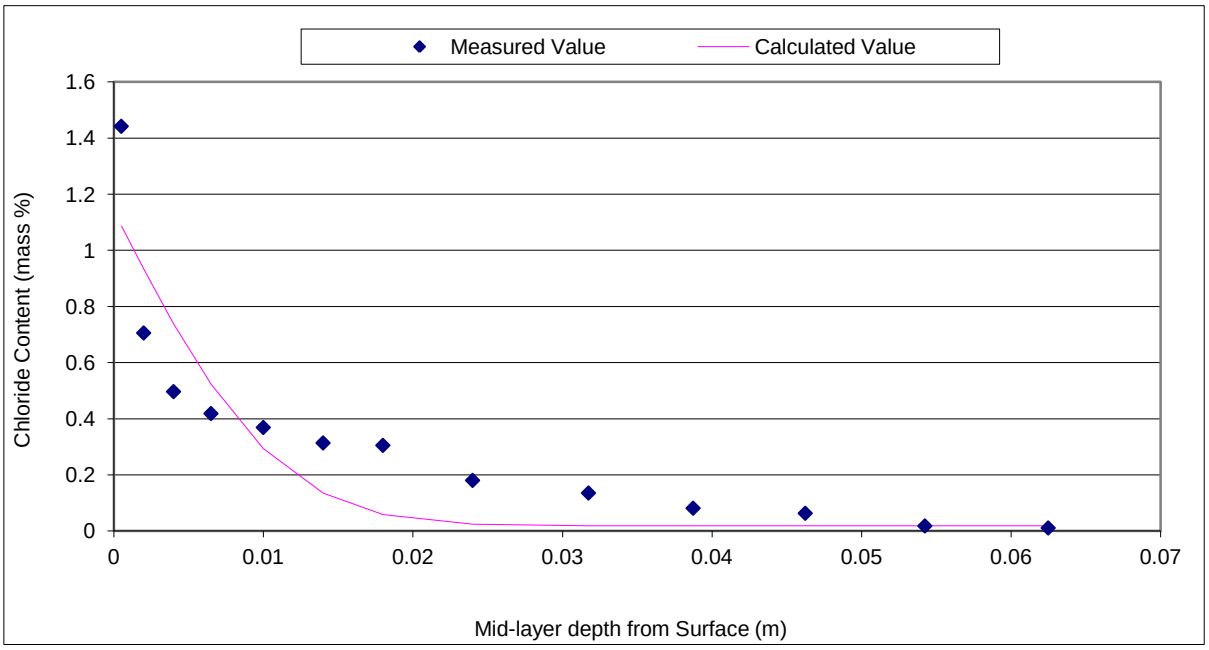

Chloride diffusion profile with best-fitted curve obtained from concrete containing 2 % BHD by weight of cement and prepared at w/c ratio of 0.6 (specimen no. 2)

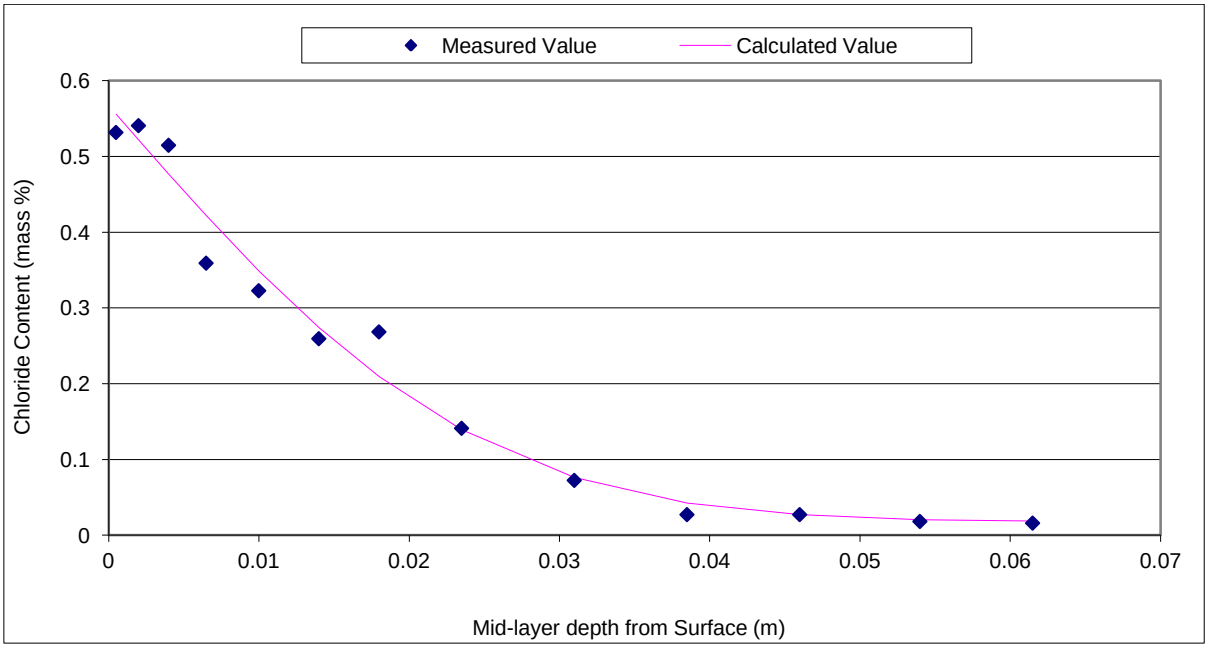

Chloride diffusion profile with best-fitted curve obtained from concrete containing 2 % BHD by weight of cement and prepared at w/c ratio of 0.6 (specimen no. 3)

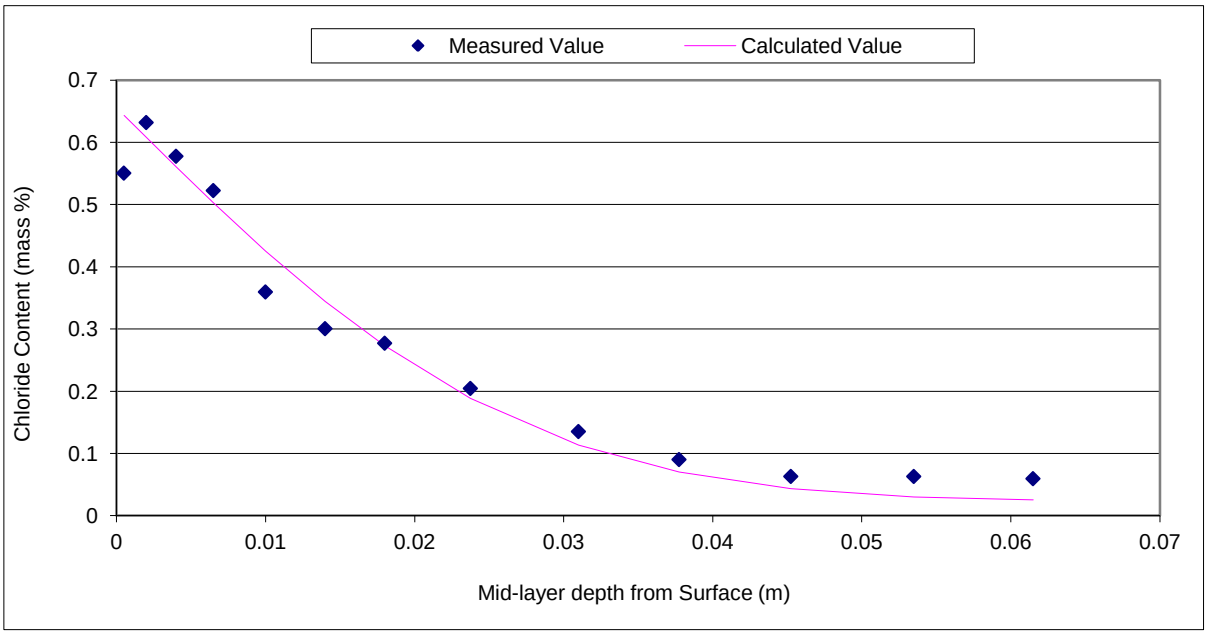

Chloride diffusion profile with best-fitted curve obtained from concrete containing 3 % BHD by weight of cement and prepared at w/c ratio of 0.6 (specimen no. 1)

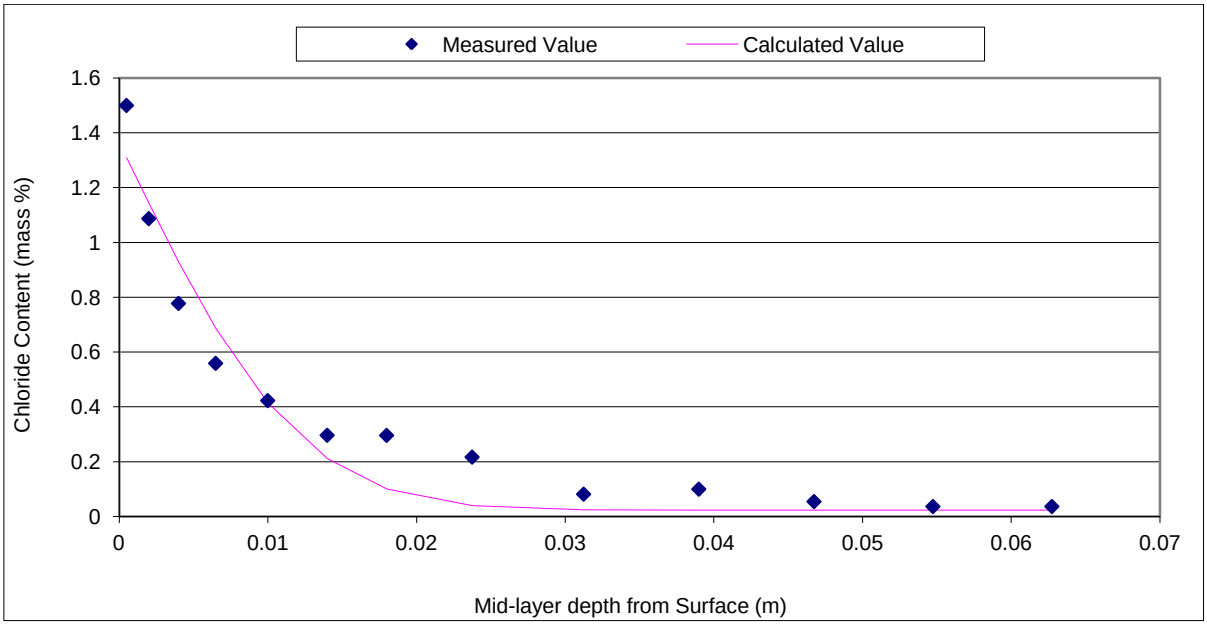

Chloride diffusion profile with best-fitted curve obtained from concrete containing 3 % BHD by weight of cement and prepared at w/c ratio of 0.6 (specimen no. 2)

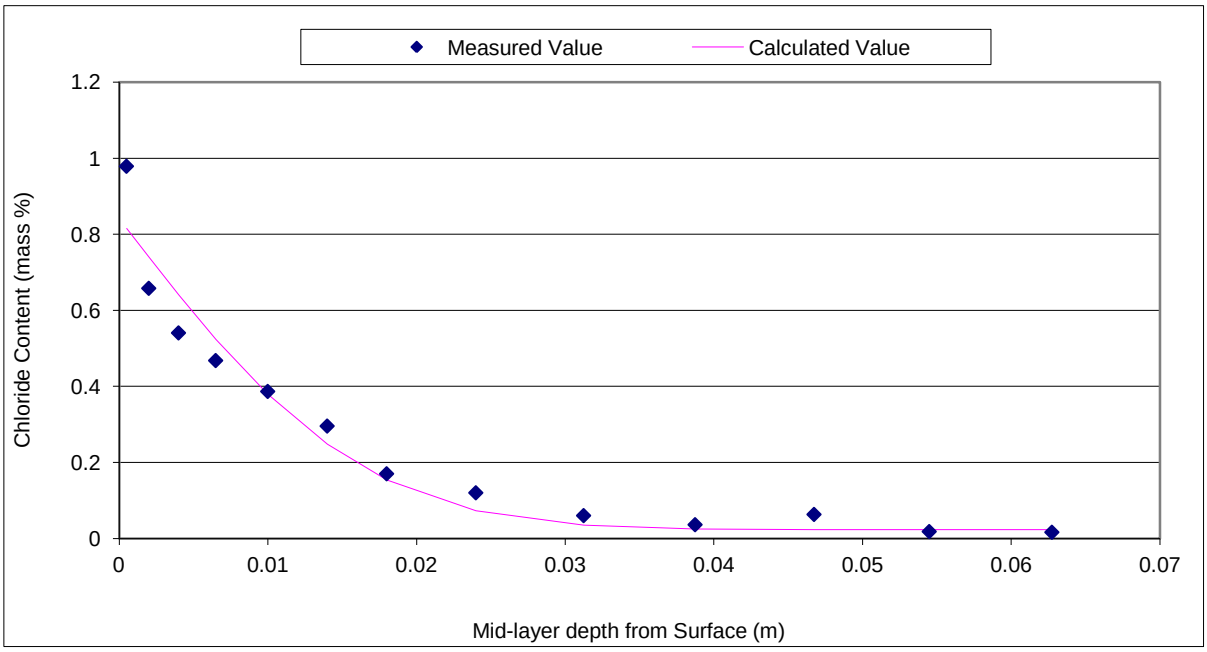

Chloride diffusion profile with best-fitted curve obtained from concrete containing 3 % BHD by weight of cement and prepared at w/c ratio of 0.6 (specimen no. 3)

Appendix E

Corrosion current density and corrosion potential data

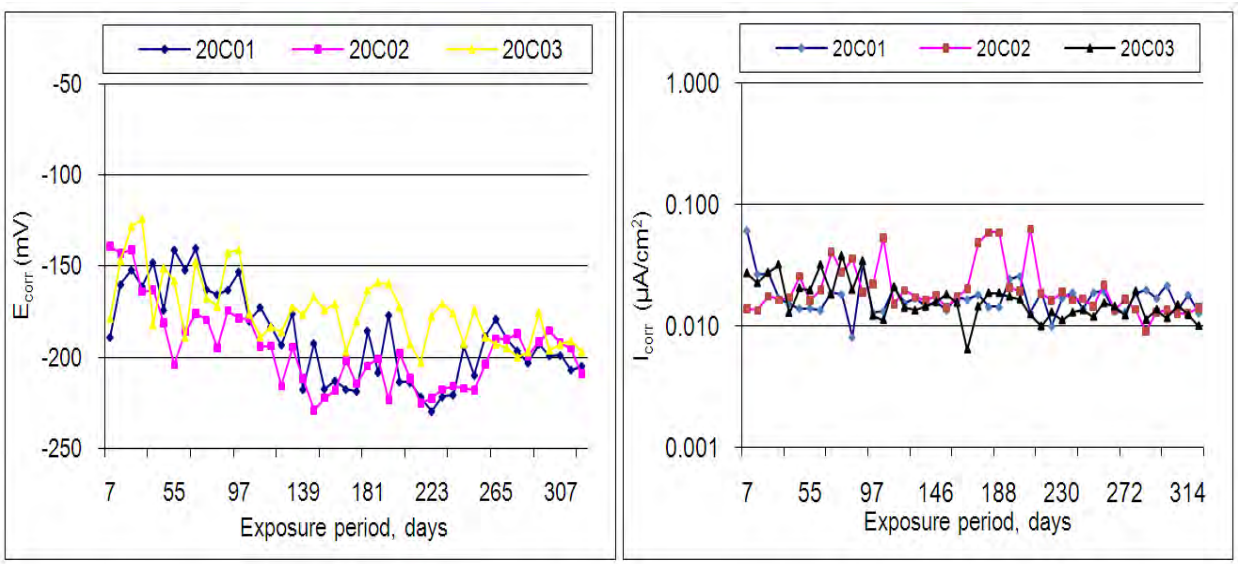

Evolution of Ecorr and Icorr of steel bar without artificial defects embedded in mortar containing no BHD and subjected to temperature of 20 C

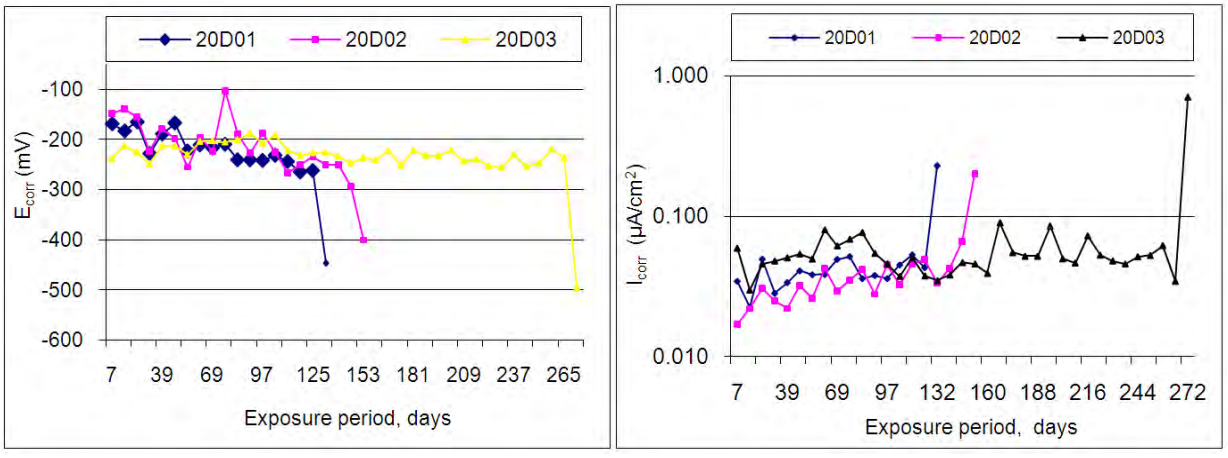

Evolution of E_{corr} and I_{corr} of steel bar with artificial defects embedded in mortar containing no BHD and subjected to temperature of 20 °C

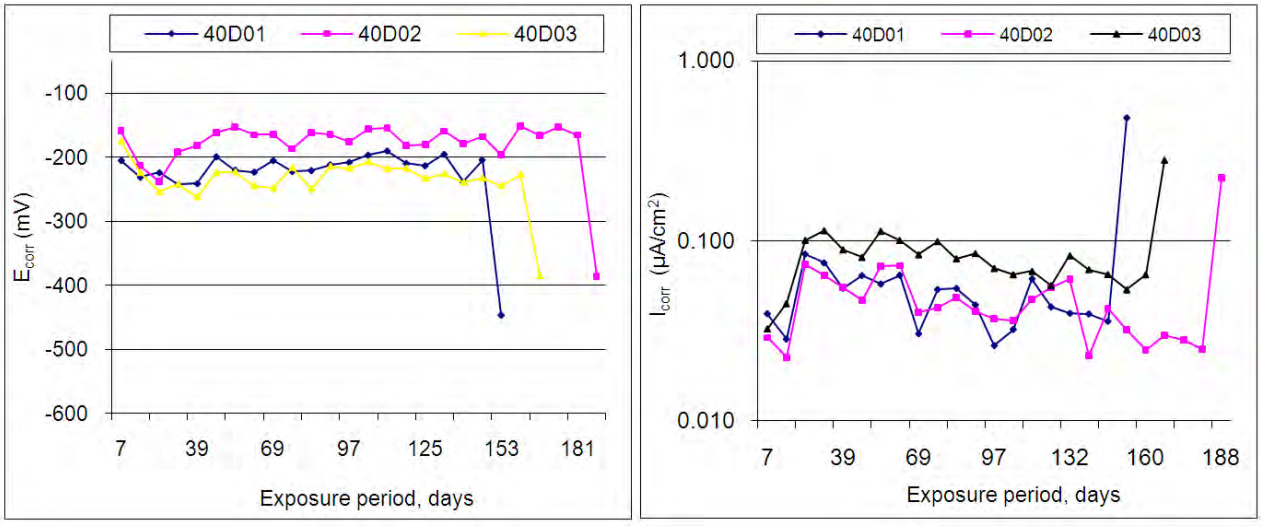

Evolution of Ecorr and Icorr of steel bar with artificial defects embedded in mortar containing no BHD and subjected to temperature of 40 ^{0}C

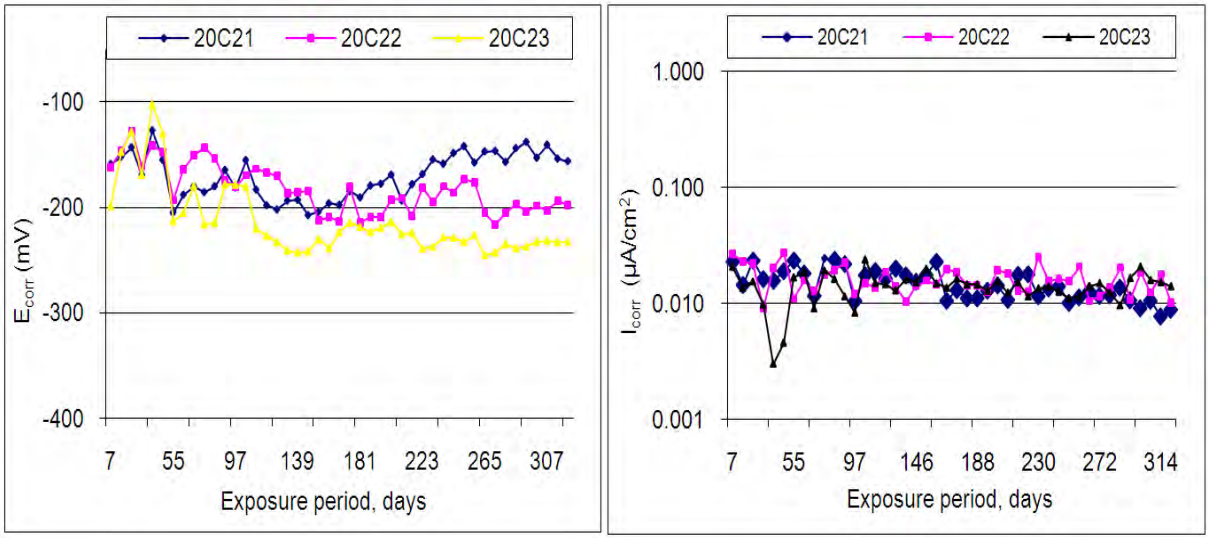

Evolution of Ecorr and Icorr of steel bar without artificial defects embedded in mortar containing 2 % BHD and subjected to temperature of 20 ^{0}C

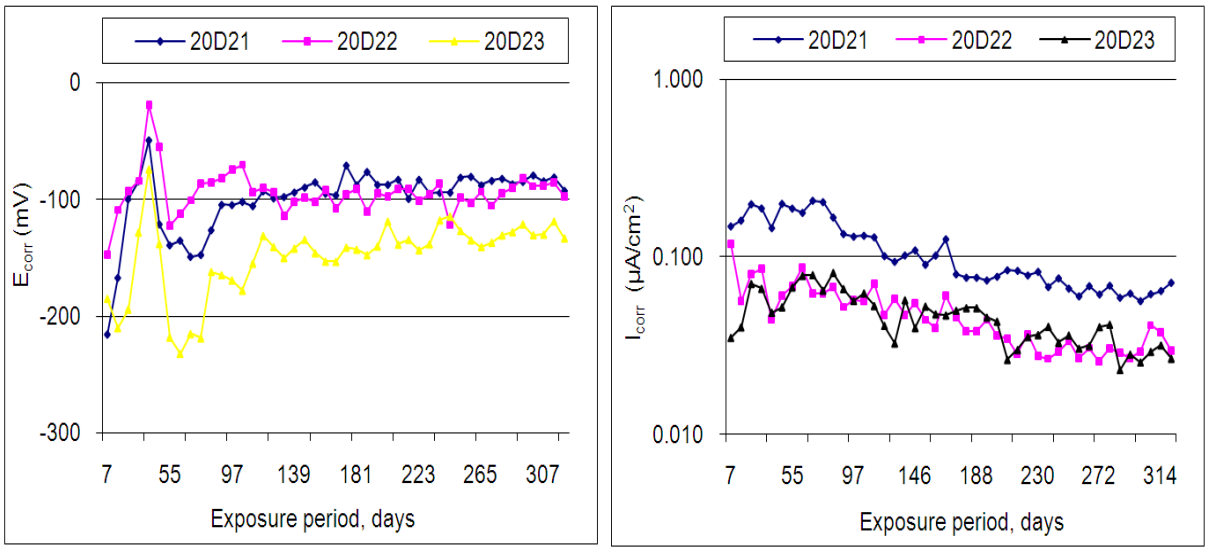

Evolution of Ecorr and Icorr of steel bar with artificial defects embedded in mortar containing 2 % BHD and subjected to temperature of 20 ^{0}C

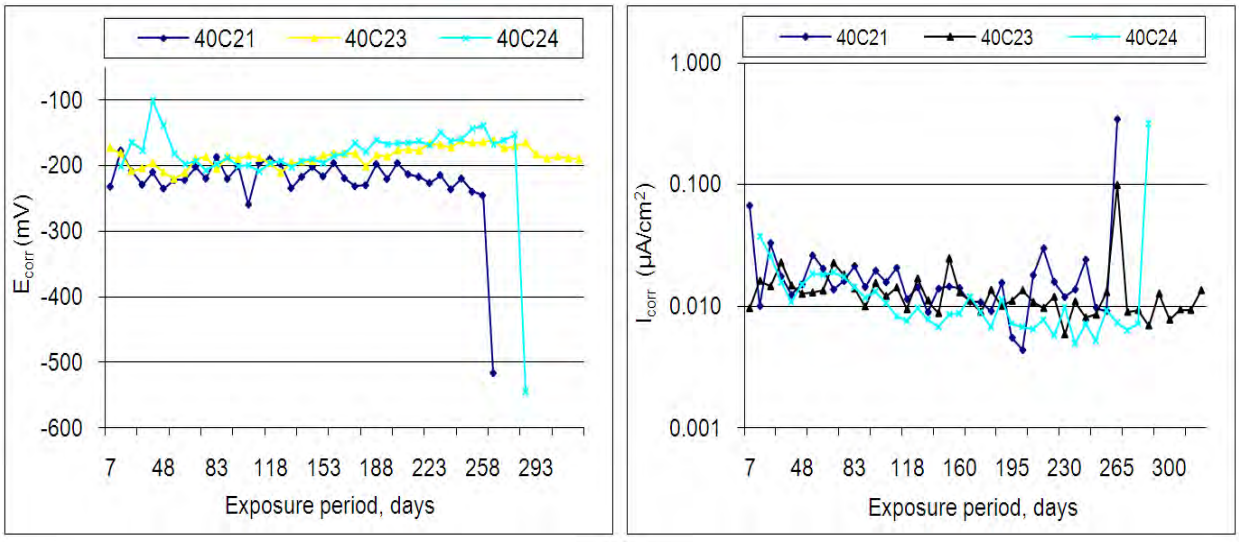

Evolution of Ecorr and Icorr of steel bar without artificial defects embedded in mortar containing 2 % BHD and subjected to temperature of 40 ^{0}C

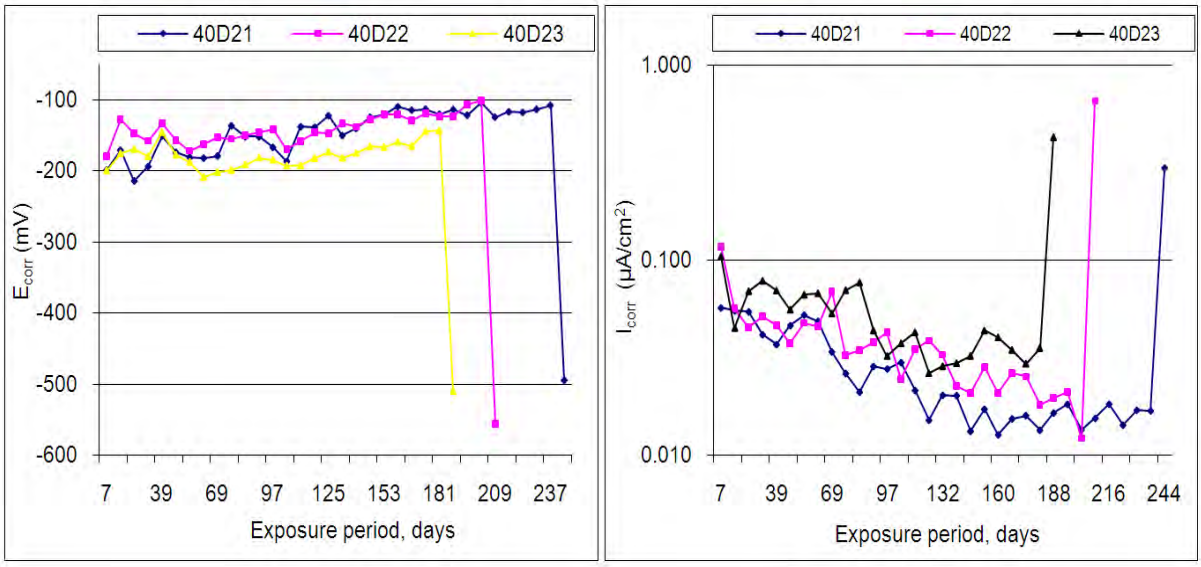

Evolution of Ecorr and Icorr of steel bar with artificial defects embedded in mortar containing 2 % BHD and subjected to temperature of 40 ^{0}C

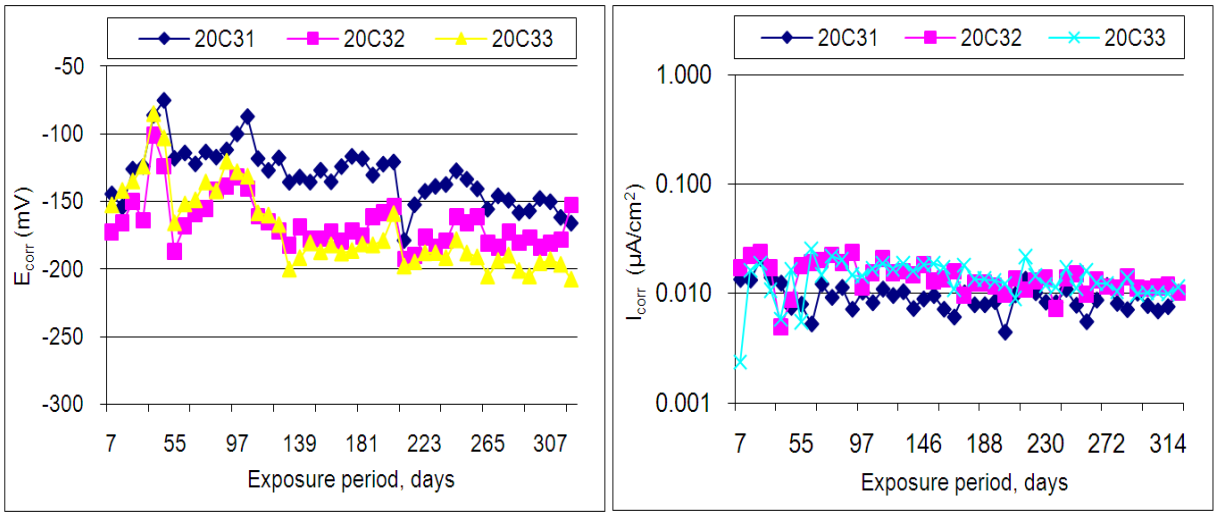

Evolution of Ecorr and Icorr of steel bar without artificial defects embedded in mortar containing 3.5 % BHD and subjected to temperature of 20 ^{0}C

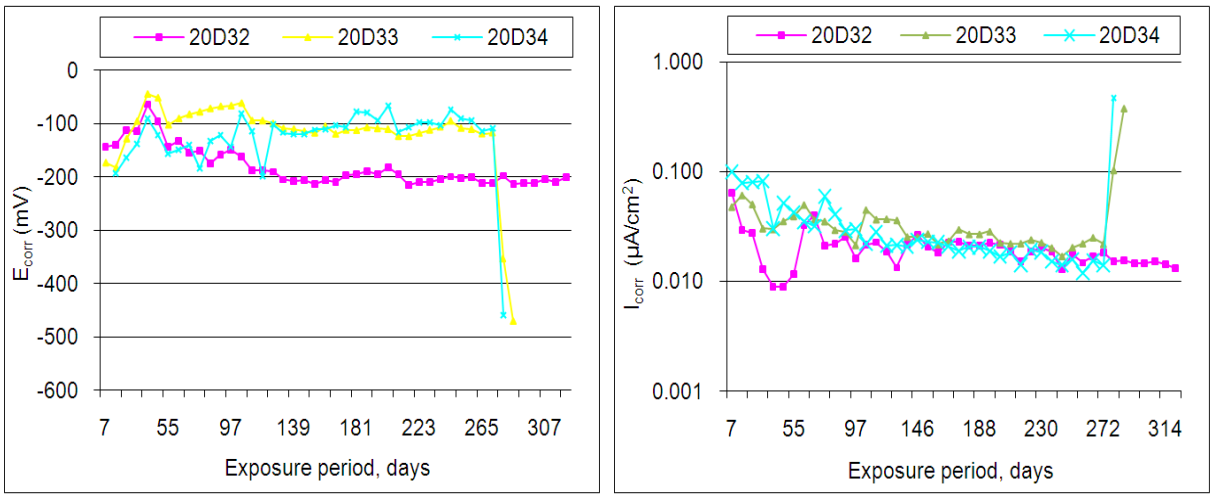

Evolution of Ecorr and Icorr of steel bar with artificial defects embedded in mortar containing 3.5 % BHD and subjected to temperature of 20 ^{0}C

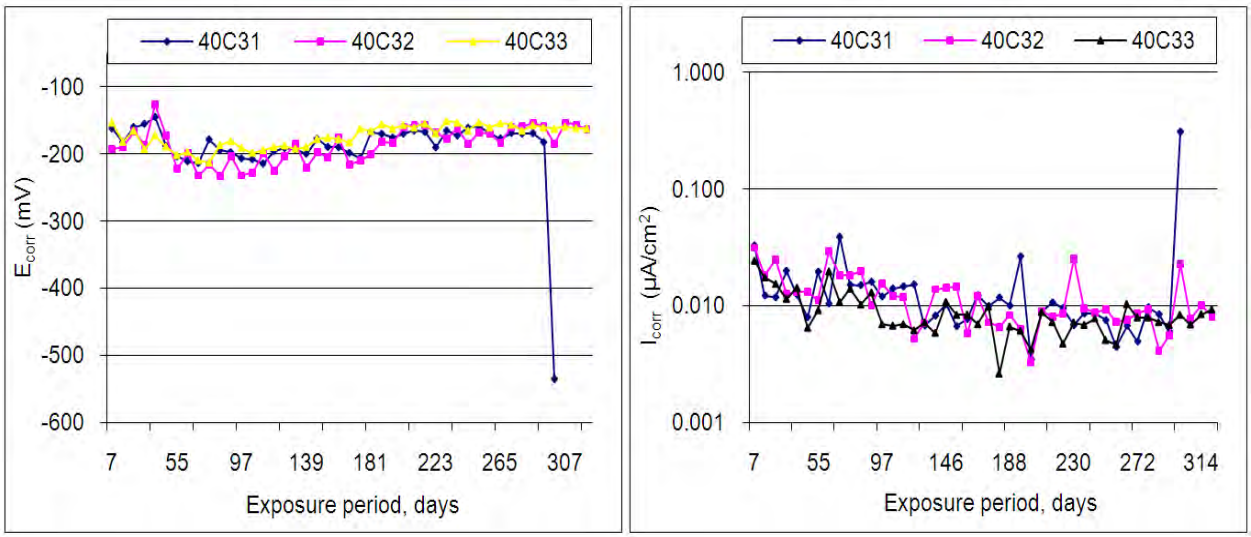

Evolution of Ecorr and Icorr of steel bar without artificial defects embedded in mortar containing 3.5 % BHD and subjected to temperature of 40 ^{0}C

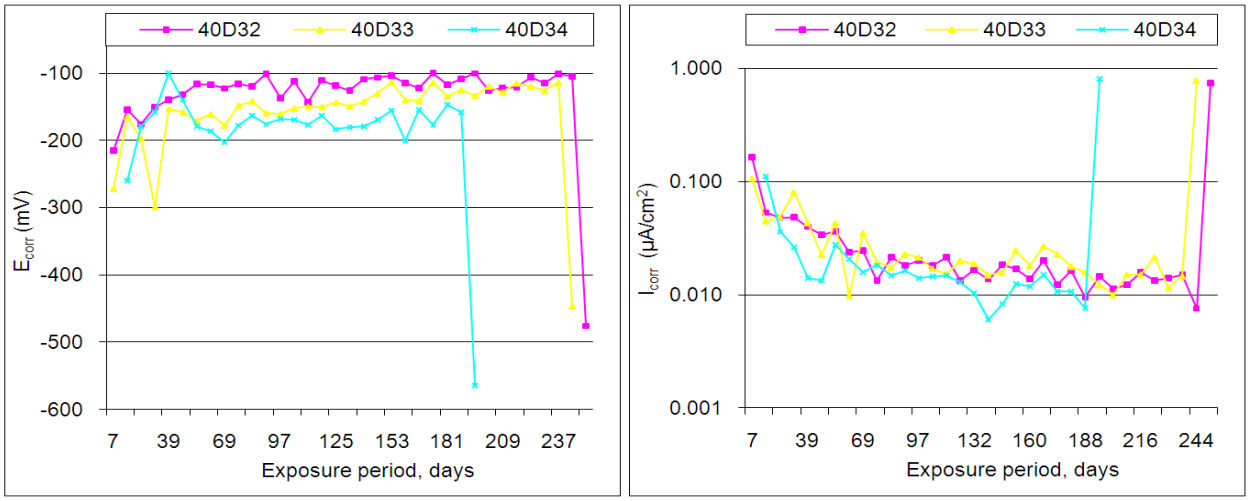

Evolution of Ecorr and Icorr of steel bar with artificial defects embedded in mortar containing 3.5 % BHD and subjected to temperature of 40 ^{0}C

Appendix F

Published work

In the basis of the work done in part A of Chapter 6, one paper was submitted for publication. More details can be found below;

1. Al Mutlaq, F.M. and Page, C.L. Effect of electric arc furnace dust on susceptibility of steel to corrosion in chloride-contaminated concrete. To be presented at the "International Symposium on Cement & Concrete Materials" (ISCCM 2011). Ningbo, China, November 7-9, 2011. Accepted.

REFERENCES

Abbasi, A.-G.F., Al-Tayyib, A.-H.J. and Al-Ali, M.B. (1992) Effect of hot weather on strength of reinforced concrete beams. **Cement and Concrete Composites**, 14: (3): 209-221.

Ahmad, S., Al-Kutti, W.A., Baghabra Al-Amoudi, O.S., et al. (2008) Compliance criteria for quality concrete. **Construction and Building Materials**, 22: (6): 1029-1036.

Ahmad, Z. (2006) "Concrete Corrosion". **Principles of Corrosion Engineering and Corrosion Control.**, Butterworth-Heinemann pp. 609-646.

Ahmed, S. (2003) Reinforcement corrosion in concrete structures, its monitoring and service life prediction--a review. **Cement and Concrete Composites**, 25: (4-5): 459-471.

Aitcin, P.C. (1994) Durable Concrete--Current Practice and Future Trends. **ACI Materials Journal-SP144-05**, 144: 85-104.

Al-Amoudi, O.S.B. and Maslehuddin, M. (1993) The effect of chloride and sulfate ions on reinforcement corrosion. **Cement and Concrete Research;(United States)**, 23: (1): 139-146.

Al-Amoudi, O.S.B., Maslehuddin, M. and Abduljauwad, S.N. (1994) Influence of sulfate ions on chloride-induced reinforcement corrosion in Portland and blended cement concretes. **Cement and concrete aggregates**, 16: (1): 3-11.

Al-Amoudi, O.S.B., Maslehuddin, M., Lashari, A.N., et al. (2003) Effectiveness of corrosion inhibitors in contaminated concrete. **Cement and Concrete Composites**, 25: (4-5): 439-449.

Al-Dulaijan, S.U., Maslehuddin, M., Al-Zahrani, M.M., et al. (2003) Sulfate resistance of plain and blended cements exposed to varying concentrations of sodium sulfate. **Cement and Concrete Composites**, 25: (4-5 SPEC): 429-437.

Al-Gahtani, H.J., Abbasi, A.G.F. and Al-Amoudi, O.S.B. (1998) Concrete mixture design for hot weather: Experimental and statistical analyses. **Magazine of Concrete Research**, 50: (2): 95-106.

Al-Mutlaq, F.M. and Chaudhary, Z.M. (2007) Effect Of Addition Of Steel Furnace By-Product On Cement Pore Solution Chemistry And Corrosion Of Reinforcing Steel. **CORROSION 2007**.

Al-Sugair, F.H., Al-Negeimish, A.I. and Al-Zaid, R.Z. (1996) "Use of electric arc furnace by-products in concrete". In 5557031, U.S.P.n. (Ed.) 5557031 ed. USA.

Al-Tayyib, A.J. and Shamim Khan, M. (1991) Effect of sulfate ions on the corrosion of rebars embedded in concrete. **Cement and Concrete Composites**, 13: (2): 123-127.

Al-yami, H.A., Al-Dubaib, M., Awan, F.M., et al. (2003) "Bag House Dust: waste material to a product". **The 4th Middle East Petrochemicals Conference and Exhibition**. Bahrain, Petrotech 2003.

Al-Zaid, R.Z., Al-Negeimish, A.I., Al-Sugair, F.H., et al. (1999) "Use of electric arc furnace dust as a retarder in concrete: a cooperative study". **Proc. 5th. Saudi Engineering Conference**. Makkah, Umm-Al-Qura University 33-42.

Al-Zaid, R.Z., Al-Sugair, F.H. and Al-Negheimish, A.I. (1997) Investigation of potential uses of electric-arc furnace dust (EAFD) in concrete. **Cement and Concrete Research**, 27: (2): 267-278.

Alonso, C., Andrade, C. and González, J.A. (1988) Relation between resistivity and corrosion rate of reinforcements in carbonated mortar made with several cement types. **Cement and Concrete Research**, 18: (5): 687-698.

Alsyed, S.H. (1997) Sensitivity of Compressive Strength of HSC to Hot-Dry Climate, Curing Regimes, and Additives. **ACI Materials Journal**, 94: (6).

Andrade, C., Alonso, C. and Gonzalez, J.A. (1990) "An initial effort to use the corrosion rate measurements for estimating rebar durability". In Berke, N.S.;Chaker, D. & Whiting, D. (Eds.) **Corrosion Rates of Steel in Concrete**. STP-1065, ASTM, American Society for Testing and Materials, Philadelphia.

Andrade, C. and Gonzalez, J.A. (1978) Quantitative measurements of corrosion rate of reinforcing steels embedded in concrete using polarization resistance measurements. **Materials and corrosion**, 29: (8): 515-519.

Anstice, D.J., Page, C.L. and Page, M.M. (2005) The pore solution phase of carbonated cement pastes. **Cement and Concrete Research**, 35: (2): 377-383.

Arliguie, G. and Grandet, J. (1990) Influence de la composition d'un ciment portland sur son hydration en presence de zinc. **Cement and Concrete Research**, 20: (4): 517-524.

Arliguie, G., Ollivier, J.P. and Grandet, J. (1982) Etude de l'effet retardateur du zinc sur l'hydratation de la pate de ciment Portland (Study of the retarding effect of zinc on the hydration of Portland cement paste). **Cement and Concrete Research**, 12: (1): 79-86.

Arya, C., Buenfeld, N.R. and Newman, J.B. (1990) Factors influencing chloride-binding in concrete. **Cement and Concrete Research**, 20: (2): 291-300.

Asavapisit, Fowler, G. and Cheeseman, C.R. (1997) Solution chemistry during cement hydration in the presence of metal hydroxide wastes. **Cement and Concrete Research**, 27: (8): 1249-1260.

Asavapisit, S., Naksrichum, S. and Harnwajanawong, N. (2005) Strength, leachability and microstructure characteristics of cement-based solidified plating sludge. **Cement and Concrete Research**, 35: (6): 1042-1049.

ASTM 1556 (2004) "Standard test method for determining the apparent chloride diffusion coefficient of cementitious mixtures by bulk diffusion". **ASTM Manual series: MNL**. ASTM International.

ASTM (1995) "Corrosion tests and Standards: Application and Interpretation". In BABOIAN, R. (Ed.) **ASTM Manual series: MNL**. 75-90.

ASTM C494/C494M -10a (2010) "Standard Specification for Chemical Admixtures for Concrete". **Book of Standards Volume: 04.02**. West Conshohocken, ASTM International

ASTM C876 (1999) **Standard Test Method for Half-Cell Potentials of Uncoated Reinforcing Steel in Concrete** American Society of Testing and Materials.

ASTM C 192/C 192M (2002) "Standard practice for making and curing concrete test specimens in the laboratory". **ASTM Manual series: MNL**. ASTM International.

ASTM C 305 (1999) "Standard practice for mechanical mixing of hydraulic cement pastes and mortars of plastic consistency". **ASTM Manual series: MNL**. ASTM International.

ASTM C 1202-94 (1994) "Standard Test Method for electrical indication of concrete's ability to resist chloride ion penetration". **ASTM Annual Book of ASTM Standards Vol. 04.02 Concrete and Aggregates**. Philadelphia.

Baghabra, A.A., Omar, S., Al-Kutti, W.A., et al. (2009) Correlation between compressive strength and certain durability indices of plain and blended cement concretes. **Cement and Concrete Composites**, 31: (9): 672-676.

Bakker, R.F. (1988) "Initiation period". In Schiessl, P. (Ed.) **Corrosion of steel in concrete: Report of the Technical Committee 60 CSC, RILEM (the International Union of Testing and Research Laboratories for Materials and Structures)**. London, Chapman and Hall 22-54.

Balderas, A., Navarro, H., Flores-Velez, L.M., et al. (2001) Properties of portland cement pastes incorporating nanometer-sized franklinite particles obtained from electric-arc-furnace dust. **Journal of The American Ceramic Society**, 84: (12): 2909-2913.

Bamforth, P.B. (2004) "Enhancing reinforced concrete durability : Guidance on selecting measures for minimising the risk of corrosion of reinforcement in concrete". Surrey.

Benjamin, S.E. and Sykes, J.M. (1990) "Chloride -induced pitting corrosion of Swedish iron in ordinary Portland cement mortars and alkaline solutions: the effect of temperature". In Page, C.L.;Bamforth, P.B. & Figg, J.W. (Eds.) **3rd International Symposium on Corrosion of Reinforcement in Concrete Construction**. Wishaw, UK.

Bensted, J. (1978) Early hydration behaviour of Portland cement in water, calcium chloride and calcium formate solutions. Part I: General aspects. **Silicates Industries**, 6: (43): 117-122.

Bensted, J. (1980) Early hydration behaviour of Portland cement in water, calcium chloride and calcium formate solutions. Part IV: Effects of intergrinding the calcium chloride and calcium formate. **Silicates Industries**, 45: (3): 67-69.

Bentz, E.C., Evans, C.M. and Thomas, M.D.A. (1996) "Chloride diffusion modelling for marine exposed concretes". In Page, C.L.;Bamforth, P.B. & Figg, J.W. (Eds.) **Fourth International Symposium on 'Corrosion of Reinforcement in Concrete Construction', Cambridge, UK**. Royal Society of Chemistry Information Services.

Berke, N.S., Hicks, M.C. and Tourney, P.G. (1993) "Evaluation of concrete corrosion inhibitors". **Proceedings of 12th International Corrosion Congress: Corrosion Control for Low-Cost Reliability Conference**. Houston, TX, NACE International pp. 19-24.

Berke, N.S. and Rosenberg, A. (1989) Technical review of calcium nitrite corrosion inhibitor in concrete. **Transportation Research Record**, 1211: (8-27).

Berke, N.S. and Sundberg, K.M. (1990) Effects of Calcium Nitrite and Microsilica Admixtures on Corrosion Resistance of Steel in Concrete. **ACI-Special Publication**, 122: 265-280.

Biffen, F.M. (1956) Determination of Free Lime and Carbonate in Calcium Sillicate Hydrates by Thermobalance. **Analytical Chemistry**, 28: (7): 1133-1136.

BRE Digest 444 (2000) "Corrosion of steel in concrete; Durability of reinforcied concrete structures". **Digest 444; Part 1**.

Brehm, F., Dal Molin, D., Vilela, A.C.F., et al. (2004) "Zinc oxide addition in cement pastes to study the viability of recycling electric arc furnace (EAF) dust in civil construction". **2nd International Meeting on Ironmaking and 1st International Symposium on Iron Ore and Parallel Event- 5th Japan-Brazil Symposium on Dust Processing-Energy-Environment on Metallurgical Industries**. Brazil, Associacao Brasileira de Metalurgia e Materiais pp. 725-733.

Broomfield, J.P. (2007) **Corrosion of Steel in Concrete: Understanding, Investigation and Repair**. 2nd Taylor & Francis.

Brown, M. (2001) **Introduction to thermal analysis: techniques and applications**. 2nd.London: Kluwer Academic.

Brown, M.C., Weyers, R.E. and Sprinkel, M.M. (2001) Effect of Corrosion-Inhibiting Admixtures on Material Properties of Concrete. **ACI Materials Journal**, 98: (3): 240-250.

BS 812-103.1 (1985) **Testing aggregates —Part 103: Methods for determination of particle size distribution — Section 103.1 Sieve tests**. BSI.

BS 8110-1 (1997) **Structural use of concrete. Code of practice for design and construction** BSI.

BS 8110-Part 1 (1985) **Structural use of concrete. Code of practice for design and construction**. BSI.

BS 8500-1 (2006) **Concrete – Complementary British Standard to BS EN 206-1 – Part 1: Method of specifying and guidance for the specifier**. BSI.

BS EN 206-1 (2000) **Concrete. Specification, performance, production and conformity** BSI.

BS EN 480-2 (2006) **Admixtures for concrete, mortar and grout — Test methods — Part 2: Determination of setting time**. BSI.

BS EN 480-4 (2005) **Admixtures for concrete, mortar and grout. Test methods. Determination of bleeding of concrete**. BSI.

BS EN 934-2 (2009) **Admixtures for Concrete, Mortar and Grout. Concrete Admixtures - Definitions, Requirements, Conformity, Marking and Labeling**. BSI.

BS EN 1992-1-1: (2004) **Eurocode 2: Design of concrete structures — Part 1-1: General rules and rules for buildings**. BSI.

BS EN 12350-2 (2000) **Testing fresh concrete-part 2: slump test**. BSI.

BS EN 12390-3 (2009) **Testing hardened concrete. Compressive strength of test specimens**. BSI

BS EN 12390-3:2009 (2009) **Testing hardened concrete. Compressive strength of test specimens**. BSI

BS EN 12504-4: (2004) **Testing concrete-part 4: Determination of ultrasonic pulse velocity**. BSI.

BS EN 12620:2002+A1:2008 (2002) **Aggregates for concrete**. BSI.

Buenfeld, N.R. and Okundi, E. (1998) Effect of cement content on transport in concrete. **Magazine of Concrete Research**, 50: 339-352.

Bungey, J.H., Millard, S.G. and Grantham, M.G. (2006) **Testing of concrete in structures**. 4th.Taylor & Francis.

Byfors, K., Hansson, C.M. and Tritthart, J. (1986) Pore solution expression as a method to determine the influence of mineral additives on chloride binding. **Cement and Concrete Research**, 16: (5): 760-770.

Cabrera, J.G. and Claisse, P.A. (1990) Measurement of chloride penetration into silica fume concrete. **Cement and Concrete Composites**, 12: (3): 157-161.

Caseres, L., Sagues, A.A., Kranc, S.C., et al. (2005) In situ leaching method for determination of chloride in concrete pore water. **Cement and Concrete Research**, 36: (3): 492-503.

Castellote, M., Menendez, E., Andrade, C., et al. (2004) Radioactively Contaminated Electric Arc Furnace Dust as an Addition to the Immobilization Mortar in Low- and Medium-Activity Repositories **Environ. Sci. Technol**, 38: (10): 2946 -2952.

Chaudhary, Z., Al-Mutlaq, F.M., Ahsan, S.N., et al. (2003) "Improving durability reinforced concrete slabs by addition of HADEED by-product (HR001)". **The 4th Middle East Petrochemicals Conference and Exhibition**. Bahrain, Petrotech 2003.

Chaudhary, Z., Al-Mutlaq, F.M. and Al-Beed, A. (2008) "Condition assessment and cathodic protection of reinforced concrete cooling tower". **NACE CORROSION 2008**. New Orleans LA, NACE International.

Cheng-yi, H. and Feldman, R.F. (1985) Influence of silica fume on the microstructural development in cement mortars. **Cement and Concrete Research**, 15: (2): 285-294.

Clark, L.A., Shammas-Toma, M.G.K., Seymour, D.E., et al. (1997) How Can We Get the Cover We Need? **The Structural Engineer**, 75: (17): 289-296.

Cooper, S. (1941) Mixed Indicator Bromocresol Green-Methyl Red for Carbonates in Water. **Industrial & Engineering Chemistry Analytical Edition**, 13: (7): 466-470.

Costa, A. and Appleton, J. (1999) Chloride penetration into concrete in marine environment—Part I: Main parameters affecting chloride penetration. **Materials And Structures**, 32: (4): 252-259.

Currie, R.J. and Robery, P.C. (1994) **Repair and maintenance of reinforced concrete** Watford: Building Research Establishment.

de Rincón, O.T.O., Castro, P., Moreno, E.I., et al. (2004) Chloride profiles in two marine structures--meaning and some predictions. **Building and Environment**, 39: (9): 1065-1070.

De Schutter, G. and Luo, L. (2004) Effect of corrosion inhibiting admixtures on concrete properties. **Construction and Building Materials**, 18: (7): 483-489.

de Vargas, A.S., Masuero, A.B. and Vilela, A.C.F. (2006) Investigations on the use of electric-arc furnace dust (EAFD) in Pozzolan-modified Portland cement I (MP) pastes. **Cement and Concrete Research**, 36: (10): 1833-1841.

Dehwah, H.A.F., Austin, S.A. and Maslehuddin, M. (2002) Chloride-induced reinforcement corrosion in blended cement concretes exposed to chloride-sulfate environments. **Magazine of Concrete Research**, 54: (5): 355-364.

Delalio, A., Bajger, Z., Balaz, P., et al. (1998) Characterization and pre-treatment of steelmaking dusts in order to recover valuable products. **Acta Metall.**, Slovaca 4: (Special issue (1)): 55-59.

Diamond, S. (1986) Chloride concentrations in concrete pore solutions resulting from calcium and sodium chloride amixtures. **Cement, Concrete and Aggregates**, 8: (2): 97-102.

Diamond, S. (2000) Mercury porosimetry: An inappropriate method for the measurement of pore size distributions in cement-based materials. **Cement and Concrete Research**, 30: (10): 1517-1525.

Dodson, V.H., Farkas, E. and Rosenberg, A.M. (1965) "Non-chloride accelerator for setting of cements". United States patent No. 3,210,207.

Domone, P. (2010) "Concrete". In Domone, P. & Illston, J.M. (Eds.) **Construction Materials: Their Nature and Behaviour**. 4TH ed., Taylor & Francis p 83-205.

Edmeades, R.M. and Hewlett, C.P. (2003) "15: Cement Admixtures". In Hewlett, P.C. (Ed.) **Lea's Chemistry of Cement and Concrete**. Oxford, Butterworth-Heinemann 1-1092.

El-Jazairi, B., Berke, N.S. and Grace, W.R. (1990) The use of calcium nitrite as a corrosion inhibiting admixture to steel reinforcement in concrete. **Corrosion of Reinforcement in Concrete**, 571-585.

El Jazairi, B. and Berke, N.S. (1990) "The use of calcium nitrite corrosion inhibitors in concrete". In Page, C.L.;Treadaway, K.W. & Bamforth, P.B. (Eds.) **In corrosion of reinforcement in concrete**. Elsevier.

EWC (2002) **European Waste Catalogue and Hazardous Waste List** [online]. http://www.environ.ie/en/Publications/Environment/Waste/WEEE/FileDownLoad,1343,en.pdf Ireland Environmental Protection Agency [Accessed 2010]

Fédération Internationale du Béton (fib) (2000) **Bond of reinforcement in concrete: state-of-art**. Switzerland: International Federation for Structural Concrete.

Feldman, R.F. (1984) PORE STRUCTURE DAMAGE IN BLENDED CEMENTS CAUSED BY MERCURY INTRUSION. **Journal of the American Ceramic Society**, 67: (1): 30-33.

Felekoglu, B., Tosun, K. and Baradan, B. (2011) Compatibility of a polycarboxylate-based superplasticiser with different set-controlling admixtures. **Construction and Building Materials**, 25: (3): 1466-1473.

Fernández-Olmo, I., Lasa, C. and Irabien, A. (2007) Modeling of zinc solubility in stabilized/solidified electric arc furnace dust. **Journal of hazardous materials**, 144: (3): 720-724.

FIP (1988) **Condensed silica fume in concrete - state of art report**. London: Thomas Telford.

Flores-Velez, L.M. and Dominguez, O. (2002) Characterization and properties of portland cement composites incorporating zinc-iron oxide nanoparticles. **Journal of Materials Science**, 37: (5): 983-988.

Gallé, C. (2001) Effect of drying on cement-based materials pore structure as identified by mercury intrusion porosimetry:: A comparative study between oven-, vacuum-, and freeze-drying. **Cement and Concrete Research**, 31: (10): 1467-1477.

Gebler, S. (1983) Evaluation of calcium formate and sodium formate as accelerating admixtures for Portland-cement concrete. **Journal of the American Concrete Institute**, 80: (5): 439-444.

Gervais, C. and Ouki, S.K. (2000) "effects of foundry dusts on the mechanical, microstructural and leaching characteristics system". In Goumans, J.J.;Woolley, G.R. & Wainwright, P.J. (Eds.) **Waste materials in construction: WASCON 2000 : proceedings of the International Conference on the Science and Engineering of Recycling for Environmental Protection**. Harrogate, England, Elsevier pp. 782-790.

Gjorv, O.E., Monteiro, P.J.M. and Mehta, P.K. (1990) Effect of condensed silica fume on the steel-concrete bond. **ACI Materials Journal**, 87: (6).

Gjørv, O.E. and Vennesland, Ø. (1979) Diffusion of chloride ions from seawater into concrete. **Cement and Concrete Research**, 9: (2): 229-238.

Glass, G.K. and Buenfeld, N.R. (1997) The presentation of the chloride threshold level for corrosion of steel in concrete. **Corrosion Science**, 39: (5): 1001-1013.

Glass, G.K., Page, C.L. and Short, N.R. (1991) Factors affecting the corrosion rate of steel in carbonated mortars. **Corrosion Science**, 32: (12): 1283-1294.

Goñi, S. and Andrade, C. (1990) Synthetic concrete pore solution chemistry and rebar corrosion rate in the presence of chlorides. **Cement and Concrete Research**, 20: (4): 525-539.

Gorst, N.J.S. and Clark, L.A. (2003) Effects of thaumasite on bond strength of reinforcement in concrete. **Cement and Concrete Composites**, 25: (8): 1089-1094.

Gouda, V.K. (1970) Corrosion and corrosion inhibition of reinforcing steel, Part 1: immersed in alkaline solutions. **British Corrosion Journal**, 5: (9): 198-203.

Gowers, K.R. and Millard, S.G. (1999) Measurement of concrete resistivity for assessment of corrosion severity of steel using Wenner technique. **ACI Materials Journal**, 96: (5).

Grosse, C.U. and Reinhardt, H.W. (2003) **New developments in quality control of concrete using ultrasound**. Berlin: DGZFP.

Gu, G.P., Beaudoin, J.J. and Ramachandran, V.S. (2001) "Techniques for corrosion investigation in reinforced concrete". In Ramachandran, V.S. & Beaudoin, J.J. (Eds.) **Handbook of analytical techniques in concrete science and technology**. William AndrewPublishing/Noyes.

Haines, P.J. (2002) **Principles of thermal analysis and calorimetry**. Cambridge: Royal Society of Chemistry.

Hamilton, I.W. and Sammes, N.M. (1999) Encapsulation of steel foundry bag house dusts in cement mortar. **Cement and Concrete Research**, 29: (1): 55-61.

Hansson, C. and Sorensen, B. (1988) The threshold concentration of chloride in concrete for the initiation of reinforcement corrosion. **Corrosion rates of steel in concrete**, 3-16.

Hansson, C.M., Frølund, T. and Markussen, J.B. (1985) The effect of chloride cation type on the corposion of steel in concrete by chloride salts. **Cement and Concrete Research**, 15: (1): 65-73.

Hansson, C.M., Poursaee, A. and Jaffer, S.J. (2007) "Corrosion of Reinforcing Bars in Concrete". USA, Portland Cement Association pp. 1-33.

Hausmann, D.A. (1967) Steel corrosion in concrete -- How does it occur. **Materials Protection**, 6: (11): 19-23.

Heikal, M. (2004) Effect of calcium formate as an accelerator on the physicochemical and mechanical properties of pozzolanic cement pastes. **Cement and Concrete Research**, 34: (6): 1051-1056.

Ho, D.W.S. and Lewis, R.K. (1987) Carbonation of concrete and its prediction. **Cement and Concrete Research**, 17: (3): 489-504.

Holden, W.R., Page, C.L. and Short, N.R. (1983) "The influence of chlorides and sulphates on durability". In Crane, A.P. (Ed.) **Corrosion of Reinforcement in Concrete Construction**. London, Society of Chemical Industry pp. 143-149.

Hooper, R., McGrath, C., Morrison, C., et al. (2002) Ferro-Silicate Slag from ISF Zinc Production as a Sand Replacement: A Review. **ACI-Special Publication**, 209: 811-838.

Hope, B.B. and Alan, K.C. (1987) Chloride Corrosion Threshold in Concrete. **ACI Materials Journal**, 84: (4).

Hoshino, M. (1989) Relation Between Bleeding, Coarse Aggregate, and Specimen Height of Concrete. **ACI Materials Journal**, 86: (2).

Houst, Y.F. and Wittmann, F.H. (2002) Depth profiles of carbonates formed during natural carbonation. **Cement and Concrete Research**, 32: (12): 1923-1930.

Hunkeler, F. (2005) "Corrosion in reinforced concrete: processes and mechanisms". In Bohni, H. (Ed.) **Corrosion in Reinforced Concrete Structures**. Cambridge, Woodhead publishing 1-42.

Hussain, Al-Gahtani, A.S. and Rasheeduzzafar (1996) Chloride threshold for corrosion of reinforcement in concrete. **ACI Materials Journal**, 93: (6): 534-538.

Hussain, Rasheeduzzafar, Al-Musallam, A., et al. (1995) Factors affecting threshold chloride for reinforcement corrosion in concrete. **Cement and Concrete Research**, 25: (7): 1543-1555.

Jarrah, N.R., Al-Amoudi, O.S.B., Maslehuddin, M., et al. (1995) Electrochemical behaviour of steel in plain and blended cement concretes in sulphate and/or chloride environments. **Construction and Building Materials**, 9: (2): 97-103.

Kayyali, O.A. and Haque, M.N. (1995) The Cl-/OH-ratio in chloride-contaminated concrete--a most important criterion. **Magazine of Concrete Research**, 47: (172): 235-242.

Khan, M.I. (2003) Isoresponses for strength, permeability and porosity of high performance mortar. **Building and Environment**, 38: (8): 1051-1056.

Khan, M.I., Lynsdale, C.J. and Waldron, P. (2000) Porosity and strength of PFA/SF/OPC ternary blended paste. **Cement and Concrete Research**, 30: (8): 1225-1229.

Khayat, K.H. (1998) Use of viscosity-modifying admixture to reduce top-bar effect of anchored bars cast with fluid concrete. **ACI Materials Journal**, 95: (2).

Komlos, K., Popovics, S., Nürnbergerová, T., et al. (1996) Ultrasonic pulse velocity test of concrete properties as specified in various standards. **Cement and Concrete Composites**, 18: (5): 357-364.

Kosmatka, S.H. (1994) Bleeding. Significance of Tests and Properties of Concrete and Concrete Making Materials. **STP-169 C, ASTM International, West Conshohocken, Pa**, 88-111.

Kropp, J. (1995) "Relations between transport characteristics and durability". In Kropp, J. & Hilsdorf, H.K. (Eds.) **RILEM Report 12: Performance Criteria for Concrete Durability**. London, Spon pp. 97-137.

Kropp, J., Hilsdorf, H.K., Grube, H., et al. (1995) "Transport mechanisms and definitions". In Kropp, J. & Hilsdorf, H.K. (Eds.) **RILEM Report 12: Performance Criteria for Concrete Durability**. London, Spon pp. 3.

Kumar, A., Komarneni, S. and Roy, D.M. (1987) Diffusion of Cs+ and Cl- through sealing materials. **Cement and Concrete Research**, 17: (1): 153-160.

Kumar, R. and Bhattacharjee, B. (2003) Porosity, pore size distribution and in situ strength of concrete. **Cement and Concrete Research**, 33: (1): 155-164.

Kumar, V. (1998) Protection of steel reinforcement for concrete- a review. **Corrosion Reviews**, 16: (4): 317- 358.

Lachemi, M., Bae, S., Hossain, K.M.A., et al. (2009) Steel–concrete bond strength of lightweight self-consolidating concrete. **Materials And Structures**, 42: (7): 1015-1023.

Laforest, G. and Duchesne, J. (2007) Investigation of stabilization/solidification for treatment of electric arc furnace dust: Dynamic leaching of monolithic specimens. **Cement and Concrete Research**, 37: (12): 1639-1646.

Lambert, P., Page, C.L. and Vassie, P.R. (1991) Investigations of reinforcement corrosion. 2. Electrochemical monitoring of steel in chloride-contaminated concrete. **Materials and Structures/Materiaux et Constructions**, 24: (5): 351-358.

Laue, W., Thiemann, M., Scheibler, E., et al. (1988) "Nitrates and Nitrites". **Ullmann's encyclopedia of industrial chemistry**. 7 ed., Wiley-Vch.

Lerch, W. (1957) "Plastic shrinkage". **ACI 52nd annual convention**. Philadelphia, ACI.

Li, C.L. and Tsai, M.S. (1993) A crystal phase study of zinc hydroxide chloride in electric-arc-furnace dust. **Journal of Materials Science**, 28: (17): 4562-4570.

Li, L., Sagues, A.A. and Poor, N. (1999) In situ leaching investigation of pH and nitrite concentration in concrete pore solution. **Cement and Concrete Research**, 29: (3): 315-321.

Lieber, W. (1968) "The influence of lead and zinc compounds on the hydration of Portland cement". **Fifth Int. Sym. on the Chemistry of Cement**. Tokyo, 444–454

Lin, Y., Kuo, S.F., Hsiao, C., et al. (2007) Investigation of pulse velocity-strength relationship of hardened concrete. **ACI Materials Journal**, 104: (4).

Lohtia, R.P. and Joshi, R. (1995) "Mineral Admixtures". In Ramachandran, V.S. (Ed.) **Concrete Admixture Handbook - Properties, Science and Technology**. 2nd Edition ed., William Andrew Publishing/Noyes 1182.

Longuet, P., Burglen, L. and Zelwer, A. (1973) La phase liquide du ciment hydrate. **Rev. Mater. Constr. Trav. Publics**, 676: 35-41.

Machado, J., Brehm, F.A., Moraes, C.A.M., et al. (2006) Chemical, physical, structural and morphological characterization of the electric arc furnace dust. **Journal of Hazardous Materials**, 136: (3): 953-960.

Mangat, P.S., Khatib, J.M. and Molloy, B.T. (1994) Microstructure, chloride diffusion and reinforcement corrosion in blended cement paste and concrete. **Cement and Concrete Composites**, 16: (2): 73-81.

Maslehuddin, M., Awan, F.R., Shameem, M., et al. (2010) Effect of electric arc furnace dust on the properties of OPC and blended cement concretes. **Construction and Building Materials**, ARTICLE IN PRESS.

Maslehuddin, M., Awan, F.R., Shameem, M., et al. (2011) Effect of electric arc furnace dust on the properties of OPC and blended cement concretes. **Construction and Building Materials**, 25: (1): 308-312.

McPolin, D., Basheer, P.A.M., Long, A.E., et al. (2005) Obtaining progressive chloride profiles in cementitious materials. **Construction and Building Materials**, 19: (9): 666-673.

Mehta, P.K. and Gjørv, O.E. (1982) Properties of portland cement concrete containing fly ash and condensed silica-fume. **Cement and Concrete Research**, 12: (5): 587-595.

Mohammed, T.U., Otsuki, N. and Hamada, H. (2003) Corrosion of steel bars in cracked concrete under marine environment. **Journal of Materials in Civil Engineering**, 15: (5): 460-469.

Monosi, S., P. Giretti, P., G. Moriconi, G., et al. (2001) Non-Ferrous Slag as Cementitious-Material and Fine Aggregate for Concrete. **ACI-Special Publication**, 202: 33-44.

Montes, P., Bremner, T.W. and Mrawira, D. (2005) Effects of calcium nitrite-based corrosion inhibitor and fly ash on compressive strength of high-performance concrete. **ACI Materials Journal**, 102: (1): 3-8.

Morrison, C., Hooper, R. and Lardner, K. (2003) The use of ferro-silicate slag from ISF zinc production as a sand replacement in concrete. **Cement and Concrete Research**, 33: (12): 2085-2089.

Mulheron, M. and Nwaubani, S.O. (1999) "corrosion Inhibitors for high performance reinforced concrete structures". In Rivera-Villarreal, J.G.C.a.R. (Ed.) **PRO 5: International RILEM Conference on The Role of Admixtures in High Performance Concrete**. France, RILEM Publications pp. 183-197.

Mustafa, M.A. and Yusof, K.M. (1991) Mechanical properties of hardened concrete in hot-humid climate. **Cement and Concrete Research**, 21: (4): 601-613.

Neville, A.M. (1995) **Properties of Concrete** 4th ed.Harlow : Longman.

Ngala, V.T. (1995) **Pore structure and diffusional properties of hardened cement pastes**. PhD, the University of Aston.

Ngala, V.T., Page, C.L. and Page, M.M. (2002) Corrosion inhibitor systems for remedial treatment of reinforced concrete. Part 1: Calcium nitrite. **Corrosion Science**, 44: (9): 2073-2087.

Ngala, V.T., Page, C.L., Parrott, L.J., et al. (1995) Diffusion in cementitious materials: II, further investigations of chloride and oxygen diffusion in well-cured OPC and OPC/30%PFA pastes. **Cement and Concrete Research**, 25: (4): 819-826.

Oh, B.H. and Jang, S. (2007) Effects of material and environmental parameters on chloride penetration profiles in concrete structures. **Cement and Concrete Research**, 37: (1): 47-53.

Oh, B.H., Jang, S.Y. and Shin, Y.S. (2003) Experimental investigation of the threshold chloride concentration for corrosion initiation in reinforced concrete structures. **Magazine of Concrete Research**, 55: (2): 117-124.

Page, C.L. (1988) "Basic principles of corrosion". In Schiessl, P. (Ed.) **Corrosion of Steel in Concrete: Report of the Technical Committee 60 CSC, RILEM (the International Union of Testing and Research Laboratories for Materials and Structures)**. London, Chapman & Hall 3-21.

Page, C.L. (1998) "Corrosion and its control in reinforced concrete". **26th annual convention of the institute of concrete technology, the sixth Sir Fredrick Lea Memorial Lecture**. Market Bosworth, The institute of concrete technology.

Page, C.L. (2007) "Corrosion and Protection of Reinforcing Steel in Concrete". In Page, C.L. & Page, M.M. (Eds.) **Durability of concrete and cement composites**. Woodhead publishing pp. 136-186.

Page, C.L. (2009) Initiation of chloride-induced corrosion of steel in concrete: role of the interfacial zone. **Materials and corrosion**, 60: (8): 586–592.

Page, C.L. and Havdahl, J. (1985) Electrochemical monitoring of corrosion of steel in microsilica cement pastes. **Materials and Structures/Materiaux et Constructions**, 18: 41-47.

Page, C.L., Lambert, P. and Vassie, P.R.W. (1991) Investigations of reinforcement corrosion. 1. The pore electrolyte phase in chloride-contaminated concrete. **Materials And Structures**, 24: (4): 243-252.

Page, C.L., Short, N.R. and El Tarras, A. (1981) DIFFUSION OF CHLORIDE IONS IN HARDENED CEMENT PASTES. **Cement and Concrete Research**, 11: (3): 395-406.

Page, C.L., Short, N.R. and Holden, W.R. (1986) The influence of different cements on chloride-induced corrosion of reinforcing steel. **Cement and Concrete Research**, 16: (1): 79-86.

Page, C.L. and Treadaway, K.W.J. (1982) Aspects of the electrochemistry of steel in concrete. **Nature**, 297: 109 - 115

Parrott, L.J. (1987) "Measurement and modelling of porosity in drying cement paste". **Mater. Res. Symp. Proc.** Wexham, UK.

Parrott, L.J. (1992) Variations of water absorption rate and porosity with depth from an exposed concrete surface: Effects of exposure conditions and cement type. **Cement and Concrete Research**, 22: (6): 1077-1088.

Parrott, L.J. (1994) Study of carbonation-induced corrosion. **Magazine of Concrete Research**, 46: (166): 23-28.

Pereira, C.F., Galiano, Y.L., Rodríguez-Pi ero, M.A., et al. (2007) Long and short-term performance of a stabilized/solidified electric arc furnace dust. **Journal of Hazardous Materials**, 148: (3): 701-707.

Pourbaix, M. (1966) **Atlas of electrochemical equilibria in aqueous solutions**. Oxford: Pergamon press.

Ramachandran, V.S. (1976) **Calcium chloride in concrete: science and technology**. London: Applied Science Publishers.

Ramachandran, V.S. (1982) "Investigation of the role of chemical admixtures in cements - a differential thermal approach". In Miller, B. (Ed.) **Thermal analysis-Proc. 7th Int. Conf. Therm. Anal.** Chichester, UK, Wily.

Ramachandran, V.S. (1995) "Accelerators". In Ramachandran, V.S. (Ed.) **Concrete admixtures handbook: properties, science, and technology**. William Andrew Publishing 1153.

Rasheeduzzafar, Al-Saadoun, S.S., Al-Gahtani, A.S., et al. (1990) Effect of tricalcium aluminates content of cement on corrosion of reinforcing steel in concrete. **Cement and Concrete Research**, 20: (5): 723-738.

Richardson, M.G. (2002) "5 Carbonation". **Fundamentals of durable reinforced concrete**. Taylor & Francis.

RILEM Committee (1988) CPC-18 Measurement of hardened concrete carbonation depth. **Materials And Structures**, 21: (6): 453-455.

Rilem TC 178-TMC (2002) 'Testing and modeling chloride penetration in concrete' - Analysis of total chloride content in concrete. **Materials and Structures/Materiaux et Constructions**, 35: (253): 583-585.

Rixom, M.R. and Mailvaganam, N.P. (1986) "accelerators". **Chemical admixtures for concrete**. 2nd ed. London, E. & F.N. Spone Ltd 300.

Roberts, M.H. (1962) Effect of calcium chloride on the durability of pre-tensioned wire in prestressed concrete. **Magazine of Concrete Research**, 14: (42): 143-154.

Rodriguez, P., Ramirez, E. and Gonzalez, J.A. (1994) Methods for studying corrosion in reinforced concrete. **Magazine of Concrete Research**, 46: (167): 81-90.

Rosenberg, A.M., Gaidis, J.M., Kossives, T.G., et al. (1977) "A corrosion inhibitor formulated with calcium nitrite for use in reinforced concrete". In Tonini, D.E. & Dean, S.W. (Eds.) **Chloride corrosion of steel in concrete**. Chicago, ASTM International.

Rosskopf, P.A., Linton, F.J. and Peppler, R.B. (1975) Effect of various accelerating chemical admixtures on setting and strength development of concrete. **Journal of Testing and Evaluation**, 3: (4): 322-330.

Rostásy, F.S., Wei, R. and Wiedemann, G. (1980) Changes of pore structure of cement mortars due to temperature. **Cement and Concrete Research**, 10: (2): 157-164.

Ryou, J.S. and Ann, K.Y. (2008) Variation in the chloride threshold level for steel corrosion in concrete arising from different chloride sources. **Magazine of Concrete Research**, 60: (3): 177-188.

Sabic (2001) "Cast-In-Place Reinforced Concrete". **Sabic Engineering Standard**. Jubail-KSA, Sabic 1-37.

Sagues, A.A., Moreno, E.I. and Andrade, C. (1997) Evolution of pH during in-situ leaching in small concrete cavities. **Cement and Concrete Research**, 27: (11): 1747-1759.

Salihoglu, G. and Pinarli, V. (2008) Steel foundry electric arc furnace dust management: Stabilization by using lime and Portland cement. **Journal of hazardous materials**, 153: (3): 1110-1116.

Salihoglu, G., Pinarli, V., Salihoglu, N.K., et al. (2007) Properties of steel foundry electric arc furnace dust solidified/stabilized with Portland cement. **Journal of environmental management**, 85: (1): 190-197.

Sawan, J.S. (1992) Strength and shrinkage of natural pozzolanic mortar in hot weather. **Journal of Materials in Civil Engineering**, 4: (2): 153-165.

SchiessI, P., Schmidt, R., International Union of, T., et al. (1990) "Bleeding of concrete". In Wierig, H.J. (Ed.) **Properties of Fresh Concrete: Proceedings of the International RILEM Colloquium**. Hanover, Chapman and Hall.

Schiessl, P. and Raupach, M. (1990) Influence of concrete composition and microclimate on the critical chloride content in concrete. **Corrosion of Reinforcement in Concrete**, 49-58.

Singh, N.B. and Abha, K. (1983) Effect of calcium formate on the hydration of tricalcium silicate. **Cement and Concrete Research**, 13: (5): 619-625.

Sofili, T. and Rastovan-Mio, A. (2004) Characterization of steel mill electric-arc furnace dust. **Journal of hazardous materials**, 109: (1-3): 59-70.

Soylev, T.A. and François, R. (2003) Quality of steel-concrete interface and corrosion of reinforcing steel. **Cement and Concrete Research**, 33: (9): 1407-1415.

Stegemann, J.A., Roy, A., Caldwell, R.J., et al. (2000) Understanding environmental leachability of electric arc furnace dust. **Journal of Environmental Engineering**, 126: 112-120.

Stern, M. and Geary, A.L. (1957) Electrochemical polarization. 1: A theoretical analysis of the shape of polarisation curves. **Electrochemical Society**, 104: 56-63.

Stern, M. and Weisert, E.D. (1959) "Experimental observations on the relation between polarisation resistance and corrosion rate". **Proceedings of the American Society for Testing and Materials**. 1280-1291.

Suryavanshi, A.K., Scantlebury, J.D. and Lyon, S.B. (1998) Corrosion of reinforcement steel embedded in high water-cement ratio concrete contaminated with chloride. **Cement and Concrete Composites**, 20: (4): 263-281.

Suzuki, K., Ohno, Y., Praparntanatorn, S., et al. (1990) "Mechanism of steel corrosion in cracked concrete". In Page, C.L.;Treadaway, K.W. & Bamforth, P.B. (Eds.) **Corrosion of Reinforcement in Concrete**. UK, Society of chemical industry pp. 19-28.

Taylor, F.W. (1997) **Cement Chemistry.** Second Ed.London: Thomas Telford Publ.

Thomas, Jameson, D. and Double, D. (1981) The effect of lead nitrate on the early hydration of Portland cement. **Cement and Concrete Research**, 11: (1): 143-153.

Thomas, M. (1996) Chloride thresholds in marine concrete. **Cement and Concrete Research**, 26: (4): 513-519.

Thomas, M.D.A. and Matthews, J.D. (2004) Performance of pfa concrete in a marine environment--10-year results. **Cement and Concrete Composites**, 26: (1): 5-20.

Thomas, M.D.A., Shehata, M.H., Shashiprakash, S.G., et al. (1999) Use of ternary cementitious systems containing silica fume and fly ash in concrete. **Cement and Concrete Research**, 29: (8): 1207-1214.

Tomosawa, T., Masuda, Y., I., F., et al. (1990) "Experimental study on the effectiveness of corrosion inhibitor in reinforced concrete". In E., V. (Ed.) **Proceedings of the international RILEM durability symposium**. London, Chapman and Hall.

Traetteberg, A., Ramachandran, V.S. and Grattan-Bellew, P.E. (1974) Study of the microstructrure and hydration characteristics of tricalcium silicate in the presence of calcium chloride. **Cement and Concrete Research**, 4: (2): 203-221.

Tritthart, J. (1989) Chloride binding in cement II. The influence of the hydroxide concentration in the pore solution of hardened cement paste on chloride binding. **Cement and Concrete Research**, 19: (5): 683-691.

Troconis de Rincón, O., Pérez, O., Paredes, E., et al. (2002) Long-term performance of ZnO as a rebar corrosion inhibitor. **Cement and Concrete Composites**, 24: (1): 79-87.

Turkmen, I., Gul, R. and Celik, C. (2008) A Taguchi approach for investigation of some physical properties of concrete produced from mineral admixtures. **Building and Environment**, 43: (6): 1127-1137.

Vassie, P. (1984) Reinforcement corrosion and the durability of concrete bridges. **P. Vassie, Proceedings, Institution of Civil Engineers(London), Part I, Design and Construction**, 76: 713-723.

Vogel, A.I. (1978) **A Textbook of Quantitative Inorganic Analysis**. Fourth Edition.London: Longman.

Walker, P.R., Batayneh, M.K. and Regan, P.E. (1997) Bond strength tests on deformed reinforcement in normal weight concrete. **Materials and Structures/Materiaux et Constructions**, 30: (201): 424-429.

Weeks, C., Hand, R.J. and Sharp, J.H. (2008) Retardation of cement hydration caused by heavy metals present in ISF slag used as aggregate. **Cement and Concrete Composites**, 30: (10): 970-978.

Wilkins, N.J. and Sharp, J.V. (1990) "Localized corrosion of reinforcement in marine concrete". In Page, C.L.;Treadaway, K.W. & bamforth, P.B. (Eds.) **Corrosion of Reinforcement in Concrete**. England, Society of chemical industry pp. 3-18.

Williamson, S.J. (1999) **The influence of concrete cover properties on the effects of reinforcement corrosion** Thesis (Ph.D), University of Birmingham.

Xia, D.K. and Pickles, C.A. (1999) Caustic roasting and leaching of electric arc furnace dust. **Canadian metallurgical quarterly**, 38: (3): 175-186.

Yokota, M., Sasaki, T., Iijima, T., et al. (2005) "Study on the change of rebar corrosion rate using ac impedance measurements in chloride containing concrete with advance of carbonation". **Proceedings EUROCORR 2005: European Corrosion Congress**. Lisbon, Portugal, EUROCORR 2005 pp. 10.

Yonezawa, T., Ashworth, V. and Procter, R.P.M. (1989) "The mechanism of fixing Cl-by cement hydrates resulting in the transformation of NaCl to NaOH". **Proceedings, 8th International Conference on Alkali-Aggregate Reaction** Kyoto, pp. 153-160.

Zheng, J. and Xinzhu, Z. (2008) Analytical solution for the chloride diffusivity of hardened cement paste. **Journal of Materials in Civil Engineering**, 20: (5): 384-391.